

STUDIES ON THE PLASTICIZATION OF POLYMERIC TABLET BINDERS

A thesis submitted by

RICHARD JOHN HOUGHTON B.Pharm., M.Sc., M.R.Pharm.S.

in partial fulfilment of the requirements for the degree of

DOCTOR of PHILOSOPHY

of the Council for National Academic Awards.

October 1990

The Department of Pharmacy,
The School of Health and Life Sciences,
Leicester Polytechnic

The work presented in this thesis was carried out under an SERC CASE Award in collaboration with Pfizer Central Research, Sandwich, Kent

STUDIES ON THE PLASTICIZATION OF POLYMERIC TABLET BINDERS

RICHARD JOHN HOUGHTON

ABSTRACT

Plasticization has been investigated with respect to the physico-mechanical properties and the tableting performance of the polymeric tablet binders HPMC, PVP and Starch 1500.

Thermodynamic criteria for polymer-solvent miscibility have been evaluated in the screening of plasticizers. Estimations of polymer-plasticizer miscibility using solubility parameters and Flory and Huggins interaction parameters show good correlation with solid-state compatibility limits. Limitations to the theoretical approach are discussed. PEG 200 is identified as the optimum plasticizer for both PVP and HPMC from the range of PEGs and glycol monomers evaluated. The crystallinity of Starch 1500 suggests that its plasticization might be unattainable.

Mechanical properties of PVP, HPMC and Starch 1500 films have been characterised by tensile stress-strain relationships. The incorporation of some potential plasticizers, or the sorption of moisture, yields weaker but more ductile films. These changes are consistent with a plasticizer activity.

The influence of moisture sorption and plasticization on the creep compliance of polymeric binder films has been studied by microindentation. The development of a computer interface for data capture and manipulation has enabled rapid and accurate quantification of important viscoelastic properties.

The role of binder plasticity in the tablettability of materials has been investigated using dicalcium phosphate and paracetamol granulates prepared by wet-massing. In the case of dicalcium phosphate, tablet tensile strength is correlated with binder tensile strength. Consequently, increasing binder plasticity results in weaker tablets. In contrast, the tensile strength and capping pressure of paracetamol tablets is initially increased with increasing binder plasticity. An optimum level of binder plasticity exists, however, above which tablet strength falls. For both substrates, increasing binder plasticity reduces tablet friability.

The influence of binder plasticity on granule deformation during compression has been studied using an instrumented press. It is deduced from Heckel plots that the consolidation of binder-massed granulates is related to binder plasticity. This is a physico-mechanical phenomenon which is independent of binder type or substrate material.

The relationship between binder plasticity and granular plasticity has been confirmed by stress-relaxation studies. Correlation of tablet capping tendency with plasto-elasticity indices indicates that ductile binder flow, during elastic strain recovery, is more important than elastic strain reduction in eliminating capping. A model has been proposed to relate binder mechanical properties to the strength, friability and capping tendency of tablets.

PRESENTATIONS AND PUBLICATIONS

Parts of the work described in this thesis have resulted in the following conference publications and presentations:

Aulton, M.E., Houghton, R.J. and Wells, J.I., (1985),
Compatibility of polymeric binders and potential plasticizers.
J. Pharm. Pharmacol., 37, Suppl., 113P.

Aulton, M.E., Houghton, R.J. and Wells, J.I., (1986),
A computer-interfaced microindenter.
Proceedings of the 5th Pharmaceutical Technology Conference,
Harrogate, U.K.

Houghton, R.J., Aulton, M.E. and Wells, J.I., (1986),
The time-dependent deformation of cast films of plasticized polymeric
tablet binders.
Proceedings of the 5th Pharmaceutical Technology Conference,
Harrogate, U.K.

Aulton, M.E., Houghton, R.J. and Wells, J.I., (1986),
The effect of plasticization on the performance of polymeric tablet
binders.
Proceedings of the 4th APGI International Conference on Pharmaceutical
Technology, Paris, France.

ACKNOWLEDGEMENTS

I wish to express my sincere thanks to Dr M. E. Aulton and Dr J.I. Wells for their continued encouragement, advice and criticisms throughout the course of this work

My thanks are also due to the following:

- The technical staff of the Department of Pharmacy, particularly Mr R. Webster.
- The Department of Chemistry, for use of the Instron Tensometer and for undertaking X-ray crystallography studies.
- Mr R.J. Burdett and The Department of Mechanical Engineering, for the use of Mayes hydraulic press.
- The Science and Engineering Research Council, for granting a CASE Award.
- Pfizer Central Research, for additional financial support and for use of technical facilities.
- Mr A.M. Twitchell and Dr D. Wong, for their friendship, encouragement and interest in the work.
- The International Development Centre, Abbott Laboratories, for access to reprographic facilities.

CONTENTS

Abstract	(i)
Presentations and Publications	(ii)
Acknowledgements	(iii)
Contents	(iv)
CHAPTER ONE INTRODUCTION	1
1.1 Preamble	1
1.2 The Deformation of Materials	2
1.2.1 Elastic Behaviour	2
1.2.2 Viscous Behaviour	4
1.2.3 Real Materials	5
1.2.4 Mechanical Models of Linear Viscoelastic Behaviour	5
1.2.4.1 The Maxwell Model	6
1.2.4.2 The Voigt Model	7
1.2.4.3 Generalised Linear Viscoelasticity	9
1.3 Evaluation of Material Behaviour During the Compression Process	11
1.3.1 Brittle Failure and Brittle Fracture Propensity	11
1.3.2 Densification and Pressure-Volume Relationships	13
1.3.2.1 The Heckel Equation	14
1.3.2.2 Applications of Pressure-Volume Relationships	17
1.3.3 Stress Relaxation	19
1.3.4 Radial Versus axial Pressure Cycles	22
1.3.5 Work of Compaction	24
1.3.6 Power	26
1.3.7 Elastic Deformation	27
1.3.7.1 Elastic Strain Recovery	27
1.3.7.2 The Poisson Ratio	28
1.3.7.3 Surface Areas	28

1.3.8	Plasticity-Elasticity Indices	29
1.3.9	Viscoelastic Deformations	32
1.4	Binder Film Formation and Deformation	33
1.5	Plasticization of Tablet Binders: Objectives and Scope of the Thesis	35
CHAPTER TWO	PLASTICIZATION AND THE THERMODYNAMICS OF POLYMER SOLUTIONS	39
2.1	Plasticization Phenomena	39
2.1.1	Intermolecular Forces	41
2.1.2	Compatibility	42
2.1.3	Ideal Solutions	44
2.1.4	Heat of Mixing	45
2.1.5	Determination of Solubility Parameters	47
2.1.6	Entropy of Mixing	49
2.1.7	Free Energy of Mixing	51
2.1.8	Phase Separation	52
2.1.9	Determination of Flory-Huggins Interaction Parameters	54
2.1.10	Application of Polymer-Solvent Phase Equilibria to Plasticization	55
2.1.11	Application of the Hildebrand-Scatchard Relationship to Polymer-Plasticizer Compatibility	56
2.2	Materials and Methods	57
2.2.1	Binding Agents	58
2.2.1.1	Polyvinylpyrrolidone (PVP)	58
2.2.1.2	Hydroxypropyl Methylcellulose (HPMC)	59
2.2.1.3	Pregelatinised Starch (Starch 1500)	60
2.2.2	Potential Plasticizers	61
2.2.3	Estimation of Polymer Solubility Parameters	61
2.2.4	Estimation of Flory-Huggins Interaction Parameters	64
2.2.5	Intrinsic Viscosities	65

2.2.6	Evaluation of Solid State Compatibility	66
2.3	Results and Discussion	67
2.3.1	Entropy of Mixing	67
2.3.2	Solubility Characteristics of PVP, HPMC and Starch 1500 in Solvents of Differing Hydrogen-bonding Propensity	69
2.3.3	Estimation of Flory-Huggins Interaction Parameters and Phase-separation Criteria	78
2.3.4	Intrinsic Viscosities	84
2.3.5	Solid State Compatibility	86
2.3.5.1	Solid State Compatibility of HPMC	88
2.3.5.2	Solid State Compatibility of PVP	91
2.3.5.3	Solid State Compatibility of Starch 1500	92
2.4	Conclusions	93
 CHAPTER THREE THE INFLUENCE OF PLASTICIZATION ON THE TENSILE PROPERTIES OF POLYMERIC TABLET BINDERS		 97
3.1	Mechanical Properties of Polymer and their Measurement	97
3.2	Mechanical Properties of Pharmaceutical Polymers	101
3.2.1	Tensile Properties of Unplasticized Polymers	101
3.2.2	Effects of Plasticizers on the Tensile Properties of Polymers	103
3.2.3	Effects of Other Inclusions on the Tensile Properties of Polymers	105
3.3	Materials and Methods	106
3.3.1	Materials	106
3.3.2	Methods	107
3.3.2.1	Film Preparation	107
3.3.2.2	Tensile Testing	110

3.4	Results and Discussion	112
3.4.1	Tensile Mechanical properties of Unplasticized Binders	112
3.4.2	The Effect of Different Plasticizers on the Tensile Properties of the Binders	118
3.4.2.1	Plasticization of PVP	118
3.4.2.2	Plasticization of HPMC	121
3.4.2.3	Plasticization of Starch 1500	123
3.4.3	The effect of Plasticizer Concentration and Conditioning Humidity	126
3.4.4	Molecular basis of Binder Plasticization	133
3.5	Conclusions	140
 CHAPTER FOUR CREEP RHEOLOGY OF POLYMERIC TABLET BINDERS		 143
4.1	Investigation of Time-dependent Deformation	143
4.2	Materials and Methods	146
4.2.1	The ICI Micro-Indenter	146
4.2.2	Data Logging Using the BBC Model B Microcomputer	148
4.2.3	Sample Preparation	151
4.2.4	Indentation Testing	151
4.3	Results and Discussion	153
4.3.1	Analysis of Creep Compliance	153
4.3.1.1	Discrete mechanical analysis of Creep Compliance	156
4.3.1.2	Continuous Spectral Analysis of Creep Compliance	158
4.3.2	Visual Evaluation of the Creep Compliance Curves	161
4.3.3	Discrete Mechanical Analysis	167
4.3.3.1	The Influence of Moisture Content on Polymer Plasticity and Elasticity	173
4.3.3.2	The Influence of Plasticizer Content on Polymer Plasticity and Elasticity	176

4.3.3.3	The Influence of Moisture Content and Plasticizer Content on Viscoelastic Deformation	176
4.3.4	Continuous Spectral Analysis	180
4.3.4.1	Continuous Retardation Spectra of Unplasticized Binders	180
4.3.4.2	The Effects of Plasticization on Continuous Retardation Spectra	183
4.4	Discussion	188
4.4.1	Mechanistic Interpretation of Viscoelastic Phenomena	188
4.4.2	Thermal Properties of Polymers - Dependence of Viscoelastic Behaviour on Temperature	189
4.4.3	Thermal Properties of Polymers - Correlation With Viscoelastic Properties of Plasticized Binders	192
4.5	Conclusions	194
 CHAPTER FIVE GRANULATION AND TABLETTING STUDIES		197
5.1	Granulation	197
5.1.1	Theories of Aggregation and Bonding	197
5.1.2	The Granulating Liquid	199
5.1.3	Processing Factors	200
5.1.4	Binders	201
5.2	The Effect of Binders on Physical Properties of Granules and Tablets	202
5.2.1	Granule Properties	202
5.2.2	Tablet Properties	203
5.2.2.1	Tablet Strength	203
5.2.2.2	Granulation Method	203
5.2.2.3	Binder Type	204
5.2.2.4	Tablet Friability and Work of Failure	205
5.3	Materials and Methods	206
5.3.1	Materials	207

5.3.1.1	Model Substrates	207
5.3.1.2	Binder and plasticizers	209
5.3.2	Methods	210
5.3.2.1	Granulation Method	210
5.3.2.2	Granule Size Distribution	212
5.3.2.3	Granule Bulk Densities	212
5.3.2.4	Tabletting	213
5.3.2.5	Determination of Tablet Physical Properties	214
5.4	Results and Discussion	215
5.4.1	Granule Properties	215
5.4.1.1	Reproducibility of the Granulation Method	215
5.4.1.2	Granulation with Water Alone	216
5.4.1.3	The Effect of Binding agents on Granule Properties	216
5.4.1.4	Granule Morphology	220
5.4.1.5	Granule Moisture Content	222
5.4.2	Tablet Properties	224
5.4.2.1	Substrate Dependent Differences	229
5.4.2.2	Binder Dependent Differences	229
5.4.2.3	The Effect of Binder Plasticization	232
5.4.2.4	The Effect of a Low Efficiency Plasticizer	236
5.4.2.5	Discussion	237
5.4.3	Tablet Work of Failure Correlation with Friability	240
5.5	Conclusions	246
 CHAPTER SIX DEFORMATION AND CONSOLIDATION OF COMPACTS		249
6.1	Introduction	249
6.2	Materials and Methods	249
6.2.1	Materials	249
6.2.2	Methods	250
6.2.2.1	The Mayes Press	250
6.2.2.2	The Punch and Die Set	251

6.2.2.3	Consolidation of Granules During Compression	252
6.2.2.4	Stress Relaxation	255
6.2.2.5	Elastic Strain Recovery	255
6.3	Results and Discussion	256
6.3.1	Pressure - Volume Relationships	256
6.3.1.1	Consolidation of the Substrates	256
6.3.1.2	The Effect of Granulation with a Binder on Granule Consolidation	261
6.3.1.3	The Effect of Binder Plasticization on Granule Consolidation	267
6.3.1.4	The Effect of a Low Efficiency	277
6.3.2	Time-Dependent Densification	278
6.3.2.1	Time-Dependent Densification of the Substrates	278
6.3.2.2	The Effect of Binder and Binder Plasticity on Time-Dependent Densification	280
6.3.3	Stress-Relaxation Studies	285
6.3.3.1	Stress-Relaxation of the Tablet Substrates	286
6.3.3.2	The Effect of Granulation with a Binder on Stress-Relaxation	290
6.3.3.3	The Effect of Binder Plasticity on Stress-Relaxation	295
6.3.3.4	The Effect of a Low Efficiency Plasticizer	301
6.4	Elastic Strain Recovery	303
6.5	Plasto-Elasticity Indices	306
6.6	Conclusions	309
CHAPTER SEVEN GENERAL CONCLUSIONS AND SUGGESTIONS FOR FURTHER WORK		313
REFERENCES		323

CHAPTER ONE

INTRODUCTION

CHAPTER ONE

INTRODUCTION

1.1 Preamble

The concept of the modern pharmaceutical tablet has its origins in 1843 when Thomas Brockedon was granted a patent for the manufacture of pills and lozenges by compaction in a die. Since then, the compressed tablet has grown in popularity and is now recognised as the most commonly utilised dosage form. The success of the tablet arises from the unique combination of benefits that it offers both to the patient and the pharmaceutical manufacturer. To the patient, it provides a compact and accurate unit dose in a palatable and easily administered form. To the manufacturer it affords a presentation that is uniform in content, is physically, chemically and microbiologically stable for prolonged periods of storage and is relatively inexpensive to manufacture and process.

The requirement for physical coherence in a compressed tablet is important for aesthetic and practical reasons. Nutter Smith (1949) discussed the need for meaningful and reproducible methods for the assessment of a tablet's resistance to "wear and tear". Flaws in the tablet may detract from the quality and appearance of the tablet and may affect the dose delivered. Additionally, the success and efficiency of operations such as tablet coating, packaging, transportation and ultimately dispensing, all depend on the initial production of a suitably robust and durable tablet.

Where the active component is a low dose drug, tableting problems can largely be avoided by the use of readily compressible diluents. Where the active component is a high dose drug comprising the largest proportion of the tablet problems are more likely, however, especially if the drug is refractory with respect to its compression properties. In such cases, the use of sufficient quantity of a compressible diluent may be precluded on the grounds of size. It may then be necessary to modify the compression behaviour of the bulk drug by the inclusion, by granulation if necessary, of a suitable binding agent.

It has long been appreciated that the ease with which a material will form a tablet (and the subsequent mechanical properties of the tablet) is a function of the way in which the material deforms in response to compressive stress. In this chapter a brief outline of the nature of material deformation is given. The literature reveals that a number of procedures have been used to assess aspects of material behaviour during the compaction process (see, for example, Krycer et al., 1982a; Marshall, 1989). The contribution of these techniques to an understanding of the role of deformation in the formation of coherent tablets, and the manner in which binders may influence the deformation, is reviewed.

1.2 The Deformation of Materials

When investigating physical and mechanical properties of elastic solids or viscous liquids, it is frequently found that deviations occur from the classical theories of elasticity or hydrodynamics. Deviations are of two kinds. Firstly, stress anomalies arise when the strain in a solid or the rate of strain in a liquid are not directly proportional to the applied stress but instead depend on the stress in a more complex manner. Secondly, time anomalies occur when the resultant stress depends not only on strain but also on the rate of strain; the observed deformation behaviour is both liquid-like and solid-like and is therefore termed viscoelasticity. Stress and time anomalies may co-exist but in the absence of the former the behaviour is said to be linear viscoelasticity. This implies that the ratio of stress to strain is a function of time alone and is independent of stress magnitude. Linear viscoelastic behaviour applies, therefore, to cases where the elastic contribution is Hookean and the viscous contribution is Newtonian. To understand viscoelasticity it is necessary first to consider the extreme examples of this behaviour exhibited by an elastic solid and a viscous fluid respectively.

1.2.1 Elastic Behavior

An ideal elastic material, which recovers its original strain after removal of an applied stress, obeys Hooke's law. This states that the stress (σ) is proportional to the linear strain (ϵ):

$$\sigma = G.E \quad (1.1)$$

where (G) is a constant of proportionality, effectively a measure of stiffness or rigidity, known as the elastic modulus or Young's Modulus. The implicit conditions of the above equation define elastic behaviour. Firstly, the strain in response to applied stress has an equilibrium value which is completely recoverable; secondly, deformation is ideally instantaneous, i.e. independent of time and lastly, the relationship of strain to stress is linear.

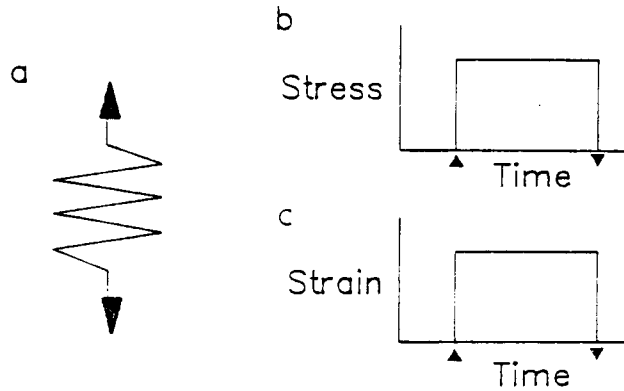
Both stress anomalies and time anomalies result in deviations from the simplest case of Hookean elasticity giving rise to other modes of deformation. Norwick and Berry (1972) have classified several types of mechanical behaviour according to the conditions obeyed by the stress-strain relationship (Table 1.1).

Table 1.1 Types of Mechanical Behaviour Classified According to the Conditions Obeyed by the Stress-Strain Relationship.
After Norwick and Berry (1972)

CONDITION	Unique Equilibrium Relationship (Complete Recovery)	Complete Instant Response	Linearity
Ideal Elasticity	YES	YES	YES
Non-linear Elasticity	YES	YES	NO
Instantaneous Plasticity	NO	YES	NO
Anelasticity	YES	NO	YES
Linear Viscoelasticity	NO	NO	YES

A simple metal spring exhibits typical Hookean behaviour and is often used as a mechanical model of ideal elastic behaviour. The stress-time and strain-time relationships are illustrated by Fig. 1.1.

Figure 1.1 The Hookean Spring



- a Mechanical Model
- b Stress vs. Time
- c Strain vs. Time

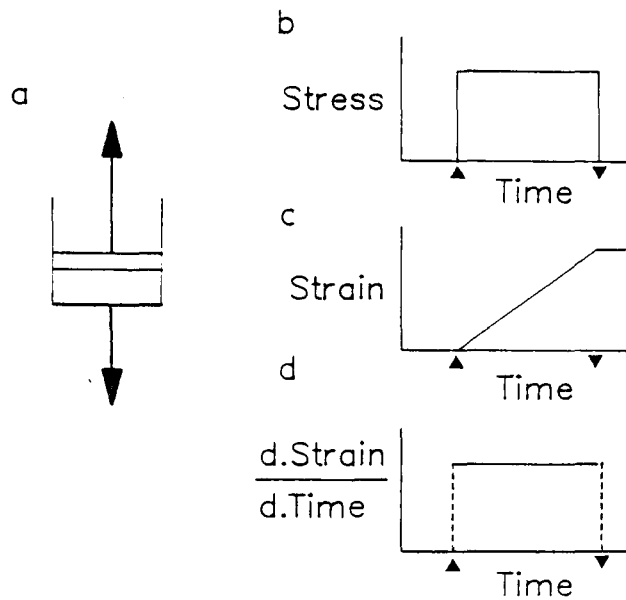
1.2.2 Viscous Behaviour

Application of a constant stress to a Newtonian viscous fluid results in a linear increase in strain with time until the stress is removed. The deformation is permanent and the original strain is not recovered. The strain-time relationship is characterised by the gradient of the stress versus strain-rate plot, i.e.

$$\eta = \sigma / \dot{\epsilon} \quad (1.2)$$

where ($\dot{\epsilon}$) is the rate of change of strain (the first differential of strain with respect to time and (η) is the Newtonian viscosity of the fluid. Newtonian viscous behaviour can be conveniently modelled by a piston and dashpot arrangement in which the dashpot cylinder is filled with a Newtonian fluid. Figure 1.2 illustrates the deformation characteristics of such a material.

Figure 1.2 The Newtonian Dashpot



- a Mechanical Model
- b Stress vs. Time
- c Strain vs. Time
- d Rate of Change of Strain vs. Time

1.2.3 Real Materials

For most materials the observed mechanical properties can only be described by a two-component system in which an ideal elastic phase is combined with an ideal viscous phase. In practice most materials show, to some extent, both elastic and viscous characteristics (Davis, 1974., Lockett, 1972). Consequently, viscoelastic behaviour covers mechanical properties from ideal elasticity to ideal Newtonian behaviour.

1.2.4 Mechanical Models of Linear Viscoelasticity

Mechanical models can be used to represent the properties of a viscoelastic material. The simplest of these use a Hookean spring combined either in series or in parallel with a Newtonian dashpot. These are the Maxwell and Voigt models respectively. Their properties have been reviewed extensively (see, for example, Costello and Goyan, 1964; Barry, 1974) and will be considered briefly here.

1.2.4.1 The Maxwell Model

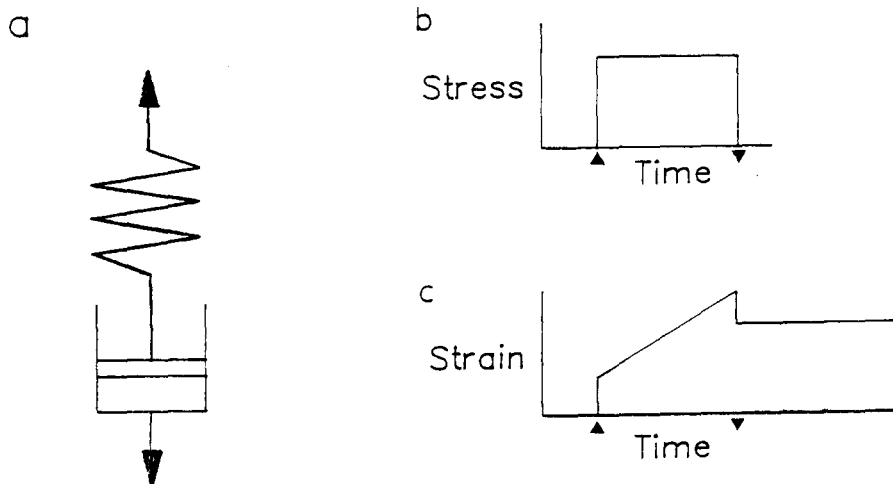
The Maxwell model, shown in Fig. 1.3, consists of a Hookean spring in series with a Newtonian viscous dashpot. The strain response with time to an applied stress reflects both viscous and elastic contributions to the resultant deformation. On application of the stress there is an instantaneous increase in strain associated with the deformation of the spring. This is followed by a linear increase in strain due to the movement of the piston of the Newtonian dashpot. On removal of the stress the elastic strain alone is recovered.

Under an applied external force the stress in the spring is equal to that in the dashpot. The total strain (ϵ) in the Maxwell model is the sum of the strains in the spring (ϵ_s) and in the dashpot (ϵ_v):

$$\epsilon = \epsilon_s + \epsilon_v \quad (1.3)$$

By convention viscoelastic deformations are studied by calculating the compliance (J) defined as the strain divided by the applied stress rather than strain itself. This has the advantage of allowing the comparison of data obtained under different stress conditions.

Figure 1.3 The Maxwell Model



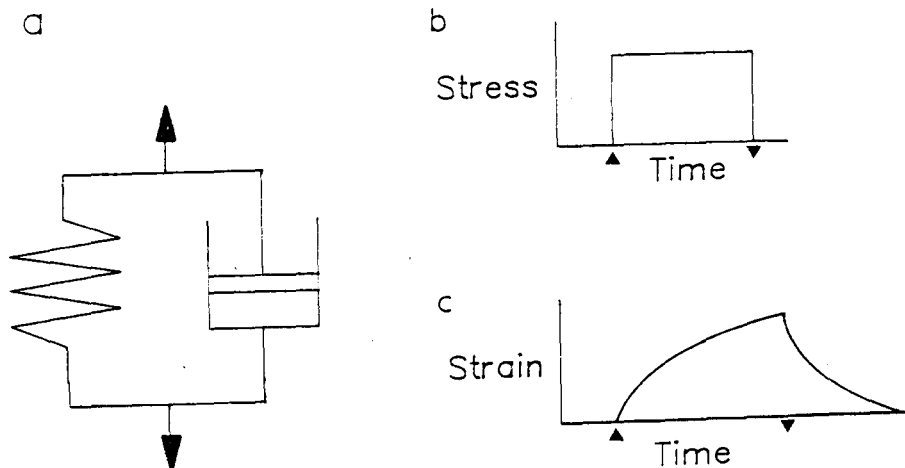
- a Mechanical Model
- b Stress vs. Time
- c Strain vs. Time

If the Maxwell model is maintained under conditions of constant strain the initial stress in the Hookean spring will be reduced by a viscous deformation in the dashpot until the stress decays to zero. This phenomena is termed stress relaxation. Measurement of stress relaxation, therefore, provides a quantitative measurement of the ability of a material to undergo plastic, non-recoverable deformation.

1.2.4.2 The Voigt Model

The Voigt model (also described as the Kelvin model) shown in Fig. 1.4, consists of a Hookean spring in parallel with a Newtonian dashpot. This provides a mechanical analogy for a material in which the response to an applied stress is not instantaneous but is retarded by viscous resistance. Removal of the stress results in a similarly retarded, but total, recovery of the strain. The Voigt model therefore exhibits the properties of creep and creep recovery.

Figure 1.4 The Voigt Model



- a Mechanical Model
- b Stress vs Time
- c Strain vs. Time



IMAGING SERVICES NORTH

Boston Spa, Wetherby
West Yorkshire, LS23 7BQ
www.bl.uk

BEST COPY AVAILABLE.

VARIABLE PRINT QUALITY

The change in strain with time is exponential and the greater the apparent viscosity of the Newtonian dashpot the greater will be the retardation. In the Voigt model, on application of an external force, the strain at any time (t) in the spring is equal to that in the dashpot and the total stress (σ_T) is the sum of the stresses in the spring (σ_s) and in the dashpot (σ_d):

$$\sigma_T = G.E(t) + \eta E'(t) \quad (1.4)$$

The Voigt model is capable of dissipating energy, a phenomenon known as internal friction. This parameter has dimensions of viscosity and may be regarded as the apparent viscosity (η) of the Newtonian dashpot. G is the rigidity modulus of the Hookean spring. Unlike the Maxwell model, the Voigt model is incapable of stress relaxation. The quantity (η)/G is the retardation time (τ) for the unit, that is the time required for strain to relax to 1/e of its initial value on removal of the stress. The retardation time is short and strain recovery is rapid where the internal friction is small compared with the rigidity modulus.

In a real material there exists a number of molecular interactions resulting in more than one retardation time. The viscoelastic behaviour of such materials can be represented by the generalised Voigt model consisting of n Voigt units in series, where n is the number of discrete retardation times. For a viscoelastic solid exhibiting limited recoverable flow the generalised Voigt model applies.

If equation 1.4 is rearranged to include the retardation time, then integration without limits for the ith. element gives equation 1.5.

$$-\ln(\sigma_i/G_i - E_i) = t/\tau_i + k_i \quad (1.5)$$

when time t = 0, strain $E_i = 0$ then $k_i = -\ln(\sigma_i/J_i)$ and

$$\ln[(\sigma_i/J_i - E_i)/G_i/J_i] = -t/\tau_i \quad (1.6)$$

Thus, the strain in the ith element is:

$$\epsilon_i = \sigma_i J_i [1 - \exp(-t/\tau_i)] \quad (1.7)$$

In terms of compliance then:

$$J_i(t) = J_i [1 - \exp(-t/\tau_i)] \quad (1.8)$$

The total strain $\epsilon(t)$ in the generalised Voigt model is the sum of the strains in the individual elements, and thus compliances in series are additive. For the case of n Voigt units in series:

$$J(t) = \sum_{i=1}^n J_i [1 - \exp(-t/\tau_i)] \quad (1.9)$$

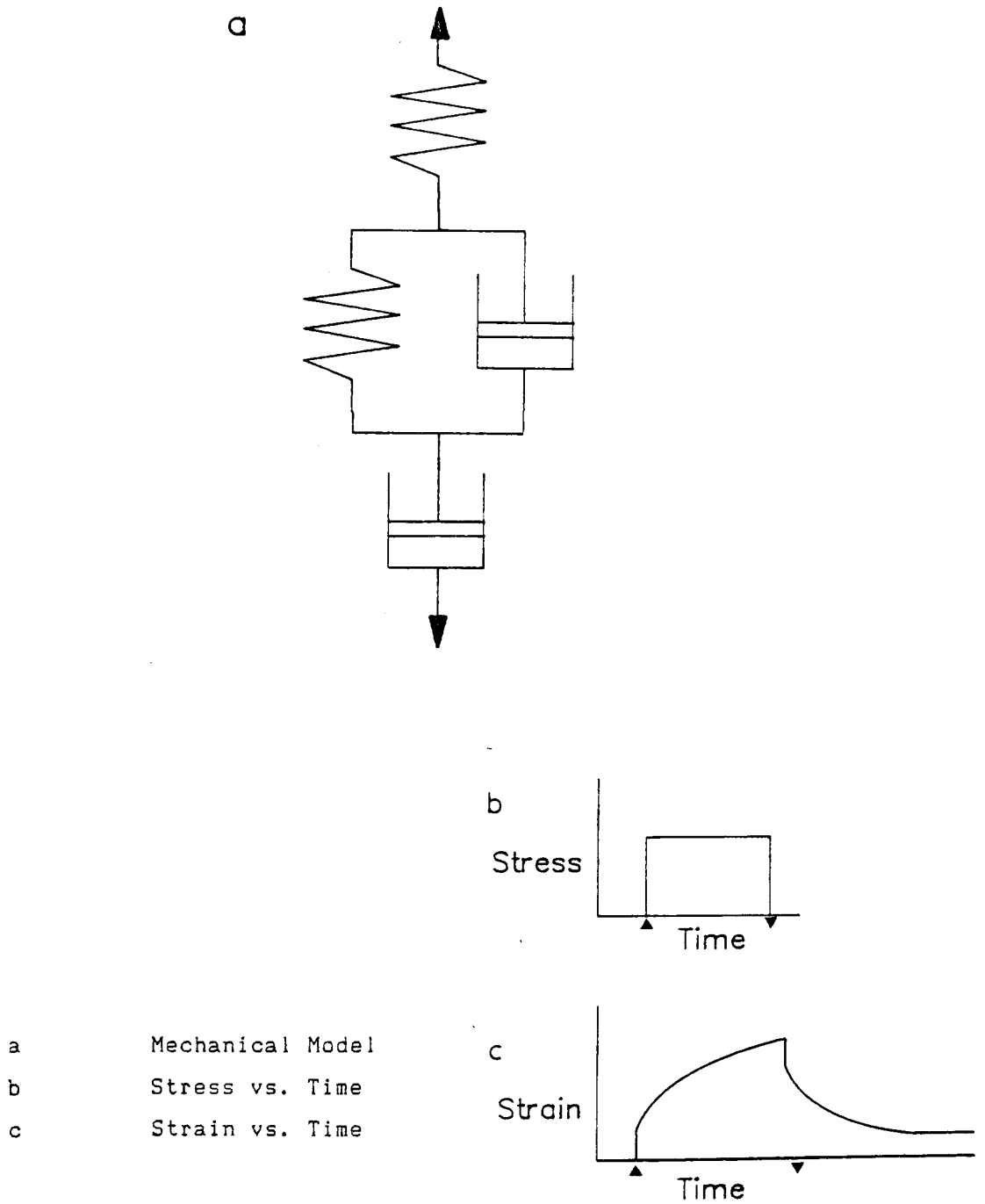
1.2.4.3 Generalised Linear Viscoelasticity

By combining a Maxwell model in series with one or more Voigt units (Fig. 1.5) a generalised model for linear viscoelastic behaviour is obtained. The strain response with time under an applied stress is represented by a plot of compliance $J(t)$ against time t and is termed a creep curve. A typical curve can be rationalised into three distinct regions. The instantaneous response and the late linear region can be represented, respectively, by the Hookean spring and the Newtonian dashpot of the Maxwell model. The intermediate curved zone can be modelled by the retarded elastic Voigt unit. An equation for the overall compliance at any time can be derived to include the contribution from each region:

$$J(t) = J_0 + \sum_{i=1}^n J_i [1 - \exp(-t/\tau_i)] + t/\eta_0 \quad (1.10)$$

where (J_0) is the instantaneous creep compliance and (η_0) is the apparent Newtonian viscosity of the late linear region. Complex viscoelastic behaviour may require more than one Voigt unit to accurately model the observed properties. The middle term of equation (1.10) will then be a summation of the contributions due to each discrete Voigt unit.

Figure 1.5 . The Generalised Model for Linear Viscoelasticity



A necessary characteristic of a linear viscoelastic material is that it obeys the Boltzmann superposition principle. Briefly, this states that if a material is subjected to a series of stresses, the total strain observed will be a linear superposition of the strain contribution for each stress over the elapsed time of stress application. The validity of this principle for polymeric systems has generally been assumed (Ferry, 1961).

1.3 Evaluation of Material Behaviour during the Compression Process

Bonding between materials subjected to dry compaction may occur as a result of plastic deformation, brittle failure, physical interlocking and also molecular diffusion, sintering or asperity melting. The process of consolidation and compact formation for a compressed powder is complex since one or more mechanisms may be involved, either simultaneously or sequentially. The two extreme types of non-recoverable deformation may be distinguished as brittle failure or plasticity. Additionally, some strain may be recovered on removal of the compressive stress, either as instantaneous (ideal) elasticity or as time-dependent viscoelasticity. Elastic strain recovery may result in a de-bonding effect. The properties of a formed compact are not, therefore, uniquely dependent on a single mode of deformation but are a result of the relative contributions of both bonding and de-bonding processes. The dominant mechanism of deformation during compression may also depend on factors such as the temperature (Britten and Pilpel, 1978) and punch strain rate or velocity (Roberts and Rowe, 1985, 1986a and 1986b; Armstrong, 1990). Binding agents incorporated into a powder by wet-massed granulation may modify the relative amounts of each type of deformation during compression.

A number of techniques have been used to characterise modes of deformation and to investigate the influence of inclusion of a binding agent. The potential for modern instrumental methods of compression analysis have been extensively reviewed (Marshall, 1989; Celik and Marshall, 1989; Doelker, 1989).

1.3.1 Brittle Failure and Brittle Fracture Propensity

Brittle failure is exhibited by materials which break only under a supra-elastic stress and is characterised by the rapid propagation of a crack under an applied stress. Griffith (1920) assumed the presence of sub-microscopic cracks in a material, which concentrate the applied stress at their tips. He suggested that, for crack propagation to occur, the release of stored elastic strain energy must be greater than the surface energy of the material (defined as the energy required to create a new surface of unit area).

Hardman and Lilley (1970) and Hersey et al. (1973) reported that lactose, dicalcium phosphate dihydrate and sucrose were fragmented during the compression process. Hiestand et al. (1977) proposed the concept of a Brittle Fracture Propensity (BFP) to quantify the tendency of materials to laminate during ejection. The method involved determining the tensile strength of compacts prepared both with and without a stress-concentrating flaw (a hole passing axially through the centre of the compact). BFP was then defined by:

$$\text{BFP} = 0.5 ([\sigma_r / \sigma_{r_0}] - 1) \quad (1.11)$$

where σ_{r_0} and σ_r were the tensile strengths of the unflawed and flawed compacts respectively.

A low BFP index indicates the ability of a material to relieve localised stresses by plastic flow. A high value for the BFP index (tending to unity) indicates a brittle material, unable to relieve stress by plastic flow and with a resultant tendency to laminate. Experimental results were reported for a range of materials. Those known to induce capping (methenamine, erythromycin base and ibuprofen) exhibited large values for BFP whereas relatively plastic materials (pregelatinised starch, spray-dried lactose and microcrystalline cellulose) had low values for BFP.

Roberts and Rowe (1986a) used a compaction simulator to evaluate BFP for "tablet-sized" cylindrical compacts of microcrystalline cellulose, Tablettose (a spray-dried lactose) and heavy magnesium carbonate. The results obtained were in good agreement with those of the earlier workers. An interesting feature of the results of Roberts and Rowe (1986a), was the increase in BFP as the upper punch velocity was increased from 3.33mm s^{-1} to 200mm s^{-1} , particularly for brittle materials such as Tablettose (a spray-dried lactose) and heavy magnesium carbonate. They considered that this may be due to an increase in the modulus of the compact. They concluded that strain rate sensitivity might provide an indication of the stress relieving ability of materials, particularly since there was little change in BFP with punch velocity for relatively plastic materials like microcrystalline cellulose. Rees (1980) had emphasised that the strength of a perfectly elastic-brittle particle shows no rate

dependence in contrast to a viscoelastic particle capable of plastic flow. Roberts and Rowe (1985, 1986) observed that consolidation of materials, such as in organic minerals, deforming by brittle fracture was independent of strain rate. The consolidation of more plastic materials, such as Avicel PH 101, maize starch and sodium chloride, was highly strain rate dependent, however.

Church and Kennerley (1984) used a four-point bending test to characterise mechanical properties of preformed compacts for a number of direct compression excipients. The stress-strain curves they obtained showed that brittle behaviour occurred irrespective of whether the material consolidated by plastic flow or fragmentation. Both the mean tensile fracture stress and the modulus of elasticity were dependent on the bonds formed during compaction, and increased with greater consolidation. As it was unlikely that compaction would affect the stiffness of the primary particles, they suggested that the modulus of elasticity for a compacted material was a function of the stiffness of the material and the extent of inter-particulate bonding.

1.3.2 Densification and Pressure-Volume Relationship

During the tableting cycle a compressive stress is applied to a loosely packed powder or granule bed resulting in volume reduction and densification of the bed. Several mechanisms of densification may operate concurrently and therefore no simple model exists to relate volume reduction and densification to the applied load. Train (1956, 1957) investigated the effect of compressive pressure on the relative volume of magnesium carbonate. He proposed that consolidation proceeded via four sequential and distinct stages, i.e initial particle rearrangement, frictional resistance to further rearrangement, plastic flow and/or crushing of particles and rebonding of particles. Train did not consider the possibility of elastic deformation in the formed compact itself.

The transmission of force through a powder bed is complex so that different pressures and densities may be detected at different positions (Train, 1957). Anomalies of force transmission may arise from the nature of the equipment used and due to the mobilisation of wall effects (Shaxby and Evans, 1923). Despite this, several useful

empirical relationships have been derived relating bed density or porosity to the applied compressive stress including those of Walker, 1923; Balshin, 1938; Cooper and Eaton, 1962 and Heckel 1961a,b.

1.3.2.1 The Heckel Equation

The equation proposed by Heckel (1961a,b) has found wide application in the study of the consolidation of pharmaceutical powder blends. He considered that the reduction of porosity with applied pressure was analogous to a first-order reaction, in which pores were considered as the reactant and the compact as the product. Expressed mathematically:

$$\ln (1 / 1-D) = K_H P + A_H \quad (1.12)$$

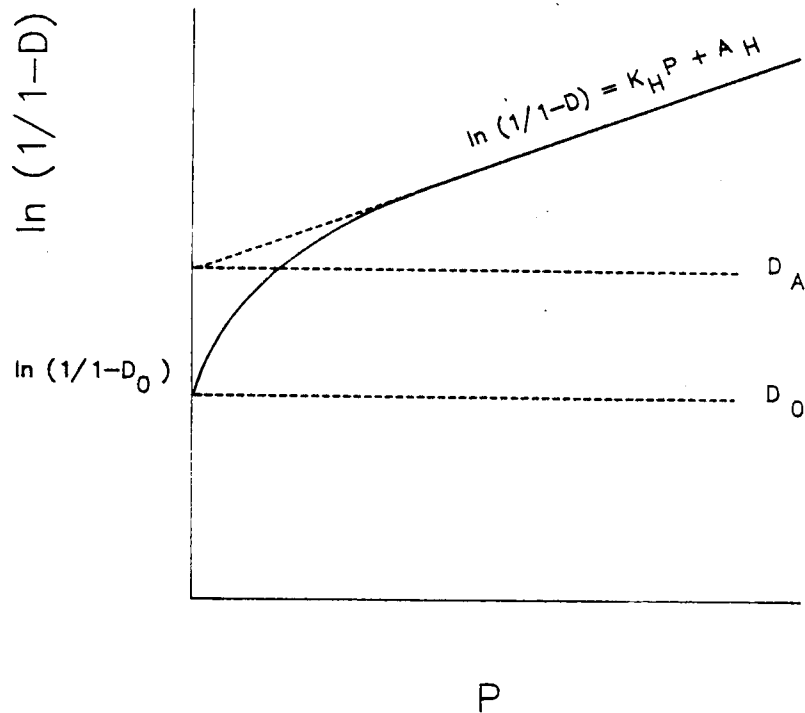
where (D) is the relative density of the compact at any applied pressure (P). The constants K_H and A_H are determined from the slope and intercept respectively of the linear portion of a plot of $\ln (1/1-D)$ against P. The intercept A_H defines two parameters. Firstly, the relative density of the material at zero pressure, expressed as $\ln (1-1/D_0)$, where D_0 is the relative density of the loose packed powder bed. Secondly, densification by movement and rearrangement of individual particles at low pressures before the occurrence of significant interparticulate bonding. This may be represented by B_H so that $A_H = \ln (1 / 1-D_0) + B_H$. The relative density contributions of the above equations are given by $D_A = D_0 + D_B$ and D_A is obtained from $A_H = \ln (1 / 1-D_A)$. D_B , which represents the density contribution from movement and rearrangement of discrete particles may be calculated where D_0 is known from experimentation. The derivation of Heckel parameters is shown in Fig. 1.6.

K_H , the slope, was considered to be an index of the ability of the compact to deform plastically and has been related to the yield strength (Y) of the material by the expression :

$$K_H = 1/3 Y \quad (\text{Heckel, 1961b}) \quad (1.13)$$

Hersey and Rees (1970) defined a yield pressure (P_Y) as the reciprocal of K_H .

Figure 1.6

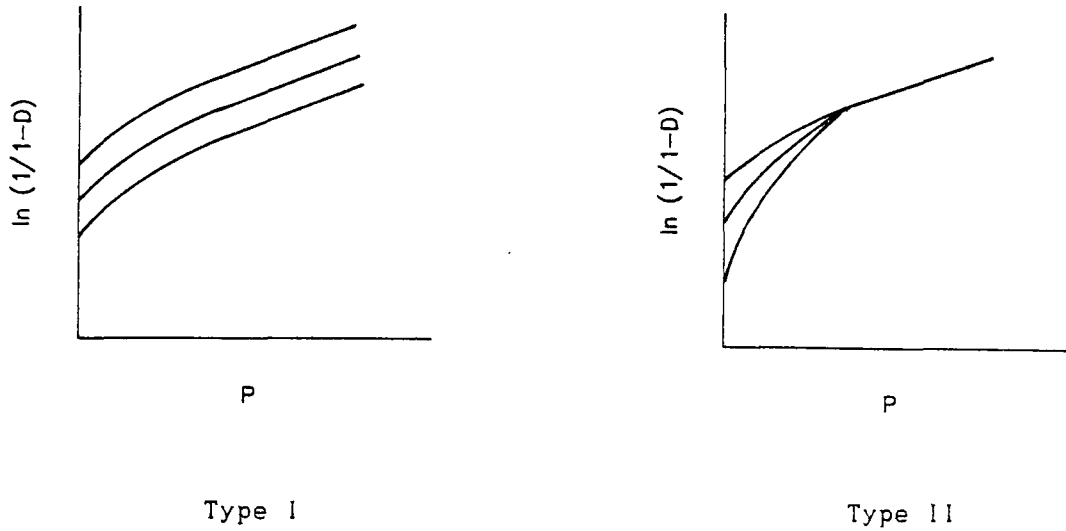
Derivation of Heckel Parameters

$$D_B = D_A - D_0$$

$$B_H = A_H - \ln(1/(1-D_0))$$

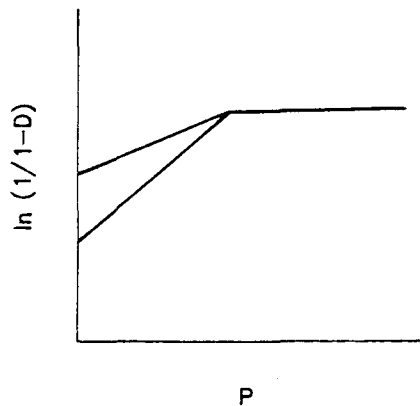
The value of the Heckel relationship lies in the fact that information may be gained both about the mechanisms of consolidation and about the apparent yield pressure of the materials examined. Hersey and Rees (1970, 1971) used the Heckel equation to investigate the consolidation of different particle size fractions of sodium chloride and lactose powders. Heckel plots were shown to be sufficiently sensitive to differentiate consolidation by plastic flow in sodium chloride and brittle failure in lactose. Two forms of the Heckel plot were subsequently proposed (Fig.1.7). Type I plots are obtained for different particle size fractions of a material which consolidates primarily by plastic flow. Variation in the initial bed density results in different final bed densities at equivalent applied pressures. Type II behaviour is shown for materials consolidating by particle fragmentation. Particle size dependence of the form of the Heckel plot occurs at low pressures only. Above a certain pressure a single relationship exists which is independent of the initial particle size and bed density. This is due to progressive fragmentation and subsequent consolidation at high pressures by plastic flow.

Figure 1.7 Forms of the Heckel Plot
 (after Hersey and Rees, 1970, 1971)



York and Pilpel (1973), in a study of the compression of some fatty acids, demonstrated the existence of another form of the Heckel plot (Fig. 1.8). The linearity of the plot at low pressures was considered to be due to the absence of an initial particulate rearrangement stage. Densification was attributed to plastic deformation and possibly asperity melting.

Figure 1.8 The Type III Form of the Heckel Plot
 (after York and Pilpel, 1973)



1.3.2.2 Applications of Pressure-Volume Relationships

Qualitative agreement between the Heckel approach to consolidation data and the Cooper and Eaton approach has been shown both for the compression behaviour of simple pharmaceutical powders (Chowan and Chow, 1980) and granulates prepared with different binders (Chowan and Chow, 1981a). Malamataris and Pilpel (1983) had concluded that the Cooper and Eaton equation was insufficiently sensitive to discriminate between different consolidation mechanisms during powder compression. Kurup and Pilpel (1978) found that the Heckel equation was more discriminating in the evaluation of the effects of excipients on the consolidation of griseofulvin/excipient blends. Similarly, Armstrong and Morton (1979) concluded that the Cooper and Eaton equation was of little value in differentiating the compression behaviour of magnesium carbonate granulated with different binding agents.

Nelson et al., (1957), investigating the influence of binder type and concentration on the compressibility of sulphathiazole granulates, showed that increasing binder concentration resulted in a reduced compact volume for equal applied pressure. Several workers have reported a decrease in yield pressure, evidenced by an increase in slope for the linear portion of the Heckel plot, as the binder concentration in a formulation was increased (Kurup and Pilpel, 1978; Armstrong and Morton, 1979; Jarosz and Parrott, 1982). In contrast, Esezobo and Pilpel (1977a) reported an increase in yield pressure for oxytetracycline granulates with increasing gelatin content, indicating an increased resistance to deformation.

Several workers have used parameters derived from the Heckel plot to investigate the effect of binder type on granule compressibility. Chowan and Chow (1981a) studied the effect of five binders on the compression behaviour of a model drug/lactose granulate. The Heckel plots indicated that among the binders studied, the sucrose granulate was the most readily compressible and the pregelatinised starch granulate was relatively less readily compressible. Plots obtained, however, deviated from ideal Heckel behaviour and exhibited a biphasic linearity. This was attributed to free moisture in the granulates which would constitute hydrodynamic resistance to consolidation at high compaction pressures whilst acting as a lubricant between the

die, punches and the compact. Armstrong and Morton (1979) demonstrated that the decrease in yield pressure with increased binder level was dependent on the type of binder. With magnesium carbonate granulates, they reported little increase in plasticity as the concentration of wheat starch or PVP was raised from 2%w/w to 4%w/w. In contrast, increasing the concentration of PEG 4000 or acacia significantly increased granule plasticity. Cutt (1983), using glass ballotini as a model non-plastic substrate, confirmed that increased polymeric binder concentration conferred increased granule plasticity and compressibility.

Several studies (Chowan and Chow, 1981b; Cutt, 1983; Reading and Spring, 1984a) have demonstrated that effect of polymeric binders on consolidation is dependent on their moisture content. Chowan and Chow (1981b) suggested that, at lower compaction pressures, higher moisture-containing granules were more compressible than lower moisture-containing granules. At higher compaction pressures, the reverse appeared to be true, due to the incompressibility of free water. The Heckel plots, therefore, exhibited a biphasic linearity. Similar results have been reported for the consolidation of milled polymeric binder films (Reading and Spring, 1983) and for the consolidation of binders used as received (Cutt, 1983). Reading and Spring (1983) concluded that, for hydrophilic polymeric binders, moisture may act as a plasticizer at low pressures and as an incompressible lubricant at higher pressures. In contrast, Cutt (1983) did not observe biphasic linearity for glass ballotini granulates compressed with binders of different moisture contents. Increased moisture contents did, however, increase the plasticity and compressibility of the granules, the magnitude of the effect being dependent on the relative hygroscopicity of the binders.

The use of Heckel plots for the evaluation of tablet binder performance may lead to erroneous conclusions unless other factors, i.e. moisture content, contact time (Rees and Rue, 1978) or strain-rate sensitivity (Celik, 1984; Roberts and Rowe, 1985, 1986b) are also considered.

1.3.3 Stress-Relaxation

Stress-relaxation, pioneered as a tool for tableting studies by Shlanta and Milosovich (1964), has been used to evaluate plastic flow during the compression process. The technique involves subjecting the test material to a sudden (ideally instantaneous) compressive stress. The strain is held constant while any resulting decay in axial stress is monitored with time. Cole et al., (1975) monitored stress decay under load for sodium chloride and potassium chloride and were able to demonstrate the occurrence of post-compression plastic flow. David and Augstberger (1977) used a stress-relaxation technique to study the extent of plastic flow in a number of direct compression bases. For materials which were found to deform plastically, an interdependence between the mechanical strength of the tablets formed and the degree of plastic flow was shown. The importance of contact time in determining the strength of tablets formed from plastically flowing materials was shown.

One disadvantage of the technique is the difficulty which exists in quantifying the rate and extent of stress-relaxation. David and Augstberger (1977) considered stress-relaxation phenomena to be analogous to the response of a discrete Maxwell unit under constant strain. The combination of an elastic parameter in series with a viscous parameter leads to the derivation of the following equation:

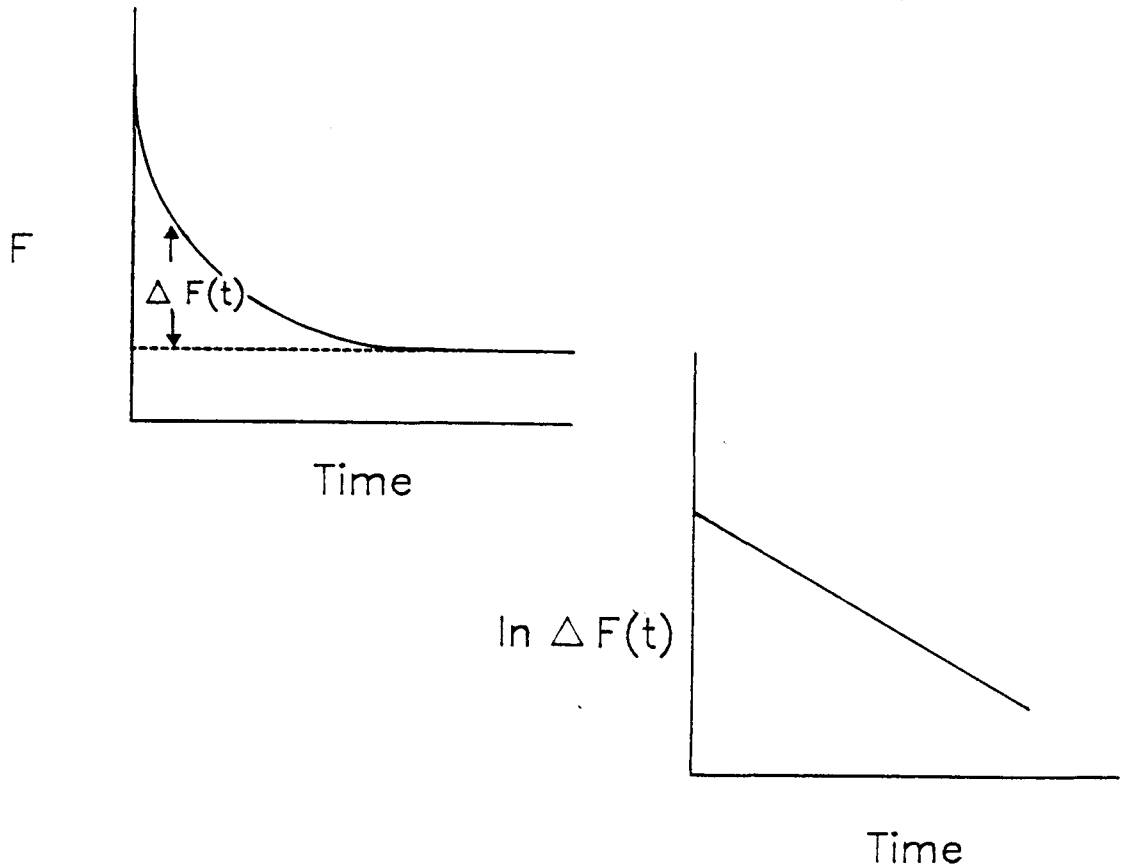
$$\ln \Delta F = \ln F_0 - kt \quad (1.14)$$

where (ΔF) is the force left in the viscoelastic region at time t , (F_0) is the initial applied force at time zero and k is the slope (viscoelastic decay rate constant). The approach is illustrated in Fig. 1.9. The constant (k) and (ΔF) are directly related to the rate and the extent of plastic flow respectively, exhibited by a compact under constant strain.

A study of the time-dependent deformation properties of direct compression excipients carried out by Rees and Rue (1978) contradicted many of the findings of David and Augstberger (1977). Unlike the earlier workers, Rees and Rue demonstrated that stress-relaxation continued for periods much greater than 10 seconds and also that

Figure 1.9

Analysis of Stress Relaxation Data
(after David and Augstberger, 1977)



dicalcium phosphate dihydrate, Sta-Rx, and Elcema did not behave as a single Maxwell unit but instead showed a spectrum of retardation times. The differences observed may be accounted for by considering the strain conditions prevailing during relaxation. Rees and Rue (1978) measured stress-relaxation under conditions approximating to constant strain. In contrast, David and Augstberger (1977) used a rotary tablet press in which near constant stress conditions would prevail at maximum compaction force due to the elastic recovery of the lower compression roller overload spring.

Hiestand et al., (1977) demonstrated that materials prone to capping exhibited slower and reduced stress-relaxation. The analysis of stress-relaxation they used involved plotting the residual stress against the logarithm of time. This has advantages in that the early portion of the time scale (arguably the most significant with regard to capping or lamination) is expanded and there is no implicit assumption that the compressed material can be characterised by a

single retardation time.

Rue et al. (1980) used stress-relaxation as a criterion to demonstrate the greater plasticity of sprayed dried granules compared with those prepared by either wet-massing or roller compaction. They suggested that this plasticity facilitated the formation of greater areas of intergranular contact during compaction, hence tablets formed from spray-dried granulates exhibited greater tensile strength than tablets formed from the other granulates. They also showed that for wet-massed granulates of paracetamol increased binder levels reduced capping tendency, either by reducing the elastic deformation of paracetamol crystals or by accommodating post-compression elastic recovery by plastic flow of the binder.

Cutt (1983) used stress-relaxation to characterise the deformation of powdered polymeric tablet binders and model granulations of glass ballotini. The results showed that increased moisture content of the binders increased plastic deformation both in the binders alone and in the model granulations. The extent of stress-relaxation was shown to be dependent on the compact porosity and, for plastic binders, this was a function both of the rate of compression and the maximum applied load. For highly plastic materials considerable deformation occurred during the initial application of load resulting in a paradoxical reduction in stress-relaxation on maintaining constant strain. Huckle (1986) confirmed the dependence of observed stress-relaxation on the compaction rate for direct compression bases (such as Avicel) consolidating by predominantly plastic flow. The stress-relaxation of materials such as dicalcium phosphate and paracetamol, consolidating primarily by brittle fracture, showed little dependence on the initial compaction rate. Cooke and Summers (1986) demonstrated that the maximum compaction load applied also affected the subsequent relaxation phenomena.

Casahoursat et al., (1988) used a Wischert model (a Hookean spring in parallel with two or more Voigt units) to linearise and characterise the stress-relaxation of a number of excipients. The fundamental validity of this approach must be questioned, however, since it implies the characteristic of retarded elasticity rather than plasticity.

1.3.4 Radial Versus Axial Pressure Cycles

In general, a stress applied to one part of a body will be transmitted to some degree to another part. The stress transmission may be resolved into two components, an axial (normal) component and a radial (shear) stress. Examination of axial to radial stress transmission during the tablet compression cycle allows quantitative evaluation of a number of fundamental material properties. The value of compaction profiles in the study of compression phenomena was first noted for ideal non-porous plugs by Long (1960). In his work it was assumed that the die was perfectly rigid, that there was no die wall friction, and the compact behaved as an ideal elastic body. When axial stress is applied the transmitted radial stress is of the same order of magnitude and the relationship is:

$$F_R = \pi F_A \quad (1.15)$$

where (F_A) is the applied axial pressure, (F_R) is the transmitted radial pressure and (π) is the Poisson ratio.

Compression cycles for anisotropic powder or granular systems usually exhibit hysteresis depending on the relative amount of plastic and elastic deformation occurring. Materials deforming predominantly by plastic flow frequently show a cycle characteristic of a constant yield stress in shear. A second type of cycle exists where the yield stress in shear is a function of the normal stress in the plane of shear. This is characteristic of a Mohr body and often obtained for materials consolidating through brittle fracture.

Leigh et al., (1967) observed that the compression cycle of paracetamol (granulated without a binder) resembled that of a Mohr body and the resultant compacts both laminated and capped. Granulation with a binder (PVP) resulted in a compression cycle characteristic of a body with constant yield stress in shear, with the elimination of lamination. They suggested that the use of compression cycles may discriminate between materials which form satisfactory tablets and those which do not. Similar results were obtained by Carless and Leigh (1974) also using paracetamol granulated with PVP.

Shotton and Obiorah (1975) showed that the compression cycle of crystalline paracetamol was characteristically elastic unlike that of Paracetamol DC (a commercial direct compression formulation containing gelatin hydrolysate as a binder). The elimination of paracetamol capping by the presence of a binder was associated with an increase in residual die wall pressure (RDWP) and a decrease in elastic recovery during decompression. Krycer et al., (1982c) substantiated this although they demonstrated that capping tendency could not be predicted solely on the basis of the RDWP. A capping index (CI), defined as the gradient of a plot of elastic recovery against RDWP, proved more useful to quantify capping tendency than RDWP alone.

The results of Obiorah and Shotton (1976) contrast with other studies on the influence of binders on the nature of compression cycles. Both paracetamol (which tended to cap) and paracetamol mixed with a gelatin hydrolysate or with water (which did not cap) exhibited compression cycles characteristic of a Mohr body. RDWP appeared, in this study, to be a better discriminator of capping tendency than any other parameter of the compression cycle. Armstrong et al., (1977) found that for ungranulated dibasic calcium phosphate or dibasic calcium phosphate granulated with a range of binders, the compression cycles resembled those of a Mohr body. The presence of a binder induced plasticity, resulting in a lower yield pressure and greater stress transmission to the die wall at pressures above the yield.

Doelker and Shotton (1977) related the mechanical properties of paracetamol and dicalcium phosphate granules prepared with different binders to their characteristic compression cycles. The crushing strength of tablets prepared from the granules was also measured and found to be dependent on the plastic deformation and fracture of the initial granules. For dicalcium phosphate tablets, the rank order for crushing strength reflected the granule strength. With paracetamol, however, the increase in bonding surface on compression reversed binder mediated effects. The weakest granules (in both cases those containing PVP) consequently produced the weakest tablets of dicalcium phosphate and the strongest tablets of paracetamol. Thus, a good conversion of axial to radial pressure was demonstrated not to be the major factor in producing compacts of high strength. The generated contact area was proposed to be a more significant factor.

1.3.5 Work of Compaction

Powders or granules having different size distributions, packing characteristics, and different relative elasticity and plasticity will absorb varying amounts of energy for equal applied compaction pressures. A measurement of the work expended during the compaction of materials can be obtained by examining the relationship between top punch displacement and the force it exerts during uniaxial compression.

de Blaey et al., (1970, 1971, 1972) pioneered the use of a uniaxial double compression technique to evaluate work expended during different stages of compaction and to relate it to tablet properties. The area under the upper punch force-displacement plot, obtained for the uniaxial compression, represents the gross work exerted by the top punch on the material compressed. The upper punch force-decompression plot represents the proportion of the work returned to the punch as a consequence of elastic strain recovery during decompression. The difference between the gross work of compression and the work of expansion represents the total work expended during a single compression-decompression cycle. de Blaey and co-workers noted that the work of expansion may be underestimated if elastic recovery continues after the top punch has lost contact with the compact. The compact is not, therefore, ejected from the die but is subjected to a second compression cycle. Since the maximum force used is the same as that of the initial compression de Blaey and Polderman (1970) assumed that no further plastic deformation would occur. Incomplete resolution of elastic expansion during the first decompression is shown by a larger work of compression for the second cycle compared with the work of expansion during the first decompression. The work required to overcome friction at the die wall can be calculated from the difference between the upper and lower punch forces. This corrected compaction force represents the force transmitted to the lower punch during uniaxial compression. Subtracting this work and the work of expansion yields an overall net work of compaction.

The work carried out on the lower punch during the second compaction, designated LPW2, has been reported to be a measure of the elastic energy recovered by the ascending punch in the first decompression (de

Blaey and Polderman, 1970; de Blaey and Polderman, 1971; de Blaey et al., 1971b). This relies on the assumptions that the compact had fully recovered elastically prior to recompression and that elastic deformation alone occurs during recompression. Krycer et al., (1982a) pointed out that those assumptions may not be strictly applicable in practice. Armstrong et al., (1982) and Jackson et al., (1982) have confirmed that the work expended during the second and subsequent compactions was not just that required to elastically deform the compact. Armstrong et al., (1982) utilised a multiple recompression technique to demonstrate the induction of plasticity in granulates by the incorporation of a binder

De Blaey et al., (1971b) demonstrated differences in the work of compression for some pharmaceuticals with variation of the binder type or granulation technique. Differences were found with respect to the gross work, elastic deformation, net work and tablet properties such as crushing strength, disintegration time and dissolution rate. In common with other workers (Polderman and de Blaey, 1971; Doelker et al., 1980) they showed that for a number of granulations, there was a linear relationship between the net work and radial tablet strength. This relationship failed, however, where capping occurred (de Blaey et al., 1971d).

Armstrong and Morton (1977) used force-displacement curves to study the effects of binder type on the plasticity and elasticity of dicalcium phosphate granulates. They ignored die wall friction and consequently their net work of compaction was calculated simply from the gross work minus the work of elasticity. They noted that the gross work of compression increased with increased binder concentration. They suggested that this was due to an increase in the resistance of the granule to deformation or an increase in the plasticity of the granule. At higher binder concentrations, proportionately more work was used to overcome the resistance to deformation of the granules. The amount of work contributing to tablet strength, therefore, remained relatively low. By calculating the ratio of net work to gross work expressed as a percentage at some arbitrary compression force, it was possible to identify the proportion of the total work that contributed to tablet strength. The results indicated that, for dicalcium phosphate granules at low binder concentrations,

starch, gelatin and methylcellulose were more effective in inducing plasticity than PVP, acacia or PEG 4000. Doelker et al., (1980); in contrast, observed that this plasticity ratio was incapable of differentiating between binder types. The ratio was increased, however, for dicalcium phosphate and paracetamol by the inclusion of a binding agent.

Upper punch force-displacement curves have also contributed to an understanding of capping phenomena. De Blaey et al., (1971c) found that the strength of compacts formed from phenacetin granulates increased with compression force until a critical force was reached. Above this critical force, which was characteristic for every granulation, the compact strength fell again. The magnitude of the critical force was influenced both by granule size and by the moisture content of the granulate. Smaller granules were better able to withstand post-compression elastic recovery, resulting in stronger tablets. Higher moisture contents in the granules caused the formation of stronger structures, although with a lower net work expenditure (de Blaey et al., 1971c, 1971d). This factor was more significant in determining the strength of the resultant compacts than was the coincident increase in elastic deformation.

Ragnarsson and Sjorgren (1985) commented that, to be able to characterise inherent deformation properties of a material using force-displacement measurements, the measurement should be unaffected by particle interactions, i.e. friction and bonding. They showed however, that unlike yield pressures derived from Heckel plots, the net work of compaction was significantly affected by particle interactions. They concluded that, although the net work of compaction might be useful as a test of inter-lot variations in compaction behaviour of materials, it was a poor measure of the plasticity of a material. In contrast, yield pressure appeared to be a more useful parameter for the evaluation of deformation properties.

1.3.6 Power

Armstrong et al., (1983) attempted to measure the power expended in the process of compression. Power consumption during the tableting process, defined as the energy expended in unit time, can be derived

in two ways. Firstly, from the area under the compression force-displacement curve (i.e. the work of compaction) divided by the time over which the force is applied. Secondly, from the applied punch force multiplied by the punch velocity at the time that force is being applied (Armstrong and Palfreyman, 1987). Armstrong (1990) suggested that the value of power determination lay in the fact that this technique alone takes into account the role that time can play in the compression process. This may not be strictly true, in view of the potential to determine apparent plastic viscosities of compressed materials by creep rheological methods (section 1.3.9).

In spite of the potential for highlighting difficulties caused by artificially long compaction times or for comparison of different types of tablet press (Armstrong, 1989), little attention has been paid to power as a compression parameter.

1.3.7 Elastic Deformation

Fell and Newton (1971) and more recently Paronen (1986) have shown that elastic deformations of a compact under load may influence the form and interpretation of the Heckel plot. Of greater practical relevance is the potentially disruptive effect of elastic strain recovery during the decompression phase of the compression cycle. The extent of de-bonding which may ensue, has been implicated by many workers as a major factor in the manifestation of capping or lamination (see, for example, Ritter and Sucker, 1980; Mann, 1984; Fassihi and Parker, 1986). In addition, slower viscoelastic recovery may also occur.

1.3.7.1 Elastic Strain Recovery

Besides the questionable use of LPW2 (defined in section 1.3.5) there are other methods available which quantify the extent of elastic strain undergone by a compact during compression. Various workers (Armstrong and Haines-Nutt, 1972, 1974; Carless and Leigh, 1974; York and Baily, 1977; Krycer et al., 1982b) have used the percentage elastic recovery (E) defined as:

$$E = (H - H_c) / H_c \times 100 \quad (1.16)$$

where (H) and (H_c) are the compact height under load and after ejection from the die respectively.

Travers et al., (1983) have shown that the axial elastic strain recovery occurs very rapidly within the die immediately stress is removed. Since compact expansions have been measured at varying times after ejection they may therefore include viscoelastic strain recovery as well as the ideally instantaneous elastic response. For instance, Krycer et al., (1982b) measured the ejected compact height after twenty-four hours, whereas Carless and Leigh (1974) and York and Baily (1977) measured the height immediately after ejection. Marshall et al., (1986) demonstrated that the axial strain recovery in ibuprofen compacts (measured two hours after compression) was dependent on the duration of the compression cycle. An increase in the duration of the compression cycle from one to ten seconds resulted in a decrease in the total strain recovery at all compaction pressures studied. They concluded that consolidation (of ibuprofen) was a balance between elastic deformation and time-dependent plasticity. Although percentage elastic recovery may not provide a direct measurement of elastic deformation, it has proved useful to quantify the disruptive effects of elastic deformation. Summers et al., (1977) employed an elastic modulus, which, like LPW2 relied on the assumption that no plastic deformation occurred on recompression of the compact.

1.3.7.2 The Poisson Ratio

The Poisson ratio (π), calculated from radial versus axial pressure cycles, has also been used to measure the ability of materials to deform elastically (Long, 1960; Leigh et al., 1967; Summers et al., 1976). However, Poisson ratios are, in actuality, strain ratios in stressed isotropic materials and may not be identical to stress ratios in powdered or granular materials which may behave anisotropically when subjected to uniaxial compression.

1.3.7.3 Surface Areas

A further insight into the elastic strain during compression has been afforded by investigations into changes in surface area during compaction. During the compaction process the overall surface area of

the consolidating mass changes due to plastic deformation or fracture of the base particles (Stanley-Wood and Shubair, 1979; 1980). Initially the specific surface rises with compaction pressure as fracture and plastic flow generate new surface. The fall in surface which follows, at higher pressures, is associated with recombination of particles. A second increase in surface area observed at much higher compaction pressures is due to disruptive elastic recovery on decompression.

Armstrong and Haines-Nutt (1974) showed that the presence of a starch binder reduced elastic recovery on decompression and eliminated the second rise in specific surface area for magnesium carbonate and for phenacetin. The strength of the compacts was correspondingly increased. Morton (1977) also showed the elimination of the second rise in the specific surface-area compression profile for magnesium carbonate granulated with wheat starch. In contrast with the previous workers, however, post-compression elastic recovery was not reduced although compact strength was increased. In the latter work, the binder was observed to accommodate post-compression strain recovery without apparent bond disruption.

1.3.8 Plasticity-Elasticity Indices

From preceding sections, it is clear that the mechanical properties of a compression-formed compact will be dependent on the relative extent of bonding (non-recoverable or plastic) deformation and de-bonding (elastic) deformation. The Brittle Fracture Propensity, discussed previously in section 1.3.1, was an example of this type of approach. Aulton and Tebby (1977) showed that the ratio of penetration distance to relaxation distance, determined from indentation testing on pre-formed compacts, was a simple but useful means of differentiating "good" and "poor" tableting materials. Since then, other workers have attempted to quantify the relative contribution of different deformations in the form of plasticity-elasticity indices and to use the resultant parameters to interpret compaction behavior. The capping index of Krycer et al., (1982b) is one example of this type of approach. Hiestand and Smith (1984) used dynamic indentation hardness measurements on compacts to define a bonding index (BI) and a strain index (SI). These were proposed to

characterise the post-compression bonding area and the relative strain that could develop during elastic recovery, respectively.

Celik and Travers (1984) proposed an alternative parameter to predict the compressional behaviour of materials and to measure the disruptive effects of elastic expansion. This parameter is the Elastic Recovery Index (ERI) defined by:

$$\text{ERI} = \text{ER}/\text{SM} \quad (1.17)$$

where (ER) is the elastic recovery of the compact during decompression (corrected for punch recovery) and (SM) is the strain movement of the compact held under a constant stress. Under identical compression conditions Avicel and Sta-Rx, which are known to be good compressible bases, exhibited the lowest ERI values. Magnesium carbonate, magnesium stearate and paracetamol, which yielded either very brittle or capped compacts had correspondingly high values for ERI. Powdered paracetamol had almost double the ERI value of its binder-containing direct compression form.

A number of other workers (Malamataris et al., 1984; Bangudu and Pilpel, 1985; Esezobo and Pilpel, 1986; Ejiofor et al., 1986; Itiola and Pilpel, 1986) have adopted a similar approach for quantifying plasto-elasticity to that of Celik and Travers (1983). Malamataris et al., (1984) defined a plasto-elasticity ratio ER/PC thus:

$$\text{PC} = \frac{H_0 - H_L}{H_0} \times 100 \quad (1.18)$$

and

$$\text{ER} = \frac{H_R - H_L}{H_L} \times 100 \quad (1.19)$$

H_0 , H_L and H_R are respectively the compact thickness at maximum compaction pressure, the compact thickness after holding for 30 seconds at maximum compaction pressure and the compaction thickness after ejection from the die. Some workers (Bangudu and Pilpel, 1985; Esezobo and Pilpel, 1986) have referred to the plastic compression (PC) as the stress relaxation (SR). Clearly, this is incorrect as the parameter recorded is a measurement of strain movement at constant

stress rather than stress decay at constant strain. Additionally, the movement measured may contain some element of viscoelastic strain and as such may not be characteristic of pure plasticity. The concept, however, is identical to that of Celik and Travers (1984) although they used a shorter holding time (10 seconds) and measured elastic recovery within the die to avoid contribution from viscoelastic effects.

Malamataris et al., (1984) and Bangudu and Pilpel (1985) showed that, for a variety of materials, an inverse relationship existed between compact strength and the ER/PC ratio. Itiola and Pilpel (1986) showed that for PVP, gelatin and methylcellulose as binders an increase in binder concentration reduced the ER/PC ratio for metronidazole granules prepared by wet-massing. The change in the ratio resulted both from a reduction in elastic recovery and an increase in plasticity. In relative terms, the increase in plasticity appeared to be more significant. Esezobo and Pilpel (1986) demonstrated that the ER/PC ratio increased with increasing compaction pressure and that this was due mainly to an increase in the elasticity component. Also for a number of materials, including paracetamol granules prepared by wet-massing with PVP 5%w/w, the plasto-elasticity ratio decreased as the temperature of compaction was raised between -10°C and 65°C. This was due both to a reduction in ER and an increase in PC and was associated with an increase in the tensile strength of the resultant compacts. They considered that these results were due to an increase in asperity melting and the formation of strongly welded bonds at high pressure. They did not consider (in the case of the paracetamol granulate) the possibility of thermally-increased plasticity in the PVP binder.

One disadvantage of the elastic recovery index or the plasto-elasticity ratio is that they fail to quantify plastic deformation occurring during the loading phase of compression. For rapid compression where the holding or dwell time is short, this may be significant. The use of plasticity-elasticity indices has contributed considerably to the understanding of how compact properties are dependent on bonding and debonding processes. The absolute values of the indices will, however, be expected to vary with the detail of the test method employed.

1.3.9 Viscoelastic Deformations

It has long been appreciated that the mechanical properties of some tableted materials may change significantly with time. Rees and Shotton (1970) attributed initial increases in the crushing strength of sodium chloride compacts to stress-relaxation. Creep strain recovery, which may contribute to the cracking of sugar coats or splitting of film coats, has been shown for a number of materials (Aulton et al., 1973; York and Baily, 1977). Rippie and Danielson (1981) and Danielson et al., (1983) studied viscoelastic behaviour of compacts by measuring stress-relaxation during the unloading and post-compression periods in the die of a rotary tablet press. These authors suggested that viscoelastic parameters could provide insight into kinetically controlled changes in structure.

Celik (1984) derived creep-compliance versus time curves for a range of direct compression bases, both from the strain movements of compacts held a constant stress and from micro-indentation tests. The deformation of Avicel PH101 and Sta-Rx was shown to be highly time-dependent, with significant retarded elastic strain in addition to plastic flow. Emcompress, a material compacting by brittle failure, showed little tendency to undergo visco-elastic or plastic strain. Using classical methods of creep analysis (Barry, 1974) it was possible to model the mechanical properties of the compacts in terms of Maxwell and Voigt units. Studies by Patel and Staniforth (1987) and Staniforth et al. (1987), using an identical technique, have also differentiated between elastic, viscoelastic and plastic deformation in direct compression bases. The creep behaviour of pharmaceutical particulate solids must, however, be complicated by the non-isotropic structure of the packed bed, fragmentation and inter-particle bonding, and the composite character of a tablet formulation.

Radebaugh et al., (1989) characterised the viscoelastic properties of compacted pharmaceutical powders using a non-destructive dynamic rheological method. The technique utilised small strain sinusoidal oscillatory torsion of compacts. It was found that the determination of fundamental viscoelastic parameters could provide an insight into the processes that result in bonding and structure formation. Radebaugh et al., (1989) proposed that their findings support the

premise that van der Waal's forces are the primary origin of bonding between particles.

Armstrong (1989) observed that further work on time-dependent factors involved in tablet compression was needed, since virtually all data so far reported were derived for single component systems. But most commercial tablets are multiparticulate systems.

Hiestand (1985) noted that the measured strength of compacts is usually greater than would be predicted from a balance of bonding plasticity and debonding elasticity. The tensile strength of a particle-particle contact will be very weak when the elastic recovery following decompression is Hertzian, i.e. the elastic energy is all dissipated in the formation of new surface. To account for stronger bonding, it is necessary to obtain post-decompression contact areas greater than produced by elastic recovery alone. Further plastic deformation during decompression must occur. This has been called "isthmus formation" (Hiestand and Smith, 1984). Hiestand et al., (1987) have proposed that, for viscoelastic materials, elastic energy dissipated during recovery may be utilised in further plastic deformation. The resultant increase in true area of contact or isthmus formation between particles accounts for the development of strong bonds. Studies in the fracture mechanics of viscoelastic materials have confirmed that ductile extension (analogous to isthmus formation) occurs at the crack tip and accounts for increased bond strength (Hiestand and Smith, 1987).

1.4 Binder Film Formation and Deformation

Many materials have been evaluated, in some manner or other, for use as binding agents in the production of compressed tablets. Willis et al., (1965) investigated a variety of polymers as potential binders in the granulation of powders. Other workers (Nelson et al., 1957; Lehrman and Skauen, 1958; Muti and Othman, 1989) have evaluated binders by considering the properties of tablets produced when using them. Mendes (1968) assessed the performance of eight binding agents by means of a "hardness-friabrasion" index of tablets produced using the respective binders. He considered that methods of assessing binders outside of tablet systems did not produce satisfactory

conclusions, although no experimental evidence was presented to support this contention.

It has been long been appreciated that the inclusion of a binding agent in a granulate may modify compression properties. Few studies have been carried out, however, to investigate how mechanical properties of the binder itself influence subsequent compression behaviour. Healey et al., (1974) studied the mechanical properties of free binder films cast from aqueous solution. Using stress-strain curves derived from tensile tests, they classified acacia and PVP as weak materials, gelatin as a hard, strong material and methylhydroxyethylcellulose and starch as hard and tough materials. PVP also exhibited the lowest modulus of elasticity, showing it to be the most readily deformed binder tested as well as having a low tensile strength. They suggested that its value as a good binder may in part be attributed to this high deformability which would aid consolidation during compaction. Gelatin possessed the highest modulus of elasticity and tensile strength (although it was shown to be brittle) and it was suggested that its value as a binder may be limited by its resistance to consolidation. Additionally, they suggested that its brittleness may result in friable granules and tablets. The high tensile strength of gelatin films, however, corresponded with its known ability to produce hard tablets.

Krycer et al., (1983) used results of their own studies, along with a retrospective review of previously published data, in a comprehensive evaluation of binders used in wet-massed granulation. Using paracetamol as the substrate material for granule and tablet studies, they concluded that the relative tablet strength and capping tendency could not be predicted by any single binder property. They considered that it was necessary to take into account four proposed determinants of binder efficacy: substrate wetting by binder solution, binder film formation and deformation properties, binder cohesion, and binder-substrate adhesion. The first and second factors were found to be significant determinants of granule and tablet strength. Tablet friability was shown to be mainly influenced by binder film-forming properties. Optimum binder efficiency was achieved when the binder solution readily wetted the substrate and was well distributed. During the compaction process, bonding was optimized when the binder

was sufficiently soft to flow plastically at low pressures, yet tough enough to withstand postcompression elastic recovery. Thus, although starch was a good film former, the tablets formed were relatively weak and very friable due to poor wetting of paracetamol by the starch paste. PEG 6000 and sucrose, both non film-forming binders, produced correspondingly friable tablets.

Reading and Spring (1984a) investigated the mechanical properties of four film-forming polymeric binders; methylcellulose, PVP, hydrolysed maize starch and a gelatin hydrolysate. Using sand as a model substrate they investigated the effects of the binders on the mechanical properties of granules and compact formed using the binders. They noted that one of the binders (maize starch) formed a viscous paste which was poorly distributed during granulation. Thus, although starch film formation was good, granulation was inefficient and the resultant compact strength low. For the other binders, a positive correlation was shown between desirable properties (compact strength and low granule friability) and the creep compliance, ultimate tensile strength and elongation at failure of the cast binder films. A negative correlation was found between compact strength and the Brinell Hardness of the films. They concluded that a good binder would be one which was strong in tension, but was readily deformable.

1.5 Plasticization of Tablet Binders: Objectives and Scope of the Thesis

In the commercial production of tablets, using high speed tablet presses, it is not uncommon to use granulated material rather than simple powder blends. In this way, a uniform flow of non-segregating and compressible material from the hopper to the die can be assured. The production of granules is usually carried out by wet-massing the powder blend with a binding agent dissolved in a suitable solvent. It was considered that the primary function of a binding agent was to facilitate adhesion between primary particles during wet-massing and maintain granular integrity after drying. However, it has become evident that the binder may significantly modify the compression properties of materials inducing a degree of plasticity which was absent in the ungranulated substrate. It has been observed that many

materials will only form coherent tablets after granulation with a suitable binder.

The incorporation of a binding agent into a granulate has been shown by several studies to increase the overall plasticity of the mass. Wells et al., (1982) proposed that this effect might be enhanced by the plasticization of the binder. A patent for this concept was subsequently applied for (European Patent Application Number 0 070 127 A2, 1982). Wells et al., (1982) evaluated the effects of a series of potential plasticizers on the tableting properties of dicalcium phosphate, lactose and paracetamol, each granulated with PVP. The influence of the plasticizer was most significant for the paracetamol compacts, which exhibited increased strength and capping pressure, and reduced friability. The tensile strength of paracetamol compacts increased with increased plasticizer levels, although friability appeared to be independent of plasticizer type or concentration. Both the tensile strength and resistance to friabrasion were improved for lactose compacts prepared using the plasticized binder. Dicalcium phosphate compacts containing plasticized binder were, however, weaker than those containing no plasticizer, although their friability was significantly lowered. It was concluded that fragmentation of dicalcium phosphate was reduced by binder plasticization, resulting in reductions in bonding and compact strength.

Similar results were reported by Krycer et al., (1983) for paracetamol granulated with PVP co-precipitated with glycerol. These workers also observed that this resulted in tablets of elevated strength and capping pressure and with an increased resistance to friabrasion. Although Wells et al., (1982) and Krycer et al., (1983) accounted for their results in terms of binder plasticization, neither group of workers presented binder deformation data to support this contention.

Reading and Spring (1984b) evaluated the influence of a number of inclusions on the mechanical properties of four polymeric tablet binders; methylcellulose, PVP, hydrolysed maize starch and a gelatin hydrolysate. In general, the inclusions resulted in the weakening of films made with the binders. They reported that PEG 600, included as a potential plasticizer, had little plasticizing effect with respect to the tensile mechanical properties of cast binder films. The

inclusion of sodium lauryl sulphate (a wetting agent) or lactose (a water-soluble tableting diluent) made some films of PVP and starch too brittle to test. Using sand as a model substrate, they also investigated the effect of binder inclusions on granule and compact properties. Inclusion of PEG 600 tended to give weak granules and compacts when included with each of the binders studied.

The concept of tablet binder plasticization is of interest for a number of reasons. Plasticization offers the potential to increase compressibility of a granular mass using the minimum quantity of binding agent. This may be important for poorly compressible drugs since the inclusion of sufficient binder to facilitate tableting may result in impaired dissolution and poor bioavailability. At a fundamental level, the ability to manipulate deformation characteristics of a polymeric binder offers considerable scope for the investigation of binder function in tablet compression. The contrasting results of Wells et al., (1982) and Reading and Spring (1984b) serve to emphasise the need for a detailed study of the phenomena of binder plasticization. Consequently, the plasticization of polymeric tablet binders forms the subject of this thesis. Objectives of the thesis include studies on the fundamental nature of plasticization, the effects of plasticization on physico-mechanical properties of polymers, and consequences for the tableting process.

No material exists as a plasticizer per se for all polymers. Consequently, Chapter two considers the fundamental molecular requirements for plasticization and attempts to relate them, in a semi-quantitative manner, to the plasticization of some polymeric tablet binders. The objective of plasticization is to modify the ductility and workability of a polymer. Characterisation of the physico-mechanical properties of some commonly used polymeric tablet binders, and the quantification of changes induced by plasticization, form the subject of Chapters three and four. The development of instrumented creep rheological techniques (Chapter four) proved particularly useful for the resolution and quantification of time-dependent and time-independent deformation of tablet binders.

The role of plasticity in the tableting performance of binding agents is investigated with respect to tablet mechanical properties (Chapter

five) and the compression characteristics of granulates (Chapter six). Wet-massed granulation is used as the method for incorporating binding agents and plasticizers into model systems for tableting. Granulation has been the subject of considerable previous work and is not, therefore, investigated other than to assure control and reproducibility of experimental methods. By the selection of tableting substrates which deform predominantly without plastic flow, it should be possible to investigate the specific influence of binder plasticity on compression characteristics. The use of an sophisticated instrumented hydraulic press enables investigation of time-dependent and time-independent deformations during tablet compression process.

The final chapter summarises the conclusions of the work and discusses their implications for tablet formulation and manufacture. Potential areas for additional research are suggested.

CHAPTER TWO

PLASTICIZATION AND THE THERMODYNAMICS OF POLYMER SOLUTIONS

CHAPTER TWO

PLASTICIZATION AND THE THERMODYNAMICS OF POLYMER SOLUTIONS

2.1 Plasticization Phenomena

Polymers are macromolecules formed from the addition of a number of repeating monomer subunits. The macromolecules may be homopolymers, composed of a single type of monomer, or copolymers consisting of two or more types of monomer. Among the naturally occurring polymers, cellulose is representative of the former type whereas proteins are the latter. The number of repeat units per macromolecule is called the degree of polymerization. Depending on functionality, i.e. the number of reactive groups of the monomer, polymers may be linear, branched or crosslinked. Small molecules and many polymers of biological origin are monodisperse, i.e. all molecules of a given pure compound have the same molecular weight. In contrast, synthetically manufactured polymers are polydisperse, consisting of macromolecules having different degrees of polymerisation. Such polymers are characterised by an average molecular weight and a molecular weight distribution.

Polymers have found wide application in the science and practice of pharmacy. Their applications include bioactive substances (e.g. insulin and heparin) packaging materials (e.g. polyethylene and polyvinyl chloride) and excipients used in formulation. In the latter case, polymeric materials have found particular application in the granulation of powder substrates and in the modification of the tablettability of such materials. In many areas of use, however, the physico-mechanical properties of a polymer "as received" do not conform with the optimum for the intended function. In such cases, the properties of the polymer may be modified by the incorporation of a second component which "plasticizes" the polymer.

Alfrey (1949) defined a plasticizer as "a non-volatile, high boiling point substance, usually a liquid, incorporated in a polymeric plastic to increase its flexibility, workability and distensibility." Boyer (1951) subdivided potential plasticizers into three types on the basis of their association with the polymer. They were considered as:

of their association with the polymer. They were considered as:

- Solvent type
 - miscible in all proportions with the polymer
 - action limited to small, localised regions
- Non-solvent type
 - partially miscible with the polymer
 - dispersed molecules act as a solvent type plasticizer
 - non-dispersed molecules form droplet-like clusters which disrupt forces between polymer chains
- Polymeric type
 - may be miscible or immiscible with the main polymer
 - form large continuous regions separating the main polymer chains to give a flexible matrix

Plasticizing efficiency declines in the order:

polymer type < non-solvent type < solvent type.

Boyer (1951) observed that polymer-type plasticizers have very low efficiency and may require large levels of incorporation to produce the desired effect.

A number of theories have been proposed to account for the action of plasticizers on the physical and mechanical properties of polymers. Broadly, these can be classified into mechanistic theories as reviewed by Ritchie (1972), or thermodynamic theories of solvent action as proposed by Doty and Zable (1946).

The viscosity theory (Jones, 1947; Leibch, 1943; Wurstlin, 1943) related the behaviour of plasticized polymer to the viscosity-temperature relationship. According to this theory, incorporation of lower viscosity plasticizers would result in softer, more ductile polymers. The lubricity theory (Ritchie, 1972) assumes that resistance to deformation in a polymer resulted from intermolecular friction. Plasticizers act as lubricants at the molecular level, facilitating easier movement of polymer chains. The mechanistic theory which has probably gained greatest credence is the gel theory originated by Manfred and Obrist (1927) and developed by Doolittle (1947, 1954). According to this theory, polymers are attracted to each other by forces originating from "active centres" along the

polymer chain. In solution, the bonds are in dynamic equilibrium and as bonds are disrupted solvent molecules are also attracted to, and compete for, the active centres. A plasticizer added to the solution will also be in competition for the unbound centres. The rigidity of an unplasticized polymer is considered to result from a three-dimensional gel structure, formed by inter-polymer bonding between active centres as solvent is removed during drying. The presence of a non-volatile plasticizer (or residual solvent) will act to mask a proportion of the active centres and consequently reduce the number of polymer-polymer bonds. The rigidity of the three-dimensional network formed after solvent removal will be decreased, allowing greater deformation before failure.

At an empirical level, mechanistic theories generally offer an adequate explanation of the influence of a plasticizer on the properties of a polymer. But mechanistic theories offer little insight into rational plasticizer choice or the fundamental nature of the polymer-plasticizer interaction. In the latter areas, theories based on the solution thermodynamics of macromolecules are potentially more useful. The development of these theories with respect to plasticization is briefly reviewed in subsequent sections.

2.1.1 Intermolecular Forces

Prior to a review of the thermodynamics influencing plasticization, it is necessary to briefly consider the nature of forces which exist between atoms and molecules. All the forces are electrostatic in origin and are ultimately based on Coulomb's Law of the attraction between unlike, and the repulsion between like charges. For non-electrolytes, Small (1953) identified the pertinent forces as London dispersion forces, dipole orientation, dipole induction, repulsion energy and hydrogen bonding. The sum of all attractive forces between uncharged molecules is often described by the term "van der Waal's forces".

Dispersion and repulsion forces are always present and, being non-directional in nature, are additive over all pairs of molecules in a liquid (Small, 1953). Dipole orientation is usually of less importance. Strong interaction requires permanent orientation of the

molecules. But a molecule favourably orientated with respect to a second molecule may be unfavorable orientated with respect to a third. Consequently, it is only when there is regular long range orientation of the molecules, as in crystals or pseudocrystalline liquids and polymers, that the dipole contribution can be large. Where this orientation is present, for example in hydrogen bonded liquids such as water, the entropy of vapourisation is abnormally high. Ordinary polar organic liquids such as ketones, ethers or esters, have entropies of vapourisation only slightly higher (if at all) than for non-polar liquids of similar boiling point. This indicates that dipole orientation can make little contribution to the net attractive force, probably because the dipoles are buried deep in the molecule. Weak dipole forces not associated with long range orientation may make a small contribution to the total attractive energy. In general, attraction due to dipole orientation can be regarded as insignificant, even for polar molecules, when compared with dispersion forces unless hydrogen bonding occurs.

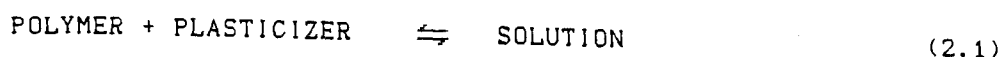
2.1.2 Compatibility

For a substance to effectively plasticize a polymer it is often stated requirement that the two components should be compatible. The use of the term "compatibility" in this sense, is somewhat different to its usual meaning in relation to pharmaceutical systems. The Pharmaceutical Codex (1979) states that "incompatibility occurs when the components of a medicine interact in such a way that the properties of the medicine are adversely affected". With respect to polymeric systems, compatibility is defined as "the miscibility on an intimate molecular scale of polymers and additives in the solid state" (Bohn, 1975). The latter definition has been adopted as the convention throughout this thesis.

In many respects, the compatibility of a potential plasticizer with a polymer can be regarded as analogous to the dissolution of the polymer in a solvent. The principles governing the solution of a polymer are not very different from those governing the solution of non-polymeric solutes. The main deviations, in concentrated solutions at least, arise from the low entropy of mixing of polymers compared with other substances. A mixture which, thermodynamically, is a single phase is

regarded as a solution irrespective of its mechanical properties. Thermodynamic factors affecting solubility can, therefore, be applied to a consideration of compatibility in polymer-plasticizer systems.

The mixing of a polymer and a potential plasticizer can be represented as an equilibrium:



In thermodynamic terms the process will be at equilibrium when the change in Gibbs free energy (ΔG) is zero. The free energy is defined as that energy which would be absorbed or liberated during a reversible process. When the free energy change is negative, the process proceeds from left to right, i.e. dissolution is spontaneous. For a reversible process, the change in free energy can be related to the change in heat content (enthalpy ΔH) or the change in randomness (entropy ΔS) by the equation:

$$\Delta G = \Delta H - T \Delta S \quad (2.2)$$

where T is the absolute temperature.

It follows that for thermodynamic compatibility or spontaneous dissolution, the balance of enthalpy and entropy of mixing must be negative. This is favoured when ΔH is negative (exothermic mixing) or when ΔS is positive (randomness or disorder is increased), ideally at a high temperature.

Crystalline polymers have a lower free energy than the corresponding amorphous polymer. For compatibility or dissolution, the free energy necessary to melt the crystalline regions must be supplied. This energy may be considerable so that highly crystalline polymers may be compatible with solvents or plasticizers only at temperatures approaching their melting points. This explains why the polymer cellulose is insoluble in water even though its monomer, dextrose, is readily soluble (Martin et al., 1983). The following discussions apply, therefore, to the dissolution and compatibility of essentially amorphous polymers.

2.1.3 Ideal Solutions

The simplest case for binary mixing occurs when the two component are similar in size, shape and molecular structure. They may then form an "ideal solution", defined as one in which Raoult's law is obeyed. This law states that the partial vapour pressure of each component of the mixture is proportional to its mole fraction in the mixture:

$$p_i = p_i^\circ X_i \quad (2.3)$$

where p_i is the partial vapour pressure of a component in the mixture, p_i° is the corresponding vapour pressure of the pure liquid and X_i is the mole fraction. Negative deviations from Raoult's law lead to increased solubility and are frequently associated with specific interaction between solute and solvent, i.e. by solvation or hydrogen bonding. Positive deviations, leading to decreased solubility, are interpreted as resulting from association of one of the components to form dimers or oligomers. Hildebrand and Scott (1950) suggest, however, that positive deviation is better accounted for by the difference in the cohesive forces (sometime termed internal pressures or cohesive energy densities) of each constituent.

The conditions for ideal mixing imply that the heat of mixing ΔH is zero, i.e. the components mix without change in enthalpy. In such cases spontaneous mixing in all proportions is assured by the change in entropy (equation 2.6). In practice, few systems obey Raoult's law and types of deviation have been classified (Hildebrand and Scott, 1950) as:

- | | |
|---------------------|---|
| Athermal solutions | - enthalpy change is zero
- entropy change is non-ideal. |
| Irregular solutions | - both enthalpy and entropy deviate from ideal |
| Regular solutions | - entropy change has the ideal value
- enthalpy change is finite |

For molecules of similar size, ΔS is nearly ideal when ΔH is zero so that athermal solutions are nearly ideal in behaviour.

2.1.4 Heat of Mixing

For the free energy of mixing (ΔG of equation 2.2) to be negative then the enthalpy or heat of mixing (ΔH_{mix}) must ideally be negative or, if positive, low enough for ΔH to be smaller than the product of T and ΔS . The heat of mixing resulting from the addition of a plasticizer to a polymer originates from three sources:

- breaking of polymer-polymer bonds (ΔH_{PP})
- breaking of plasticizer-plasticizer bonds (ΔH_{LL})
- formation of polymer-plasticizer bonds (ΔH_{PL})

The magnitude of the heat of mixing is determined by the nature and strength of the intermolecular bonds involved and is given by:

$$\Delta H_{mix} = \Delta H_{PP} + \Delta H_{LL} - 2 \Delta H_{PL} \quad (2.4)$$

The dissolution of a polymer in a solvent is frequently observed to be endothermic, with ΔH_{mix} positive and thus tending to oppose the dissolution process. Hildebrand and Scott (1950), in their development of the theory of regular solutions, proposed that the heat of mixing of two non-electrolytes (denoted by subscripts 1 and 2) was positive and could be described by:

$$\Delta H_{mix} = [(E_1/V_1)^{0.5} - (E_2/V_2)^{0.5}]^2 V_m \phi_1 \phi_2 \quad (2.5)$$

where ΔH_{mix} is the overall heat of mixing, V_m is the total volume of the mixture, E is the energy of vapourisation, V is the molar volume of the components and ϕ is the volume fraction of the components.

The quotient (E/V) is the energy of vapourisation per cubic metre (in Jm^{-3}) and is termed the cohesive energy density (CED). Equation 2.5 may be rearranged to give:

$$\Delta H_{mix}/V_m \phi_1 \phi_2 = [(E_1/V_1)^{0.5} - (E_2/V_2)^{0.5}]^2 \quad (2.6)$$

The overall heat of mixing per cubic metre at a given concentration is given by the square of the difference between the square roots of the CEDs. The square root of the CED has been assigned the symbol ξ and has the units $(Jm^{-3})^{0.5}$.

The heat of mixing depends, therefore, on the term $(\delta_1 - \delta_2)^2$. If the heat of mixing is not to be too great to prevent miscibility, this term should be relatively small. When the term equals zero, then mutual solubility is ensured by the increase in entropy on mixing. $(\delta_1 - \delta_2)^2$ tends to zero as δ_1 tends to δ_2 . This implies that if the values of two substances are nearly equal, then they will be thermodynamically compatible and mutually miscible. For this reason δ has been termed the solubility parameter. Equation 2.5 is then expressed in the form of the Hildebrand-Scatchard equation:

$$\Delta H_{mix} = V_1 (\delta_1 - \delta_2)^2 \phi_2 \quad (2.7)$$

The molar CED for a liquid is defined as the energy required to break all the intermolecular contacts in one mole of the liquid. It is therefore equivalent to the internal energy of vaporisation to an ideal gas, providing that the intramolecular contacts are similar in the liquid and gas states. Ideal gases mix without heat change. If the CED of a mixture of liquids is greater than the sum of the CEDs of its components, however, heat is liberated, i.e. H_{mix} is negative and mutual solubility is ensured since the entropy change is always positive. The converse situation occurs when the CED of the mixture is less than the sum of the CEDs of its component liquids. In this case H_{mix} may be so positive as to outweigh the influence of entropy, resulting in a net positive free energy change. Such a solution (sic) if formed will spontaneously demix.

A number of assumptions are implicit in the derivation of the Hildebrand-Scott heat of mixing model:

- that the geometric mean approximation is valid, i.e the CED of a pair of dissimilar molecules is approximately equal to the geometric mean of the CEDs for the corresponding pairs of similar molecules
- that the molar volumes of the solvent and solute are not significantly different
- that the interaction forces result from a uniform force field surrounding the molecules, with no account being taken of polarity, solvation or specific molecular interaction

These conditions are only fulfilled for relatively small non-polar

molecules, so that application of the model to polymer-plasticizer mixtures can only give a qualitative interpretation of the heat of mixing. Nevertheless, the model provides a useful starting point for the prediction of polymer-plasticizer compatibility. According to this theory, essentially amorphous polymers should be miscible or compatible with liquid plasticizers of similar ϵ , without the need for chemical similarity or specific molecular interaction.

In the Flory-Huggins theory of polymer solutions (Flory, 1942; Huggins, 1942a,b,c) the heat of mixing for a polymer and solvent is assumed to be positive and is given by the van Laar expression:

$$\Delta H_{MIX} = \chi RT n_1 \phi_2 \quad (2.8)$$

where n_1 is the number of moles of component 1 (the solvent), ϕ_2 is the volume fraction of component 2 (the polymer) and χ is the Flory-Huggins interaction parameter. The nature and significance of this parameter is discussed in section 2.1.7.

2.1.5 Determination of Solubility Parameters

The solubility parameter for a solvent can be readily calculated. Methods for the calculation of solubility parameters from physical constants have been reviewed by Burrell (1975). The most accurate and direct method for obtaining the solubility parameter of a solvent is from its latent heat of vapourisation. The energy of vapourisation (E_v) to a gas at zero pressure is given by:

$$E_v = H_v - RT \quad (2.9)$$

where H_v is the latent heat of vapourisation at temperature $T(K)$ and R is the gas constant. The solubility parameter ($\epsilon(Jm^{-3})^{0.5}$) is then obtained from the square root of the CED (E_v/V) where V is the molar volume of the solvent in cubic metres. For many solvents, direct measurement of the heat of vapourisation at the desired temperature may not be readily available. In such cases methods must be used to estimate the heat of vapourisation, for example, the Clausius-Clapeyron equation. Probably the most convenient estimation is Hildebrand's equation:

$$H_{2s} = 23.7 T_b + 0.020 T_b^2 - 2950 \quad (2.10)$$

where H_{2s} is the latent heat of vapourisation at 25°C and T_b is the solvent boiling point in K.

Other methods for determining the solubility parameter exist, for example the relationship between δ and surface tension (Hildebrand and Scott, 1950). The solubility parameter of a polymer (or any non-volatile substance) cannot, however, be determined directly because most polymers cannot be volatilised without decomposition. Small (1953) and Hoy (1970) have produced tables of molar attraction constants which allow the estimation of solubility parameters from structural formulae, molecular weight, and density. Molar attraction constants are additive over the formula and are related to δ by:

$$\delta = \rho \Sigma G/M \quad (2.11)$$

where ρ is the density of the compound, G is the molar group attraction constant and M is the molecular weight. The method cannot be applied to alcohols, amines, carboxylic acids or other strongly hydrogen bonding compounds unless such groups constitute only a small part of the molecule and the contribution to the total CED is correspondingly small. In spite of the limitations, the method does provide a potential means of determining the solubility parameter for a polymer. There are drawbacks, however, in that the molecular weight and density of a polymer are rarely known with any certainty.

In practice δ is usually obtained for polymers from their solubility data (Burrell, 1975). Solvents of gradually increasing δ can be arranged such that a given polymer is soluble in all solvents grouped within a certain range. The midpoint of the range may be taken as the solubility parameter value of the polymer. The solubility parameter of a polymer is, therefore, defined as being the same as that of a solvent in which the polymer will mix (a) in all proportions, (b) without heat change, (c) without volume change and (d) without reaction or specific association. The solubility parameter of polymers which are rubber-like or can be readily cross-linked can be estimated from swelling values (Bristow and Watson 1958a). The polymer is immersed in a series of liquids of varying δ . Being cross-linked,

the polymer will not dissolve but will imbibe liquid and swell to varying degrees. The amount of swelling should be greatest in the liquid having the same δ as the polymer. By inference, the soluble none cross-linked polymer has the same value of δ .

In practice it has been found necessary to consider a hydrogen bonding parameter as well as the cohesive energy density. Hydrogen bond energies are difficult to determine, however, and their accuracy may be questioned. It has been usual therefore to arrange solvents qualitatively into three classes, poorly H-bonding (hydrocarbons and their halo-, nitro-, and cyano-substituted products), moderately H-bonding (esters, ethers, ketones) and strongly H-bonding (alcohols, amines, amides, carboxylic acids, aldehydes).

A further refinement to the solubility parameter concept is the extended solubility parameter approach of Hansen (1967a,b). He introduced the three-dimensional solubility parameter to provide information about the nature and relative quantitative contributions of dispersion, polar and hydrogen bonding interactions to the solubility parameter. According to this theory, the solubility parameter is related to the relative dispersion (δ_d), polar (δ_p) and hydrogen bonding (δ_h) contributions by the following equation:

$$\delta = (\delta_d^2 + \delta_p^2 + \delta_h^2)^{0.5} \quad (2.12)$$

2.1.6 Entropy of Mixing

The entropy of mixing (S) can be considered as the increase in the disorder of a system due to the formation of a mixture. The entropy change is always positive and tends to promote mixing. If W_1 and W_2 are the probabilities of a random mix and complete segregation respectively the entropy of mixing, according to the Boltzmann equation, is:

$$\Delta S = k \ln(W_1 / W_2) \quad (2.13)$$

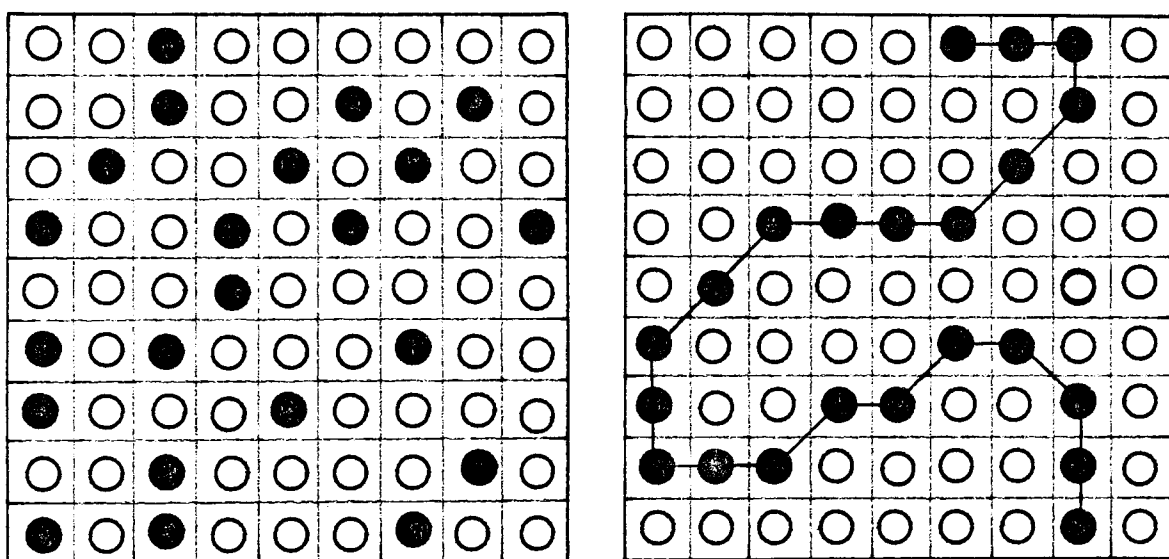
k of equation (2.13) is the Boltzmann constant. Flory (1942) and Huggins (1942a,b,c) independently evaluated the quotient (W_1 / W_2) for polymer-solvent systems. They considered the constituent molecules of

a solution to be arranged on a theoretical regular lattice, defined so that each solvent molecule occupied one site whilst each polymer molecule occupied a succession of nearest neighbour sites. This is illustrated by Fig. 2.1.

Figure 2.1 Two-Dimensional Lattice Models

a. Mixture of Two
Non-polymer Liquids

b. Polymer Molecule located
in The Liquid lattice



The configurational entropy change, due to the increase in the number of ways of arranging solvent and polymer molecules on the lattice when a solution was formed, was given by:

$$\Delta S = -R [n_1 \ln \varnothing_1 + n_2 \ln \varnothing_2] \quad (2.14)$$

where R is the Gas constant, n_1 and n_2 are the number of moles and \varnothing_1 and \varnothing_2 are the volume fractions of solvent and polymer respectively in the mixture.

Gee (1947) estimated the magnitude of ΔS for the mixing of liquids with a molar volume of 100cm^3 and polymers with a molar volume of 100000cm^3 . On mixing one cm^3 of each at room temperature the entropy increases (expressed as the product of entropy and temperature) were about:

Liquid + Liquid	34.7 J
Liquid + Polymer	17.4 J
Polymer + Polymer	0.03 J

The entropy of mixing was estimated to be much lower for the mixing of a liquid and polymer than for the mixing of two liquids of low molar volume. The entropy of mixing for two large volume polymers was so small that even a small positive value for the heat of mixing would render the free energy of mixing positive (equation 2.2) with resulting immiscibility.

2.1.7 Free Energy of Mixing

By the use of a semi-empirical heat of mixing term (the Flory-Huggins interaction parameter χ), Huggins (1947) combined equations 2.2, 2.8 and 2.14 to express the free energy of mixing as:

$$\Delta G_{mix} = RT [n_1 \ln \phi_1 + n_2 \ln \phi_2 + \chi n_1 \phi_2] \quad (2.15)$$

The first two terms in the parentheses, representing entropy contributions, are negative. The third term, representing the enthalpy contribution, is positive and opposes dissolution. The parameter χ (sometimes represented as μ) is a dimensionless quantity characterising the interaction energy for a given polymer-solvent pair divided by kT (Flory, 1953). The quantity χkT represents the free energy of transfer of a molecule of solvent from the pure solvent phase to the pure polymer phase. In fact, the parameter χ is composed of two terms, one an temperature-dependent enthalpy term, the other a temperature-independent entropy-related term. χ can, therefore, be represented as:

$$\chi = \chi_H/kT + \chi_S \quad (2.16)$$

The heat of mixing (ΔH) is then defined as:

$$\Delta H = X_m \bar{v}_1 \bar{v}_2 \quad (2.17)$$

2.1.8 Phase Separation

Differentiation of equation (2.15) with respect to n_1 gives the partial molar free energy of mixing

$$\begin{aligned} \Delta \bar{G}_1 / RT &= \ln a_1 \\ &= \ln \bar{v}_1 + (1 - 1/m) \bar{v}_2 + \chi \bar{v}_2^2 \end{aligned} \quad (2.18)$$

where a_1 is the activity of the solvent and m is the ratio of the molar volume of the polymer to that of the solvent.

For most polymer-solvent combinations, χ is positive and increases with decreasing temperature as the solvent becomes poorer. ΔG_{mix} and $\Delta \bar{G}_1$ therefore become progressively less negative until, at a critical value χ_c , they become positive and demixing or phase separation occurs. In binary polymer-solvent systems, equilibrium between two phases requires that $\Delta \bar{G}_1 / RT$ be the same in both phases. This corresponds to the requirement that the first and second derivative of $\Delta \bar{G}_1 / RT$ with respect to \bar{v}_2 be zero. Applying this requirement to equation (2.16) (see for example, Doolittle, 1954) result in expressions for the critical composition S_c and χ_c at the critical solution temperature T_c , to the molar volume ratio m :

$$S_c = m^{0.5} / (1 + m^{0.5}) = 1 / m^{0.5} \quad (2.19)$$

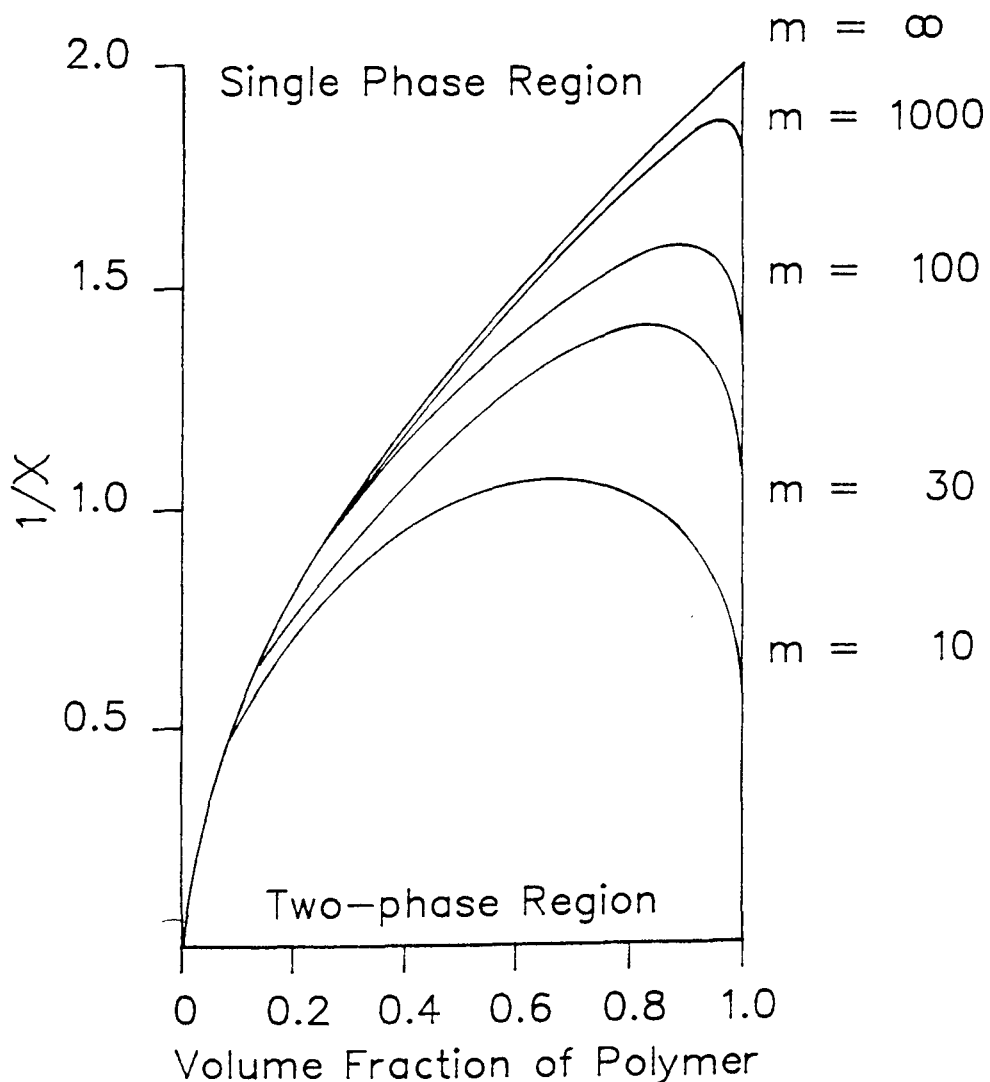
$$\chi_c = (1 + m^{0.5})^2 / 2m = 0.5 + (1 / m^{0.5}) \quad (2.20)$$

The critical solution temperature (also called upper consolute temperature) is the temperature above which solution is complete across the complete concentration range. Phase separation occurs below T_c . Equation 2.20 indicates that, as the ratio m increases (with increased polymer molecular weight, for example) χ_c falls. The critical value exceeds 0.5 by a small increment, which depends on the polymer molecular weight. At infinite molecular weight χ_c equals 0.5. It should be noted that some polymer-solvent systems (for example HPMC in water) exhibit phase separation when the temperature is raised. Inverted solubility phenomena (more commonly referred to

as thermal gelling) is generally caused by a competition between polymer-polymer association and solvation. This results from heterogeneity of the polymer or solvent, giving rise to two distinctly different types of polymer-solvent interactions. Of the two interactions one corresponds to a positive and one to a negative heat of mixing, and two χ values may be required to represent the situation (Doty, in Doolittle, 1954).

Using the preceding equations (2.18 - 2.20) Small (1953) and others have determined the conditions for the equilibrium of two phases by numerical calculation. The theoretical phase equilibrium diagram for selected values of the molar volume ratio m is shown in Fig. 2.2.

Figure 2.2 Phase Equilibrium In Binary Solvent-Polymer Systems
(After Small, 1953)



For convenience, Small used $1/X$ as the ordinate. Other workers (for example, Shultz and Flory, 1952) have employed temperature as the ordinate although the form of the plot is identical. Doolittle, 1954 has noted that practically determined phase equilibrium plots show good agreement with calculated plots for different molecular weight fractions of a polymer. The significant feature of the plots is the extreme asymmetry such that the curves almost coincide with the X axis for low ϕ_s values. Thus, the theory predicts that the solvent is readily soluble in the polymer even at large values of X , but the polymer will dissolve in the solvent only very near the critical point, and then only to a small extent. At values of X lower than X_c (or lower than the limiting value of 0.5) miscibility is complete. Areas above the curves in Fig. 2.2 are single-phase regions representing complete thermodynamic miscibility. Those beneath the curve represent two-phase regions of partial miscibility. When m is large, the critical composition is nearly all solvent.

Below the critical temperature, i.e. when $X > X_c$, the phases exist as a highly swollen polymer gel in equilibrium with substantially pure solvent. The nature of the curves shown in Fig. 2.2 explain why certain liquids may cause swelling of a polymer accompanied by negligible solubility. For example, even at a X value of 1.0, about 30% (by volume) of the solvent would be imbibed by the polymer at equilibrium. Obviously, two phases must be present and it is clear from the asymmetry of Fig. 2.2 that the second phase will be essentially pure solvent. But it may be present in such a small amount as to be unnoticeable.

2.1.9 Determination of Flory-Huggins Interaction Parameters

Values of X have been determined for a number of polymer-plasticizer systems. Anagnostopolos et al. (1967) measured X for various PVC-plasticizer blends by the depression of crystalline melting point technique. Good correlation was observed between values of X and the incidence of exudation of plasticizer from a standard PVC formulation. Where X was less than 0.5 for any system the polymer and plasticizer were thermodynamically compatible at all compositions. The technique, which is relatively simple in application, is unfortunately only of use for polymers having a definite crystalline

structure which can be visualised using hot-stage optical microscopy.

Other methods which have been applied with some success include measurement of swelling in cross-linked polymers (Bristow and Watson, 1958a) and measurement of intrinsic viscosity (Bristow and Watson, 1958b, 1958c). In the former case, the method is of use only for rubbers or polymers showing rubber-like behaviour. The latter method utilises the relationship:

$$0.5 + x^{0.5} - \chi = V_1 / K \{ ([\eta]^{1.66} / [\eta]_0^{0.66}) - [\eta] \} \quad (2.21)$$

where x is the polymer chain length, V_1 is the molar volume of the plasticizer, $[\eta]$ is the intrinsic viscosity of the polymer in the plasticizer, $[\eta]_0$ is the intrinsic viscosity of the polymer in a theta solvent, and K represents a term which is dependent on the specific volume of the polymer and its molecular weight.

Values for K in equation (2.21) have only been evaluated for a few rubbers. The intrinsic viscosity method is of interest to pharmacy, however, since Entwistle and Rowe (1979) have used the measurement of intrinsic viscosities to characterise interactions between the film coating polymers, Pharmacoat 606 (an HPMC) and ethylcellulose, and commonly used plasticizers. From the form of Equation (2.21) it can be seen that, generally, the lower the magnitude of χ the higher will be the intrinsic viscosity. The rank correlation for compatibility between a given polymer and a series of potential plasticizers may well be somewhat different, however, depending on whether χ or $[\eta]$ is used as the criterion.

2.1.10 Application of Polymer-Solvent Phase Equilibria to Plasticization

A potential plasticizer for a given polymer can be regarded as a specialised type of solvent. It follows from the preceding discussion that, for a given polymer-plasticizer mixture at a specified temperature, if the interaction parameter χ is greater than χ_c the system is thermodynamically incompatible. Two phases will be formed, the composition being determined by the value χ . Where χ is less than χ_c , the polymer and plasticizer will be compatible or mutually

miscible in all proportions. When the molar volume ratio m is very large, χ must be less than or equal to 0.5 in order to ensure miscibility throughout the entire range of composition. The magnitude of the difference between χ and χ_c characterises the degree of compatibility. For example, where χ is only slightly less than χ_c , a reduction in the temperature of the system may reduce the solvent efficacy sufficient to cause phase separation.

Doolittle (1954) observed that there appeared to be a strong correlation between χ values and plasticizing ability. In the case of polyvinyl chloride (PVC), for example, the best plasticizers were dibasic esters and phosphate esters having molecular weights of about 300 or more. These systems had very low χ values and were miscible in all proportions. In contrast, hydrocarbon molecules having large values of χ tended to separate out until the equilibrium (two-phase) composition was attained. This action is known as "sweating out". The relationship between χ , phase separation and plasticizer efficiency has been demonstrated by Anagnostopoulos et al. (1965).

2.1.11 Application of the Hildebrand-Scatchard Relationship to Polymer-Plasticizer Compatibility

The heat of mixing defined by the Hildebrand-Scatchard equation (2.7) can be used to replace the term χH the heat contribution to the Flory-Huggins interaction parameter (equation 2.15) so that:

$$\chi = \chi_s + V_1 (\epsilon_1 - \epsilon_2)^2 / RT \quad (2.22)$$

The formation of a single phase compatible polymer-plasticizer mix occurs when χ is less than χ_c . Combining equations 2.20 and 2.22 results in the following expression for compatibility:

$$(1 + m^{0.5})^2 / 2m > \chi_s + V_1 (\epsilon_1 - \epsilon_2)^2 / RT \quad (2.23)$$

The term χ_s is dependent on the effective coordination number z of the quasi-lattice assumed in the derivation of Flory and Huggins original model. In theory χ_s should be equal to $1/z$. In fact this is true only for the simplest lattice model where the polymer is

considered to be a rod composed of cubic monomers of coordination number $z = 6$. In all other cases χ_s is larger and experimental values generally range from 0.3 to 0.5. If an average value for χ_s of 0.4 is assumed, then expression 2.23 can be used to express the likelihood of compatibility in terms of the maximum allowable difference in polymer and plasticizer solubility parameters, i.e.

$$\Delta\epsilon_{MAX} = (\epsilon_1 - \epsilon_2) \quad (2.24)$$

Thus giving:

$$\Delta\epsilon_{MAX}^2 = RT [((1 + m^{0.5})^2 / 2m) - \chi_s] / V_1 \quad (2.25)$$

On this basis the criterion for compatibility would be that $(\epsilon_1 - \epsilon_2)$ should be less than ϵ_{MAX} where the subscripts 1 and 2 denote the plasticizer and polymer respectively. Since the difference is squared, this is true for both positive and negative values of ϵ_{MAX} . The condition for polymer-plasticizer compatibility can therefore be expressed as: $\epsilon_1 - \Delta\epsilon_{MAX} > \epsilon_2 < \epsilon_1 + \Delta\epsilon_{MAX}$

Using equation 2.25 values for ϵ_{MAX} can be estimated. AT 25°C with $RT = 2477.66 \text{ Jmol}^{-1}$ then, for a polymer and plasticizer of molar volumes 20000cm^3 and 200cm^3 respectively and $\chi_s = 0.4$, then $\epsilon_{MAX} = 2.54 (\text{Jm}^{-3})^{0.5}$.

2.2 Materials and Methods

Until comparatively recently, the use of plasticizers in polymers of pharmaceutical interest has been limited to the field of tablet film coating and packaging materials. Plasticizing agents have been added to film coating solutions to improve the film forming properties of the coating solution and enhance the servicability of the dried coat. Interest has been expressed in the incorporation of plasticizing agents into polymeric binding agents used in wet-massed granulation, with the view to enhancing overall compactability and reducing capping tendency (Wells and Khan, 1982; Wells et al., 1982; Krycer et al., 1983).

To be effective a plasticizer must interpose itself between polymer chains, reducing inter-chain forces, thereby extending and softening the polymer matrix. Efficiency is not, however, an absolute property of a plasticizer since it is dependent on the end use properties. The rank order of a series of plasticizers can vary considerably according to the property measured (Rowe, 1982). In consequence it is usual to define the most efficient plasticizer as one that gives the best balance of end properties for the amount incorporated. It follows that to be most effective the plasticizer must be compatible with the polymer. To date, the choice of plasticizers for tablet film coats has generally been empirical. The solubility parameter approach to polymer - plasticizer compatibility has been used with some success for ethylcellulose film coats (Entwistle and Rowe, 1979; Abdul-Razzak, 1983). A thermodynamic approach was adopted here, therefore, to study factors affecting the compatibility of polymeric binders and potential plasticizers.

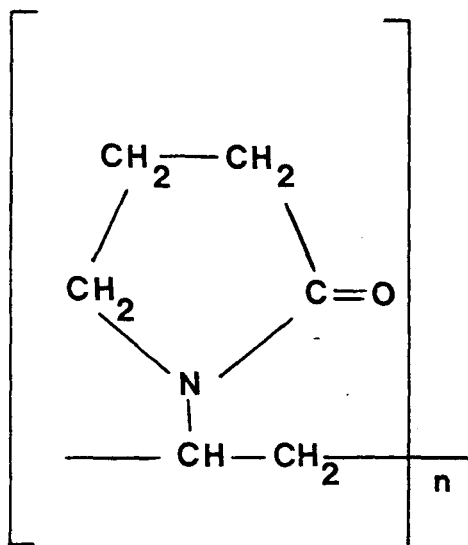
2.2.1 Binding Agents

Film-forming polymers commonly used as binders in aqueous wet-massed granulation were selected to give a range of physical and mechanical properties. These were:

2.2.1.1 Polyvinylpyrrolidone (PVP)

PVP is widely used in the pharmaceutical industry as a tablet binder, solubilizer and thickening agent. It is manufactured by the polymerization of the monomer N-vinylpyrrolidone to yield a linear polymer with the structure shown in Fig. 2.3. A number of molecular weight grades (varying with the degree of polymerization) are commercially available. Number average molecular weights (M_n) typically range from 1300 to 360000 Da. Grades used in the present work were Kollidon K25 and K90 (BASF UK Ltd.) having number average molecular weights of 10000 and 360000 Da respectively. PVP is readily soluble in many solvents, including water, and is very hygroscopic.

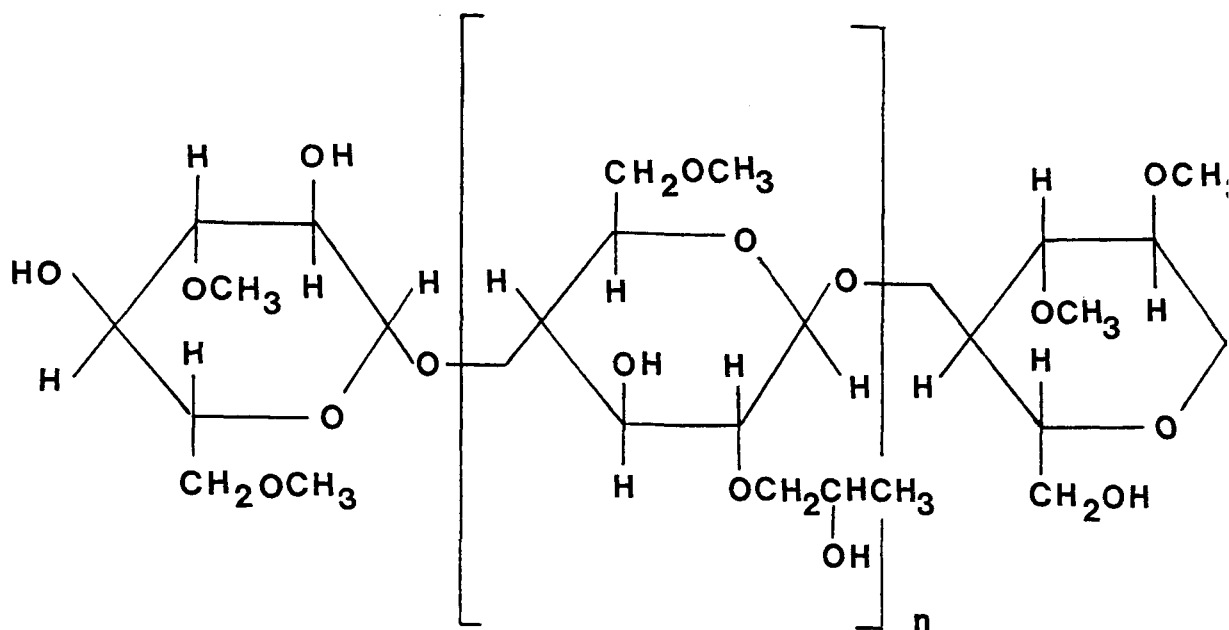
Figure 2.3 Molecular Structure of Polyvinylpyrrolidone



2.2.1.2 Hydroxypropyl Methylcellulose (HPMC)

HPMC is derived from cellulose, a linear polymer containing repeating anhydroglucose units. Treatment of the cellulose with methyl chloride and propylene oxide in turn, result in methoxyl and hydroxypropoxyl etherification on the hydroxyl groups of the anhydroglucose backbone. The general structure of HPMC is shown in Fig. 2.4. The principal use of HPMC is as a film-former in the film coating of tablets. A range of viscosity grades, determined by the molecular weight and its distribution, are available. Lower viscosity grades are particularly suited to aqueous film coating and are also employed as binders in wet-massed granulation. Higher viscosity grades are used in solvent film coating and as matrix-formers in the formulation of controlled release dosage forms. HPMC is readily soluble in water and some organic solvents. The material used in the present work was a low viscosity grade, Methocel E5 (Colorcon Ltd.).

Figure 2.4 Molecular Structure of Hydroxypropyl Methylcellulose



2.2.1.3 Pregelatinised Starch (Starch 1500)

Pregelatinized starch is widely used as an excipient in the formulation of solid dosage forms. Applications include its use as a filler in capsule and direct compression tablet formulations and as a binder in conventional wet-massing. Starches consist of a mixture of two polysaccharides, amylose and amylopectin. The relative amounts depend on the source of the starch but are usually about 30% amylose to 70% amylopectin (Merck 1983). Amylose is a linear polymer composed of α -1,4 anhydroglucose units. Amylose shows a marked tendency to associate due to hydrogen bonds between the linear chains and is the main film former of starch. Amylopectin, in contrast, has a highly branched structure consisting of short amylose chains connected via α -1,6-linkages. Pregelatinised starch is a physically modified corn starch which differs from compendial maize starch principally in its increased cold water solubility. The material used in the present work was Starch 1500 (Colorcon Ltd.).

2.2.2 Potential Plasticizers

No compound exists as a universal plasticizer per se for all polymers. In fact, a molecule which is an efficient plasticizer for one polymer may be less efficient for a second polymer or may not act as a plasticizer at all. A number of general requirements for a suitable plasticizer have evolved, however, and these can be summarised as:

- compatibility (miscibility with the polymer)
- efficiency (producing the optimum balance of end properties)
- permanence (high boiling point and low volatility)

The intended use of the polymers selected for the present work, i.e. tablet binders in aqueous wet-massing, imposed additional criteria with respect to plasticizer selection. Thus, the potential plasticizers should exhibit good aqueous miscibility and low toxicity. The compounds selected in this work for screening as potential plasticizers consequently comprised a number of polyhydric alcohols and polyethylene glycols. In addition, a history of usage (particularly with HPMC) suggested that the compounds listed below were particularly worthy of evaluation.

- Ethylene glycol
- Propylene glycol
- Hexylene glycol
- Glycerol
- Polyethylene glycols (PEGs) 200, 400, 600, 1500, 4000 and 6000

All of the potential plasticizers used were reagent grade, supplied by BDH Ltd., Poole, Dorset. Ethylene glycol, although not meeting the criteria for low toxicity, was included as the monomeric subunit of the PEGs.

2.2.3 Estimation of Polymer Solubility Parameters

The compatibility of an amorphous polymer and plasticizer is dependent primarily upon the heat of mixing. The magnitude of the heat of mixing is determined, to a great extent, by the difference between the solubility parameters of the polymer and plasticizer. It follows that, when the solubility parameter for a potential plasticizer is approximately equal to that of a polymer, the heat of mixing will be

small. Thermodynamic compatibility is then assured by the entropy of mixing. A comparison of the difference between the solubility parameter values for a polymer and potential plasticizers should, therefore, provide a guide to their compatibility in the solid state.

In this work, solubility parameters were determined using the method of Burrell (1975). This involved determining the solubility parameter range of each polymer in three classes of solvent (capable of poor, moderate or strong hydrogen-bonding). The solvent groups have been selected so that the values increase in reasonable constant steps within each hydrogen-bonded class. A solubility parameter range (rather than a single value) is obtained for the polymer. This has the advantage of indicating the practical allowable difference which can be tolerated between the absolute values for the polymer and solvent.

The solvent spectra proposed by Burrell (1975) and given in Table 2.1 were used, supplemented by additional solubility data published by the suppliers of the polymers. Other workers, for example Iyengar and Erickson (1967), have used solvent spectra covering a wider range of values. The probability of specific interaction of the polymer with solvents such as water having very high ϵ values and strong hydrogen-bonding propensity leads to some doubt as to the validity of polymer values obtained using such solvents.

A sample of each polymer, 1g in each case, was taken and added to 100ml of the solvent at room temperature. After agitation the resultant mixture was observed. If the mixture formed was a single phase with absence of turbulence or gel particles, the polymer was judged soluble. In cases where solubility was not immediately apparent, the mixture was heated to about 60°C, to speed dissolution, and observed again after cooling to room temperature.

Solubility parameter values of solvents which do dissolve the polymer mark the limits of the solubility range. The mid-points of the solubility parameter ranges can be taken as single value parameters for some purposes. Gee (1943) has pointed out, however, that these values will not necessarily agree with values obtained by other methods.

Table 2.1 Solvent Spectra for Determining Solubility Parameter Ranges
(after Burrell, 1975)

Solvent	Solubility Parameter δ (Jm^{-3}) ^{0.5}
<u>Poorly Hydrogen Bonded</u>	
n-Pentane	14.3
n-Heptane	15.1
Methylcyclohexane	16.0
Toluene	18.2
Tetrahydronaphthalene	19.4
o-Dichlorobenzene	20.5
1-Bromonaphthalene	21.7
Nitroethane	22.7
Acetonitrile	24.3
Nitromethane	26.0
<u>Moderately Hydrogen Bonded</u>	
Diethyl ether	15.1
Diisobutyl ketone	16.0
n-Butyl acetate	17.4
Methyl proprionate	18.2
Dibutyl phthalate	19.0
Dioxane	20.4
Dimethyl phthalate	21.9
2,3-Butylene carbonate	24.8
Propylene carbonate	27.2
Ethylene carbonate	30.1
<u>Strongly Hydrogen Bonded</u>	
2-Ethyl hexanol	19.4
Methyl Isobutyl Carbinol	20.5
2-Ethylbutanol	21.5
n-Pentanol	22.1
n-Propanol	24.3
Ethanol	26.0
Methanol	29.7

2.2.4 Estimation of Flory-Huggins Parameters

In view of the limitations placed on the experimental measurement of the value of the interaction parameter at room temperature (25°C) was estimated by recourse to equation (2.22):

$$\chi = \chi_s + V_1 (\epsilon_1 - \epsilon_2)^2 / RT$$

All symbols are as previously defined. The value of χ_s , the entropic contribution to the Flory-Huggin interaction parameter, was taken to be 0.4, consistent with experimentally determined values (Hildebrand and Scott, 1950). Thus, by substituting values of the solubility parameter for polymer and potential plasticizer, and the molar volume of the potential plasticizer, the value of χ for the system can be estimated. Values of χ for binders HPMC and PVP, and the potential plasticizers were calculated using solubility parameter data given in Table 2.2.

Table 2.2 Some Physico-chemical Properties of Potential Plasticizers
(after Burrell (1975))

Potential Plasticizer	Molar Mass (Da)	Molar Volume (cm ³ at 25°C)	Solubility Parameter (Jm ⁻³)
Water	18.0	18.0	47.9
Ethylene glycol	62.1	55.8	29.7
Propylene glycol	76.1	73.3	25.8
Glycerol	92.1	73.4	33.8
Hexylene glycol	118.2	128.4	19.8
PEG 200	200	177.4	24.5
PEG 400	400	354.6	24.5
PEG 600	600	531.9	24.5
PEG 1500	1500	1239.6	24.5
PEG 4000	4000	3300.3	24.5
PEG 6000	6000	4950.5	24.5

Note: Data for PEGs is derived from nominal molar masses and densities given by BDH Ltd., Poole, Dorset

2.2.5 Intrinsic Viscosities

A number of terms can be used to describe the viscosity of a solvent, solution or dispersion. The intrinsic viscosity $[\eta]$ is of particular value since it provides a simple but quantitative evaluation of the interaction between a polymer and solvent (or potential plasticizer). $[\eta]$ is usually determined graphically from a plot of specific viscosity (η_{sp}) or the natural log of relative viscosity ($\ln\eta_{REL}$) against concentration from the intercept of an extrapolation to zero concentration. Intrinsic viscosities have the dimensions of reciprocal concentration, and where the concentration is expressed in gdl^{-1} , the intrinsic viscosity has units of dl.g^{-1} .

Inn the present work, intrinsic viscosities were determined for the soluble polymers, HPMC and PVP in potential plasticizers where adequate solubility was found. Solutions in the concentration range 0.1 to 0.3 g.dl^{-1} (corrected for the moisture content of the polymer) were prepared in each solvent/plasticizer. Solutions were ultrasonicated for 30 minutes then allowed to stand for 24 hours to achieve full solvation of the polymer. After making up to volume with the solvent, the viscosity of each solution was measured at $25.0^\circ\text{C} \pm 0.2^\circ\text{C}$ using an Ubbelodhe capillary viscometer. The viscometers used were all works calibrated and were chosen to give efflux times sufficiently long to avoid the need for a kinetic correction. The method employed was essentially that specified in B.S. 188 (1977) with the exception that the viscometers were cleaned prior to each determination with a proprietary cleaning agent (Decon 90) rather than chromic acid. The viscosity of the pure solvents was also determined as above.

The kinematic viscosity (ν) in $\text{mm}^2.\text{s}^{-1}$ was calculated from the efflux time (t) using the following relation:

$$\nu = C.t \quad (2.26)$$

where C was the calibration constant ($\text{mm}^2 .\text{s}^{-2}$) for the viscometer used.

Graphical determination of intrinsic viscosity is laborious especially where many solvent systems are to be evaluated. Single point methods

for determining intrinsic viscosity overcome this limitation but many are applicable only to specific polymer-solvent combinations. Such methods include the Schulz-Blaschke and Matthes intrinsic viscosity determination for PVP (Buhler and Klodwig, 1984). Rudin and Wagner (1975) reported the development of a single point method, showing excellent agreement with multipoint intrinsic viscosities, for a wide range of polymers and solvents. This method was successfully used to determine intrinsic viscosities of cellulose ethers used for tablet film coating (Entwistle and Rowe, 1979) and was therefore employed in the present work.

2.2.6 Evaluation of Solid State Compatibility

In this work, the optical method of detecting incompatibility was selected since the technique is simple and provides information about the nature of the incompatibility. In addition, the problems caused by the influence of residual solvent on the glass transition temperature of the polymer (Tan and Challa, 1976) could be avoided. Polymer-plasticizer blends were prepared by making an aqueous solution of the polymer to which was added the aqueous miscible plasticizer in quantities up to 50% by weight of the final dried film. Polymer solutions were prepared using the following methods:

HPMC E5: Solutions of HPMC (10% w/w) were prepared by dispersing the polymer in about half of the required amount of hot water. When the polymer was adequately wetted cold water was added with stirring to give the final required weight.

PVP K25 and PVP K90: A quantity of PVP to give either a 10% w/w solution (PVP K90) or a 50% w/w solution (PVP K25) was dispersed in slightly less than the total required amount of cold water. When the polymer was adequately hydrated, the solution was made up to weight with cold water. The dissolution of PVP in water was accompanied by the evolution of heat indicative of specific interaction between the solvent and polymer, probably the hydrogen bonding of water to the oxygen of the pyrrolidone ring.

Starch 1500: Initial studies indicated that the pregelatinized starch, when simply slurried in cold water, failed to form a coherent

film. Consequently, the more traditional method of starch gelation was used to yield films suitable for compatibility studies. A 5% w/w gel was prepared by dispersing the starch in slightly less than the required amount of cold water, heating to 90°C, and maintaining this temperature for 15 minutes with constant stirring. After cooling the gel was adjusted to weight by the addition of cold water.

Double distilled water was used as the vehicle for all the polymers; dispersion of the polymers was achieved by means of an Ultra Turrax turbine mixer. The mass of polymer taken for the solutions was corrected for the moisture content of the polymer. Potential plasticizers were added to give the required loading to the freshly prepared polymer solutions. Liquid plasticizers were added directly to the solution with vigorous stirring. Solid plasticizers, i.e. the higher molecular weight PEGs, were dissolved in a small quantity of water prior to addition to the polymer solution to ensure homogeneity. The polymer-plasticizer blends were stored overnight for air bubbles to be removed before casting onto cleaned and degreased petri dishes. The casts were then dried in a laminar flow screen under ambient conditions (20 - 25°C, 40 - 60% RH). Unplasticized polymer solutions were also cast as controls.

Dried films were examined visually, using low power magnification where necessary, for evidence of incompatibility, i.e. phase separation as indicated by blooming (loss of film clarity and lustre) or exudation of plasticizer from the polymer matrix. Films showing no immediate sign of incompatibility were re-examined after one week at room conditions.

2.3 Results and Discussion

2.3.1 Entropy of Mixing

Table 2.3 shows the calculated configurational entropy of mixing, calculated using Equation 2.14, for the polymers PVP K25, PVP K90 and HPMC E5 with a range of potential plasticizers.

Table 2.3 Estimated Entropy of Mixing for Some Polymeric Binders and Potential Plasticizers at 25°C

Plasticizer	Molar Volume (cm ³)	Entropy of Mixing (J)		
		PVP K25 (mol. vol.) 23000 cm ³	HPMC (mol. vol.) 261000 cm ³	PVP K90 (mol. vol.) 932000 cm ³
Water	18.0	95.5	95.4	94.4
Ethylene Glycol	55.8	30.8	30.7	30.4
Propylene Glycol	73.3	23.5	23.4	23.2
Glycerol	73.4	23.5	23.4	23.2
Hexylene Glycol	128.4	13.4	13.4	13.3
PEG 200	177.4	9.7	9.7	9.6
PEG 400	356.4	4.9	4.8	4.8
PEG 600	531.9	3.2	3.2	3.2
PEG 1500	1239.6	1.5	1.4	1.4
PEG 4000	3300.0	0.6	0.5	0.5
PEG 6000	4950.0	0.4	0.4	0.3

Molar volumes for PVP, HPMC and the plasticizers were estimated from molecular weight and density data supplied by the respective suppliers (BASF, Colorcon and BDH). The data was expressed in terms of the energy change occurring at room temperature (25°C) on mixing 1 cm³ of each component. It was not possible to reasonably estimate the molar volume of Starch 1500, hence the entropy of mixing could not be calculated. To a first approximation, the magnitude of the entropy change would probably be similar to that observed for the other polymers.

The results show that the entropy of mixing is relatively insensitive to the size of the polymer, but falls markedly as the molar volume of the plasticizer increases. Water, being a small molecule, is a good

solvent in terms of entropy. Practical experience substantiates this since HPMC and PVP are readily soluble in water at room temperature. For the glycols, particularly the PEGs, the configurational entropy of mixing is very much reduced, however. The free energy of mixing ultimately determines miscibility between polymer and plasticizer. This depends on the balance between enthalpy and entropy changes as noted previously (Equation 2.2). Where the entropy change is small, the enthalpy of mixing becomes the significant factor. In such cases even a small positive enthalpy would give a positive free energy of mixing, resulting in immiscibility. Data presented in Table 2.3 suggests that, since the entropy of mixing will be small, compatibility between polymeric tablet binders and plasticizer will be dependent on the size of the enthalpy change.

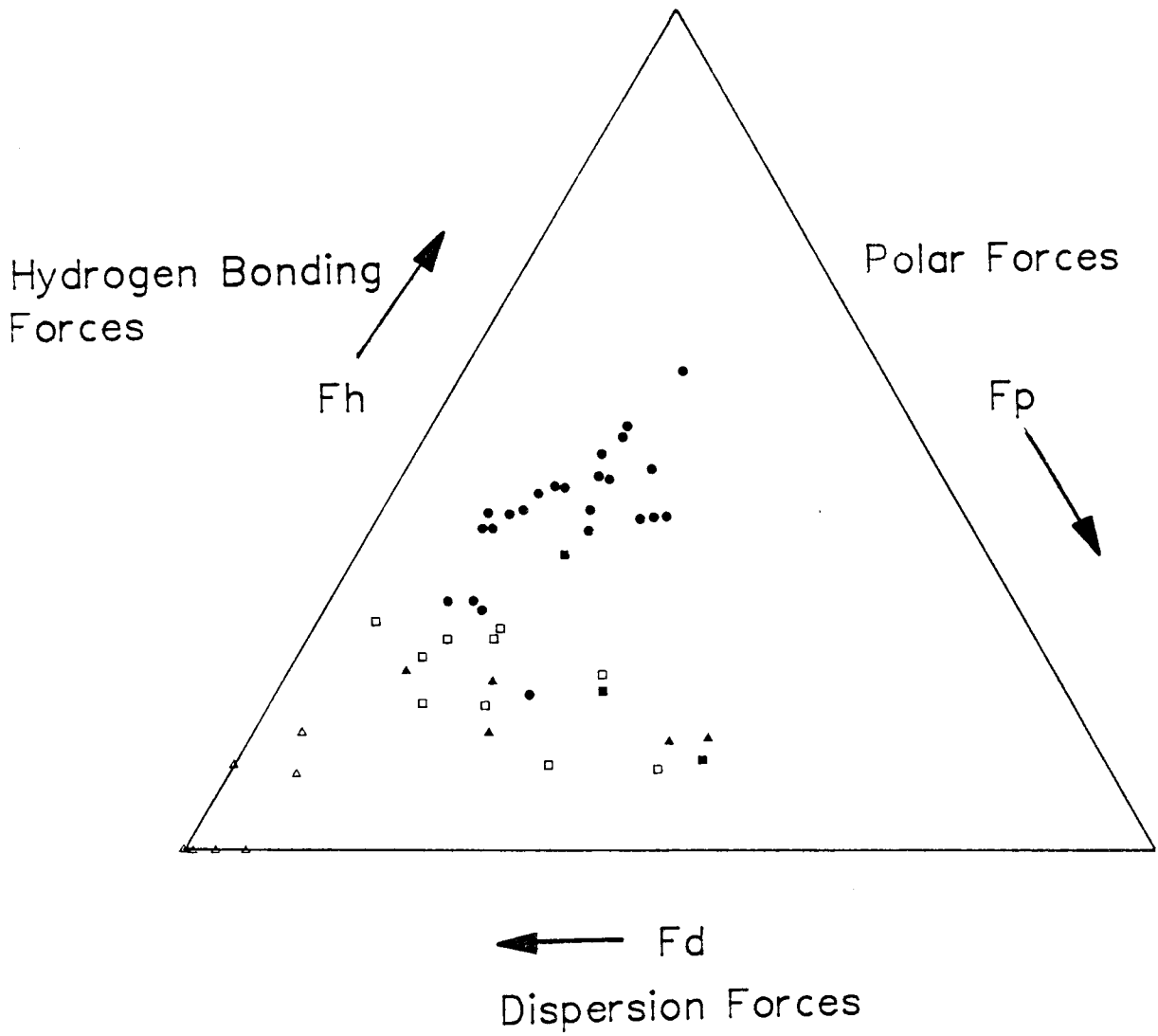
2.3.2 Solubility Characteristics of PVP, HPMC and Starch 1500 in Solvents of Differing Hydrogen-bonding Propensity

The solubility characteristics of PVP (K25 and K90), HPMC (E5) and Starch 1500 in solvents of strong, moderate and poor hydrogen-bonding propensity are shown in Figs. 2.5 to 2.7.

Data were compiled from estimations of the solubility of each polymer in the solvents comprising Burrell's solvent spectra and was supplemented by published solubility results. The data is represented by ternary solubility plots, in which the axes represent the relative fractional contributions of dispersion, polar and hydrogen-bonding components of the solvent solubility parameter. Relative fractional contributions for the solvents were abstracted from the literature (Hansen and Skarrup, 1967; Burrell, 1983). It has been suggested that the data could be presented in terms of a three-dimensional volume although this is harder to visualise than the ternary solubility plot.

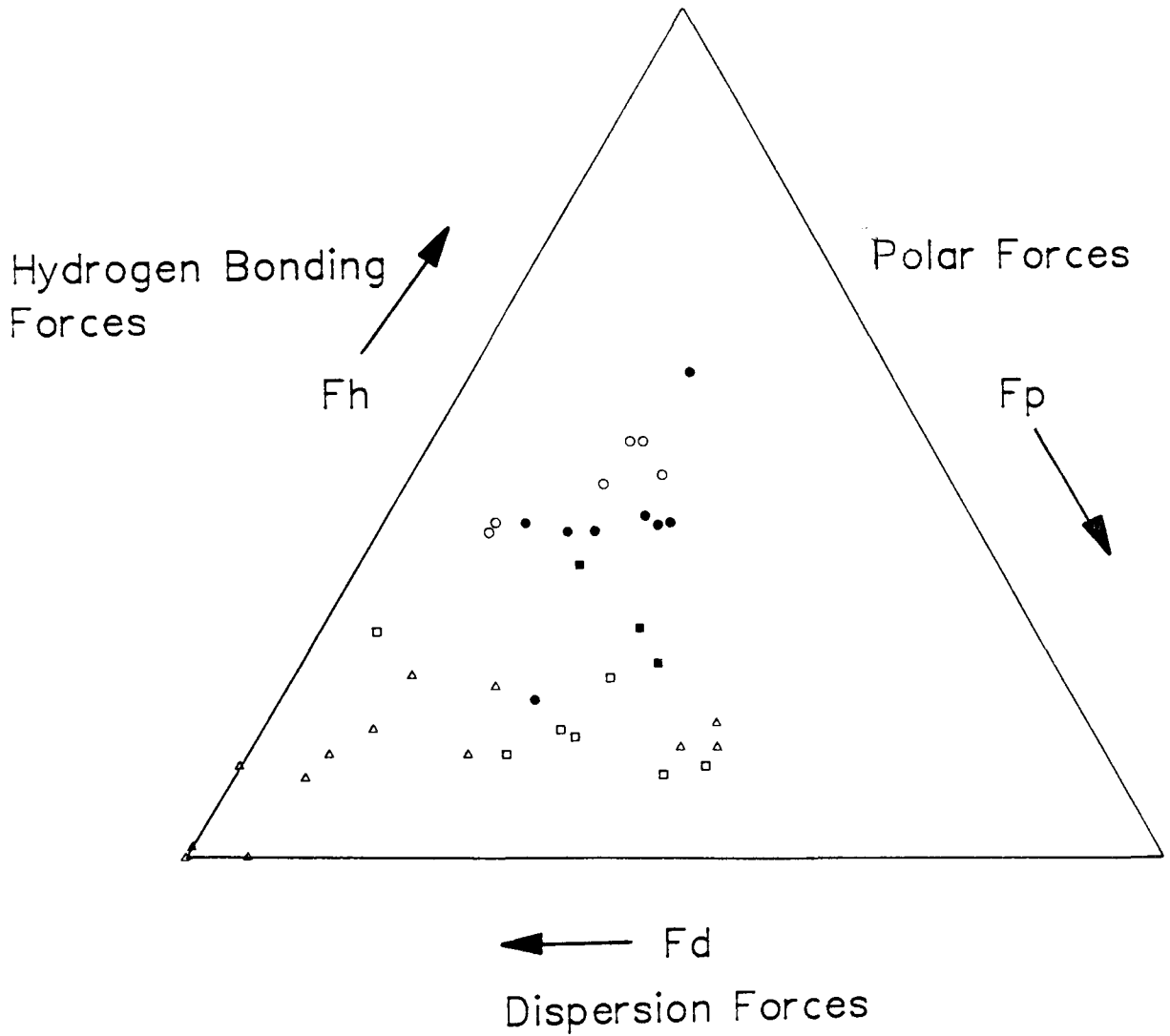
The allowable solubility parameter ranges for room temperature dissolution of the polymeric binders are given in Table 2.4. The solubility parameter limits reported do not necessarily correspond directly with Burrell's solvent spectra since published solubility data for additional solvents was included.

Figure 2.5 Ternary Solubility Diagram For PVP



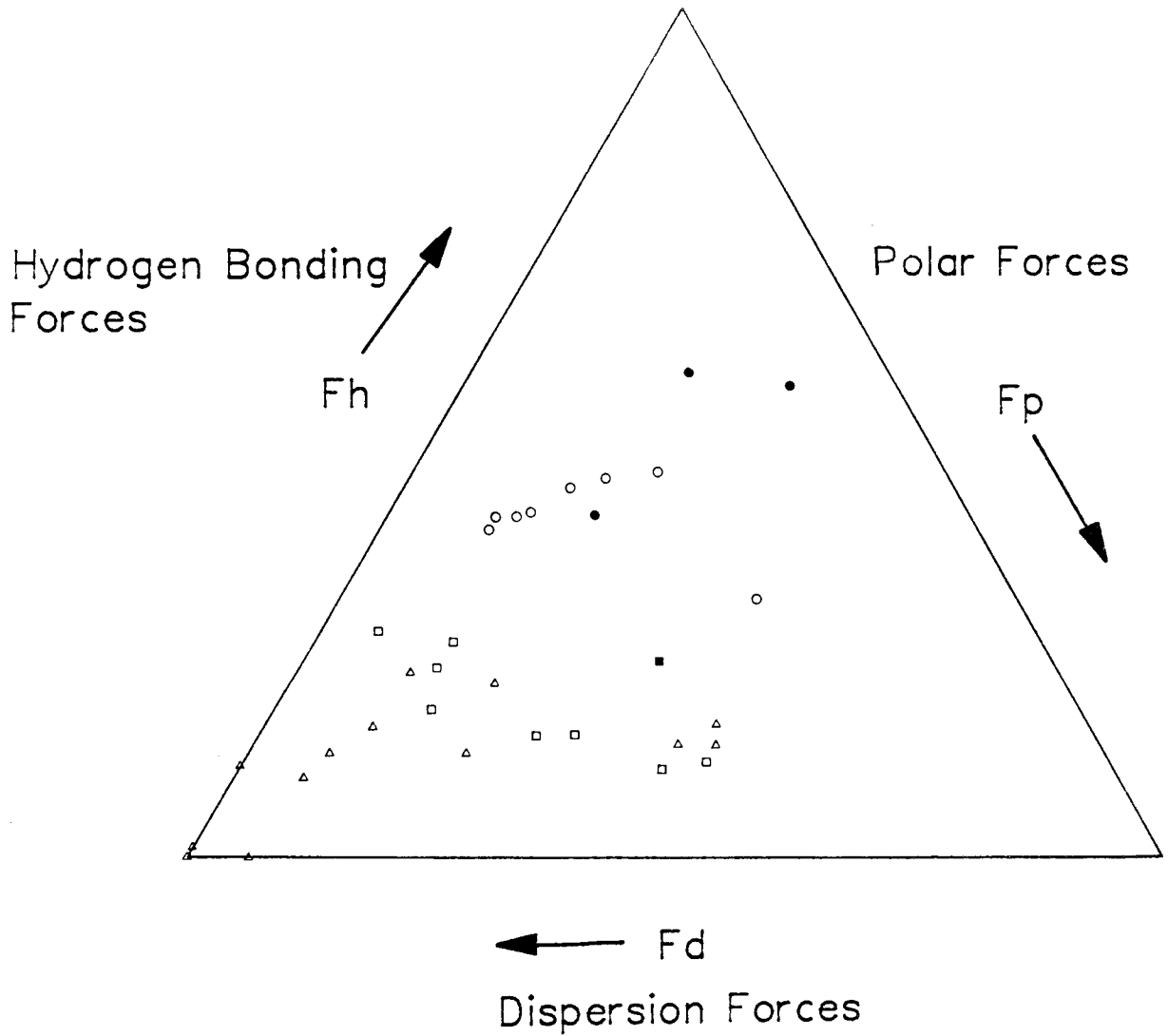
Solvent	Non-solvent	
●	○	Strongly Hydrogen-bonded
■	□	Moderately Hydrogen-bonded
▲	△	Weakly Hydrogen-bonded

Figure 2.6 Ternary Solubility Diagram For HPMC



Solvent	Non-solvent	
●	○	Strongly Hydrogen-bonded
■	□	Moderately Hydrogen-bonded
▲	△	Weakly Hydrogen-bonded

Figure 2.7 Ternary Solubility Diagram For Starch 1500



Solvent	Non-solvent	
●	○	Strongly Hydrogen-bonded
■	□	Moderately Hydrogen-bonded
▲	△	Weakly Hydrogen-bonded

Table 2.4 Solubility Parameter Ranges for Polymeric Binding Agents in Solvents Of Different Hydrogen Bonding Propensity

Polymer	Solubility Parameter Range (Jm^{-3}) ^{0.5}		
	Poorly H-bonded	Moderately H-bonded	Strongly H-bonded
HPMC	-	21.7 - 24.8	20.7 - 25.6
PVP	19.4 - 26.0	20.5 - 30.1	19.4 - 29.7
Starch 1500	-	-	47.9

PVP exhibited solubility in all three solvent classes. No difference in solubility characteristics was detected for two molecular weight fractions of PVP (K25 and K90). This implies that the nature and magnitude of inter-polymer forces are very similar over the molecular weight range considered. Only poorly and moderately hydrogen-bonded solvents with low solubility parameter were non-solvents for PVP. The ternary solubility diagram (Fig. 2.5) indicates that non-solvents for PVP are characterised by high fractional dispersion contributions to the overall solubility parameter. In contrast, solvents exhibit high fractional polar and/or hydrogen-bonding contributions. PVP was readily soluble in strongly hydrogen-bonding solvents, such as glycerol or water, having solubility parameters in excess of those comprising Burrell's solvent spectra. The dissolution of PVP in such solvents probably involves specific molecular interaction (hydrogen-bonding) and the evolution of heat when PVP dissolves in water supports this.

Construction of the ternary solubility diagrams reveals some inconsistencies in dissolution behaviour. For example, 1-4 dioxane ($\delta = 20.5 (Jm^{-3})^{0.5}$) is a non-solvent for PVP while ethyl lactate, having the same solubility parameter and hydrogen-bonding propensity, is a solvent. The difference in solubility results from the greater relative polar and hydrogen bonding contributions to the solubility parameter of ethyl lactate.

Unlike PVP, HPMC exhibits no appreciable solubility in poorly hydrogen bonded solvents. In moderately and strongly hydrogen bonded solvents, dissolution over a range of solubility parameters was observed. The ternary solubility plot for HPMC (Fig. 2.6) indicates, however, that criteria for dissolution of HPMC are much more stringent than for PVP. Many liquids having large fractional hydrogen bonding contributions are solvents for PVP but are non-solvents for HPMC. In common with PVP, inconsistencies in the solubility spectrum for HPMC were observed. For example, HPMC is freely soluble in acetic acid ($\epsilon = 20.7 \text{ (Jm}^{-3})^{0.5}$), formic acid ($\epsilon = 24.8 \text{ (Jm}^{-3})^{0.5}$) and furfuryl alcohol ($\epsilon = 25.6 \text{ (Jm}^{-3})^{0.5}$) but is sparingly soluble in the alcohols (2-ethyl butanol, n-pentanol and n-butanol) of intermediate solubility parameter. The statement that a polymer will be soluble in all solvents between its upper and lower solubility parameter limits (Burrell, 1975) is, therefore, over-simplistic. The relative contributions of dispersion, polar and hydrogen bonding to the overall solubility parameter are significant, even with solvents of the same nominal hydrogen bonding propensity.

Starch 1500 shows no appreciable room temperature solubility in any of the solvents comprising Burrell's solvent spectra. The literature indicates a similar dearth of room temperature solvents for starches, although Cowie (1965) observed that amylose (a component of starch) was readily soluble in ethylenediamine and dimethylsulphoxide and soluble, to a lesser extent, in formamide and water. These were presented as solvents in Fig. 2.7. The very poor solubility characteristics can be explained in terms of the molecular structure of starches which, unlike PVP or HPMC, exhibit a large degree of pseudocrystalline order. This is readily detectable by the birefringence which is visible when starch grains are viewed between crossed polarising filters. The physical modification involved in the production of pregelatinised starches may disrupt the gross crystallinity of the grain but does not disrupt crystallinity at the molecular level. In consequence, pregelatinised starches exhibit low solubility, even in strongly hydrogen-bonding solvents, at temperatures below the crystalline melting point.

The allowable solubility parameter limits for solubility for the three polymers in poor, moderate and strong hydrogen-bonding solvents are

reported in Table 2.4. Single value solubility parameters (calculated as the middle of the range and expressed to one decimal place) are recorded in Table 2.5 along with the allowable difference for polymer solubility.

Table 2.5 Single Value Solubility Parameters

Binder	Solubility Parameter (Jm^{-3}) ^{0.5}		
	Poorly H-bonded	Moderately H-bonded	Strongly H-bonded
HPMC	-	23.2 ± 1.6	23.1 ± 2.5
PVP	22.7 ± 3.3	25.3 ± 4.8	24.5 ± 5.2

Burrell (1975) commented that mid-range values might not agree with single point solubility parameters obtained from other methods such as viscometry or swelling measurements. At present, there appears to be no other published data on experimentally determined solubility parameters for PVP, HPMC or Starch 1500. Rowe et al. (1986) calculated solubility parameters for a range of cellulosic film coating materials, using group molar attraction constants reported by other workers. The following values were reported for HPMC:

16.1 (Jm^{-3})^{0.5} (method of Small, 1953)

21.5 (Jm^{-3})^{0.5} (method of Hoy, 1970)

24.4 (Jm^{-3})^{0.5} (method of van Krevelen and Hoftyzer, 1976)

Experimental results for HPMC (Table 2.5) show reasonable agreement with solubility parameters calculated using the group molar attraction constants of Hoy (1970) and van Krevelen and Hoftyzer (1976). However, the solubility parameter calculated using the data of Small (1953) is much smaller and clearly falls outside of the experimentally established limits for HPMC solubility. This discrepancy is probably due to the arbitrary low molar attraction constant assigned by Small

to the hydroxyl group (present in large numbers in HPMC) compared to the constants assigned by the other workers. The practical use of solubility parameters calculated using molar group attraction constants is limited, however, since no account is taken of the influence of hydrogen bonding. In contrast, solvent spectra determinations have the advantage of indicating practical solubility parameter limits for a polymer in solvents of different hydrogen bonding propensity. But it was not possible to determine solubility parameter limits for Starch 1500 using the solvent spectra method due to its minimal solubility in any class of solvent. On the basis of intrinsic viscosity measurements in a mixed solvent system, Cowie (1963) suggested that amylose (the minor component of starch) had a solubility parameter of about $25 \text{ (Jm}^{-3}\text{)}^{0.5}$. No estimate was made for the solubility of amylopectin. On a practical basis, the solubility characteristics of starches, including Starch 1500, are determined by the predominant polymer crystallinity.

One criterion for polymer-plasticizer compatibility is that the difference between the solubility parameter values for the polymer and plasticizer should be less than some maximum limiting value. If the molar volumes of the polymer and plasticizer are known, an estimate of this limit can be made by recourse to Equation 2.25. Determination of the solubility parameter ranges for the polymers, however, gives a practical evaluation of the limit. Applying this concept to the potential plasticizers, solubility parameter differences between the binders PVP and HPMC and potential plasticizers were calculated. These are reported in Table 2.6.

Solubility parameters for the plasticizers were abstracted from the literature. Values for the monomeric glycols were those obtained from the latent heats of vaporisation as published by Burrell (1975). The low volatility of polyethylene glycols meant that solubility parameter values could not be determined directly. Solubility parameter ranges for the dissolution of Carbowax 4000 in solvents of different hydrogen bonding propensity have been published (Burrell, 1975). It was established empirically, that the solubility parameter range in strongly hydrogen-bonded solvents ($\delta = 19.4 \text{ to } 29.7 \text{ (Jm}^{-3}\text{)}^{0.5}$) was applicable to all PEGs in the molecular weight range 200 to 6000 Da.

Table 2.6 Solubility Parameter Differences Between Potential Plasticizers and Polymeric Binding Agents

	Solubility Parameter (Jm^{-3}) ^{0.5}	Solubility Parameter Difference (Jm^{-3}) ^{0.5}	
		HPMC	PVP
Ethylene glycol	29.9 ⁽¹⁾	6.8	5.4
Propylene glycol	25.8 ⁽¹⁾	2.7	1.3
Hexylene glycol	19.8 ⁽¹⁾	-3.3	-4.7
Glycerol	33.8 ⁽¹⁾	10.7	9.3
PEG 200	24.6 ⁽²⁾ (23.7 ⁽³⁾)	-1.5 (0.6)	0.1 (0.8)
PEG 400	24.6 ⁽²⁾ (23.2 ⁽³⁾)	-1.5 (0.1)	0.1 (1.3)
PEG 600	24.6 ⁽²⁾ (20.5 ⁽⁴⁾)	-1.5 (2.6)	0.1 (4.0)
PEG 1500	24.6 ⁽²⁾	-1.5	0.1
PEG 4000	24.6 ⁽²⁾ (23.7 ⁽⁵⁾)	-1.5 (0.6)	0.1 (0.8)
PEG 6000	24.6 ⁽²⁾ (23.7 ⁽⁵⁾)	-1.5 (0.6)	0.1 (0.8)

(1) Burrell (1975)

(2) Burrell (1975) - derived from midpoint of solubility range

(3) Vaughan (1985) - single point solubility parameter

(4) Kawakimi et al. (1976) - single point solubility parameter

(5) Otozai and Toyama (1976) - single point solubility parameter

Note: Data in parentheses refer to published single point solubility parameters and the respective solubility parameter difference.

The midpoint of the range for Carbowax 4000 was taken to be the solubility parameter for PEGs. But, with the exception of PEG 1500, single value solubility parameters for PEGs were also reported in the literature and these values were included in the data for Table 2.6 for comparison. In all cases, the single point solubility parameters for PEGs fell within the solubility parameter ranges reported for Carbowax 4000. With the exception of PEG 600, the single point values showed reasonably good agreement with the midpoint of the solubility parameter range. The potential plasticizers (including the solid PEGs) were all classified as strongly-hydrogen bonded solvents because of the presence of hydroxyl groups. Consequently, solubility

parameter differences were calculated using the mid-range single value solubility parameters for PVP and HPMC in strongly hydrogen-bonded solvents.

Comparison of the data in Tables 2.5 and 2.6 show that, with the exception of ethylene glycol and glycerol, all the potential plasticizers had solubility parameters which fell within the practically determined compatibility limits for PVP. In the case of propylene glycol and the polyethylene glycols (with the exception of PEG 600) the solubility parameter difference was small. This implied almost ideal miscibility, since the heat of mixing would be so low, that the free energy change would be determined primarily by the positive entropy of mixing.

The solubility parameter differences for PVP with ethylene glycol and glycerol exceeded the apparent compatibility limits determined from Burrell's solvent spectrum. But it is well known that both ethylene glycol and glycerol are solvents for PVP, falling within the solubility limits defined by Fig. 2.5. The magnitude of the solubility parameter differences indicated that, in thermodynamic terms at least, they were poor solvents and dissolution occurred only because of specific interaction (presumably hydrogen bonding). The thermodynamic inferiority of solvents having a large solubility parameter is supported by observations (Blecher et al. (1983)) that methanol ($\delta = 29.7 \text{ (Jm}^{-3}\text{)}^{0.5}$) is a better solvent for PVP than water ($\delta = 47.9 \text{ (Jm}^{-3}\text{)}^{0.5}$).

With HPMC, the solubility parameter differences between the polymer and potential plasticizers (Table 2.6) indicated thermodynamic incompatibility or immiscibility in all cases apart from the PEGs. With the exception of PEG 600, the PEGs considered all exhibited solubility parameter differences which fell within the practical limits for compatibility.

2.3.3 Estimation of Flory-Huggins Interaction Parameters and Phase Separation Criteria

The solubility parameter approach offers a semi-quantitative

indication of compatibility based on the heat of mixing. It suffers, however, in that it does not readily quantify the degree of polymer-plasticizer interaction. In this respect the Flory-Huggins interaction parameter χ is important since it provides a quantitative index of interaction also taking account of the influence of plasticizer molar volume on compatibility. The Flory-Huggins interaction parameter characterises the degree of interaction between a polymer and a solvent or potential plasticizer. Where χ is less than the limiting value of 0.5, the theory predicts miscibility in all proportions. Values above 0.5 indicate progressively lower degrees of interaction between polymer and plasticizer and a greater tendency to phase separation. Where χ for a system exceeds a critical value χ_c , determined by the ratio of the polymer and plasticizer molar volumes, phase separation is assured. The critical interaction parameter χ_c and the associated critical composition ϕ_c at phase separation have been defined earlier (section 2.1).

In the present work, published data for the molecular weight and density of the polymers and plasticizers was used to calculate the respective molar volume ratios and estimate the critical values, χ_c and ϕ_c . This data for PVP K25, K90 and HPMC E5 with the potential plasticizers, is reported in Table 2.7.

Referring to Table 2.7 it can be seen that for both PVP K90 and HPMC, χ_c is small (tending to the limiting value of 0.5 with the monomeric glycols) and the critical composition ϕ_c is nearly all solvent. This is a consequence of the large molar volume ratios (m) for these polymers and the potential plasticizers. This is true even for the higher molecular weight PEGs which have considerably greater molar volumes than the monomers. PVP K25, in contrast, has a smaller molar volume and correspondingly smaller molar volume ratios with the plasticizers, particularly with the higher molecular weight PEGs. This is not significant for the monomer plasticizers, however, and χ_c still tends to 0.5 with a critical composition which is nearly all solvent.

Table 2.7 Phase Separation Criteria

Plasticizer	PVP K25			HPMC E5			PVP K90		
	m	χ_c	ϕ_c	m	χ_c	ϕ_c	m	χ_c	ϕ_c
Ethylene glycol	412	0.55	0.95	4677	0.51	0.99	16702	0.51	0.99
Propylene glycol	314	0.56	0.95	3560	0.52	0.98	12715	0.51	0.99
Hexylene glycol	179	0.58	0.94	2031	0.52	0.98	7253	0.51	0.99
Glycerol	314	0.56	0.95	3560	0.52	0.98	12715	0.51	0.99
PEG 200	130	0.59	0.92	1471	0.53	0.97	5254	0.51	0.98
PEG 400	65	0.63	0.89	732	0.54	0.96	2615	0.52	0.98
PEG 600	43	0.66	0.84	491	0.55	0.96	1752	0.52	0.98
PEG 1500	19	0.76	0.82	211	0.57	0.93	752	0.54	0.96
PEG 4000	7	0.95	0.73	79	0.62	0.97	282	0.56	0.94
PEG 6000	5	1.07	0.68	53	0.65	0.88	188	0.57	0.93

Note:

χ_c critical interaction parameter for phase separation

ϕ_c critical composition for phase separation (plasticizer volume fraction)

m polymer/plasticizer molar volume ratio

In the case of PVP K25 and the higher molecular weight PEGs, the molar volume ratio is considerably smaller. As a consequence, χ_c is larger and the critical composition contains a higher proportion of the polymer. Thus, the theory predicts that the plasticizers will be less soluble in PVP K25 than in PVP K90 or HPMC. Conversely, PVP K25 will be more soluble in the plasticizers than either PVP K90 or HPMC.

Table 2.8 reports the interaction parameters for PVP K25, PVP K90 and HPMC E5 with the potential plasticizers, calculated at 25°C using Equation (2.22). The value of the interaction parameter χ is determined by the sum of the enthalpy and the entropy contributions.

Table 2.8 Flory - Huggins Interaction Parameters for Potential Plasticizers and Polymeric Binding Agents

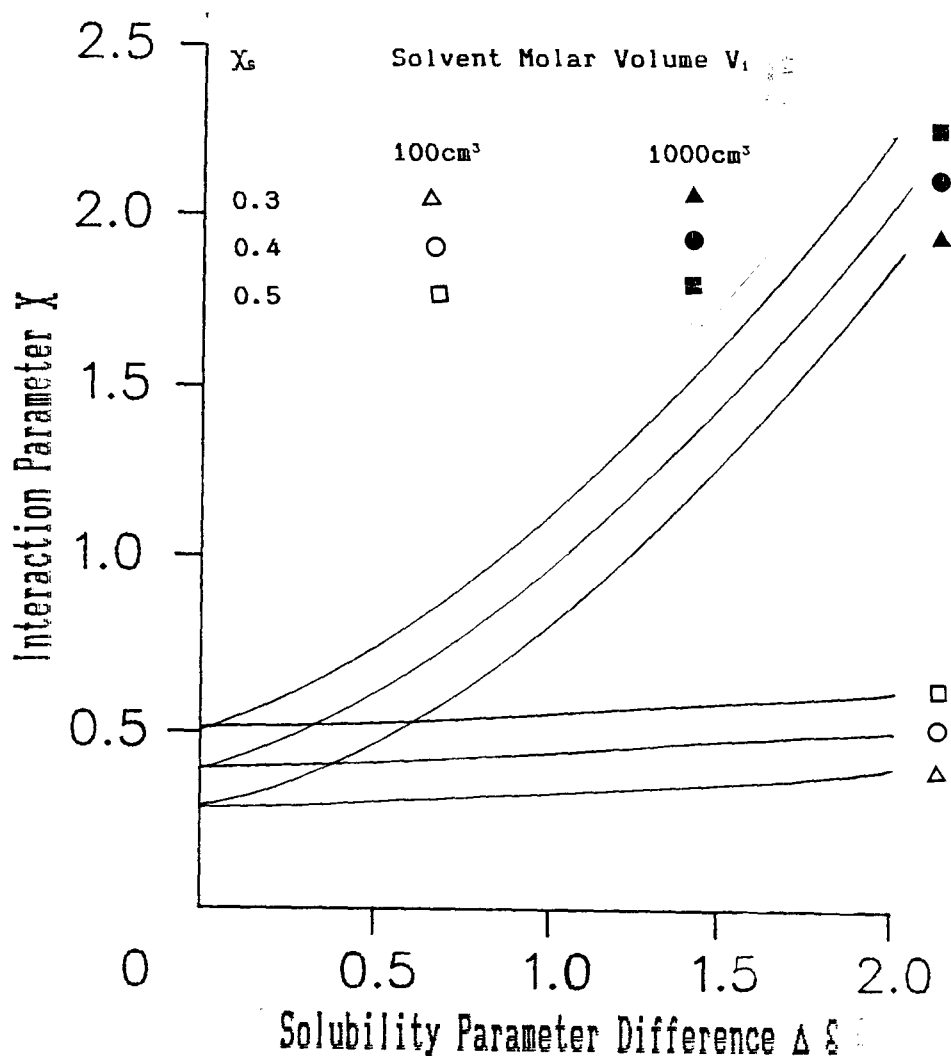
Plasticizer	Flory - Huggins Interaction Parameter (χ)					
	HPMC E5			PVP		
	χ_H	χ		χ_H	χ	
Ethylene glycol	1.04		1.44	0.65		1.05
Propylene glycol	0.21		0.61	0.05		0.45
Hexylene glycol	0.56		0.96	1.14		1.15
Glycerol	3.34		3.74	2.56		2.96
PEG 200	0.16	(0.03)	0.56	0.0007	(0.05)	0.4007
PEG 400	0.32	(0.001)	0.72	0.0014	(0.24)	0.4014
PEG 600	0.48	(1.45)	0.88	0.0021	(3.43)	0.4021
PEG 1500	1.12		1.52	0.005		0.405
PEG 4000	2.99	(0.48)	3.39	0.013	(0.85)	0.413
PEG 6000	4.49	(0.72)	4.89	0.02	(1.28)	0.42

Note:

χ_H is the enthalpic contribution to the total interaction parameter. Figures in parentheses are χ_H values determined using single point solubility parameters for PEGs.

Estimation of the enthalpy contribution χ_H is dependent only on the molar volume of the plasticizer and the assumptions implicit in the determination of the polymer and plasticizer solubility parameters. This value is given in Table 2.8 in addition to the total parameter. The magnitude assigned to the entropy contribution is, however, an estimate based on generic values reported for other systems and as such has no practical basis. Typically, χ_S is reported to have values in the region 0.3 - 0.5 and a value of 0.4 was therefore selected for the present work. The value chosen for χ_S may have a considerable influence on the magnitude of χ . Figure 2.8 illustrates the theoretical variation of χ with χ_S for different plasticizer molar volumes and solubility parameter differences.

Figure 2.8 Dependence of χ on χ_s , Solubility Parameter Difference and Solvent Molar Volume



The resulting plots lead to a number of observations. When the potential plasticizer is a relatively small molecule, the Flory-Huggins interaction parameter is highly dependent on χ_s and is relatively independent of any difference between the solubility parameter of polymer and plasticizer. In contrast, where the potential plasticizer has a large molar volume, the magnitude of the solubility parameter difference becomes critical. Small deviations of the plasticizer solubility parameter from that of the polymer result in a large interaction parameter irrespective of the value of χ_s .

Data presented in Table 2.8 suggest that none of the potential plasticizers are thermodynamically ideal for HPMC since, in all cases, the interaction parameter χ exceeded the critical value χ_c . The

results consequently predict that a mixture of HPMC with any of the plasticizers will form a two-phase system. The asymmetry of the theoretical phase equilibrium curve (Fig. 2.2) indicates that one phase will be almost pure plasticizer or solvent (polymer-poor), while the other will be a solution of the plasticizer in the polymer (polymer-rich). Depending on the magnitude of the interaction parameter, the molar volume ratio and the relative proportions of polymer and plasticizer, the amount of plasticizer in the polymer-poor phase may be so small as to be practically undetectable. The system may appear to be a compatible single phase although, in reality, two phases must be present.

The magnitude of the interaction parameters, and the phase equilibrium curves (Fig. 2.2) appropriate to the molar volume ratios suggest that PEG 200 and propylene glycol would exhibit the greatest apparent compatibility with HPMC. Hexylene glycol, ethylene glycol and the other liquid PEGs would be expected to exhibit a reduced but still considerable solubility in HPMC. In contrast, the large interaction parameters evident for glycerol and the higher molecular weight PEGs indicated that solubility of the plasticizer in the polymer would be far more limited. For the homologous series of polyethylene glycols, χ increased with increasing molecular weight consistent with decreasing solubility in HPMC.

With the exception of hexylene glycol, the potential plasticizers exhibited greater interaction with PVP than with HPMC as demonstrated by the lower values for the interaction parameter. Values of χ for PVP with the polyethylene glycols and propylene glycol were less than 0.5. This was indicative of thermodynamic compatibility or miscibility at all compositions. As with HPMC, the interaction parameter increased as the molecular weight of the PEGs increased. But this was insignificant due to the close similarity of the solubility parameters for PVP and the PEGs. Hexylene glycol, ethylene glycol and glycerol all had interaction parameters which exceeded the critical value χ_c indicating the probability of phase separation. χ values for hexylene glycol and ethylene glycol were considerably lower than for glycerol consistent with greater solubility in the polymer. The interaction parameters reported are identical for PVP K25 and K90 since the same solubility parameter was assigned in each case.

However, the lower polymer/plasticizer molar volume ratios in the case of PVP K25 would result in lower solubility of the plasticizer in the polymer for two-phase systems.

2.3.4 Intrinsic Viscosities

Intrinsic viscosities were determined using the single-point model developed by Rudin and Wagner (1975). The model assumes the existence of non-interpenetrating solvated polymer entities. Consequently solution concentrations used must be small to avoid intermolecular interference. The equations required to calculate $[\eta]$ are summarised below.

The volume fraction (\emptyset) of swollen polymer molecules in solution at a concentration C (g cm^{-3}) is given by:

$$\emptyset = (0.524 C \epsilon_0) / (0.524 \rho + C \epsilon_0 - 1) \quad (2.27)$$

ρ is the solid density of the polymer (g cm^{-3}) and ϵ_0 , the infinite dilution swelling factor, is given by:

$$\epsilon_0 = \rho [\eta] / 2.5 \quad (2.28)$$

The application of Equation 2.27 is limited to concentrations such that $0 < C < 0.524\rho$ because of the assumption in the model of a high concentration boundary condition corresponding to cubic packing of uniform spheres. The Newtonian flow of suspensions of polymeric spheres is described by:

$$\eta_0/\eta = 1 - 2.5\emptyset + 11\emptyset^5 - 11.5\emptyset^7 \quad (2.29)$$

where η_0 and η are solvent and solution viscosities respectively. If the ratio η_0/η is known at a single concentration, then Equation 2.29 can be solved for \emptyset . The resulting value and known C yield a value for ϵ_0 in Equation 2.27 and this enables $[\eta]$ to be obtained from Equation 2.28. Equations 2.27 and 2.28 can be combined to give:

$$[\eta] = \emptyset (1.31\rho - 2.5C) / (C \rho) (0.524 - \emptyset) \quad (2.30)$$

Equations 2.29 and 2.30 will therefore yield $[\eta]$ from known η_0/η and corresponding C.

The roots of Equation 2.29 may be solved, for example, by successive quadratic factorisation. Only one of the seven roots obtained is real, positive and in the range $0 < \theta < 0.524$ as required by the model. There is therefore no ambiguity in the value of θ required to yield $[\eta]$. In the present work, θ was determined by an algorithm written in BASIC for the BBC microcomputer. Equation 2.29 was evaluated using incremented values of θ within the limits 0 to 0.524 until agreement with experimentally determined values for η_0/η to a precision of ± 0.000001 was obtained. The value of θ obtained was then used, with the appropriate value for C, to give $[\eta]$ (Equation 2.30).

A number of workers have determined the value of the interaction parameter from determinations of the intrinsic viscosity of a polymer in various solvents. The method requires a knowledge of polymer properties which have been enumerated for very few polymers and as such the method is limited in its general applicability. However, the equation used (Equation 2.21) implies an inverse form of relationship between the interaction parameter χ and the intrinsic viscosity $[\eta]$. Determination of $[\eta]$ for the polymer-plasticizer systems used in the present work therefore provides a direct experimental check on the reliability of conclusions drawn from the interaction parameter data.

Intrinsic viscosities determined at 25°C for PVP and HPMC in the liquid plasticizers are reported in Table 2.9.

HPMC was insufficiently soluble in ethylene glycol, hexylene glycol or glycerol to allow viscosity measurements to be made. This is in excellent agreement with conclusions drawn from solubility parameter data and the magnitude of the interaction parameters. Intrinsic viscosity was maximal in PEG 200 and only marginally lower in propylene glycol. Increasing the molecular weight of the PEGs resulted in a reduction in the measured intrinsic viscosity. These results correlated directly with the degree of interaction determined from estimations of the Flory-Huggins interaction parameter.

Table 2.9 Single Point Intrinsic Viscosities of Some Polymeric Binders

Solvent/Plasticizer	Intrinsic Viscosity [η] (dl g ⁻¹)		
	PVP K25	HPMC E5	PVP K90
Ethylene Glycol	0.16	N/E	1.62
Propylene Glycol	0.23	0.58	1.88
Hexylene Glycol	0.21	0.49	1.60
Glycerol	0.15	N/E	1.55
PEG 200	0.24	0.60	1.93
PEG 400	0.21	0.56	1.69
PEG 600	0.17	0.51	1.11

N/E Not evaluated

Similar results were observed both for PVP K25 and PVP K90. The order of magnitude of difference in intrinsic viscosities for the K25 and K90 grades reflected their difference in molecular weight. With the PVPs, intrinsic viscosities were considerably lower with glycerol and ethylene glycol, in agreement with the magnitude of χ for these solvents.

2.3.3 Solid State Compatibility

The "acid test" of the thermodynamic approach to the problem of polymer-plasticizer compatibility is to determine whether predictions made on the basis of solubility parameters or interaction parameters are substantiated in practice. This involves the preparation of polymer-plasticizer mixtures and examining for evidence of phase separation. Suitable mixes may be prepared from the condensed state or melt, or by casting a film from a common solvent. The latter method was chosen in the present work using water (double distilled) as the solvent.

Some criteria for discerning compatibility have been defined by Bohn (1975). These are:

Transition temperature measurements: Where the polymer and plasticizer have glass transition temperatures (T_g) or melting points sufficiently far apart to be resolved by differential thermal analysis (DTA) or differential scanning calorimetry (DSC), then compatibility is indicated by the disappearance of the single component isotherms. Compatible blends therefore show a single T_g .

Optical Methods: Compatibility is indicated by the clarity of a film, cast from a homogeneous solution of the polymer-plasticizer. Films exhibiting no heterogeneity when examined under considerable magnification are considered to be compatible. Unlike transition temperature, the optical method offers the advantages of ease and simplicity.

The transition temperature method provides a relatively unambiguous method of assessing compatibility, although some blends may give complex thermograms which cannot readily be evaluated (Entwistle and Rowe, 1979). Bohn (1975) suggested that the optical method might prove ambiguous when polymer and plasticizer have the same refractive index. This limitation is rarely a problem in practice since phase-separated plasticizers may also be detected by tactile means. Visual and tactile methods form the basis of ASTMs D2383-69 and D3291-74 for the determination of plasticizer compatibility in PVC plastics.

Unplasticized HPMC E5 and PVP K90 readily formed continuous films which were perfectly transparent and homogeneous. PVP K25 was a much poorer film former, frequently cracking and crazing on drying, although film fragments were transparent and homogeneous. This was considered to be because of its considerably lower molecular weight. Coherent Starch 1500 films could only be formed after gelation and were translucent and inhomogeneous. Polymer films were also prepared with increasing levels of the potential plasticizers. The cast, dried films were evaluated visually and by tactile examination for evidence of incompatibility or phase separation. Incompatibility was defined as any reduction in film clarity (blooming) in comparison with the unplasticized controls or any oily exudation of the liquid

Plasticizers. The effective compatibility limit was then defined by the level of plasticizer incorporation (weight in weight) at which incompatibility was first detected. The observations, summarised in Table 2.10, indicated considerable differences in compatibility between the polymers and the plasticizers. Nevertheless, a number of general trends were evident.

Table 2.10 Binder - Plasticizer Compatibility in the Solid State

Plasticizer	Binder			
	HPMC	PVP K25	PVP K90	Starch 1500
Ethylene glycol	20E	C	C	50 (10E)
Propylene glycol	50E	C	C	50 (10E)
Hexylene glycol	30E	C	C	5B
Glycerol	20E	C	C	50 (10E)
PEG 200	50E	C	C	30 (10B)
PEG 400	40E	C	C	20 (10B)
PEG 600	30E	C	C	5B
PEG 1500	30B	5B	10B	5B
PEG 4000	20B	1B	5B	5B
PEG 6000	17.5B	0.5B	2.5B	5B

Key to symbols:

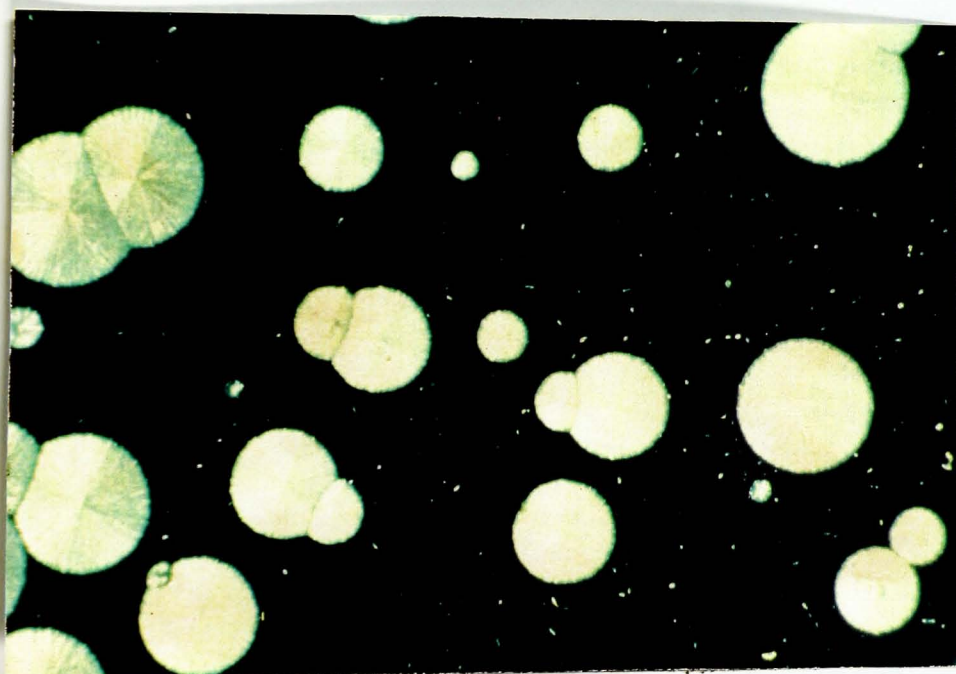
- C compatible (miscible) in all proportions
- B incompatible (film appears opaque or bloomed)
- E incompatible (plasticizer detectable as oily exudate, film clarity as control)

2.3.5.1 Solid State Compatibility of HPMC

HPMC was observed to be incompatible with all of the plasticizers considered, although the level of plasticizer at which incompatibility was detected varied between plasticizers. PEG 200 and propylene glycol exhibited the greatest "apparent" compatibility. Phase separation by exudation was detected only after inclusion of 50% plasticizer by

weight in the film. Phase separation for the other glycol monomers occurred at considerably lower levels. In the case of hexylene glycol exudation was noted at the 30%w/w inclusion level, while for glycerol and ethylene glycol this was reduced to 20%w/w. The apparent compatibility showed a consistent decrease with increasing molecular weight for the polyethylene glycols. Incompatibility with the solid PEGs was detected as an opaque bloom, although only PEG 6000 exhibited a lower compatibility limit than the liquid plasticizers. Inspection of the HPMC-solid PEG films indicated that the solid PEGs phase-separated as distinct crystal spherulites. These are illustrated in Fig. 2.9.

Figure 2.9 Phase Separation of PEG 1500 in Aqueous-Cast HPMC Films
(Viewed under crossed polarising filters)



From the arguments developed in preceding sections, it was expected that none of the potential plasticizers screened would be ideally compatible, i.e. miscible in all proportions with HPMC. On the basis of solubility parameter estimations, the glycol monomers were identified as non-solvents for HPMC unlike the polyethylene glycols. In the latter case, similarity between polymer and plasticizer solubility parameters was indicative of potential miscibility.

In all cases, the magnitude of Flory-Huggins interaction parameters calculated for HPMC and the potential plasticizers was greater than the limiting value of 0.5 or the critical value χ_c . Incompatibility, characterised by the formation of two-phase systems, was consequently not unexpected. However, because of the asymmetry of polymer-solvent phase diagrams, those plasticizers which were non-solvents could be soluble in the polymer to a considerable extent. Determinations of χ suggested that optimum interaction would be between HPMC and low molecular weight liquid PEGs and propylene glycol. These data agreed well with polymer-plasticizer interactions determined directly by intrinsic viscosity measurement, as would be expected from the interrelation of χ and $[\eta]$ (section 2.1.8).

Limits of apparent compatibility in aqueous cast films (Table 2.10) paralleled the estimated magnitude of the Flory-Huggins interaction parameters. This reflected the enhanced solubility of the plasticizer in the polymer at lower values of χ . The nature of the phase-solubility curve indicated that two phases must coexist even at compositions below that when phase separation was detected. But for plasticizers, such as PEG 200 or propylene glycol, the amount of plasticizer exuded was at such a low level as to be undetectable. The film compositions at which incompatibility was detected for HPMC - PEG 400 mixes and HPMC - PEG 4000 mixes, were in reasonable agreement with values determined using differential thermal analysis (Okhamafe and York, 1983). The high values of χ estimated for glycerol or the higher molecular weight PEGs were indicative of poor polymer-plasticizer interaction and low solubility of the plasticizer in the polymer (in addition to low solubility of the polymer in the plasticizer). This was confirmed by results of the solid state compatibility studies.

2.3.5.2 Solid State Compatibility of PVP

Both low (K25) and high (K90) molecular weight grades of PVP, exhibited complete compatibility with the glycol monomers and the low molecular weight liquid PEGs. In all cases, the films retained the clarity and homogeneity of the unplasticized controls. At plasticizer levels in excess of 50%w/w, however, the blends increasingly adopted the consistency of a highly viscous solution rather than an amorphous solid film. Solid PEGs were observed to be incompatible with PVP and, in common with HPMC, the apparent compatibility limit decreased with increasing PEG molecular. The greater compatibility of solid PEGs with PVP K90 compared with PVP K25 reflected the difference in molecular weight between the two polymers.

Only glycerol and ethylene glycol exhibited solubility parameter values (Table 2.6) outside of the range, as defined by Burrell's solvent spectra (1975), for PVP. On this basis alone, compatibility would be expected with all of the potential plasticizers except glycerol and ethylene glycol. Flory-Huggins interaction parameters for PVP with propylene glycol or the PEGs were calculated to be less than 0.5 indicating miscibility in all proportions. But, as noted earlier, the higher molecular weight solid PEGs proved to be incompatible with PVP in spite of their calculated low values for χ . This deviation from expected behaviour could arise from a number of factors such as the very low entropy of mixing for polymer blends or the propensity of solid PEGs for crystalline alignment. These factors, operating independently or in concert, tend to oppose ideal miscibility in polymer systems. Values of χ greater than 0.5 for PVP with ethylene glycol, hexylene glycol or glycerol indicated a progressive decrease in polymer-plasticizer interaction. This was substantiated by intrinsic viscosity measurements.

The total compatibility of glycerol and ethylene glycol with PVP was not expected in view of the solubility parameter differences and the relatively large values for χ . Similar discrepancies in the solubility characteristics of ethyl cellulose have been noted recently. Robinson (1989) observed that ethyl cellulose was soluble in ethanol and methanol with calculated χ values of 1.56 and 1.95 respectively. This behaviour is explained by the limitations of the solubility

parameter approach and the Flory-Huggins theory when specific polymer-solvent association occurs. Water, for example, dissolves PVP by forming hydrogen bonds with the oxygen group of the pyrrolidone ring. This reaction exhibits a negative heat of mixing which ensures complete miscibility. In the context of the present work, it seems probable that glycerol and ethylene glycol behave in an analogous manner.

2.3.5.3 Solid State Compatibility of Starch 1500

Starch 1500, consistent with its very poor solubility characteristics, exhibited the lowest compatibility with the potential plasticizers. Hexylene glycol and polyethylene glycols (with the exception of PEG 200 and PEG 400) caused blooming in cast films at loadings of only 5% w/w. Furthermore, incorporation of the "plasticizers" impaired film formation when compared with the unplasticized control. Starch films containing hexylene glycol or the solid PEGs were qualitatively weaker and showed a tendency to powder. Films containing PEGs 200 and 400 at levels up to 30%w/w and 20%w/w respectively, at first appeared identical in appearance to the unplasticized control. Similarly propylene glycol, ethylene glycol and glycerol inclusion at levels up to 50%w/w appeared compatible at first. However, after storage for one week under ambient conditions, phase separation was apparent in films containing 10%w/w or more of the above mentioned potential plasticizers. In the case of the PEGs this was evident as blooming, whereas exudation of glycerol, propylene glycol and ethylene glycol occurred. This may be due to a synerisis-type response. Tactile evaluation suggested that the extent of exudation was lower for glycerol than for propylene glycol or ethylene glycol.

The poor miscibility of Starch 1500 with the potential plasticizers is consistent with the strong intermolecular forces associated with a high degree of polymer crystallinity. Plasticization of such polymers is generally limited. It appears likely, therefore, that satisfactory plasticization of Starch 1500 will not be feasible in practice.

2.4 Conclusions

For a plasticizer to modify effectively the mechanical properties of a polymer, the two components must be brought into intimate, molecular mix. The miscibility of a polymer and plasticizer is essentially determined by the same considerations which apply to non-polymeric solutes and solvents, i.e. the free energy of mixing must be negative. This condition is achieved when the net balance of the heat of mixing and the entropy of mixing is negative. This is favoured by a large positive entropy change or a large negative heat of mixing. As a general observation, the converse situation is true for mixtures involving polymers. It was possible to estimate the configurational entropy of mixing, for mixtures of PVP or HPMC with potential plasticizers, by means of the lattice model discussed in section 2.5. The entropy change for polymer-plasticizer mixes was considerably smaller than for analogous aqueous solutions, decreasing significantly with increasing plasticizer molar volume. It was inferred from these results that the sign and magnitude of the free energy of mixing would be determined primarily by the heat of mixing. On this basis even small positive heats of mixing would lead to immiscibility

According to the theory of Regular Solutions proposed by Hildebrand and Scott (1950), the heat of mixing for two components will be zero when their solubility parameters are the same. Under such conditions, miscibility will be assured even when the entropy of mixing is very low. Using Burrell's solubility spectra (1975), supplemented by manufacturers solubility data it was possible to estimate the effective solubility parameters of PVP and HPMC in solvents of differing hydrogen-bonding propensity. PVP was soluble in solvents which were poor, moderate or strongly hydrogen bonded across a wide range of solubility parameters. The solubility parameter requirements for HPMC were much stringent and, while solubility in some moderate and strongly hydrogen bonded solvents was observed, solubility in poorly hydrogen-bonded solvents was precluded. Starch 1500 exhibited exceedingly limited solubility even in strongly hydrogen-bonded solvents. This was a result of the crystalline nature of starches and, as a consequence, it was not possible to estimate the solubility parameter of Starch 1500.

Using published values for the relative fractional dispersion, polar and hydrogen bonded solubility parameters for known solvents and non-solvents, the solubility characteristics of the polymers could be represented by ternary solubility diagrams. This had the advantage of highlighting those solvent characteristics essential for miscibility or compatibility. It was noted that solvents of the same solubility parameter and nominal hydrogen-bonding propensity could either be solvents or non-solvents, depending on their relative fractional solubility parameters.

On the basis of solubility parameters, monomer glycols were identified as non-solvents for HPMC. This implied that their potential as plasticizers would be limited by incompatibility. PEGs exhibited single-point solubility parameters which were similar to that for HPMC and there was considerable overlap of the solubility parameter ranges. PEGs were expected to be better solvents for HPMC and, consequently, to exhibit greater compatibility as plasticizers. Solubility parameter data for PVP indicates compatibility with all the plasticizers considered with the exception of ethylene glycol and glycerol. The latter solvents have solubility parameters which exceed the range defined by Burrell (1975) although, in practice, PVP is soluble in both. The apparent failure of the theory is a consequence of the limits imposed on the range of solvents comprising the solubility spectra. Dissolution in solvents which exhibit very high cohesive energy densities, such as ethylene glycol or glycerol, almost certainly proceeds via interactions involving a negative heat of mixing. The basis of the determination of polymer solubility parameters by the solubility approach is thus invalidated. Other workers, have used solvents covering wider ranges of solubility parameter but these were not used for the aforementioned reason.

Solubility parameters for HPMC determined in present work show reasonably good agreement with the value determined from molar group attraction constants (Rowe et al. 1986). To date, no comparable values have been published for PVP so a similar comparison could not be made.

The lattice model for polymer dissolution provides a complementary approach to the problem of polymer plasticization. The theory (by

means of the Flory-Huggins parameter, χ) enables a quantitative evaluation of the interaction between a polymer and a diluent such as a solvent or plasticizer. The theory also defines the conditions under which a mixture of the two components will exist as a single compatible phase or will separate into two immiscible phases.

In the present work it was not possible to determine χ directly, but estimations were possible using data for the polymer solubility parameter, the polymer and plasticizer molar volumes and an assumed value for the entropic contribution to χ . Data for HPMC indicates that none of the potential plasticizers are thermodynamically ideal since, in all cases, χ exceeds the limiting critical value of 0.5. This supports the qualitative predictions based on solubility parameters alone.

It is apparent from the asymmetry of the polymer-solvent phase equilibrium diagram, that non-solvents for a polymer may dissolve in the polymer to a considerable degree. This has important consequences for the case of plasticization, since plasticizers which are thermodynamically incompatible may nevertheless facilitate some modification of the mechanical properties of the polymeric matrix.

It is clear from the preceding work that the use of high molecular weight PEGs as plasticizers for PVP, HPMC or Starch 1500 is thermodynamically unsound. The low entropy of mixing and the size and crystallinity of solid PEGs all act to oppose miscibility. The latter factor is probably of greatest importance and is likely to lead to complex effects in films. Thus, although high molecular weight PEGs apparently soften HPMC films, i.e. reduce the Brinell hardness, the Young's modulus of elasticity may exceed that of the unplasticized film (Rowe, 1976a). Masilungen and Lordi (1984) using penetration mode thermomechanical analysis showed that PEG 4000 was more efficient than propylene glycol in reducing the softening temperature of HPMC films. PEG 4000 was incorporated at levels at which, from the present work, crystallisation could occur so it seems likely that the softening measured would be a function of PEG crystalline melting in addition to HPMC softening. In general terms, then, it is clear that while similarity of the polymer and plasticizer solubility parameters

sufficient when either component has significant crystalline order.

From the preceding thermodynamic considerations and the results of solid state compatibility testing, PEG 200 has been identified (from those screened) as the optimum potential plasticizer both for HPMC and PVP. In contrast, the limited compatibility of Starch 1500 with any of the potential plasticizers suggests that satisfactory plasticization may be unattainable.

The practical objectives of plasticization are, of course, to increase the ductility, flexibility, extensibility and workability of a polymer. Compatibility or miscibility of polymer and plasticizer at the molecular level is a necessary pre-condition to achieve this. But knowledge of the extent of miscibility or the molecular interaction involved, does not enable any prediction or inference of the degree of mechanical modification which may be achieved. A number of methods have been employed to characterise the mechanical properties of a polymer-plasticizer matrix. Tensile mechanical testing is one such method which is relatively simple in application but enables quantification of a number of fundamental properties. The influence of plasticizer type and level of incorporation on the tensile properties of polymeric tablet binders, consequently forms the subject of the following chapter.

CHAPTER THREE

THE INFLUENCE OF PLASTICIZATION ON THE TENSILE PROPERTIES OF POLYMERIC TABLET BINDERS

CHAPTER THREE

THE INFLUENCE OF PLASTICIZATION ON THE TENSILE PROPERTIES OF POLYMERIC TABLET BINDERS

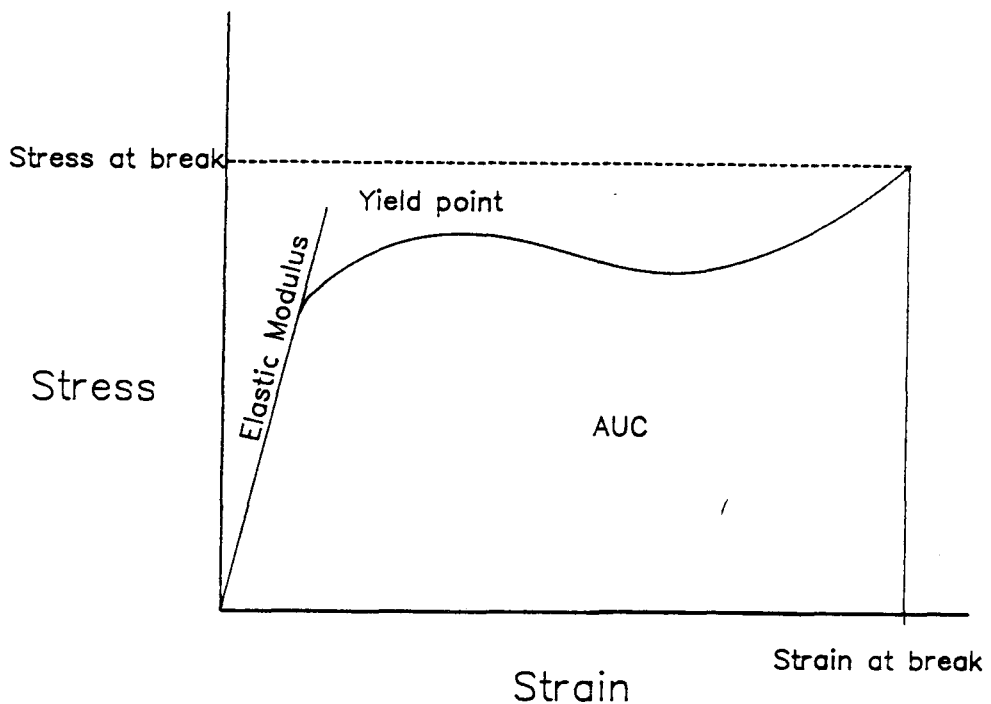
3.1 Mechanical Properties of Polymers and Their Measurement

Most real materials, when subjected to some external stress, deform in a manner which has the characteristics both of elasticity and plasticity. Banker (1966) considered that the mechanical strength and bonding ability of polymers arose from forces of cohesion within the material and adhesion between the material and its substrate. The magnitudes of these forces depend on the molecular size and structure of the polymer. Intermolecular forces are generally very much weaker than intramolecular forces, but polymers of sufficiently high molecular weight may give rise to large numbers of intermolecular bonds resulting in high cohesive strength. The observed mechanical properties of polymers are a function of "free volume" (discussed in Chapter four) and thus will be modified by the presence of diluent molecules (plasticizers and residual solvents) and environmental temperature (Ferry, 1961). Depending on environmental temperature or composition, the mechanical properties of high molecular weight polymers may range between an almost ideal elastic state to an almost Newtonian viscous state. The observed properties will also be dependent on the test methodology, particularly strain rate.

For high polymers there are five distinctly different regions of viscoelastic behavior; glassy, transition, rubbery, rubbery liquid, and liquid (Toblosky, 1971). While the change between regions is, in some respects, analogous to a phase change in true solids or liquids, it is not sharply defined and is gradual. Whereas temperature and pressure are the independent variables for phase change, temperature and strain rate (or duration of straining) are responsible for viscoelastic transitions. True plasticization results in a lowering of the glass transition temperature (T_g) of the polymer-plasticizer blend. The influence of plasticization on the observed viscoelastic behaviour can therefore be interpreted in a manner analogous to the effect of increasing temperature.

Quantification of deformation, for example by measuring the elongation of a material with increasing tensile load, enables information about fundamental mechanical properties to be derived. Figure 3.1 shows a typical plot of strain against applied stress (usually derived from a plot of displacement against applied force) for a material tested to failure in tension.

Figure 3.1 Typical Plot of Applied Stress Against Strain for a Material Tested to Failure in Tension



Analysis of the plot allows the determination of a number of mechanical properties. The initial linear portion of the curve indicates that the deformation obeys Hooke's law, i.e. the induced strain is directly proportional to the applied stress. The modulus of elasticity, or Young's modulus (E), is obtained from the slope of the regression of stress (σ) on strain (ϵ):

$$E = \frac{\sigma}{\epsilon} \quad (3.1)$$

When a material is stressed beyond its elastic limit it may fail

directly or it may continue to deform in a non-linear manner. Some materials, although not all polymers, show a distinct yield point, i.e. the first point on the stress-strain curve at which an increase in strain occurs without an increase in stress. By convention the yield strength, a measure of a material's resistance to permanent deformation, is defined:

$$\text{Yield Strength} = \frac{\text{force at yield point}}{\text{original cross-sectional area of test sample}} \quad (3.2)$$

The yield strength may also be defined in terms of the stress at which a material exhibits a specified limiting deviation from the proportionality of stress to strain. The ultimate tensile strength (UTS) is determined from the maximum applied force:

$$\text{UTS} = \frac{\text{maximum force before failure}}{\text{original cross-sectional area of test sample}} \quad (3.3)$$

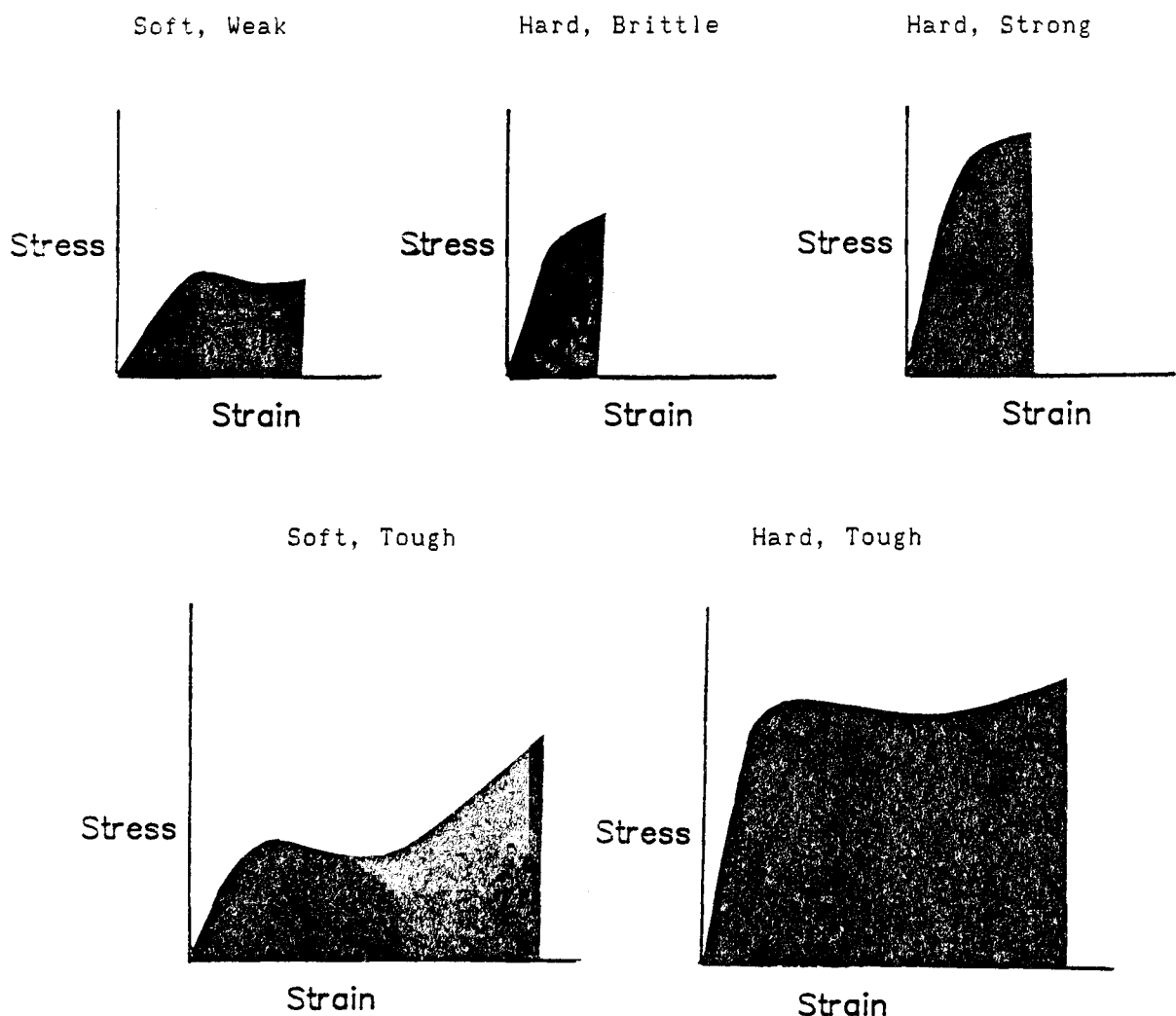
Where the maximum force occurs at the yield point, the ultimate tensile strength is termed "tensile strength at yield". Similarly, where the maximum force occurs at the break point, the ultimate tensile strength is termed "tensile strength at failure or break". A measure of the overall extensibility of the material is obtained from the strain (often expressed as a percentage) at failure. The area under the stress-strain curve (AUC) is a measure of the material's toughness and is equal to the work expended in straining unit volume of the sample to failure.

Different materials may exhibit different characteristic stress-strain relations. A number of workers (Carswell and Nason, 1944; Lever and Rhys, 1968) have classified material properties on the basis of their characteristic stress-strain curves. The classification of Lever and Rhys (1968) is given in Table 3.1. Stress-strain curves typical of these types of material are shown in Fig. 3.2.

Table 3.1 Classification of Material Properties on the Basis of Tensile Deformation (after Lever and Rhys, 1968)

Material classification	Yield point	Strain at failure	Modulus of elasticity
Soft, weak	low	low	low
Soft, tough	low	high	low
Hard, brittle	not defined	low	very high
Hard, strong	high	moderate	high
Hard, tough	high	high	high

Figure 3.2 Characteristic Stress-Strain Curves For Different Types of Materials (After Carswell and Nason, 1944)



In the case of high polymers, the five distinct regions of viscoelastic behavior may be characterised by the type of stress-strain curve exhibited by a polymer in a particular region. At low temperature, i.e. below the glass transition region, or at very high strain rates a polymer behaves as an elastic glass. Tensile strength and elastic modulus are relatively high, but extensibility is low. As the temperature is raised, the polymer enters the transition region. Tensile strength and elastic modulus are decreased, but extensibility is increased. Polymers in this region, may show a ductile type of stress-strain curve, characterised by an elastic portion, a sudden fall-off of stress with increasing strain; then as strain is increased further the stress increases again. This process may be accompanied by the formation of a neck in the sample and is called cold-drawing. As the temperature is increased further (or strain rate is decreased) the polymer enters a region called the rubbery plateau. In this region long segments of the molecular chain are free to move, but they are constrained from slipping relative to each other by cross-links or entanglements. In the rubbery state, the polymer may be capable of undergoing considerable extension but, on removal of stress, returns to its original state. At still higher temperatures, the region of rubbery flow is attained. The polymer remains elastic and rubbery, but also has a finite component of plastic flow due to failure of cross-links or disentanglement. Finally, at the highest temperatures or after long periods of straining, nearly all cross-links and entanglements are uncoupled and the polymer flows as a viscous liquid.

3.2 Mechanical Properties of Pharmaceutical Polymers

The physical and mechanical properties of polymers of pharmaceutical interest have been examined by a number of workers. Much of this work has been carried out to assess film coating materials. Several papers have, however, addressed the relationship between mechanical properties and the performance of polymeric tablet binders.

3.2.1 Tensile Properties of Unplasticized Polymers

Munden et al., (1964) investigated the tensile properties of cast

films of vinyl, acrylic and cellulosic polymers. They reported that the quantity and nature of residual solvent in the films affected the mechanical properties, although no detailed results were given.

Healey et al., (1974) produced the first significant paper characterising the tensile mechanical properties of hydrophilic polymers used as pharmaceutical tablet binders. Using the classification of Carswell and Nason (1944) they determined that the stress-strain curves for PVP (K29-32) and acacia were characteristic of weak materials; gelatin curves were characteristic of a hard, strong material, whilst curves for methylhydroxyethyl cellulose and starch were characteristic of hard, tough materials. The effect of moisture content on the properties of the polymers varied with the type of polymer and with the transition between bound and free water.

Reading and Spring (1984a) investigated the effect of tensile strain rate and film curing temperature, as well as moisture sorption, on the mechanical properties of cast films of some polymeric tablet binders (gelatin hydrolysate (Byco C), maize starch, methyl cellulose (Methocel A15) and PVP (40,000 Da)). PVP was shown to have significantly lower values for Young's modulus, ultimate tensile strength and toughness than the other three binders. Methylcellulose, however, exhibited significantly greater values of ultimate tensile strength, toughness and strain at failure. Both the strain rate and film moisture content (controlled by conditioning humidity) had significant effects in most cases. Increased moisture content was generally associated with a weakening of the films. An increase in strain rate resulted in a rise in Young's modulus, except for PVP which was unchanged, and a decrease in strain at failure. With the exception of PVP, which was unaffected, drying the films at 60°C rather than 20°C increased the film brittleness.

Ononokpono and Spring (1988a) studied the tensile properties of methylcellulose and gelatinised maize starch films over a range of thicknesses from 6 to 70 μm . They found there was a linear relation between film thickness and tensile strength, toughness, elastic resilience and elongation at failure. Young's modulus increased with decreasing film thickness particularly for films with a thickness less than 15 μm . They concluded that, since binder films within a tablet

granulation would have a thickness of only 0.1 to 0.2 μ m, they would be much weaker and more brittle than implied from previous tests on thicker films.

Comparison of the results of various studies is limited since, as Lever and Rhys (1968) noted, the properties of polymers cannot be compared when different test protocols are used to determine them. Other workers have remarked on the difficulties in extrapolating the results of free-film studies to the mechanical behaviour observed in a real system (Allen et al., 1972). Banker et al., (1966) suggested that free-film evaluation should not be the sole criterion for accepting or rejecting potential film coating materials. In contrast, Kanig and Goodman (1962) and Hawes (1978) made the important point that there are considerable benefits in studying free films in the absence of other variables. Zatz et al., (1968) considered that free films only provided a model for evaluating gross properties, giving limited information on the molecular interactions which determined those properties. They suggested that the study of insoluble monolayer films at the air/water interface would give more fundamental information, but presented no results for such studies. Mendes (1968) also considered that techniques for evaluating binders in isolation from tablet systems were unreliable. No evidence or comparisons were offered to substantiate this view.

Radebaugh et al., (1988) suggested that data obtained from puncture and shear tests would complement the information obtained from more commonly used tensile tests.

3.2.2 Effects of Plasticizers on The Tensile Properties of Polymers

Plasticization is often necessary to improve both the workability and the servicability of a polymer. This is true for many film coating polymers. Wells et al., (1982) and Krycer et al., (1983) have also demonstrated improved tableting performance for PVP binder, through the inclusion of potential plasticizers. The bulk of information on the plasticization of pharmaceutical polymers continues to relate mainly to film coating.

Porter and Ridgway (1977) observed that the inclusion of increasing amounts of diethyl phthalate resulted in a decrease in the ultimate tensile strength of some enteric coating polymers. Hawes (1978) reported the plasticization of HPMC by glycerol and PEG 400. Entwistle and Rowe (1979) studied the influence of chain length (for a series of dialkyl phthalates) and molecular weight (for a series of ethylene glycol derivatives) on the mechanical properties of ethylcellulose and HPMC respectively. A correlation was found between the intrinsic viscosity of polymer/plasticizer solutions and the tensile strength, strain at failure and work of failure of cast films. Within an homologous series of plasticizers, the magnitude of the mechanical properties exhibited a minimum when the intrinsic viscosity was at a maximum. No such correlation was found with plasticizers of different structures. A reduction in the tensile strength of ethylcellulose films with increasing content of diethylphthalate was observed by Vemba et al., (1980). In contrast, they found little change with the addition of glycerol, soya oil or PEG 400. Delporté (1980) observed a reduction both in the elastic modulus and the limit of elastic deformation as the level of PEG 400 or propylene glycol in HPMC films was increased. Reductions in the strength of sprayed HPMC films with increasing concentrations of propylene glycol, glycerol, PEG 400 or PEG 4000 were reported by Porter (1980).

The effects of glycerol inclusion, polyethylene glycol inclusion and moisture sorption on tensile properties of cast HPMC films was reported by Aulton et al., (1981). Incorporation of glycerol resulted in a reduction in the tensile strength and elastic modulus and an increase in extensibility. The magnitude of the effects increased as the level of glycerol was increased. Similar effects were observed with PEG inclusion but plasticization efficiency increased with decreasing PEG molecular weight, possibly due to the greater number of plasticizer molecules available to interact with the polymer. Conditioning the films at high humidity resulted in significant changes in the mechanical properties consistent with a plasticizer action. The plasticization of acrylic copolymer films, prepared from pseudo-latex aqueous dispersions, by inclusion of different glycols was observed by Dittgen (1984). He also concluded that plasticization efficiency increased with decreasing glycol molecular weight.

Okhamafe and York (1983) observed that increasing concentrations of PEGs 400 and 1000, progressively lowered the tensile strength and Young's modulus of cast HPMC films. The addition of polyvinyl alcohol (PVA) lowered the tensile strength and Young's modulus although to a lesser extent than the PEGs. PEGs generally increased the extensibility of the films while PVA reduced it implying that, unlike PEGs, PVA inhibited polymer chain mobility. PEG 400 was found to be a more effective plasticizer than PEG 1000, in agreement with the earlier findings of Entwistle and Rowe (1979) and Aulton et al., (1981).

Reading and Spring (1984b) observed that PEG 600, included as a potential plasticizer, showed no evidence of plasticization in cast films of four polymeric tablet binders. Cast films containing PEG 600 at concentrations up to 10% w/w were, without exception, weaker, less extensible and had a higher Young's modulus than the unmodified films.

3.2.3 Effects of Other Inclusions on Tensile Properties of Polymers

The effect of non-plasticizer inclusions on the tensile properties of pharmaceutical polymers has been investigated primarily with respect to film coating formulation. This is also of relevance to the performance of binders used in wet-massed granulation since dissolution of drug or excipients in the binder solution, and redeposition during drying, may affect the subsequent performance of the binder.

A decrease in the tensile strength of cast HPMC films with increasing content of titanium dioxide was noted by Hawes (1978) although the inclusion of a water-soluble dye had no significant effect. Porter (1980) found a significant reduction in the tensile strength of sprayed HPMC films with increasing inclusion of titanium dioxide and also with the inclusion of an aluminium lake. Delporte (1980) found that increasing the titanium dioxide content of HPMC films resulted in a increased modulus of elasticity but little change in the limit of elasticity. Abdul-Razzak (1980) showed a marked reduction in the work of failure of HPMC films with increased solids content. There was a general shift towards a more brittle state.

Reading and Spring (1984b) examined the effects of lactose and sodium lauryl sulphate on the tensile properties of films prepared from four polymeric tablet binders. The inclusions resulted in a reduction of the ultimate tensile strength of all the binders tested, and made some films of PVP and starch too brittle to test.

Tobolsky (1971) suggested that filled or pigmented polymer films might be analysed in a manner analogous to suspensions. Rowe (1983), using this concept, applied a modified Einstein equation to calculate modulus enhancement in pigmented HPMC tablet film coating formulations. Okhamafe and York (1984, 1985) observed that the inclusion of pigments or fillers, talc and titanium dioxide, generally reduced tensile strength and extensibility while increasing Young's modulus of HPMC films. The magnitude of the effect was a function both of filler morphology and of filler-polymer interaction. The latter was characterised in terms of an acid-base proton transfer concept.

Dittgen (1984) observed that the inclusion of some drugs resulted in a plasticization action on acrylic copolymer films, while others produced films which were significantly more brittle than the parent polymer.

3.3 Materials and Methods

3.3.1 Materials

The polymeric binders, HPMC, PVP K90 and Starch 1500, used in the previous chapter were also used in the investigation of tensile properties. PVP K25 was not investigated because of its very poor film forming characteristics. Potential plasticizers, including the low molecular weight liquid PEGs and glycol monomers, were selected from those screened on the basis of interaction and compatibility results presented in the previous chapter. Thus, the higher molecular weight solid PEGs were not evaluated in HPMC or PVP films on the grounds of their poor compatibility and tendency to phase separate. Similarly, hexylene glycol and PEGs of molecular weight 400 or higher were not evaluated for the plasticization of Starch 1500.

3.3.2 Methods

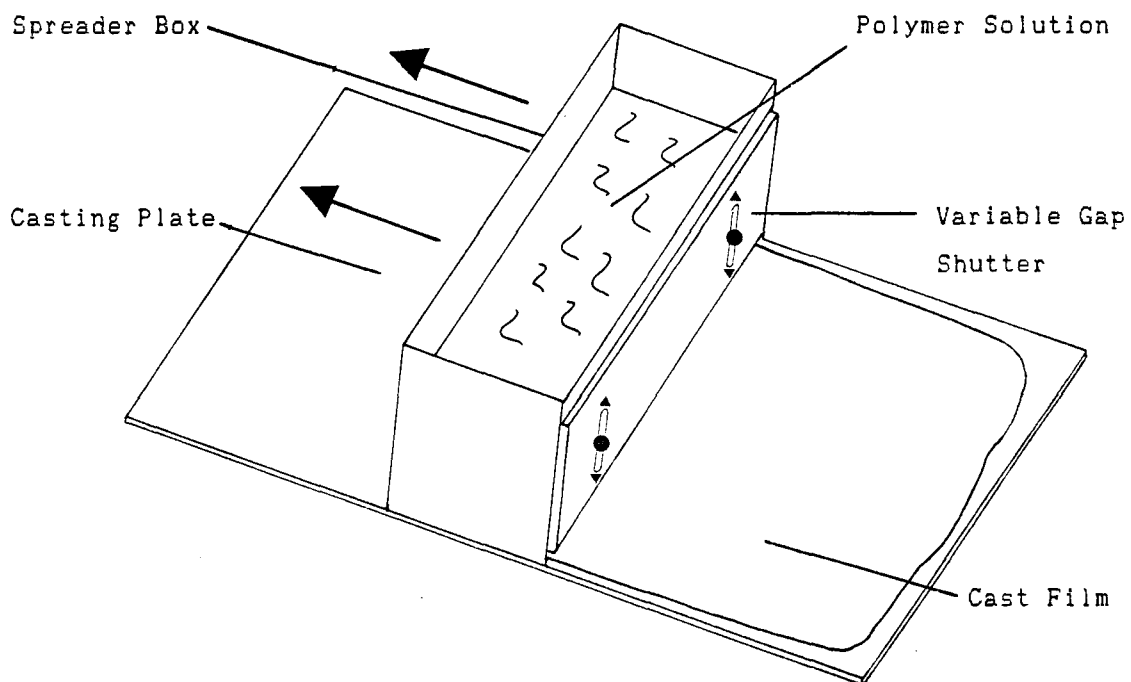
The observed tensile mechanical properties of a material may vary with the method of specimen preparation and with the speed and environment of testing. Consequently, where precise comparative results are required these factors must be carefully controlled. The presence of defects in specimens for tensile testing act as sites for stress concentration, causing erroneous results due to early fracture. Rigid, thick specimens are commonly prepared in a "dumbbell" shape to eliminate stress concentrations at the grips and to confine the failure zone (ASTM D 638). In the case of thin plastic sheets and films, however, the specimen cannot support an ordinary extensometer, and the actual gauge length of the specimen is made uncertain by the curvature in the edges of the dumbbell shape. ASTM D 882 standard test methods for tensile properties of thin plastic sheeting, therefore specifies that the test sample should consist of strips of uniform width and thickness. Test specimens should have a nominal width of between 5.0mm and 25.4mm. A width-thickness ratio of at least eight should be used since narrow specimens magnify the effects of edge strains or flaws. The test method advises that the utmost care should be taken in the cutting of specimens to prevent nicks and tears which would tend to cause premature failure by tearing or shear. In the present study, the test methods of ASTM D 882 (1980 revision) were adopted, to assure standardisation and reproducibility of the tests.

3.3.2.1 Film Preparation

Binder solutions, with or without the inclusion of potential plasticizers, were prepared as described previously (Chapter Two, section 2.2.7) for the solid-state compatibility studies. Preliminary studies were carried out to identify suitable substrates on to which the binder films could be cast. A suitable surface would be adequately wetted by the binder solution, whilst allowing removal of the dried film without excessive damage. Degreased scratch-free glass plates were found to be suitable both for HPMC and Starch 1500. PVP adheres too strongly to glass and cast films were subject to damage on attempt to remove them. Polymethyl methacrylate (Perspex) was eventually identified as a suitable substrate for the casting and successful removal of PVP films.

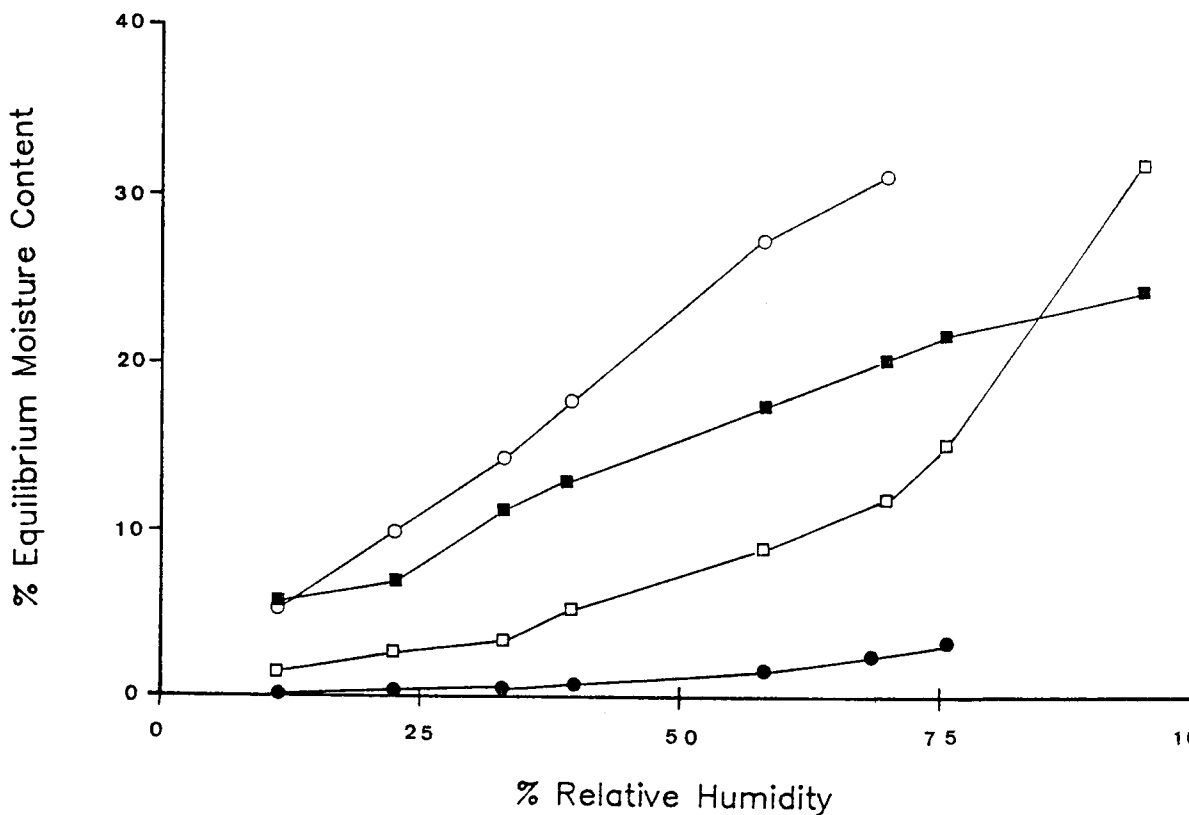
Films were cast using the specially constructed spreader box (similar to a spreader for TLC chromatography plates) shown in Fig. 3.3. A variable gap shutter enabled films of varying thicknesses to be cast. Empirically, it was established that a spreader gap of about 1.0mm resulted in dried polymeric films with thicknesses in the range 80 to 100 μ m. Films were dried overnight at ambient temperature and relative humidity (20 - 25°C, 45 - 55% RH) in a laminar flow cabinet to minimise the risk of dust contamination of the films. Film strips of 6.5mm width were cut with a steel template using a surgical scalpel. For each polymer-plasticizer combination, not less than five test strips were cut, both along the axis of casting and normal to the axis of casting. Cut films were checked for thickness at four points over the gauge length (40.0 mm) using a dial micrometer (Mercer,). Films showing any variation in thickness greater than 5 μ m were rejected, as were any films showing entrapment of air bubbles or dust, or any nicks or flaws, particularly along the cut edge.

Figure 3.3 Film Casting Apparatus



Films were conditioned prior to testing by storage for seven days in hygrosats over saturated solutions of either potassium acetate or sodium bromide, at a temperature of 20°C. These solutions maintained relative humidities of 22.5% and 59.5% respectively (Nyquist 1985). Equilibrium moisture sorption curves for the polymer batches used in this work (determined by the methods of Callaghan et al., 1982), are shown in Fig. 3.4. Data for sucrose, a non-polymeric crystalline binder, was also included. The tensile properties of sucrose were not studied because it fails to form coherent films. But use of this material was made in some later studies.

Figure 3.4 Equilibrium Moisture Sorption Curves for the Polymers



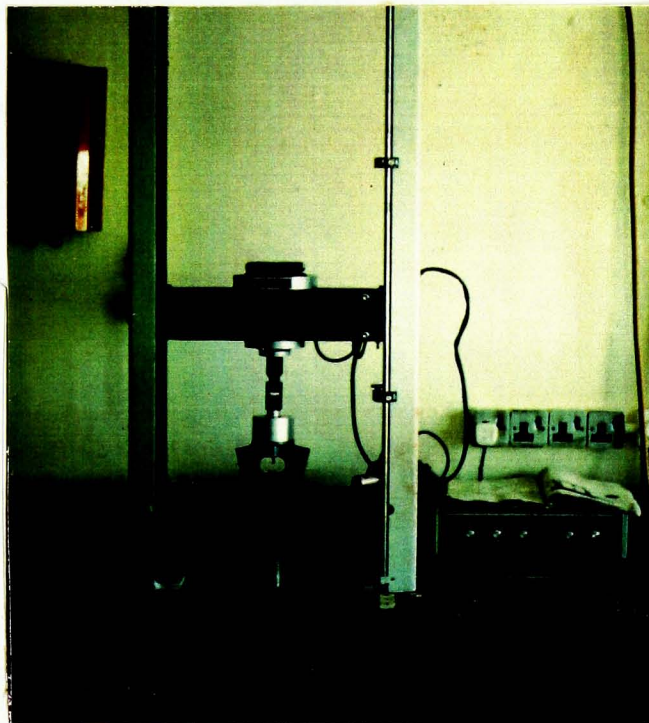
Binder

PVP K90	○	HPMC E5	□
Starch 1500	■	Sucrose	●

3.3.2.2 Tensile Testing

Conditioned film samples were tested to failure in tension using an Instron 1026 tensometer (Instron, High Wycombe, Bucks, UK) shown in Fig. 3.5.

Figure 3.5 The Instron 1026 Tensometer



The test strips were mounted in standard compression grips, lined with double sided adhesive tape to minimise slippage and uneven stress distribution. The test conditions used are summarised in Table 3.2.

Table 3.2 Summary of Tensile Testing Conditions

Load Cell type 2512-117	50 N fullscale
Strain Rate	5 mm min ⁻¹
Gauge Length	40 mm
Chart Speed	200 mm.min ⁻¹
Chart Magnification Ratio	40
Film thickness	80µm - 100µm nominal
Film width	6.5 mm
Equilibration Conditions	22.5% RH at 20°C 59.5% RH at 20°C

In order to prevent re-equilibration of film specimens during the testing procedure, the relative humidity during testing was maintained at the same value as that for the conditioning of the samples. This was achieved by enclosing the Instron crosshead and sample grips within a portable environmental chamber ("Atmos Bag", Sigma Chemicals) containing the required saturated salt solution. Test films were introduced into the Atmos Bag in their equilibration hygostat. The bag was then resealed and allowed to re-equilibrate to the required relative humidity. Glove ports in the Atmos bag allowed subsequent manipulation and testing of specimens without exposure to ambient humidity. Testing was carried out under conditions of ambient temperature which fell within the range 20°C to 25°C.

Specimens failing at some obvious flaw or at the grip contact point were discarded and retests made. For each successful tensile test, Young's Modulus, yield strength (where clearly defined), ultimate tensile strength and percentage strain at failure were calculated as described in section 3.1. The work required to cause failure in the specimen, was determined from the mass of chart paper corresponding to the area below the force-displacement curve and the film thickness. This was compared against the mass of paper corresponding to a standard work of failure of 5 MJm^{-3} for a film of $100\mu\text{m}$ thickness.

The rate of grip separation during tensile testing was calculated according to ASTM D 882 by the equation:

$$A = B \times C \quad (3.4)$$

where A is the rate of grip separation (mm.min^{-1}), B is the initial grip separation or gauge length (mm) and C is the initial strain rate ($\text{mm.mm}^{-1}\text{min}^{-1}$). For modulus of elasticity determination and/or percentage elongations at break of up to 20%, C is specified as $0.1 \text{ mm.mm}^{-1}\text{min}^{-1}$. With a gauge length of 40 mm, the required rate of grip separation was 4 mm.min^{-1} . Since this was unattainable on the Instron tensometer, the nearest alternative of 5 mm.min^{-1} was used throughout.

3.4 Results and Discussion

3.4.1 Tensile Mechanical Properties of Unplasticized Binders

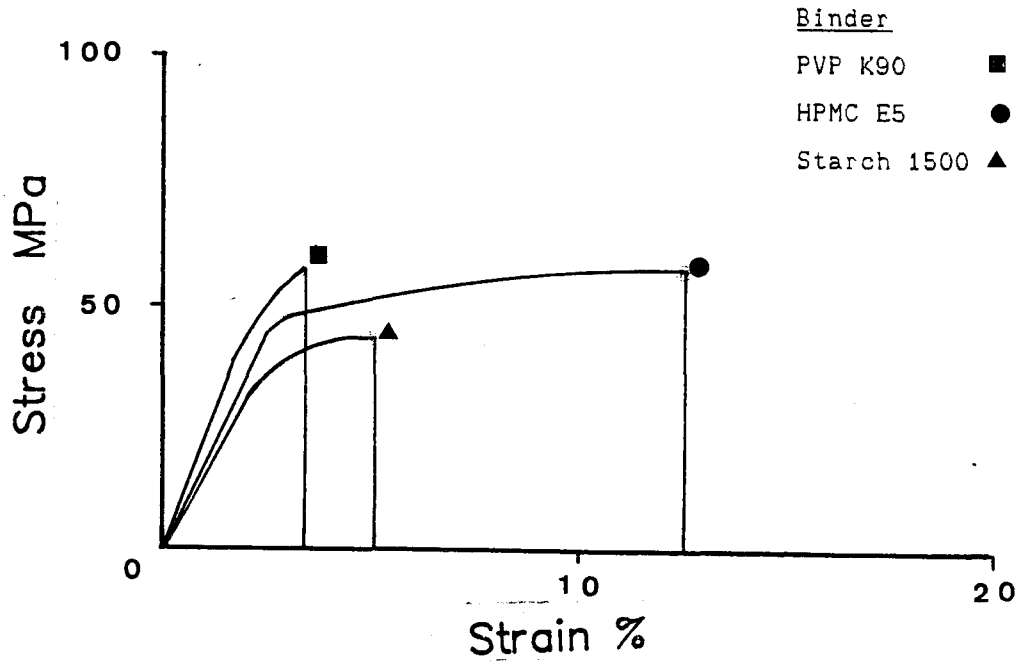
The results for tensile properties of the unplasticized binders after equilibration at either 22.5% RH or 59.5% RH are given in Table 3.3. Application of a Student t-test revealed no statistically significant anisotropy between films cut along the axis of casting or cut normal to the axis of casting. Consequently, results were pooled and represent not less than ten observations. Coefficients of variation were in the order of 10% for ultimate tensile strength and Young's modulus and in the order of 20% and 25% respectively for strain at break and toughness. This magnitude of variability was consistent with that reported by other workers (see for example, Reading and Spring, 1984a). Humidity control during the actual testing procedure by use of the "Atmos Bag" produced no apparent benefit with respect to the reproducibility of repeated measurements. Representative stress-strain curves for the unplasticized binders are shown in Figs. 3.6a and 3.6b.

Table 3.3 Mechanical Properties of Some Polymeric Tablet Binders

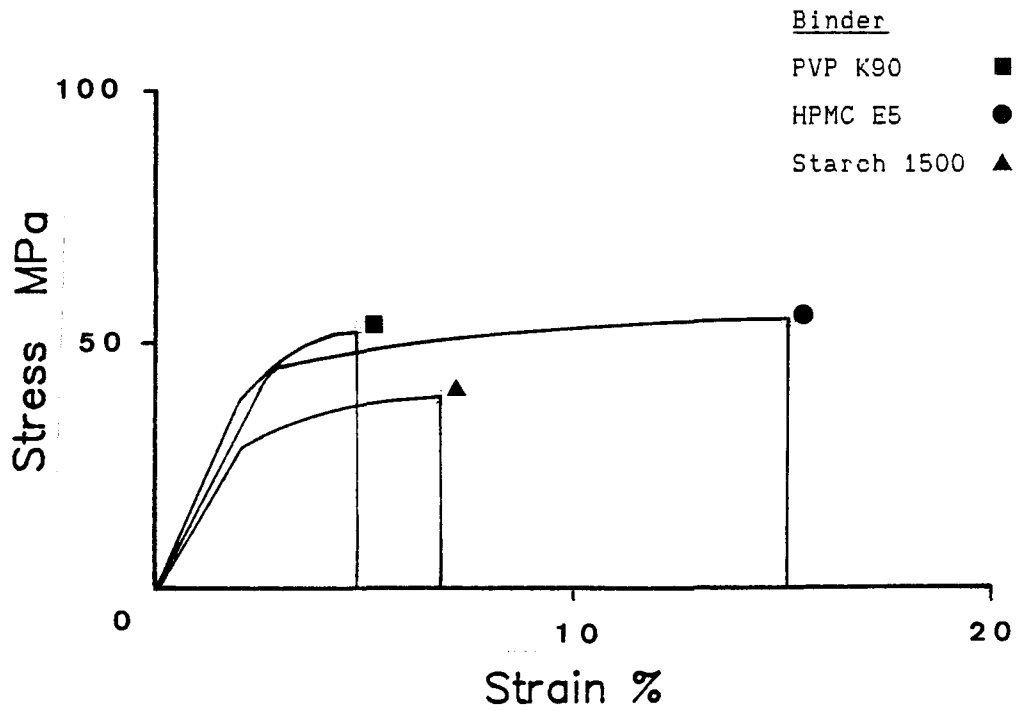
Binder	Young's Modulus MPa	UTS at Yield MPa	UTS at Break MPa	Strain at Break %	Work of Failure MJm ⁻³
22.5% RH					
PVP	2226	-	57.2	3.4	1.21
HPMC	1755	-	57.4	12.5	6.08
Starch	1573	-	43.5	5.1	1.55
1500					
59.5% RH					
PVP	1888	-	51.9	4.8	1.69
HPMC	1610	-	54.4	15.1	6.99
Starch	1415	-	39.4	6.8	1.99
1500					

Figure 3.6 Tensile Deformation of Polymeric Binders

a. 22.5% RH



b. 59.5% RH



Stress-strain diagrams were reconstructions derived from the mean values for the tensile properties. A distinct, ductile-type yield point was not evident for any of the polymers irrespective of conditioning humidity. All showed deviation from a linear stress-strain relationship, however. The observed strain increased with increasing stress up to the point of break. Ultimate tensile strengths were therefore defined as tensile strength at break.

The polymers tested exhibited markedly different tensile properties as shown in Fig. 3.6. Of the three polymers, PVP was the most rigid and the least deformable. This was in contrast with the observations of Healey et al., (1974). When stressed beyond the elastic limit, PVP showed little further extensibility before failing. HPMC had a similar ultimate tensile strength to PVP but was less rigid and was capable of withstanding considerable strain without break. Starch 1500 had an intermediate extensibility but was weaker and less rigid than the other polymers. For equivalent applied stresses Starch 1500 would consequently undergo a considerable greater extent of elastic strain than other polymers. From the shape of the characteristic stress-strain curves and the magnitude of the tensile properties, a qualitative classification of material characteristics was possible. Using the criteria of Carswell and Nason (1944), PVP was classed as a hard, brittle material and HPMC as a hard, tough material. Starch 1500 was classified as a soft, weak material.

Increasing the moisture content of the films, by equilibrating at 59.5% RH rather than 22.5% RH resulted in qualitatively similar results for all three polymers. In all cases, the increased moisture content resulted in a reduction in tensile strength and Young's Modulus and an increase in extensibility. The balance of these changes was such that, in each case, the toughness of the film was increased at the higher moisture content. Thus, although the films were weaker in terms of their ultimate tensile strength, greater expenditure of work was required to cause failure by virtue of the increased extensibility. In relative terms, the influence of increased moisture content was greater for PVP and Starch 1500 than for HPMC. This reflects the greater affinity for moisture shown by PVP and Starch 1500 at 59.5% RH. Although moisture does not conform to any traditional definition of a plasticizer (on account of its high

volatility and low permanence), the changes in tensile properties that it produced were consistent with a plasticizer action.

Strict comparison of results presented here with those of other workers was limited. This was because of differences in test protocols adopted (strain rates and conditioning humidities, for instance) and polymer grades used. However, some general observations regarding similarities and differences could be made.

Results for HPMC agreed well with results of Aulton et al., (1981) who also concluded that unplasticized HPMC was a tough polymer. This similarity was expected since the test protocols adopted were practically identical. The magnitude of the tensile parameters were also in reasonable accord with results of Entwistle and Rowe (1979) and Porter (1980).

Tensile properties for PVP were considerably different from those reported by Healey et al., (1974) or Reading and Spring (1984a). PVP was characterised by Healey and co-workers as a weak material and, although Reading and Spring did not classify the polymers that they evaluated, their results supported this classification. The difference between results reported here and those of the previous workers can be attributed to the difference in molecular weight of polymer used. Both the latter workers used low molecular weight polymers (K29-32 and 40,000 Da grades respectively). Low molecular weight polymers are usually relatively weak but as the molecular weight is increased the strength also increases (Alfrey, 1948). The higher molecular weight of the K90 grade of PVP used in the present work resulted in a higher tensile strength and elastic modulus than previously reported. The magnitude of the strain at failure was, however, similar.

Results for the tensile properties of gelatinised Starch 1500 fell within the range of results reported for gelatinised maize starch (Healey et al., 1974; Reading and Spring, 1984a). Healey et al., (1974) reported higher values for tensile strength and Young's Modulus and concluded that maize starch was a hard, tough material. The results of Reading and Spring (1984a) and of the present study, however, indicate that gelatinised starches are relatively weak materials, with low extensibility. More recently, Ononokonpono and

Spring (1988b) observed considerably greater extensibility than reported previously for gelatinised maize starch films. Since the method of film preparation and testing were identical to those used by Reading and Spring (see Reading, 1984) the difference in results is difficult to explain. It is conceivable that the thinner films used by Ononokonpono and Spring (1988b) may have influenced the results. The same workers have, however, demonstrated that polymeric films tend to become more brittle and less extensible with reducing film thickness (Ononokonpono and Spring, 1988a). Results presented here indicate that, after gelation, the tensile properties of Starch 1500 are similar to those of unmodified maize starch.

The characteristic shape of the stress-strain curve yielded qualitative information about the viscoelastic nature of the polymers. Published literature on glass transition temperatures (T_g) (Table 3.4) indicates that, at the temperature of testing, both PVP and HPMC would be considerably below the temperature of their glass transition.

Table 3.4 Published Data on the Values for the Glass Transition Temperature of Some Pharmaceutical Polymers

Polymer	Glass Transition Temperature °C	Reference
Polyvinylpyrrolidone	175	Nielsen (1977)
	175	Tan and Challa (1976)
Hydroxypropyl- methylcellulose	177	Entwistle and Rowe (1979)
	155	Okhamafe and York (1985)
	180 (DSC) 169 - 174 (DTA)	Sakellariou et al (1985)

To date, no value has been reported for the glass transition of Starch 1500. Eith et al., (1987) commented, however, that the glass transition temperature of starches containing about 14% moisture would be around 50°C above room temperature. In view of the physico-chemical similarities between Starch 1500 and unmodified starches, it seems reasonable to assume that their glass transitions would also be similar. It would be expected, therefore, that glassy elasticity

would be the dominant factor determining the shape of the stress-strain curves.

The stress-strain curve for PVP was characteristic of a brittle, glassy material with a high Young's Modulus and tensile strength but with low extensibility. The stress-strain curve for Starch 1500 was also more characteristic of a predominantly elastic material rather than a ductile or plastic material. The rigidity of PVP originates from extensive dipole-dipole association between adjacent molecules (Blecher et al., 1976). Starch 1500, on the other hand, is typical of a highly crystalline polymer. It is probably most appropriate to regard starch as a filled polymer, since structurally it consists of an amorphous matrix (predominantly branched amylopectin) containing discrete crystalline regions (predominantly aligned amylose chains) (Merck, 1983). The presence of crystalline domains within the starch film resulted in low ductility and an essentially elastic-type stress-strain curve.

HPMC had a similar tensile strength and modulus to PVP and its glass transition temperature was also considerably above ambient temperature. However, greater extensibility before failure resulted in a stress-strain curve more characteristic of a polymer in the transition state. This is most probably due to the presence of the hydroxypropyl and methyl substituents on the cellulose backbone preventing extensive molecular alignment. This explains why, although HPMC exhibits some degree of crystallinity (Okhamafe and York, 1983), this is not predominant.

The effect of moisture sorption in increasing extensibility whilst reducing rigidity and ultimate tensile strength is consistent with an increase in free volume and consequently greater segmental mobility. The ability of sorbed moisture to reduce the glass transition temperature of the hydrophilic polymers investigated is well documented in the literature (Tan and Challa, 1976; Okhamafe and York, 1983; Eith et al., 1987).

3.4.2 The Effect of Different Plasticizers on the Tensile Properties of the Binders

The influence of different potential plasticizers on the tensile properties of the polymeric binders was investigated at a fixed loading of 10% (by weight in the film), for films conditioned at 22.5% RH. Those potential plasticizers which showed particularly limited compatibility (i.e. solid PEGs and, in the case of Starch 1500, hexylene glycol) were not screened. As a general principle, materials of low compatibility exhibit phase-separation and, consequently, are inefficient plasticizers (Doolittle, 1954). The observations of Rowe (1976), Aulton et al., (1981) and Sakellariou et al., (1986) substantiate this principle for cellulosic polymers plasticized with high molecular weight PEGs.

The influence of potential plasticizers on the tensile properties of PVP K90, HPMC E5 and Starch 1500 is reported in following sections.

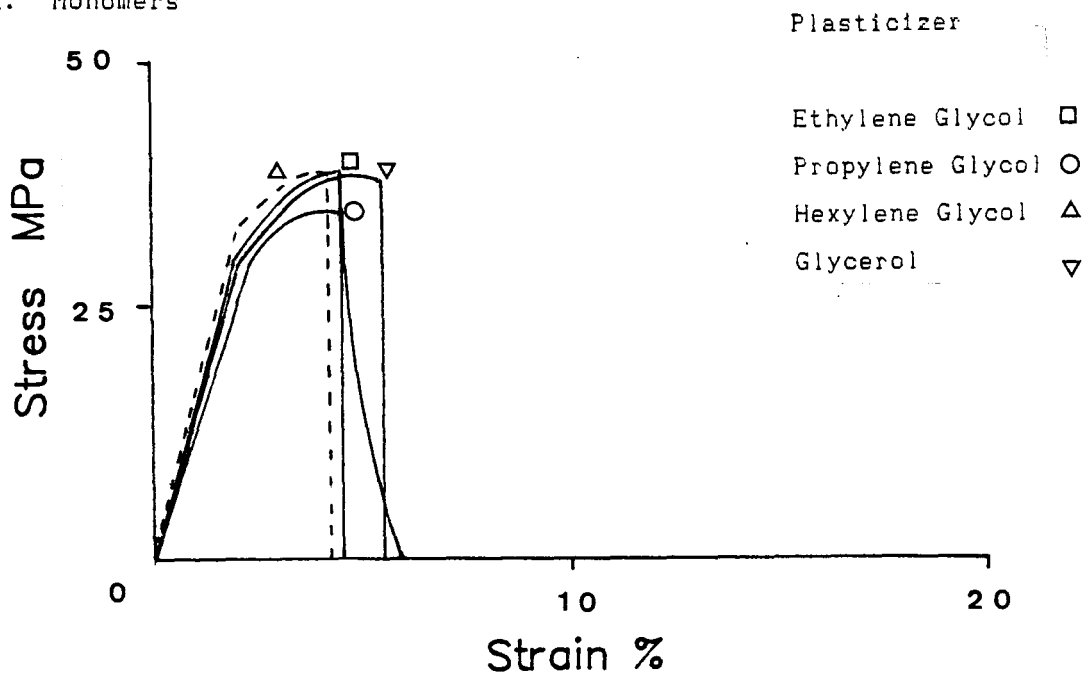
3.4.2.1 Plasticization of PVP

All of the potential plasticizers screened for PVP showed evidence of plasticizer activity. This was apparent from the decrease in tensile strength and Young's modulus and the increased extensibility compared with the unplasticized film (section 3.4.1). The characteristic shape of the stress-strain curves (Figs. 3.5a and b) and the derived parameters (Table 3.5) revealed considerable differences in the effect magnitude.

Incorporation of the glycol monomers resulted in significant decreases in the strength and modulus of the films with only small increases in extensibility. As a result, films containing the monomers had toughnesses which were similar to, or lower than, that of the unplasticized film. The PEGs were generally more efficient in reducing modulus and strength and also facilitated greater extensibility. As a result PEG-plasticized films were considerably tougher than the unplasticized film. The plasticization efficiency of the PEGs increased with decreasing molecular weight, as observed for HPMC-PEG systems (Aulton et al., 1981). The trend did not include the monomer, ethylene glycol, however.

Figure 3.5 Effect of Different Plasticizers on Stress-Strain Relationships for PVP

a. Monomers



b. PEGs

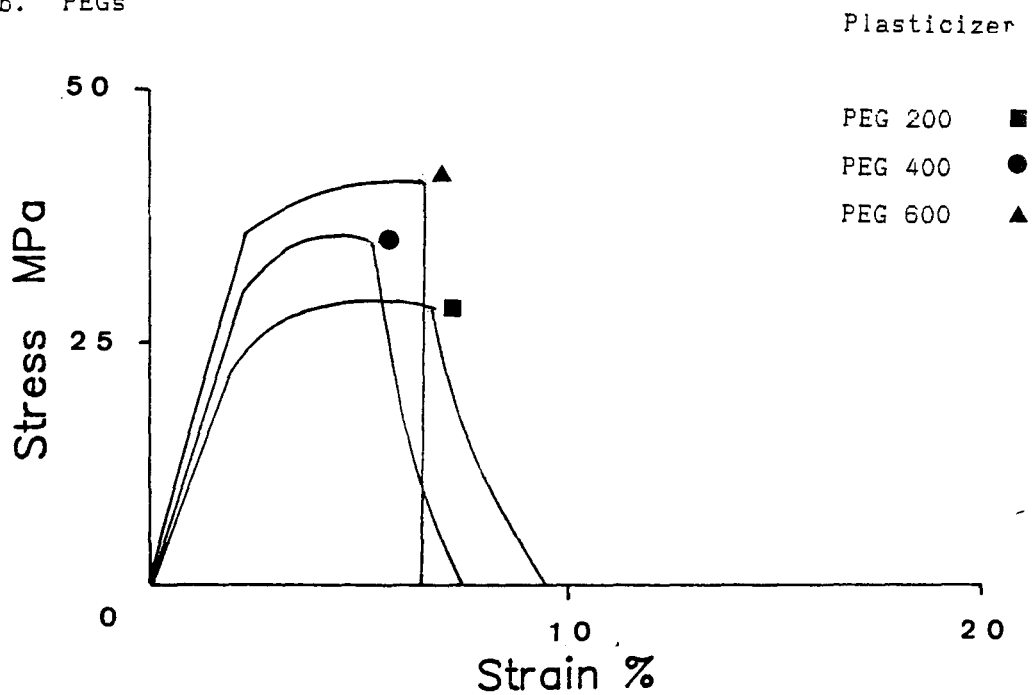


Table 3.5 Effect of Different Plasticizers on the Tensile Properties of PVP

Plasticizer (10% by weight)	Young's Modulus MPa	UTS at Yield MPa	UTS at Break MPa	Strain at Break %	Work of Failure MJm ⁻³
Hexylene glycol	1622	-	40.1	4.2	1.13
Glycerol	1569	-	38.2	5.5	1.43
Propylene glycol	1480	35.2	-	5.9	1.25
Ethylene glycol	1538	-	39.1	4.5	1.18
PEG 200	1179	28.8	-	8.2	1.75
PEG 400	1372	35.4	-	7.4	1.67
PEG 600	1595	-	38.0	6.5	1.79

Differences in plasticizer efficiency were also reflected in the shape of the stress-strain curves. Films plasticized with hexylene glycol, ethylene glycol, glycerol or PEG 600 deformed in a brittle-elastic manner. The films plasticized with propylene glycol, PEG 400 or PEG 200, however, exhibited yield points and more ductile stress-strain relations. Increasing plasticizer efficiency was therefore implicated in a qualitative shift in the viscoelastic nature of the tensile deformation.

These results contrast with those of Reading and Spring (1984b) who reported that the inclusion of PEG 600 produced no evidence of plasticization in PVP. The latter workers observed that while inclusion of PEG 600 at levels up to 10% reduced the ultimate tensile strength, this was associated with increased rigidity and decreased extensibility. The differences observed, probably result from the

molecular weight of the PVPs used. The low molecular weight PVP used by Reading and Spring (1984b) would be less amenable to effective plasticization due to reduced compatibility and also due to its lower intrinsic tensile strength. The increase in modulus with increased concentration of PEG 600, observed by the previous workers, is harder to explain. It is possible that increased segmental mobility associated with plasticizer inclusion may facilitate greater alignment between adjacent polymer chains during solvent removal. The resulting pseudo-crystalline matrix may then exhibit a paradoxical increase in rigidity.

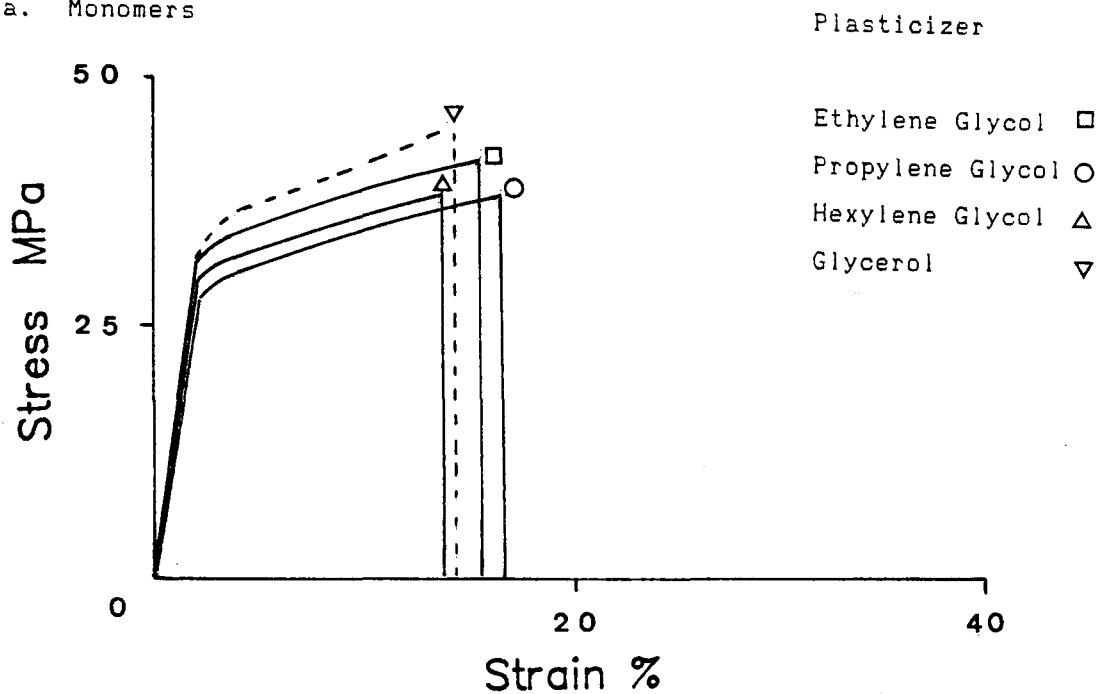
3.4.2.2 Plasticization of HPMC

The stress-strain curves (Figs. 3.6a and b) and tensile parameters (Table 3.6) were substantially in agreement with the observations of previous workers. Both the glycol monomers and the PEGs resulted in plasticization of the HPMC matrix, characterised by decreased ultimate tensile strength and elastic modulus and increased elongation at failure. In all cases, the increased extensibility was insufficient to compensate for the reduction in stiffness and tensile strength. Thus, all the plasticizers evaluated resulted in films of lower toughness than the unplasticized polymer.

Generally, the PEGs possessed greater plasticization efficiency than the monomers. The extent of plasticization achieved with the PEGs increased with decreasing molecular weight, in agreement with the observations of other workers (Entwistle and Rowe, 1979; Aulton et al., 1981 and Okhamafe and York, 1983). However, as noted for PVP (Section 3.4.2.1) this trend did not extend to include the monomer, ethylene glycol. Inspection of Table 3.6 indicated that propylene glycol was the most efficient plasticizer of the monomer glycols. Entwistle and Rowe (1979) have suggested that this molecule interacts strongly with HPMC. The latter workers also suggested that glycerol had little or no interaction with HPMC. Nevertheless, glycerol was also found to exert a plasticizer action on HPMC, consistent with the observations of Delporte (1980) and Aulton et al., (1981). Hexylene glycol produced the smallest increase in extensibility although it was more effective than either ethylene glycol or glycerol in reducing strength and stiffness.

Figure 3.6 Effect of Different Plasticizers on Stress-Strain Relationships for HPMC

a. Monomers



b. PEGs

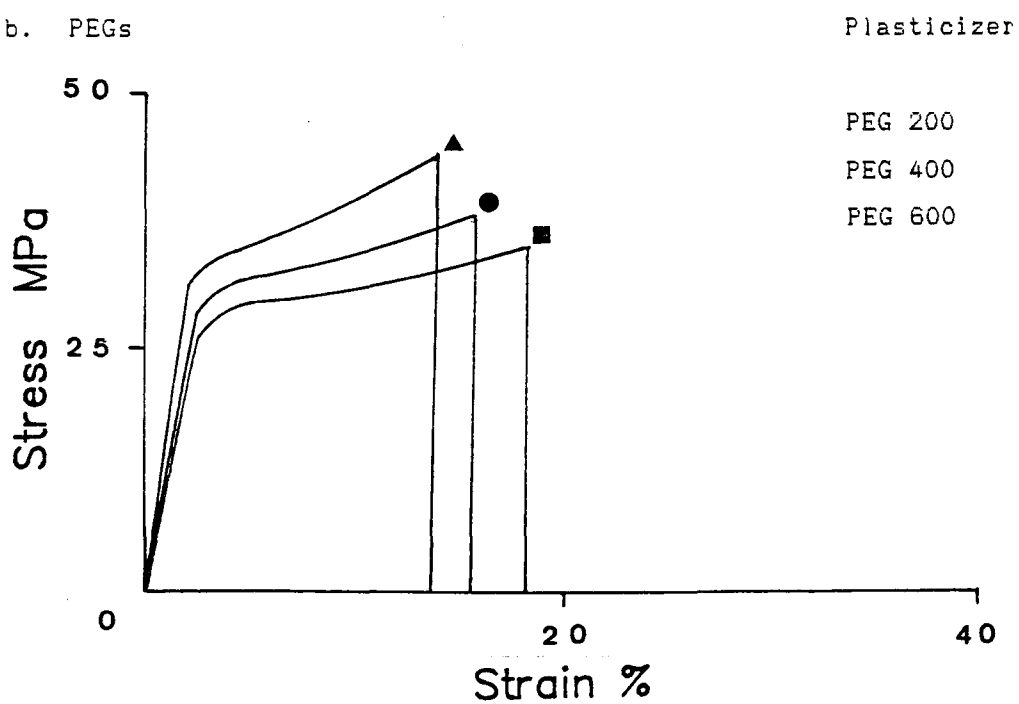


Table 3.6 Effect of Different Plasticizers on the Tensile Properties of HPMC

Plasticizer (10% by weight)	Young's Modulus MPa	UTS at Yield MPa	UTS at Break MPa	Strain at Break %	Work of Failure MJm ⁻³
Hexylene glycol	1509	-	39.7	13.7	4.35
Glycerol	1594	-	42.2	15.4	5.45
Propylene glycol	1410	-	38.9	16.5	5.20
Ethylene glycol	1687	-	45.7	14.2	5.33
PEG 200	1252	-	34.7	18.1	5.26
PEG 400	1357	-	38.7	15.5	4.83
PEG 600	1494	-	44.8	13.7	4.76

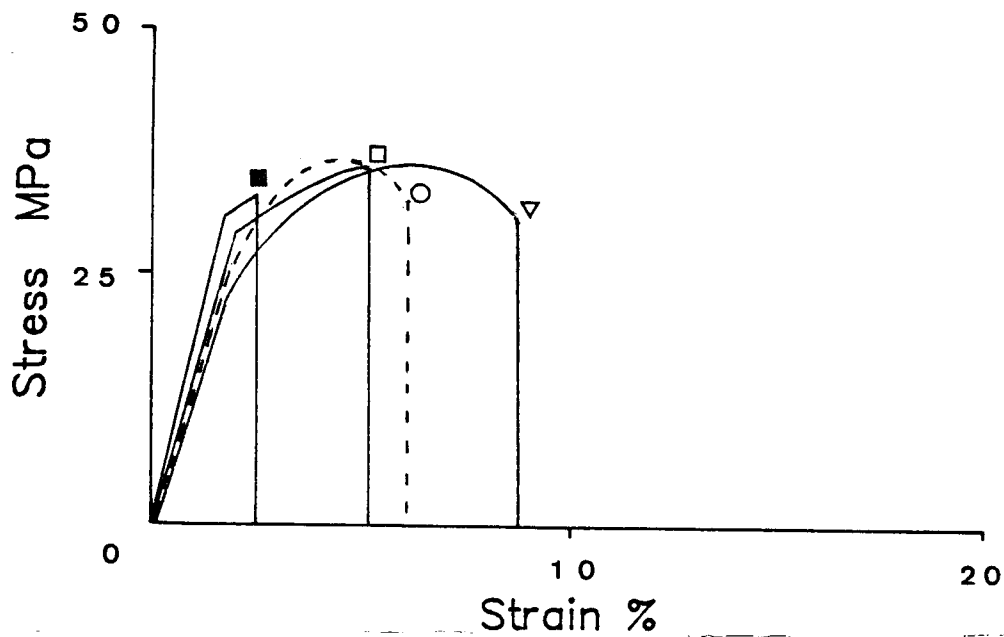
At the level of incorporation used for the present study, none of the plasticizers induced a distinct yield point in the stress-strain curve. The characteristic shape of the curves was in all cases similar to that of the unplasticized polymer. This implied that, at a qualitative level, the viscoelastic nature of the plasticized and unplasticized polymer matrix was essentially the same.

3.4.2.3 Plasticization of Starch 1500

The effect of potential plasticizers on the stress-strain relationship for Starch 1500 is shown in Fig. 3.7. The respective mechanical parameters are reported in Table 3.7.

The monomeric glycols all showed evidence of plasticization with a reduction in elastic modulus and tensile strength combined with increased extensibility. For glycerol and propylene glycol, the increased extensibility resulted in an increased film toughness even though these films had a lower strength than the unplasticized film.

Figure 3.7 Effect of Different Plasticizers on Stress-Strain Relationships for Starch 1500



Plasticizer

Ethylene Glycol □ Propylene Glycol ○
 Glycerol ▽ Peg 200 ■

Table 3.7 Effect of Different Plasticizers on the Tensile Properties of Starch 1500

Plasticizer (10% by weight)	Young's Modulus MPa	UTS at Yield MPa	UTS at Break MPa	Strain at Break %	Work of Failure MJm ⁻³
Glycerol	1403	37.9	-	8.6	2.48
Propylene glycol	1471	36.8	-	6.1	1.77
Ethylene glycol	1479	-	36.4	5.2	1.38
PEG 200	1793	-	33.1	2.5	0.55

With ethylene glycol, however, toughness was lower than that of the unplasticized film. The inclusion of glycerol or propylene glycol resulted in the induction of yield into the tensile deformation of the starch films. This was not observed with ethylene glycol.

The rank order of plasticizing efficiency generally reflected the relative hygroscopicity (or humectancy) of the glycols. This is in agreement with observations that humectants plasticize starch in a non-specific manner by binding more water into the system (Davidson, 1983). A further potential explanation is that the glycols act as non-interacting hydrodynamic modifiers, existing as discrete fluid domains within the matrix. This interpretation is consistent with the poor solubility performance of Starch 1500 noted in Chapter Two.

Ononokocono and Spring (1988b) investigated the effects of inclusion of propylene glycol on the tensile properties of gelatinised maize starch films. They found that although the strength and rigidity of the films were reduced, there was no increase in elongation at failure and they concluded that plasticization did not occur. It should be noted, however, that the extensibility of their unplasticized films was around twice that observed in the present work although ultimate tensile strength and elastic moduli were similar. A valid comparison between their results and those presented here is not really possible because of differences in film preparation and testing. Skultety and Sims (1987) have shown that, unlike PEG 400 or glycerol, propylene glycol was readily lost from cellulosic film coatings at process temperatures between 40 °C and 60 °C. A similar loss of propylene glycol from starch films might also have occurred at the drying temperature of 45 °C used by Ononokocono and Spring (1988b). This may account for the absence of plasticization reported.

Inclusion of PEG 200 resulted in film weakening and embrittlement, even though low molecular weight PEGs are relatively hygroscopic (and thus potentially capable of binding moisture within the film). The weakening and embrittlement of starch films by the inclusion of PEGs has also been observed by other workers (Reading and Spring, 1984b; Ononokocono and Spring, 1988b) although explanations for this behaviour have not been advanced.

3.4.3 The Effect of Plasticizer Concentration and Conditioning Humidity

The influence of increasing plasticizer concentration on the tensile properties of the binders was investigated using plasticizers exhibiting optimum efficiency. PEG 200 had been identified as the most efficient plasticizer both for PVP and HPMC films, whereas glycerol was more effective for Starch 1500. Moisture was also observed to influence the tensile properties of hydrophilic polymers in a manner consistent with plasticization. Since moisture interacts at a molecular level in a manner analogous to plasticizers it was probable that the observed tensile properties would reflect both moisture and plasticizer content. The tensile properties of the plasticized films were therefore examined after equilibration both at 22.5% RH and 59.5% RH.

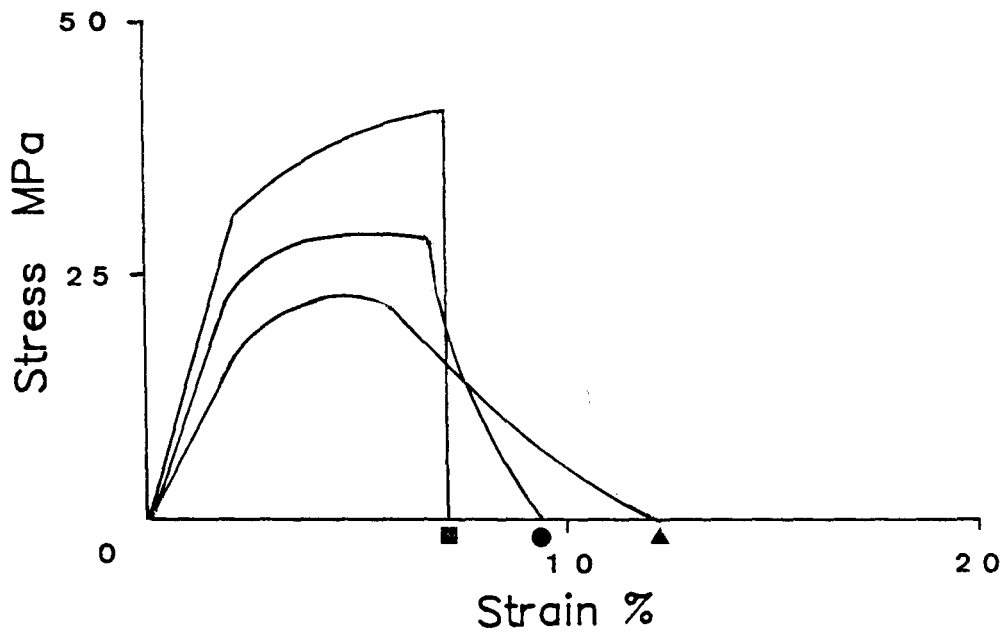
PEG 200 and glycerol were incorporated into HPMC and Starch 1500 films respectively at levels up to 30% by weight of the film. The upper limit for plasticizer inclusion was determined by the limit of compatibility and onset of phase separation determined in Chapter Two. PEG 200 was incorporated into PVP films at levels up to 15% by weight of the film. At higher levels of inclusion, PVP films were too soft and ductile to allow coherent test samples to be cut. This indicated that, on a qualitative basis, PEG 200 was a more effective plasticizer for PVP than for HPMC. This observation was in agreement with earlier observations that PVP-PEG 200 systems exhibited total compatibility while HPMC-PEG 200 systems exhibited only partial compatibility.

The characteristic stress-strain curves for polymer films containing increased plasticizer levels are shown in Figs. 3.8 to 3.10. The derived tensile properties given in Tables 3.8 to 3.10.

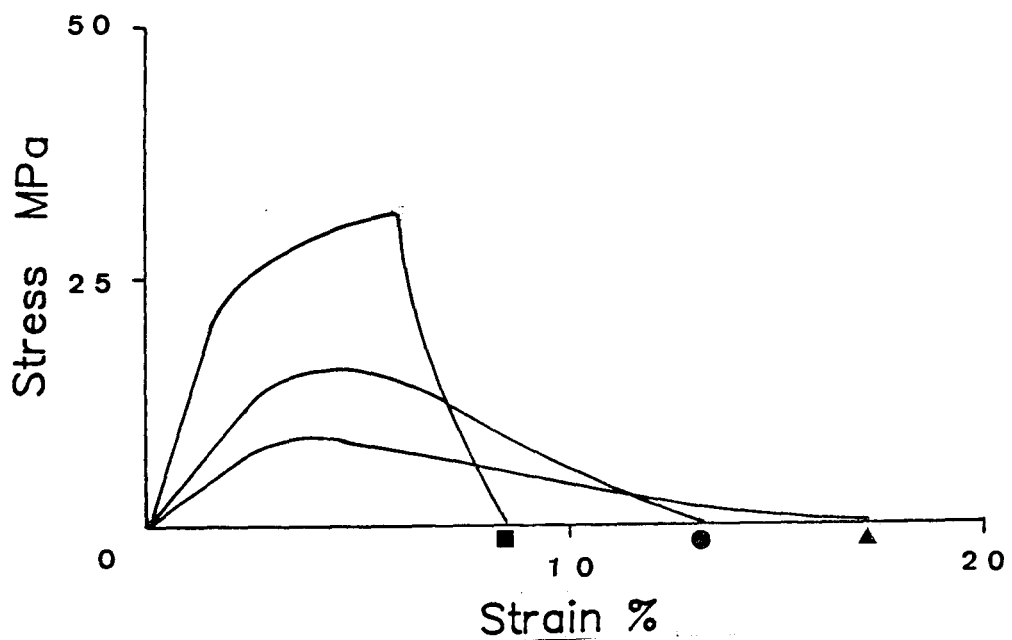
Examination of the curves indicated that the response to increasing plasticizer level was the same for the three polymers. As the plasticizer level was increased, the rigidity and strength of the films was progressively reduced whilst the strain at failure was increased. The magnitude of the respective tensile parameters confirmed this.

Figure 3.8 Effect of Plasticizer Concentration on the Tensile Properties of PVP

22.5% RH



59.5% RH

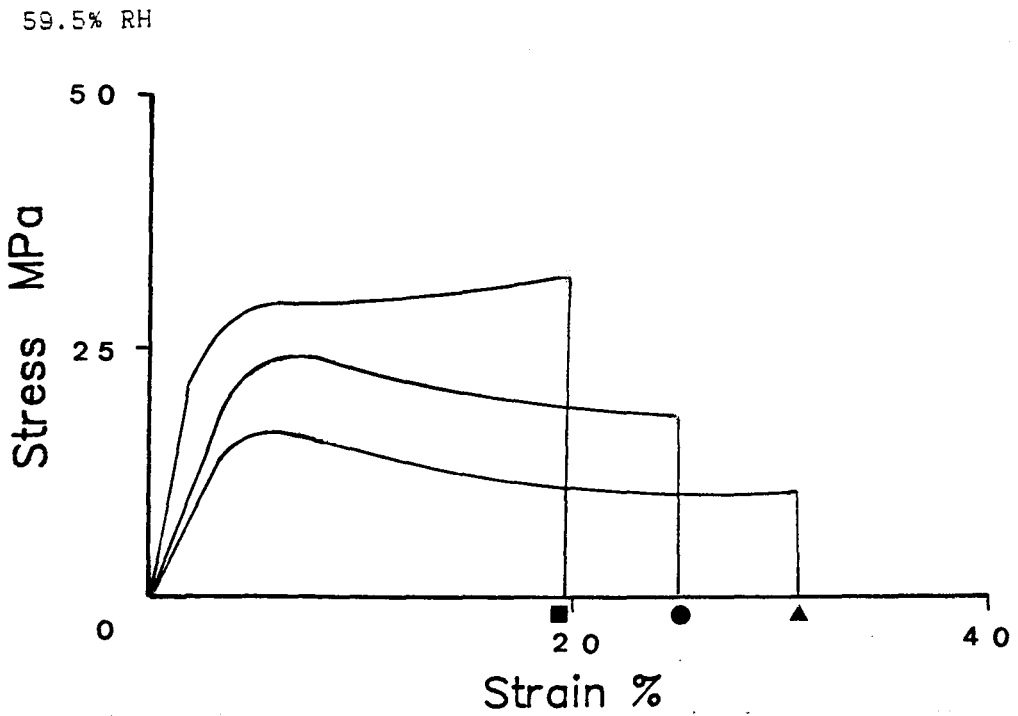
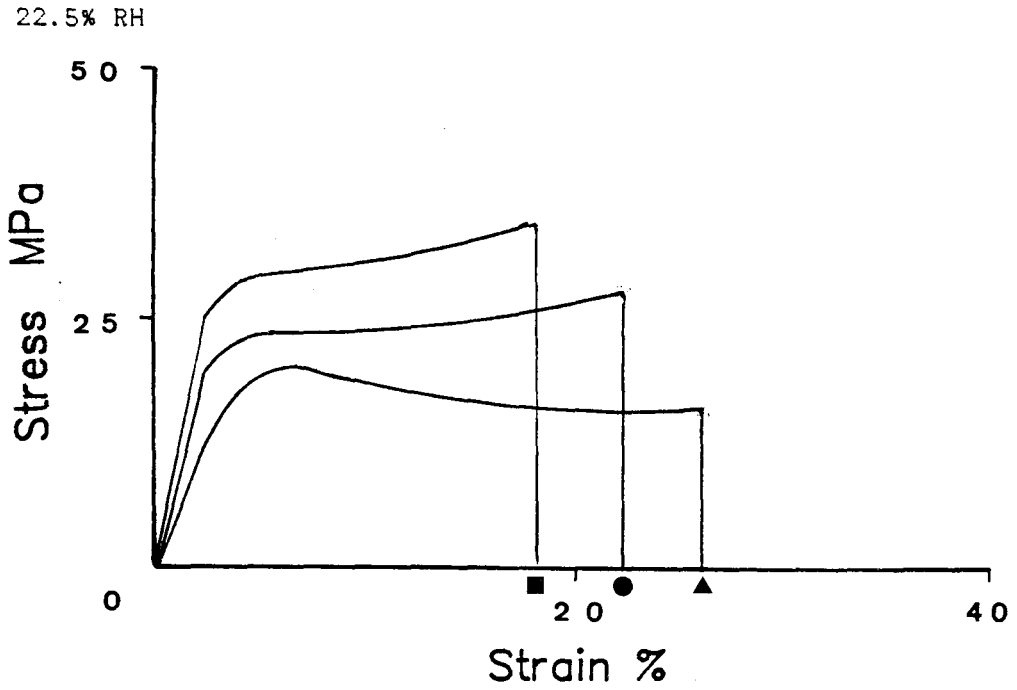


Plasticizer Concentration

PEG 200 5% w/w ■ PEG 200 10% w/w ● PEG 200 15% w/w ▲

Figure 3.9

Effect of Plasticizer Concentration on the Tensile Properties of HPMC



Plasticizer Concentration

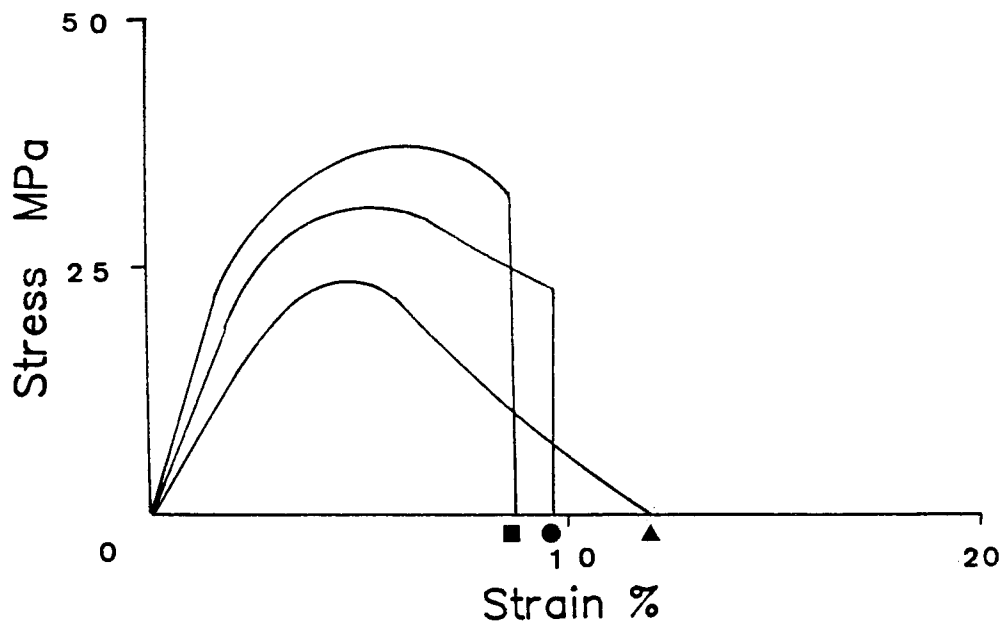
PEG 200 10% w/w ■

PEG 200 20% w/w ●

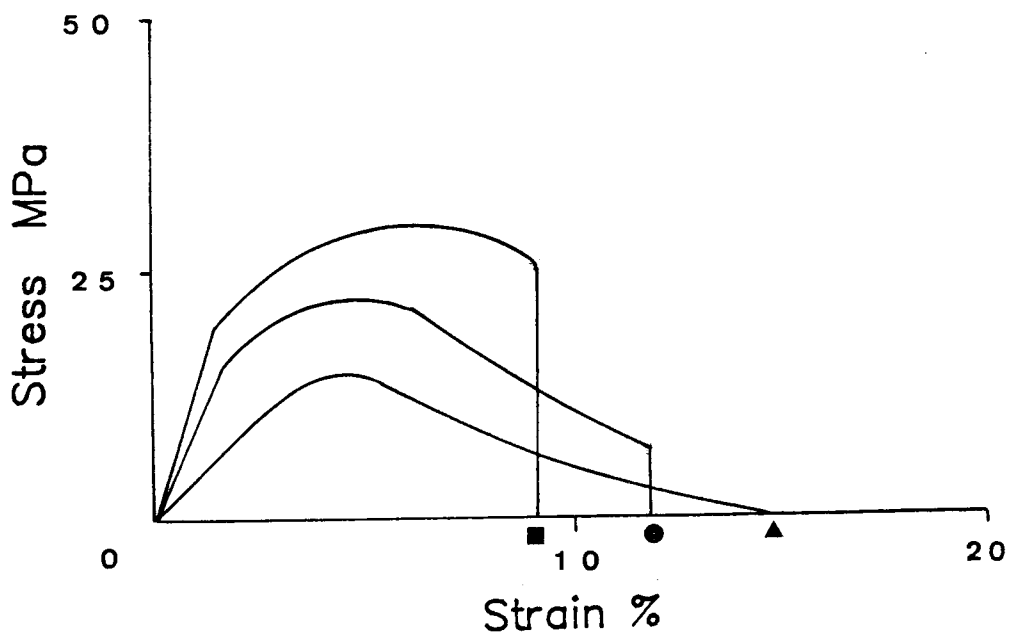
PEG 200 30% w/w ▲

Figure 3.10 Effect of Plasticizer Concentration on the Tensile Properties of Starch 1500

22.5% RH



59.5% RH



Plasticizer Concentration

Glycerol 10% w/w ■ Glycerol 20% w/w ● Glycerol 30% w/w ▲

Table 3.8 Effect of Plasticizer Concentration on the Tensile Properties of PVP

Plasticizer level in film (% by weight)	Young's Modulus MPa	UTS at Yield MPa	UTS at Break MPa	Strain at Break %	Work of Failure MJm ⁻³
22.5% RH					
0%	2226	-	57.2	3.4	1.21
5%	1452	-	41.3	7.1	2.16
10%	1179	28.9	-	9.3	1.75
15%	785	22.6	-	12.0	1.48
59.5% RH					
0%	1888	-	51.9	4.8	1.69
5%	1322	-	30.0	8.5	1.69
10%	508	22.1	-	13.2	1.08
15%	312	9.0	-	17.3	0.77

Table 3.9 Effect of Plasticizer Concentration on the Tensile Properties of HPMC

Plasticizer level in film (% by weight)	Young's Modulus MPa	UTS at Yield MPa	UTS at Break MPa	Strain at Break %	Work of Failure MJm ⁻³
22.5% RH					
0%	1755	-	57.4	12.5	6.80
10%	1252	-	34.7	18.1	5.26
20%	855	-	27.5	22.3	5.03
30%	498	20.2	-	26.0	4.12
59.5% RH					
0%	1610	-	54.4	15.1	6.99
10%	1220	-	31.9	19.7	5.53
20%	557	24.4	-	24.8	4.86
30%	440	17.3	-	31.0	3.64

Table 3.10 Effect of Plasticizer Concentration on the Tensile Properties Starch 1500

Plasticizer level in film (% by weight)	Young's Modulus MPa	UTS at Yield MPa	UTS at Break MPa	Strain at Break %	Work of Failure MJm ⁻³
22.50% R.H.					
0%	1573	-	43.5	5.1	1.55
10%	1403	37.9	-	8.6	2.48
20%	1065	31.3	-	9.6	2.23
30%	688	24.2	-	12.0	1.43
59.5% R.H.					
0%	1415	-	39.4	6.8	1.99
10%	1327	34.8	-	9.2	2.23
20%	903	27.1	-	11.9	1.75
30%	420	19.8	-	14.2	1.06

Plasticized films of PVP and Starch 1500 equilibrated at 22.5% R.H showed increased toughness compared with the unplasticized films (Table 3.3). Plasticized films of HPMC, however, required less expenditure of work to cause failure than the unplasticized film. The work involved in causing tensile failure (as reflected by the area under the stress-strain curve) depends on the magnitude of the tensile strength, the strain at failure and the elastic modulus. In the case of PVP and Starch 1500, the increase in strain at failure due to plasticization was sufficient to yield films which were tougher than the unplasticized film. The converse was true for HPMC though. With increased plasticizer loading, the increased strain at failure was insufficient to compensate for the reduced tensile strength resulting in a progressively decreased toughness.

At equivalent plasticizer levels, plasticized films equilibrated at the higher relative humidity exhibited apparently greater plasticity since the tensile strength and elastic modulus were reduced, whilst strain at failure was increased. For all three polymers, however, the

toughness of the plasticized films tended to be lower than that of the corresponding unplasticized film. This indicated that the combined activity of both moisture and plasticizer resulted in a relatively greater decrease in tensile strength and modulus, compared with the increase in extensibility. The combined effect of plasticizer and water molecules may represent simply an independent but additive activity. Since the plasticizers and water are miscible in all proportions, however, the observed tensile response may reflect greater compatibility and plasticization efficiency by a binary solvent system.

At the conditioning humidity of 59.5% RH, incorporation of plasticizer resulted in the production of very weak, deformable films. At the maximum level of plasticizer inclusion, PVP films had only 17.3% of the strength of the unplasticized film. Corresponding strength reductions for HPMC and Starch 1500 were 31.8% and 50.2% respectively. The strain attained before failure was greatly increased, however. Maximum strain increases were 3.60 times, 2.05 times and 2.08 times for PVP, HPMC and Starch 1500 respectively compared with the unplasticized films. The apparent greater proportionate increase in plasticity of PVP compared with the other binders may reflect the initial brittle-elastic nature of this polymer. The observed behaviour may also reflect the extent of compatibility between PVP and plasticizer and the greater tendency to sorb moisture.

Examination of the shape of the stress-strain curves revealed that the increased plasticizer levels were also associated with qualitative changes in viscoelasticity. As the level of plasticizer was increased, there was a general trend towards a more ductile mode of deformation. This was particularly marked for PVP and Starch 1500 where the deformation of the unplasticized polymer was essentially brittle-elastic (Fig. 3.4). Inclusion of 10% of PEG 200 or glycerol induced a distinct yield point in PVP and Starch 1500 films respectively. At the higher conditioning humidity, PVP films strained beyond their yield point continued to extend with decreasing stress up to the point of failure. The resultant stress-strain curves were characteristic of a polymer in the rubbery (viscous) flow state (Toblosky, 1971). With HPMC, a distinct yield point was evident only at 30% plasticizer inclusion (or 20% at the higher relative humidity)

although the shape of the curve indicated a more ductile deformation. Several workers have observed that PVP fails to form coherent films at relative humidities above 65% (Healey, 1976; Reading, 1983). This occurs because the extent of moisture sorption is sufficient to reduce the glass transition temperature to below ambient (Tan and Challa, 1976; Oksanen and Zografis, 1990). The shape of the stress-strain curves suggested that the glass transition temperature of plasticized PVP films equilibrated at 59.5% RH was also close to the temperature of testing. The induction of yield in all the polymers provided confirmatory evidence that the incorporation of plasticizer was associated with increased plastic or non-recoverable deformation. Induction of yield was also associated with necking of the test specimen. This was apparent for all the polymers but was more pronounced for plasticized PVP films equilibrated at the higher relative humidity.

One consequence of the induction of yield is that stored elastic strain may be translated into further plastic deformation in a manner analogous to stress relaxation. Since plasticization facilitates greater strain before failure, it seems likely that greater elastic strain dissipation may be tolerated without rupture of the binder film. This behaviour may have important consequences for the performance of a binding agent incorporated into a tablet formulation.

3.4.4 Molecular Basis of Binder Plasticization

There are a number of theories of plasticizer action which provide an adequate mechanistic interpretation of the results reported here (see, for example, Ritchie, 1972). Of these, the gel theory (Doolittle, 1947; 1954) has probably gained greatest acceptance. At an empirical level, the gel theory provides a model which adequately explains the plasticization phenomena observed in the preceding sections. Aulton et al. (1981) used this theory to explain the influence of moisture sorption and plasticization on the mechanical properties of cast films of HPMC. Okhamare and York (1983) also considered that plasticizer

action involved severance of bonds between adjacent segments of the film-former in which the plasticizer then became sandwiched. In order to understand the plasticization process in general, and differences in plasticizer efficiency in particular, it is necessary to consider the nature of the polymer-plasticizer interaction.

Okhamafe and York (1983) suggested that the principle bonding between HPMC polymer chains in an unplasticized film would be through hydrogen-bonding of the hydroxyl groups. Although starches are a composite of two polymers, amylose and amylopectin, the same probably interaction applies. The extent of hydrogen-bonding between linear amylose chains accounts for the extensive crystallinity and the consequent large heat of fusion of starches (Davidson, 1983). PVP chains, in contrast, associate through dipole-dipole interaction (Eblecher et al., 1983), although the positive heat of mixing on addition of water indicates that the pyrrolidone oxygen may bond with molecules containing sufficiently electropositive hydrogen atoms. The interaction (and thus the modification of tensile mechanical properties) of sorbed moisture with the hydrophilic polymers used here was mediated via hydrogen-bonding.

Without exception, all of the potential plasticizers screened in this and the previous chapter are capable of hydrogen-bonding. The monomeric glycols are all regarded as examples of strongly hydrogen-bonding solvents (Burrell, 1983). PEG chains, in common with PVP, associate primarily through dipole-dipole interactions although the terminal hydroxyl groups are capable of hydrogen-bonding. The ether oxygen of the PEGs is also capable of hydrogen bonding with suitable reagents. Empirical selection of the glycols or PEGs as potential plasticizers has, in the past, been based on the assumption that the primary interaction with the polymer was via hydrogen-bonding. The fact that this principle is not generally applicable to all pharmaceutical polymers has been demonstrated by Kent and Rowe (1978).

The relative effectiveness of plasticizers to modify the tensile properties of HPMC, PVP or Starch 1500 (Section 3.4.2) does not support a generalised hydrogen-bonding mechanism for plasticizer activity. Consideration of the molecular weight and structure of the

Plasticizers (Chapter two) suggests that, if hydrogen-bonding were the determining factor for plasticizer efficiency, the lower molecular weight glycol monomers would be most effective. Using the number of hydroxyl groups per unit molar mass as a criterion of hydrogen bonding capability, the following rank order for plasticizer efficacy is expected:

Ethylene glycol = Glycerol > Propylene Glycol > Hexylene Glycol > PEG 200 > PEG 400 > PEG 600

A similar rank order, favouring the lower molecular weight monomers, would be obtained if plasticizer efficacy was determined on a colligative basis, i.e. on the number of plasticizer molecules available for interaction as suggested by Aulton et al., (1981):

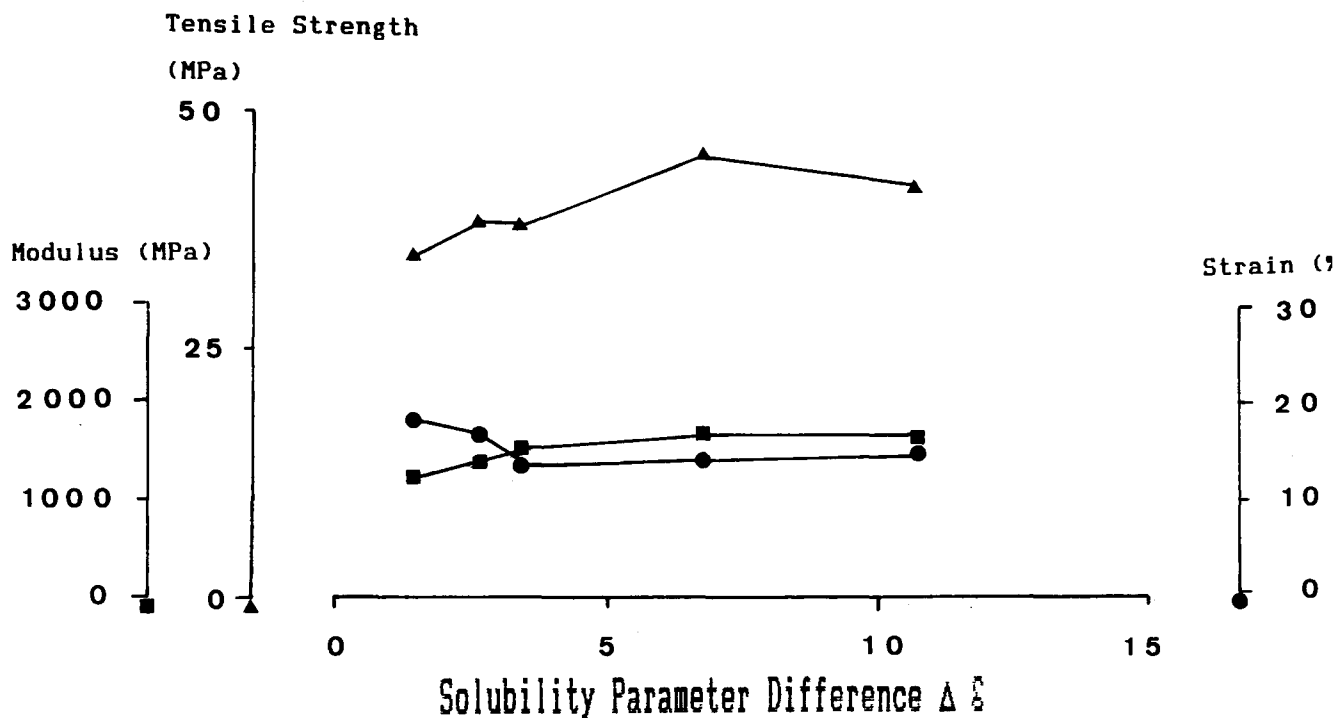
Ethylene glycol > Propylene Glycol > Glycerol > Hexylene Glycol > PEG 200 > PEG 400 > PEG 600

Inspection of the data presented in Section 3.4.2 indicated that these empirical rank correlations were not substantiated for HPMC, PVP or Starch 1500. Consequently, the thermodynamic approach to polymer-plasticizer compatibility was examined as an alternative explanation. Within the limitations of the thermodynamic approach it was expected that the observed tensile rank correlations would follow the relationships established for polymer-plasticizer compatibility. This was tested by plotting tensile properties of HPMC and PVP films against solubility parameter difference and estimated Flory-Huggins interaction parameter for each plasticizer. The resulting plots are shown in Figs. 3.11a-b and 3.12a-b for HPMC and PVP respectively. In all cases the plots showed an inflection (consistent with greater plasticizing efficiency) as either the solubility parameter difference tended to zero, or the interaction parameter tended to 0.5 or less. The rank correlation for plasticization efficiency, therefore, followed that established for polymer-plasticizer compatibility. It was apparent that non hydrogen-bonding interactions (dispersion forces and dipolar forces) played a significant role both in the solubility behaviour and in the effective plasticization of HPMC and PVP.

Correlations between solubility parameters and plasticization efficiency have been observed for ethylcellulose (Entwistle and Rowe, 1979; Abdul-Razzak, 1980). A similar correlation between the

Figure 3.11 Variation of Tensile Properties of HPMC With Thermodynamic Parameters

a. Solubility Parameter



b. Interaction Parameter

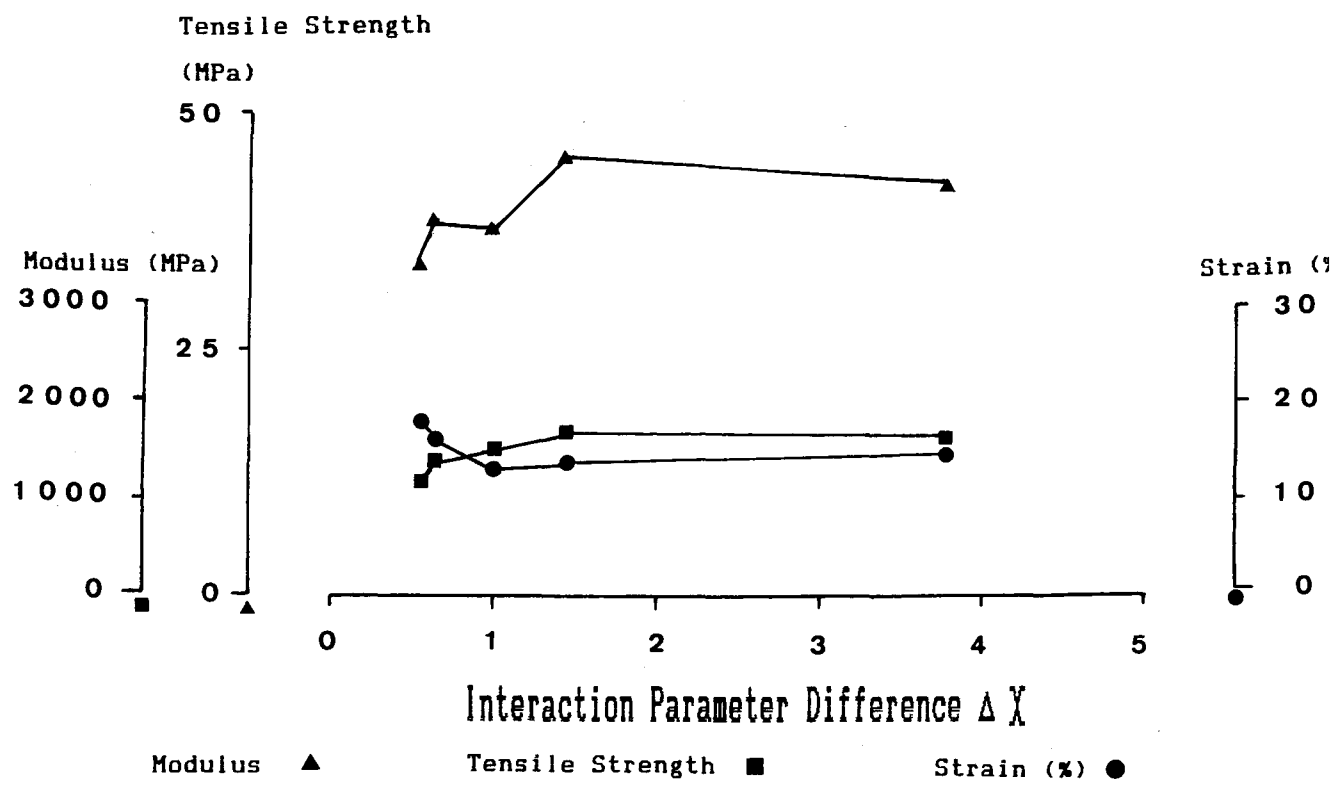
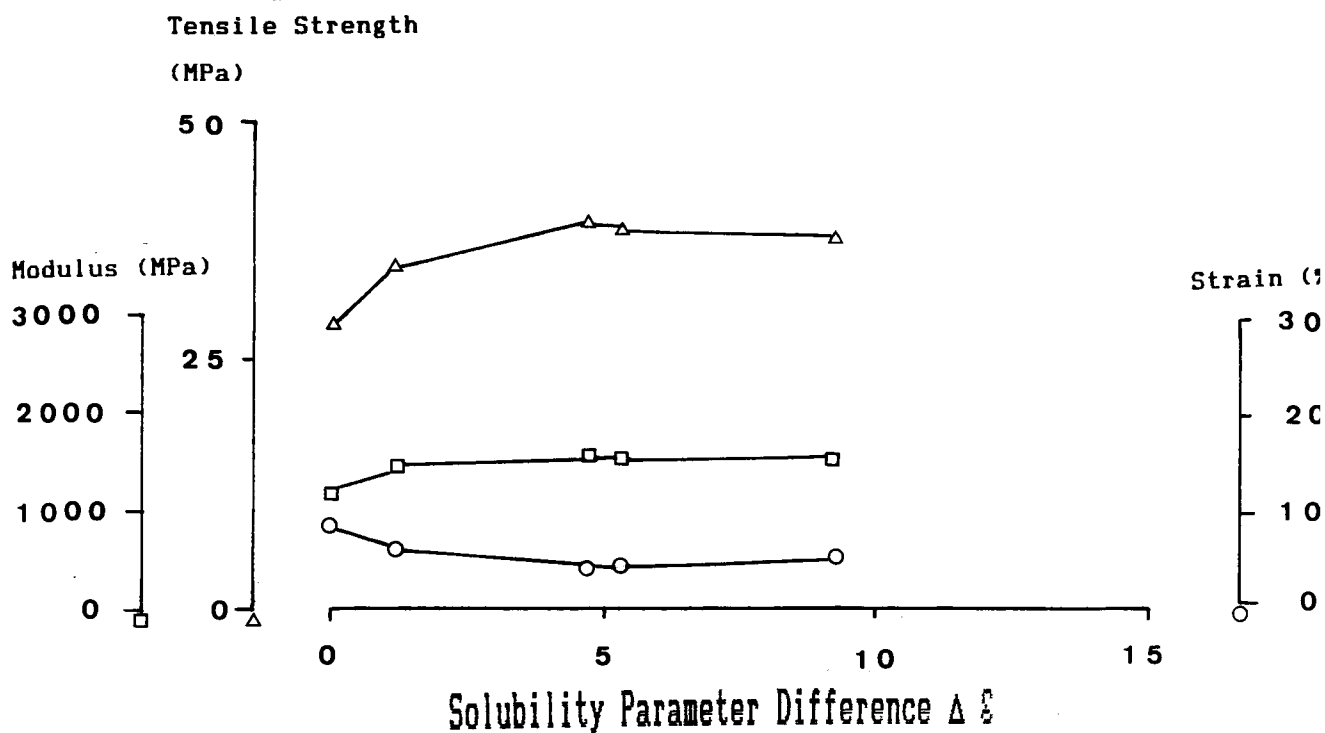
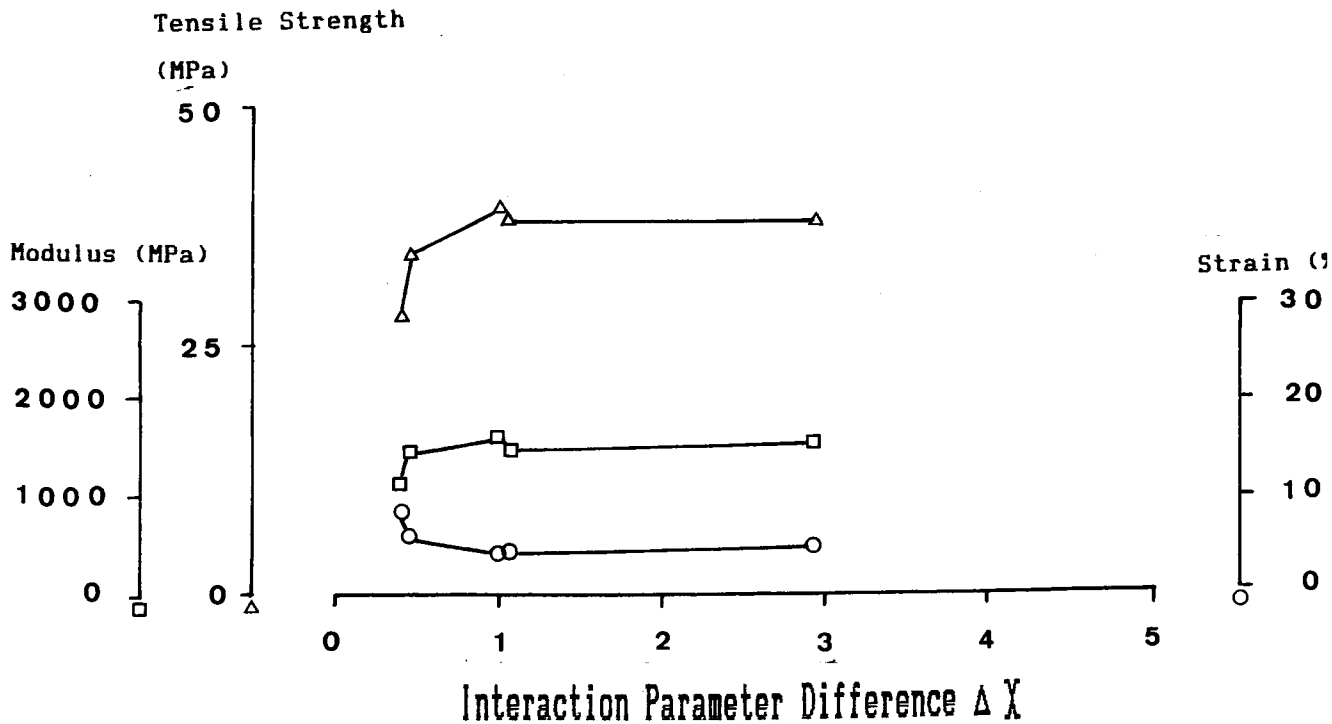


Figure 3.12 Variation of Tensile Properties of PVP With Thermodynamic Parameters

a. Solubility Parameter



b. Interaction Parameter



Modulus Δ / Tensile Strength □ Strain (%) ○

interaction parameter and plasticizer efficiency has been demonstrated for polyvinyl chloride (Doty and Zable, 1946; Boyer and Spencer, 1947; Anagnostopoulos, 1965).

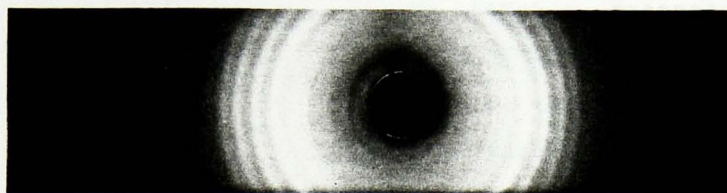
Molecules having limited thermodynamic compatibility may still exhibit plasticizer activity, as in the case of glycerol and ethylene glycol (non-solvents for HPMC and poor solvents for PVP). The ability of non-solvents to plasticize HPMC is a consequence of the asymmetry of the polymer-solvent phase equilibrium (Fig. 2.2) and the resultant solubility of the plasticizer in the polymer. The ability of ethylene glycol and glycerol to increase the plasticity of PVP films probably results from solvation of the ketone oxygen by hydrogen bonding. This would probably be accompanied by the evolution of heat in a manner analogous to dissolution of PVP in water.

In the construction of Figs. 3.11 and 3.12 the tensile properties of films plasticized with PEG 200 were used. The higher molecular weight PEGs showed reduced plasticization efficiency although the magnitude of their solubility parameters and interaction parameters were similar. Previous workers have explained this in terms of the increased hydrogen-bonding capacity of lower molecular weight PEGs and in terms of the increased number of molecules available for interaction. On this basis, the monomer, ethylene glycol, would be expected to be a superior plasticizer to the PEGs. But this was not observed either with HPMC or PVP. The decrease in polymer-plasticizer compatibility with a reduction in the polymer-plasticizer molar volume ratio was predictable from theory and was substantiated in practice. The decrease in PEG plasticization efficiency with increasing molecular weight was, therefore, a consequence of the effect of relative molecular volume on compatibility.

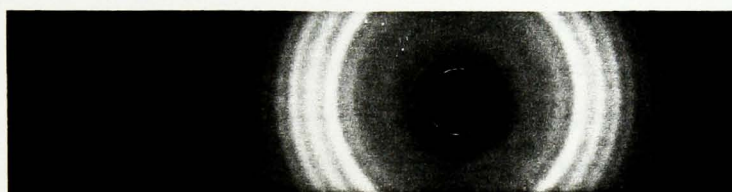
The presence of extensive crystallinity in a polymer presents a considerable physico-chemical obstacle to effective polymer-plasticizer compatibility and plasticization. The ability of glycerol and propylene glycol to exert significant plasticizer activity was consequently unexpected. Okhamafe and York (1983) observed that the addition of a plasticizer eliminated crystallinity in HPMC. X-ray crystallographic examination of unplasticized and glycerol-plasticized Starch 1500 films (Fig. 3.13) revealed no difference in the spectra.

Figure 3.13 X-Ray Crystallographs of Unplasticized and Glycerol-Plasticized Starch 1500

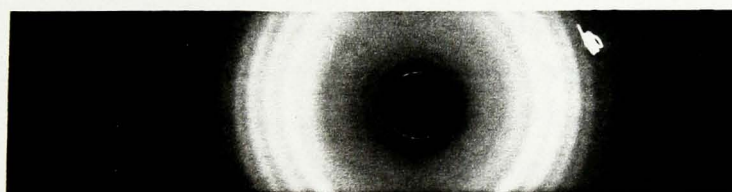
Gelatinised Starch 1500
(Unplasticized)



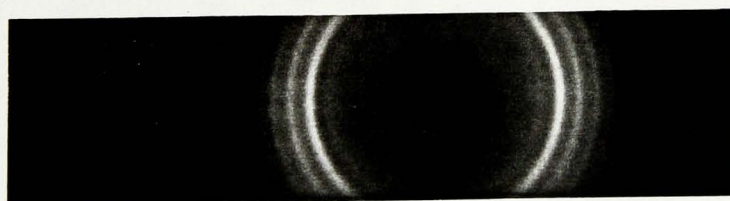
Gelatinised Starch 1500
+ Glycerol 10% w/w



Gelatinised Starch 1500
+ Glycerol 20% w/w



Gelatinised Starch 1500
+ Glycerol 30% w/w



Elimination of crystallinity could not, therefore, account for the observed plasticization. This indicates that the action of glycerol is mediated only within the amorphous (amylopectin) component of starches. The starch matrix is perhaps best regarded as a filled polymer (i.e. an amorphous polymer containing a dispersed solid). The plasticizing effects of added glycerol are therefore analogous to the addition of a plasticizer to a filled polymer (Rowe, 1983; Okhamafe and York 1984b).

3.5 Conclusions

Using tensile test methods, considerable differences were observed between the mechanical properties of three commonly-used polymeric tablet binders. From the shapes of the characteristic stress-strain curves and the magnitude of the derived tensile parameters PVP was classified as a hard, brittle material; HPMC was classified as a hard, tough material and Starch 1500 as a soft, weak material. These results showed some similarities and some differences with the observations of other workers. The differences could largely be accounted for in terms of test methodology or the grade of polymer used.

Increased moisture content of the polymers or inclusion of sufficiently compatible (potential) plasticizers resulted in significant changes in the tensile mechanical properties of cast films which were consistent with a plasticizer activity. The reduction in elastic modulus implied that plasticized polymers were capable of greater elastic strain. The increased extensibility coupled with induction of yield suggested, however, that elastic strain could be dissipated more readily by plastic flow, without failure of the film. At low levels of plasticizer inclusion, there was a concurrent increase in film toughness. However, as the plasticizer level was further raised, the film toughness decreased since the increased extensibility was insufficient to compensate for reduction in film strength.

Increased moisture sorption or incorporation of a plasticizer resulted in changes in the shape of the stress-strain curve, indicating qualitative modification of the viscoelastic properties of the polymer matrix. As the plasticizer level was increased PVP films were transformed from glassy-brittle to a rubbery-liquid state. Similarly, increased plasticizer levels resulted in a shift in Starch 1500 properties from predominantly glassy to a more ductile transition state. The stress-strain curve for unplasticized HPMC was characteristic of a polymer in the transition state, but plasticization resulted in a more ductile type of deformation. The increased extensibility and decreased modulus of plasticized HPMC films, indicated a transition towards the rubbery state. The general

trend common to all the polymers, was a shift to decreased elastic rigidity and increased ductility.

Explanation of the observed plasticization phenomena was possible by reference to the thermodynamic factors controlling polymer-plasticizer compatibility and to the gel theory of plasticization. The two concepts offer a complementary approach to an understanding of the plasticization process. The relative hydrogen-bonding potential between polymer and plasticizer alone, was not adequate to explain the plasticizing efficiency of different molecules. There was, however, good agreement between the observed tensile properties and the extent of compatibility as determined by solubility parameter and interaction parameter considerations. Further, the asymmetry of the polymer-plasticizer phase diagram predicted from thermodynamic theory, provided an explanation for the observed ability of poorly interacting non-solvents to exert a plasticizer action. While application of thermodynamic principles establishes the quantitative limits for effective plasticization, gel theory provides a model mechanism by which the process can proceed (Doolittle, 1954). The Flory-Huggins interaction parameter, which characterises the magnitude of the polymer-plasticizer interaction, can be regarded as analogous to the affinity of a plasticizer for polymer active centres in the gel theory.

The value of tensile testing in determining fundamental properties of materials is subject to certain limitations. The quantitative values obtained are dependent to a great extent on the test protocol adopted and may be influenced by the rate of strain and the method of sample preparation. Nevertheless, the use of a fixed strain rate and controlled method of sample preparation enabled comparative data to be obtained on the effects of plasticization on rigidity, strength and gross deformability of polymeric binders. Tensile tests performed at a single strain rate, however, yield little fundamental information about time-dependent viscoelastic and plastic components of deformation. Changes in the characteristic shape of the stress-strain curves indicated that both moisture sorption and plasticization produced in changes in the viscoelastic nature of the binder film. Results indicated a qualitative shift in viscoelastic nature, from predominantly elastic in the unplasticized polymer, to progressively

more viscous with increased plasticizer content.

Literature reviewed in Chapter one indicates that tablet formation in general, and the compression performance of binders in particular, is intimately associated with non-recoverable or time-dependent plastic deformation. Quantification of the time-dependent deformation of polymeric binders and its modification by plasticization, should give a greater insight into some fundamental properties determining the tableting performance of binders. Consequently, resolution and quantification of the discrete components of viscoelastic deformation, by use of creep rheological methods forms the subject of the following chapter.

CHAPTER FOUR
CREEP RHEOLOGY OF POLYMERIC TABLET BINDERS

CHAPTER FOUR

CREEP RHEOLOGY OF POLYMERIC TABLET BINDERS

4.1 Investigation of Time-dependent Deformation

A number of techniques have been utilised to investigate time-dependent deformation in materials of pharmaceutical importance. Stress-relaxation, in particular, has been widely used in tableting research. Stress-relaxation studies on film-forming polymers have been limited, however, probably because of difficulties in mounting the sample to limit slippage at the grips during testing. Castello and Goyan (1964) used this method to investigate viscoelasticity of glycerogelatin films used in the manufacture of soft gelatin capsules. Thermally aged films showed decreased initial rigidity moduli and decreased equilibrium moduli compared with unaged films, this being consistent with a thermally-mediated crystalline-amorphous transition in the glycerogelatin melt.

Probably the most informative technique for studying time-dependent deformation is the creep test in which an (ideally) instantaneous stress is imposed on a sample at zero time and maintained at a constant value whilst the resulting strain is measured with time. Creep rheological methods have been applied to a wide range of materials of pharmaceutical interest including polymers. Micro-indentation techniques, in which the penetration of a loaded probe into a test specimen is determined as a function of time, have proved to be particularly informative. Monk and Wright (1965) described the construction and use of a pneumatic micro-indentation apparatus for measuring the hardness of paint films. The precision of the instrument and its application in characterising the viscoelastic properties of thin polymer films have been discussed by Morris (1970, 1973). The change in indentation geometry as indentation depth increases with time, and the consequential change in stress conditions, potentially limited use of the apparatus for fundamental studies. However, the theoretical approach of Lee and Radok (1960) applied to a spherical indenter probe enabled creep compliance to be evaluated despite the change in stress conditions during indentation.

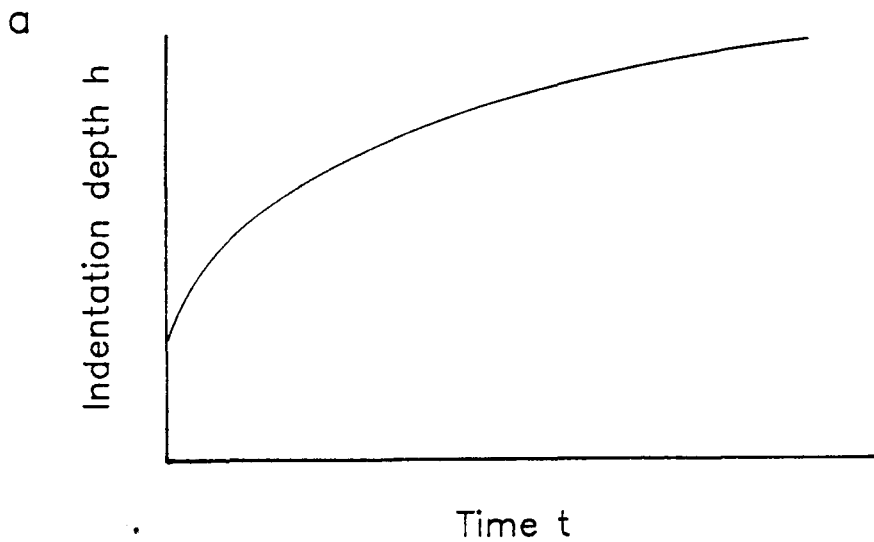
Several workers have used micro-indentation to characterise mechanical properties of tablet film-coating polymers and to assess the performance of potential plasticizers. Rowe (1976a) used the ICI micro-indenter to measure the elastic properties and hardness of HPMC coatings on tablets. Incorporation of glycerol and propylene glycol into HPMC films resulted in films which were softer and more elastic. A similar effect was noted with low molecular weight liquid PEGs. With higher molecular weight solid PEGs an increase in elastic modulus occurred which, in the case of PEG 20000, exceeded the modulus of the unplasticized film. The molecular weight of the PEGs did not appear to have a significant effect on the Brinell hardness of the film although in all cases the hardness was less than that of the unplasticized film. Rowe (1976b) also used the technique to investigate the effect of the molecular weight of various grade of HPMC on film properties. Increasing molecular weight produced films of greater Brinell hardness and elastic modulus.

Porter and Ridgway (1977) used an ICI micro-indenter to evaluate polyvinyl acetate-phthalate (PVAP) and cellulose acetate-phthalate (CAP) films in situ on tablet cores. At low plasticizer concentration CAP films exhibited much greater surface hardness than PVAP films. But an increase in plasticizer level resulted in a decrease in hardness for both films, with CAP hardness approaching that of PVAP.

Aulton et al., (1980), using the vertical displacement indentation tester of White and Aulton (1980), reported indentation-depth profiles recorded over a 600 second period, for unplasticized and plasticized films of HPMC cast from aqueous solution. They showed that both sorbed moisture and the presence of a plasticizer increased time-dependent indentation compared with the unmodified polymer. Although Aulton et al., (1980) did not present their results in the form of a creep profile, the viscoelastic nature of HPMC deformation was clearly evident. Subsequently, Aulton (1982) questioned the validity of using unique single point hardness values for such polymers. The indentation profile of a polymer may not achieve an equilibrium depth thus hardness apparently decreases with time. Indeed, depending on the time of indentation, equivalent hardnesses may be obtained for polymers of vastly differing viscoelastic properties as illustrated by Fig. 4.1.

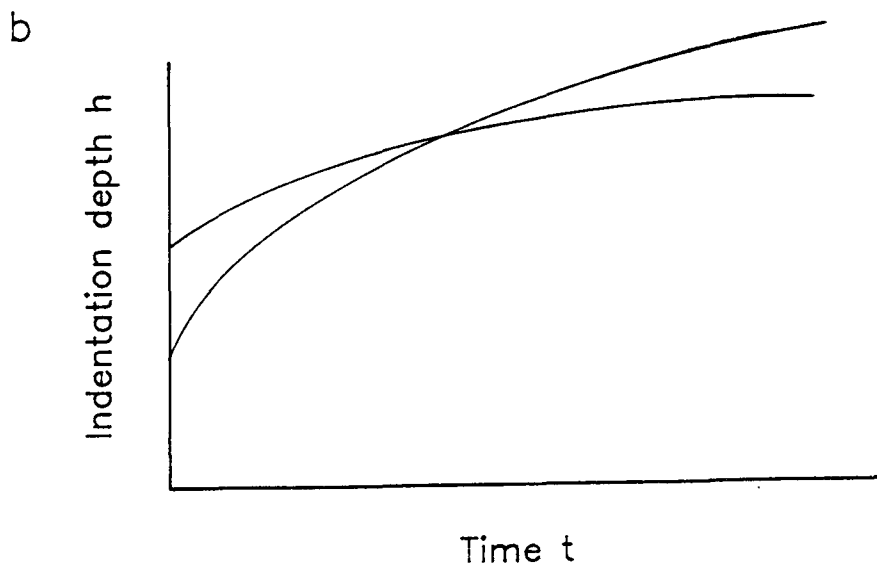
Figure 4.1 Indentation Depth versus Time Profiles of Two Polymer Formulations with Different Deformation Characteristics

(After Aulton, 1982)



$$\text{Brinnell Hardness HB} = \frac{F}{\pi Dh}$$

where F is the load applied, D is the indenter diameter and h is the indentation depth. But which h ?, which t ?



The indentation depth versus time profiles of two polymer formulations with different deformation characteristics

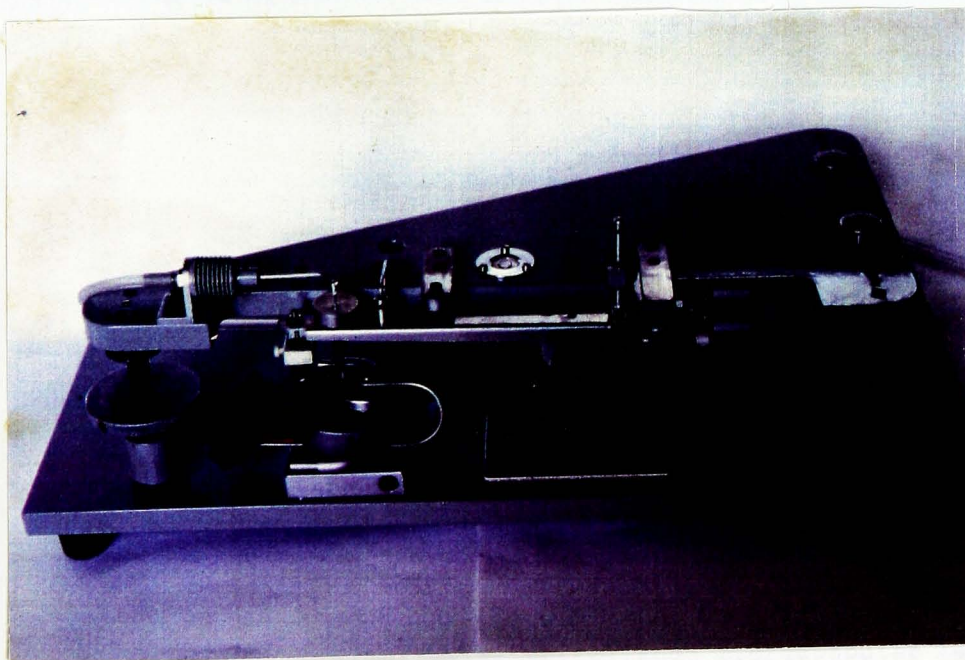
Application of micro-indentation techniques for the evaluation of polymeric tablet binders has been more limited although Rubenstein and Healey (1973) used the method to investigate moisture effects on gelatin binder films. Reading and Spring (1984a) used an ICI micro-indenter to study the hardness and creep compliance of a series of hydrophilic polymeric tablet binders. The binders they examined were gelatin (Byco C), maize starch, methycellulose (Methocel A15) and polyvinyl pyrrolidone (40000 Da.). Creep curves were determined for 120 seconds under load and for 240 seconds in recovery. Brinell hardness of all films was decreased with increasing moisture content. Creep curves determined for films conditioned at 12% RH were elastic in nature with no time dependency under load. Conditioning at 81% RH (58% RH for PVP) resulted in films which deformed both elastically and plastically.

4.2 Materials and Methods

4.2.1 The ICI Micro-indenter

The basic instrument, first described by Monk and Wright (1965), is shown in Fig. 4.2.

Figure 4.2 The ICI Micro-indenter



It consists of a triangular shaped main chassis of steel plate, which is supported on the base plate by three adjustable legs. Two of the legs enable coarse and fine adjustments for raising or lowering the main chassis or for zeroing the instrument. The coarse adjustment has a single screw thread of 20 threads per inch (tpi). The fine adjustment has a differential thread of 26 tpi and 28 tpi so that one revolution of the adjustment wheel gives a vertical movement of 20 μm at the position where the test sample is mounted. This wheel is graduated in divisions of 0.5 μm and can be used to calibrate the instrument. A beam mounted on brass crossed flexure bearings has adjustable counter-balance weights at one end. At the other end are mounted an adjustable weight for setting the neutral stability of the beam, an oil-filled dashpot damper and the indenter needle. The basic instrument was modified as follows: In place of the flapper of the original flapper/nozzle pneumatic amplifier, a steel armature (LVDT core) was fitted. The nozzle of the pneumatic amplifier was removed and replaced with the body of a sub-minutire linear variable differential transformer (LVDT) (model 222-00005, RDP Electronics, Wolverhampton). The output of the energised LVDT was dependent on the depth of penetration of the steel armature into the LVDT body and was accurate to $\pm 0.1 \mu\text{m}$.

The test specimen was mounted on a rigid platform immediately below the indenting sphere of the indenter needle. The indenting load was pneumatically lowered onto the beam immediately above the indenter tip by means of a bellows system. As the specimen was indented, the vertical movement of the indenter sphere and hence the depth of indentation was gauged by the change in output from the LVDT. An amplifier (model 2027A, RDP Electronics, Wolverhampton) and stabilised power supply (model 2031, RDP Electronics, Wolverhampton) energised the primary coil of the LVDT at 5KHz, 5V RMS and demodulated the output of the secondary coils to give a signal between 0V d.c. and 10V d.c. at full scale displacement of the transducer. The amplifier gain may be adjusted to give an output suitable to drive a digital voltmeter, a chart recorder or, as in this case, suitable for conversion to a digital signal by means of an analogue-to-digital converter (ADC). This digital signal was then suitable for data logging and manipulation using established microcomputer techniques.

4.2.2 Data Logging Using the BBC Model B Microcomputer

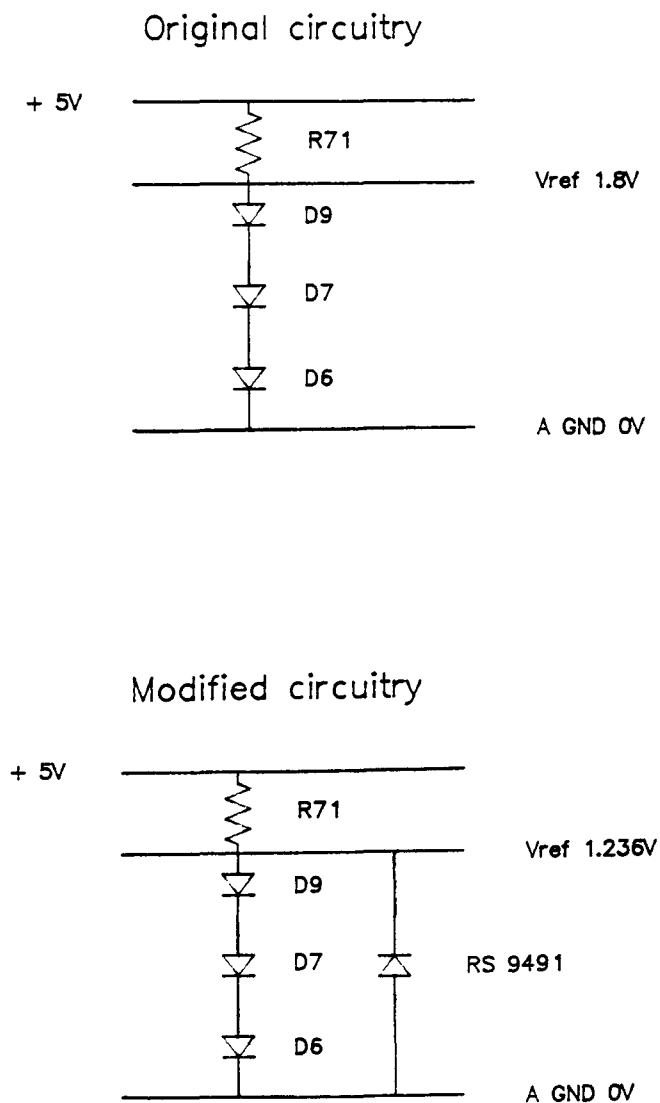
In the present work a BBC model B microcomputer (Acorn Computers, Cambridge) with disc storage capability was used for data logging and manipulation. Although not a purpose built data-logger, the BBC model B has a number of features which make it attractive for this type of application. In particular, the BBC model B contains an internal four channel ADC which is readily accessed via the analogue port (more commonly used to input games paddles and joysticks). Control of the ADC is easily achieved by commands contained in BBC BASIC and data logging rates of 25 Hz (four channel sequentially) or up to 100 Hz (single channel) can be attained without resort to machine code programming. Using structured BASIC and the graphics capabilities of the BBC microcomputer data analysis and presentation is relatively straightforward.

To optimise the data logging capabilities of the BBC model B the original ADC microchip was replaced by an upgraded device (μ Pd 7002C-1, NEC Corporation, Japan) with a typical resolution of 10 bits. Ideally the device should yield 12 bit resolution, however, some resolution is lost due to electronic noise associated with the circuitry of the ADC. This noise has been shown to be distributed normally about the true mean value, consequently, where the analogue signal is changing relatively slowly, software averaging can be used to reduce the influence of noise (Beverly, 1983). Using an appropriate machine code routine, resolutions of 11 bit (40msec per sample) and 12 bit (160ms per sample) were obtained.

Analogue-to-digital conversions using the BBC microcomputer are performed by successive approximations to an internal reference voltage generated by the voltage drop across three silicon diodes. The reference voltage equivalent to 4096 byte was nominally 1.8V. On the microcomputer used in this work, the reference voltage was 1.890V on power-up falling to 1.798V after 6 hours and failing to stabilise even after 24 hours. This variation was unacceptable for absolute measurement of displacement using the LVDT. Two approaches were possible to overcome this problem; the provision of an external reference voltage, e.g. a Weston standard cell at 1.018V, or the incorporation of an external voltage reference such as a zener or band

gap diode between the Vref (reference voltage) pin and the analogue ground pin of the ADC device. The latter option was found to be satisfactory using a low current band gap diode (Radiospares, RS 9491) with a nominal breakdown or zener voltage of 1.26V. Since the breakdown voltage is less than the original reference voltage the internal diodes do not conduct and do not affect the accuracy of the additional reference diode. The modifications to the circuit are shown in Fig. 4.3. With the RS 9491 diode fitted a reference voltage of 1.235V was obtained on power-up settling to a steady 1.236V after a few minutes. No further drift in the reference voltage was observed after monitoring for 24 hours.

Figure 4.3 ADC Circuit Modification To the BBC Model B Microcomputer



When calibrating the ICI microindenter the gain of the transducer amplifier was adjusted such that a full scale deflection of $6\mu\text{m}$ at the indenter sphere produced an analogue output of 1.000V. Calibration was carried out in situ using a load of 20g on a glass microscope slide as a reference surface by means of the graduated fine adjustment wheel. The fine adjustment wheel was adjusted to give displacements of 0 to $6\mu\text{m}$ in increments of $0.5\mu\text{m}$. At each interval, the digital byte value corresponding to the d.c. voltage induced in the LVDT was recorded. From the regression of digital byte value on displacement, calibration constants for the data-logging software were derived. Calibration data is shown in Table 4.1.

Table 4.1 Calibration Data for the BBC Interfaced ICI Microindenter

Vertical displacement at the indenter sphere (μm)	Digital byte value
0.0	0
0.5	282
1.0	541
1.5	805
2.0	1119
2.5	1438
3.0	1687
3.5	1945
4.0	2209
4.5	2448
5.0	2726
5.5	3007
6.0	3305
Regression coefficient r	= 0.9997
Slope (bytes/ μm)	= 547
Intercept (bytes)	= 13

4.2.3 Sample Preparation

In the previous chapter it was shown that the extent of tensile plasticity in a plasticized polymer film was generally dependent on the extent of polymer-plasticizer compatibility. Using both mixing thermodynamics and an assessment of tensile mechanical properties, optimum plasticizers for some commonly used tablet binders were identified. These were PEG 200 for PVP and HPMC respectively, and glycerol for starch. Consequently, in subsequent studies, the optimum plasticizers were utilised in preference to other glycols exhibiting plasticizing activity.

The preparation of polymer solutions, with or without plasticizer, was carried out as described previously. The following systems consisting of polymer and the optimum plasticizer were utilised:

- PVP + 0% - 15w/w PEG 200
- HPMC + 0% - 30w/w PEG 200
- Starch 1500 + 0% - 30w/w glycerol

Films of about 100 μ m thickness were cast onto degreased and dried glass microscope slides and were subsequently dried for twenty four hours in a laminar flow cabinet under ambient temperature and humidity. Samples of the dried films were then transferred to hygrometers containing either a saturated solution of potassium acetate or sodium bromide giving 22.5% RH and 59.5% RH respectively at 20°C (Nyqvist, 1983). Films were equilibrated for not less than seven days prior to indentation testing. In addition, samples of the unplasticized polymers were also stored at near zero relative humidity over phosphorous pentoxide. This was to allow assessment of material properties with the minimum of influence from sorbed moisture. The design and operation of the Instron tensile tester precluded this type of experiment in the previous chapter.

4.2.4 Indentation Testing

The modified ICI indentation tester was mounted within a glove box to enable relative humidity during testing to be maintained as closely as possible to the storage humidity of the test samples by use of the appropriate saturated salt solutions. The equilibrated test samples

were rapidly transferred to the indenter glove box prior to testing and the humidity allowed to re-equilibrate before performing a test. The test variables and conditions used are summarised in Table 4.2.

Table 4.2 Indentation Test Variables

Variable	Procedure	Comments
Indentation load	20g (unplasticized films) 10g (plasticized films) 1g (some PVP films only)	Determined by experiment to achieve indentations of 0-6µm over the test duration.
Indenter tip	Sapphire sphere 1.550mm diameter	To achieve measurable indentation at low load and determine creep compliance in spite of changing indentation geometry.
indentation duration	1000 seconds under load	Period over which linearity of the creep compliance curve is attained. Determined by experiment.
	Long term runs carried out for 5000 seconds under load	To confirm time at which the creep curve attains linearity.
Equilibrium conditions:		
Temperature	20°C ± 2°C	
Relative humidity	0% RH 22.5% RH 59.5% RH	To study polymer properties at low moisture content. To study influence of moisture sorption on viscoelastic properties.

With the test sample rigidly clamped beneath the indenter tip, the indenting probe was gently lowered onto the surface of the test film until it just touched the film surface. The output of the LVDT at this point was then zeroed electronically and this was recorded as zero penetration depth (digital byte value = 0) by the data-logging system. The indenting load was lowered on to its stage above the indenter probe by a pneumatic bellows system. This ensured uniform and reproducible load application. Collection of time-indentation depth coordinates was initiated automatically as soon as the applied load caused measurable indentation into the test film. The voltage output of the LVDT during indentation was recorded as digital byte values which were then converted to displacements in μm . At the end of an indentation test, the logged data was converted to the form of a creep compliance curve by means of software specifically written for this work (see section 4.3.1). Data captured by the BBC microcomputer were stored on floppy discs, to allow for future graphical examination and analysis by discrete mechanical analysis and continual spectral analysis.

4.3 RESULTS AND DISCUSSION

4.3.1 Analysis of Creep Compliance

Data obtained from the ICI microindenter was in the form of a depth of indentation versus time profile. In order to yield the most information it was necessary to convert this data to the form of a creep curve. However, as a test sample is indented by the indenter sphere the indentation geometry and hence the stress conditions are continually changing. A solution to the problem of the partial penetration of an incompressible semi-infinite plane viscoelastic surface by a smooth rigid sphere has been suggested by Lee and Radok (1960). They derived the following equation:

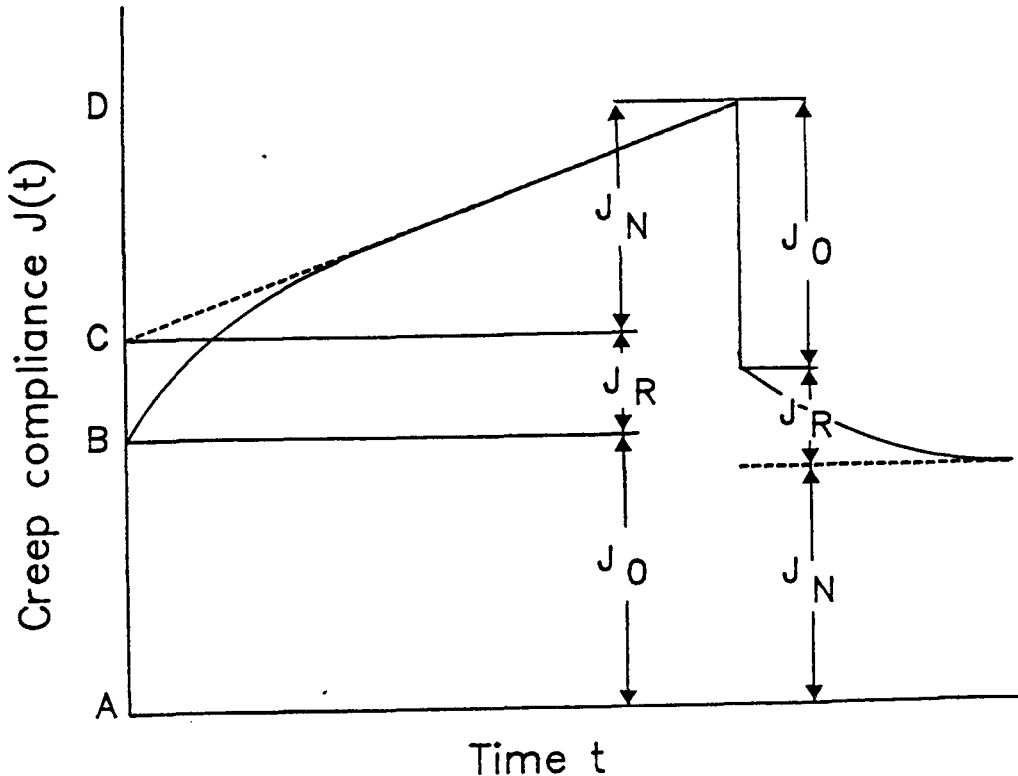
$$J(t) = (16/3) R^{0.5} (1/F) h(t)^{3/2} \quad (4.1)$$

where $J(t)$ is the overall creep compliance at time t , R is the radius of the indenting sphere, F is the indenting force, and $h(t)$ is the depth of indentation at time t . By the incorporation of constants

into the software, indentation depth was converted to creep compliance using the equation of Lee and Radok (1960) and the data stored on floppy disc for further analysis. In the present work indentation profiles were determined only under load and not in recovery. The stress conditions with application of load on a spherical indenter are given explicitly by the solution to the equation of Lee and Radok (1960). On removal of the indenting load, however, the prevailing stress conditions are something of an unknown quantity. The observed strain recovery may be a function of stress transmission from the test sample to the indenter sphere (decreasing with time as the sample recovers) and of the elastic recovery of the crossed flexure bearings of the indenter beam.

Figure 4.4 shows an idealised creep compliance curve annotated with the three discrete components of creep, described below. Analysis of such a curve is carried out using the classical methods reviewed by Barry (1974).

Figure 4.4 An Idealised Creep Curve



1. A - B is the region of instantaneous elastic deformation. The compliance (J_0) is obtained by dividing the shear strain $\epsilon_0(t)$ measured at the onset of applied shear stress (i.e. at time $t = 0$) by the shear stress σ .

$$J_0 = \epsilon_0(t)/\sigma = 1/G_0 \quad (4.2)$$

G_0 is the shear elastic modulus.

2. B - C is the retarded elastic region with a compliance (J_R). Using mean values for the parameters:

$$J_R = J_M [1 - \exp(-t/\tau_M)] = \epsilon_R(t)/\sigma \quad (4.3)$$

where J_M is the mean compliance of all the bonds involved and τ_M is the mean retardation time ($= J_M / \eta_M$). η_M is the mean viscosity associated with the retarded elastic region and $\epsilon_R(t)$ is the strain in this region. This holds where the retarded elastic behavior can be characterised by a single Voigt unit. Where more than one Voigt unit is necessary J_R is a summation of the individual compliances of all the Voigt units involved:

$$J_R = \sum_i^n J_i [1 - \exp(-t/\tau_i)] \quad (4.4)$$

3. C - D is the linear region of non-recoverable (Newtonian viscous) compliance J_N where:

$$J_N = t/\eta_0 = \epsilon_N(t)/\sigma \quad (4.5)$$

η_0 is the apparent Newtonian viscosity of viscous flow and $\epsilon_N(t)$ is the strain. In this region bonds may rupture so that the time required for them to reform is greater than the test period and the entities flow past each other.

On removal of the indenting stress there is some strain recovery; an instantaneous elastic recovery (D - E) of the same magnitude as the initial elastic deformation (A - B) followed by a retarded elastic recovery (E - F) equivalent to (B - C). In the viscous region (C - D)

bonds are irreversibly broken and the initial structure is not recovered, i.e. the deformation is plastic and permanent.

4.3.1.1 Discrete Mechanical Analysis of Creep Compliance

Characterisation of the creep curve in terms of Maxwell and Voigt mechanical models is termed discrete mechanical analysis. The viscoelastic response can then be quantified in terms of the mechanical properties of the Hookean spring and the Newtonian dashpot. Classical analysis of the creep curve using graphical techniques is illustrated in Fig. 4.5 (a-c).

The instantaneous elastic compliance J_0 is obtained directly from the creep curve as time tends to zero. The rigidity modulus G_0 is given by the reciprocal of J_0 . The apparent Newtonian viscosity η_0 associated with the compliance of non-recoverable deformation is obtained from the slope of the late linear portion of the creep curve since:

$$J_n = t/\eta_0 \quad (4.6)$$

Resolution of the discrete Voigt units required to model the retarded elastic region is achieved graphically using an exponential stripping technique. The retarded elastic compliance J_R is the summation of compliances due to the individual Voigt units:

$$J_R = \sum_i^n J_i [1 - \exp(-t/\tau_i)] \quad (4.7)$$

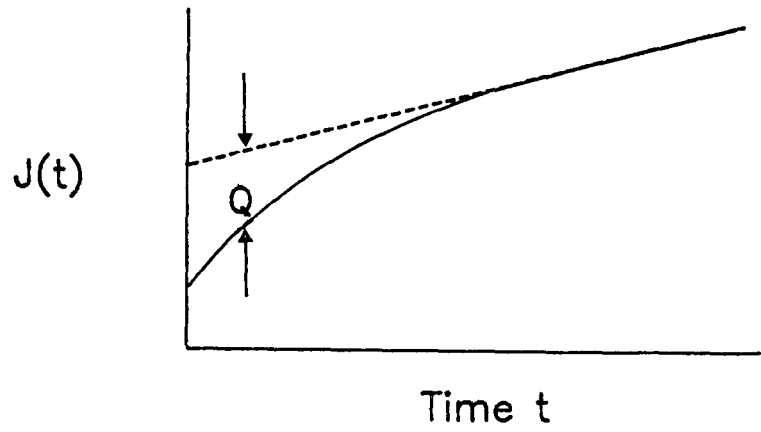
Expanding the expression and defining a function Q such that:

$$Q = \sum_i^n J_i \exp(-t/\tau_i) \quad (4.8)$$

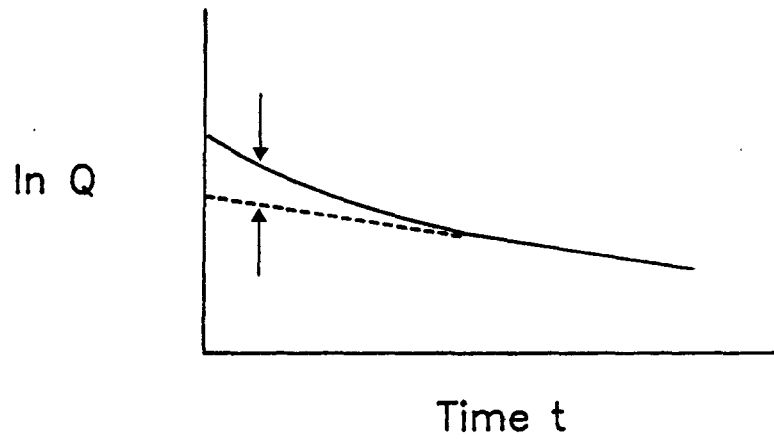
Q represents the distance at any time t between the curved portion of the creep curve and the extrapolated late linear region, assuming that linearity is attained, (Fig. 4.5a).

Figure 4.5 Discrete Mechanical Analysis of the Creep Curve Using Graphical Techniques

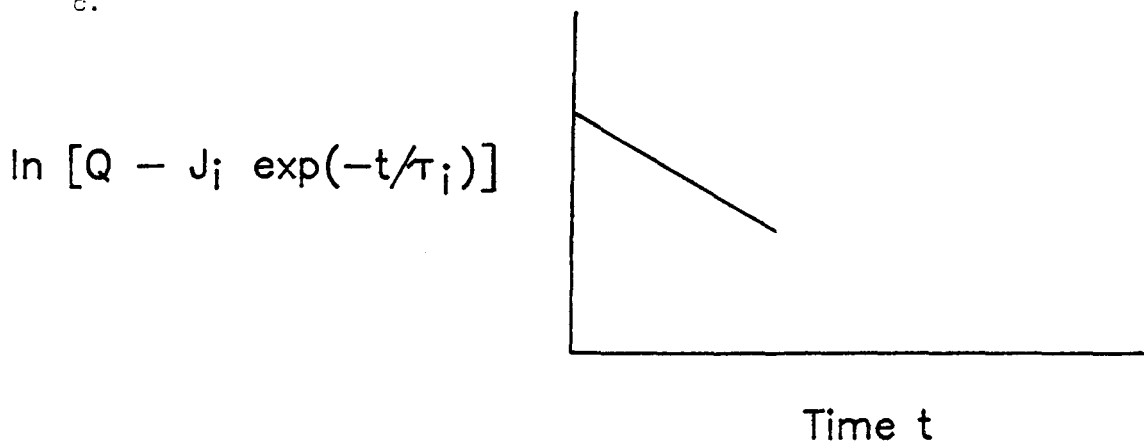
a.



b.



c.



Ignoring the summation and expressing the equation logarithmically then:

$$\ln Q = \ln J_1 (-t/\tau_1) \quad (4.9)$$

$\ln Q$ is then plotted against time (Fig. 4.5b). At late times the plot tends to linearity. The intercept of the extrapolated linear plot and the reciprocal of the slope gives the compliance J_1 and retardation time τ_1 respectively for the first Voigt unit. The apparent viscosity of the dashpot component of the Voigt unit is given by:

$$\eta_1 = \tau_1 / J_1 \quad (4.10)$$

Non-linearity at early times indicates the presence of more than one resolvable Voigt unit. The magnitude of the compliance and retardation time of the second Voigt unit is found by plotting:

$\ln [Q - J_1 \exp(-t/\tau_1)]$ against time, equivalent to the distance between the curved region at early times and the extrapolated late linear region (Fig. 4.5c). The general process is repeated for subsequent Voigt units until the early time data is linear.

4.3.1.2 Continuous Spectral Analysis of Creep Compliance

An alternative to discrete mechanical analysis is the use of continuous spectral analysis. The creep compliance curve can be manipulated so as to construct a continuous spectrum of retardation times. This spectrum represents viscoelasticity in a more generalised manner than functions such as $J(t)$ although graphical construction is still tedious and interpretation of the spectra obtained is difficult. The number of Voigt units in the retarded elastic region of the creep curve is regarded as extending to infinity, and the retardation spectrum L , is defined by the continuous analogue of creep compliance:

$$J(t) = J_0 + \int_{-\infty}^{\infty} L(\tau) [1 - \exp(-t/\tau) \ln \tau + t/\eta_0] \quad (4.11)$$

L has the nature of a distribution function with the dimensions of

compliance. This treatment accepts that in a complex (real) material there is such a large number of different molecular interactions that a wide range of retardation times exist, but that differences between adjacent retardation times may be infinitesimal. The complete spectrum may extend over several orders of magnitude, so by convention a logarithmic representation is used. Maxima in the spectrum indicate concentrations of retardation processes (which are time-dependent elastic strain mechanisms at a molecular level) as measured by their contribution to the overall compliance.

Methods for the construction of retardation spectra have been described by Alfrey (1948) and Schwarzl and Staverman (1952). The value of the distribution function $L(\tau)$ at any time can be derived from a first order differential approximation:

$$L(\tau) = d [J(t) - t/\eta_0] / d \ln t \quad (4.12)$$

$$: t = 2\tau$$

The elastic component of creep compliance $(J(t) - t/\eta_0)$ derived from the creep curve is plotted against $\ln(t)$. The gradient of this curve is calculated at selected points providing the data to calculate $L(\tau)$. This method has the disadvantage that η_0 must be known, i.e. the steady state region of viscous flow must be attained. Where the linear viscous region is not reached, for example in systems where several hours are required to ensure that all Voigt units are fully extended, a second order approximation may be used:

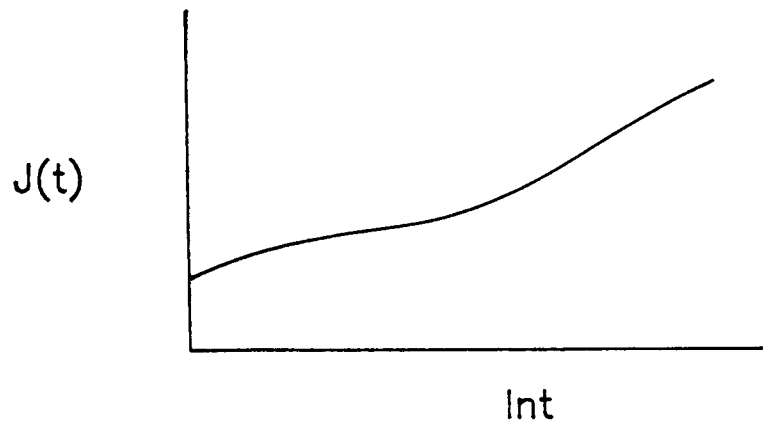
$$L(\tau) = d [J(t) - dJ(t) / d \ln t] / d \ln t \quad (4.13)$$

Application of the second order approximation (Schwarzl and Staverman, 1952) is illustrated in Fig. 4.6.

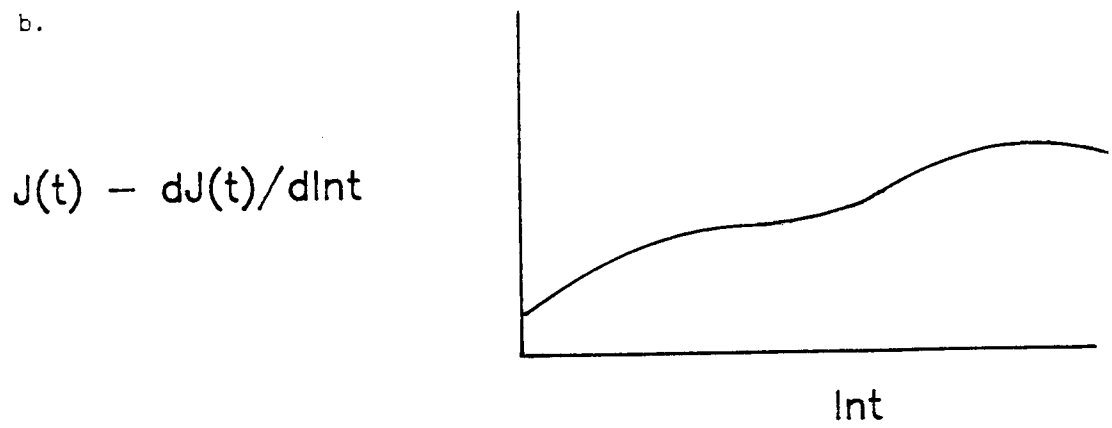
Both discrete mechanical and continual spectral analysis traditionally require laborious and potentially inaccurate graphical analysis. For the present work, several programs were written in BASIC to carry out the above data analyses rapidly and with accuracy. Validation of the programs was carried out by comparing the results of manual graphical analysis and computer-aided analysis of the same creep curve.

Figure 4.6 Continuous Spectral Analysis of the Creep Curve Using a Second Order Approximation

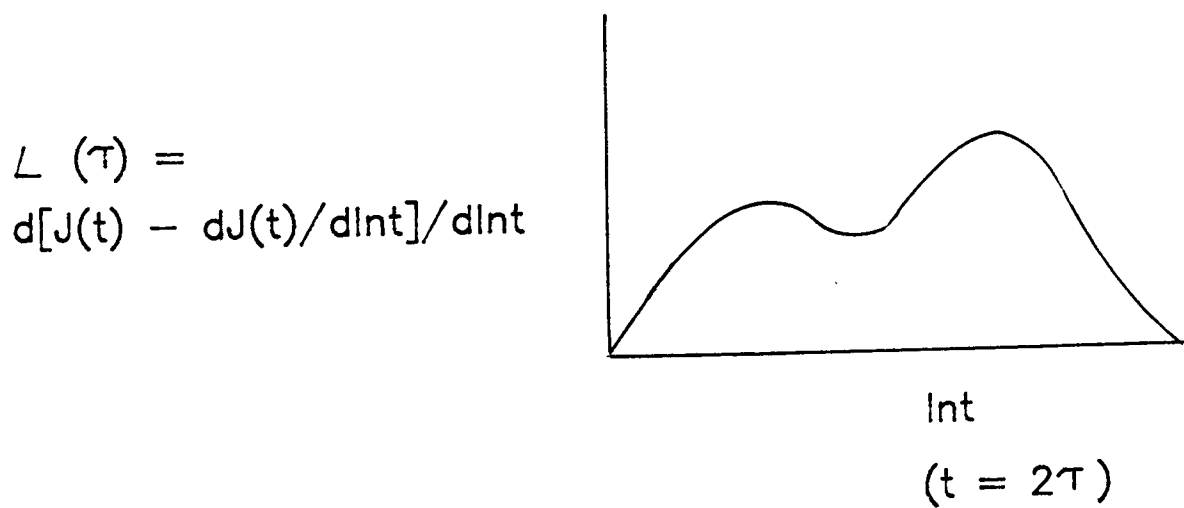
a.



b.



c.



4.3.2 Visual Evaluation of the Creep Compliance Curves

Figures 4.7, 4.8 and 4.9 show the creep compliance profiles for unplasticized films of PVP, HPMC, and Starch equilibrated at 0% RH, 22.5% RH and 59.5% RH. Indentation profiles were recorded over a period of 1000 seconds. Qualitatively, the curves for each polymer were very similar. In all cases there was an initial elastic deformation followed by time-dependent viscoelastic and/or plastic deformations. Visual examination of the creep compliance profiles suggested that in all cases linearity was attained within the test duration.

Figure 4.7 Influence of Moisture on the Creep Compliance of PVP Films

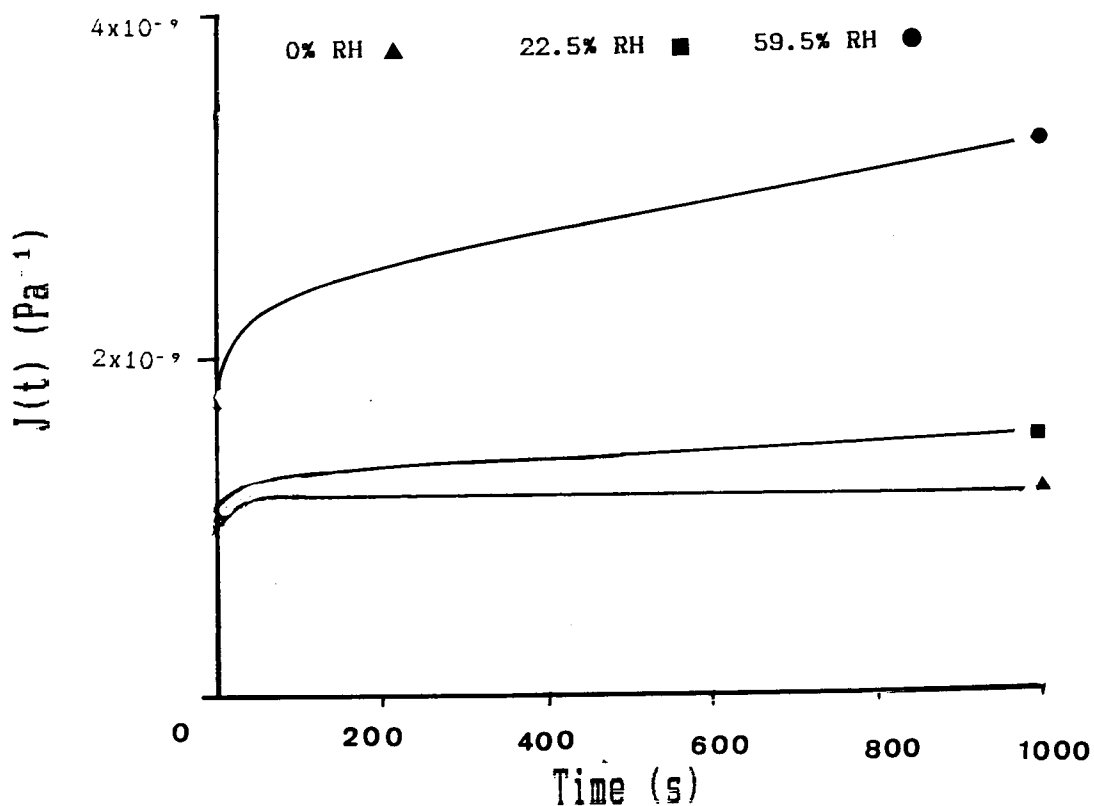


Figure 4.8 Influence of Moisture on the Creep Compliance of HPMC Films

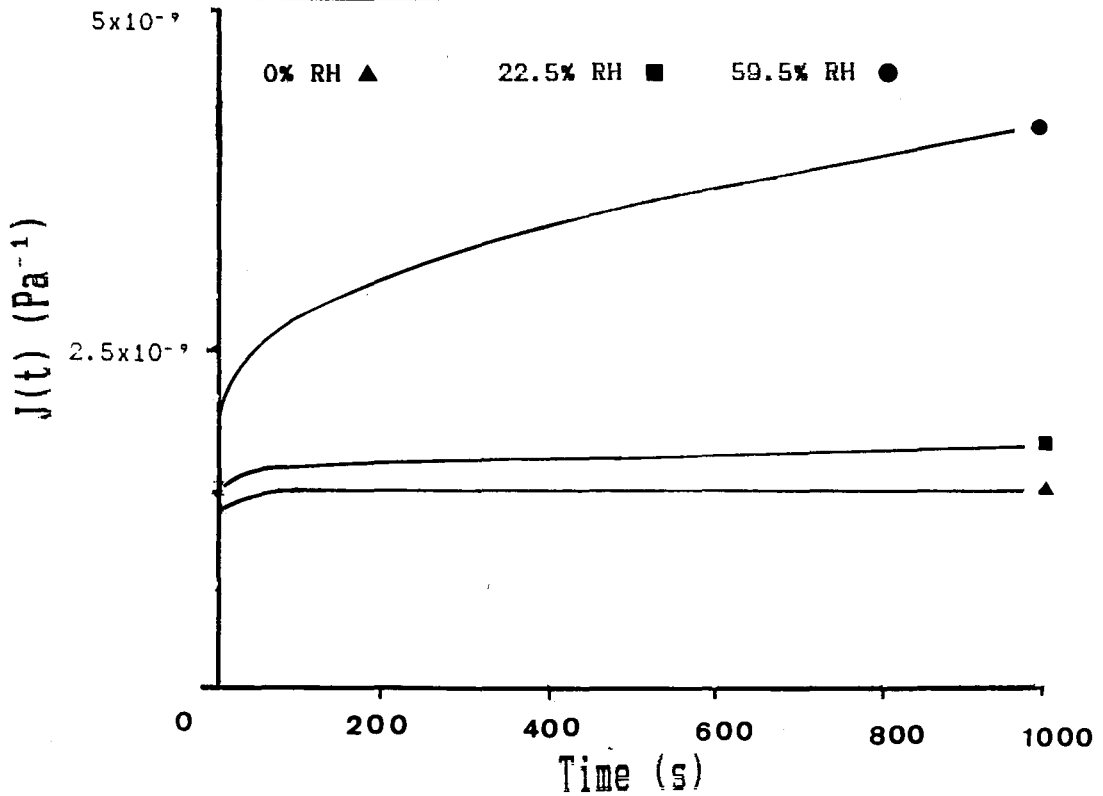
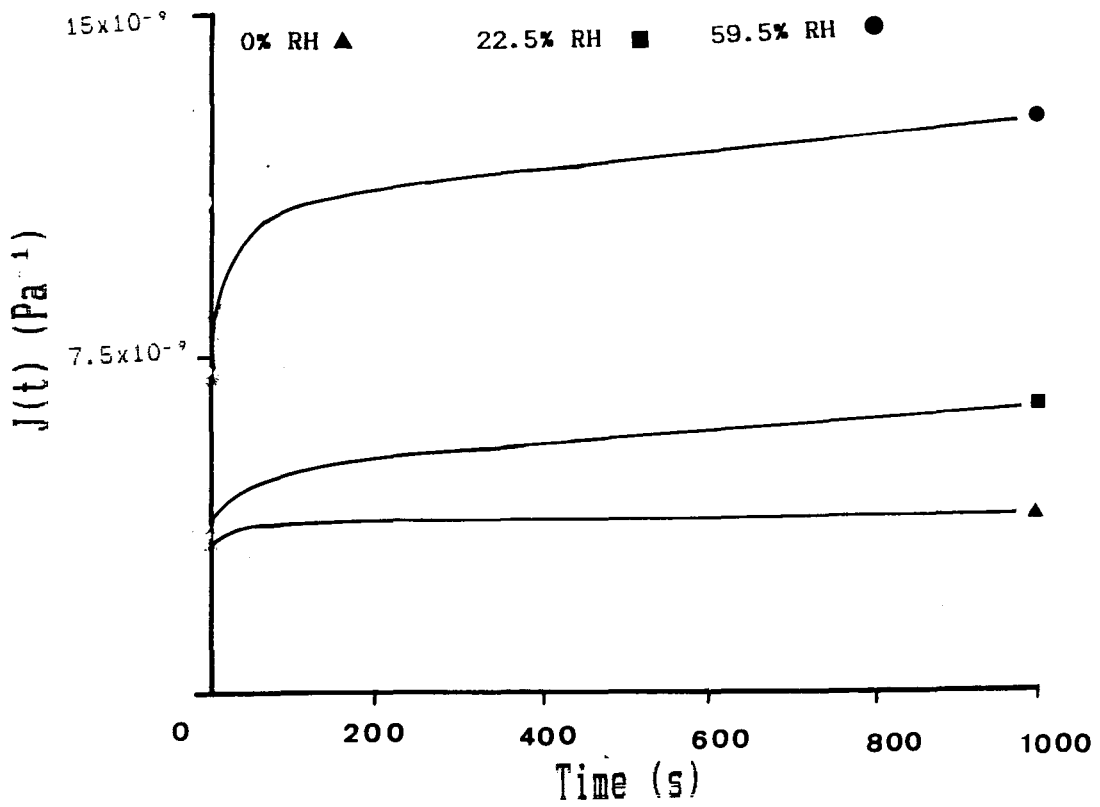


Figure 4.9 Influence of Moisture on the Creep Compliance of Starch 1500 Films



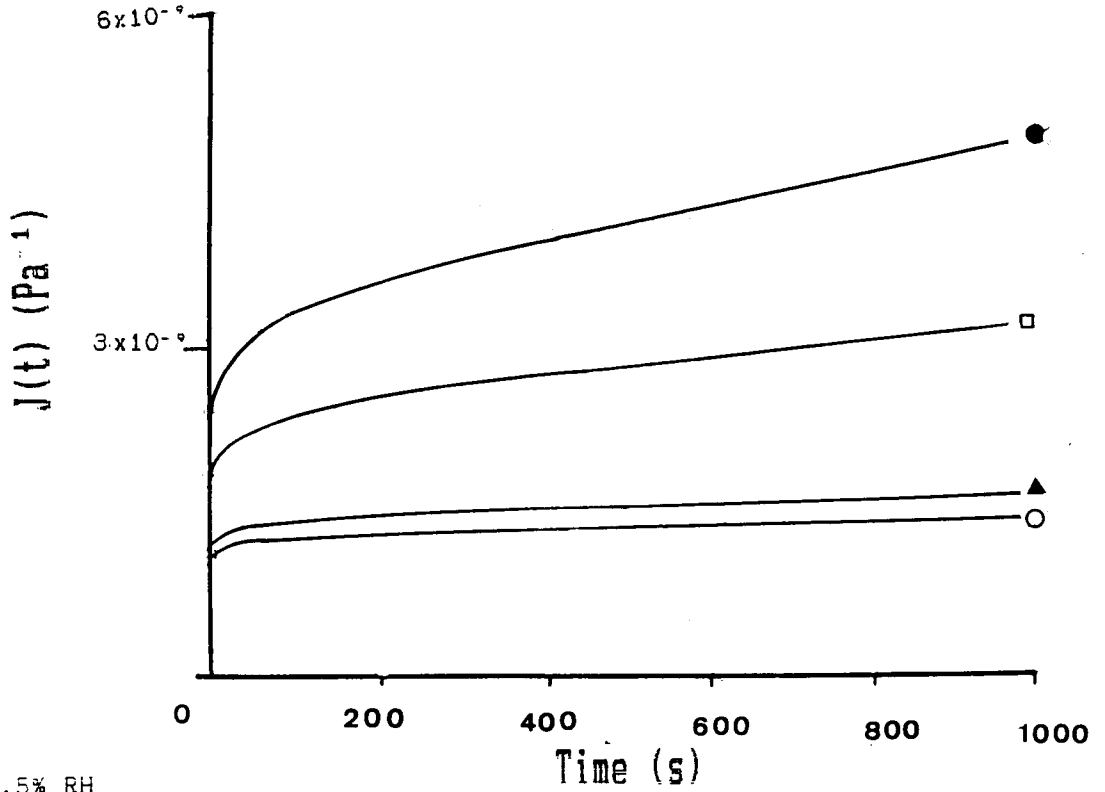
PVP and HPMC films equilibrated at 0% RH exhibited a relatively short viscoelastic period and attained an equilibrium compliance after about 100 seconds with no further indentation penetration detectable. This behaviour was typical of glassy-brittle materials and is classified as anelasticity (see Table 1.1). In contrast, Starch 1500 films equilibrated at 0% RH, showed a small but significant increase in creep compliance over the total duration of indentation. Equilibration of films at 22.5% RH and 59.5% RH produced corresponding increases (although small in the former case) in the magnitude of instantaneous elastic compliance and time-dependent viscoelastic and plastic compliances. This indicated that increased moisture content resulted in films which were both softer and more ductile. Significantly, for PVP and HPMC, an increase in moisture content was associated with a change in the creep compliance profile from anelastic to viscoelastic. The creep compliance, thus, did not attain an equilibrium value but continued to increase with time due to viscoelastic and plastic strain.

The effects of plasticization on the creep compliance profiles for the polymers are shown in Figs. 4.10a-b to 4.12a-b. Changes in the profiles with increasing plasticizer content were qualitatively similar to those observed with increasing moisture content. Thus, an increase in PEG 200 concentration in HPMC and PVP films or glycerol in Starch 1500 films produced an increase in the magnitude of the instantaneous elastic compliance and an increase in time-dependent viscoelastic and plastic compliances. The magnitude of deformation was higher for film samples equilibrated at 59.5% RH than at 22.5% RH.

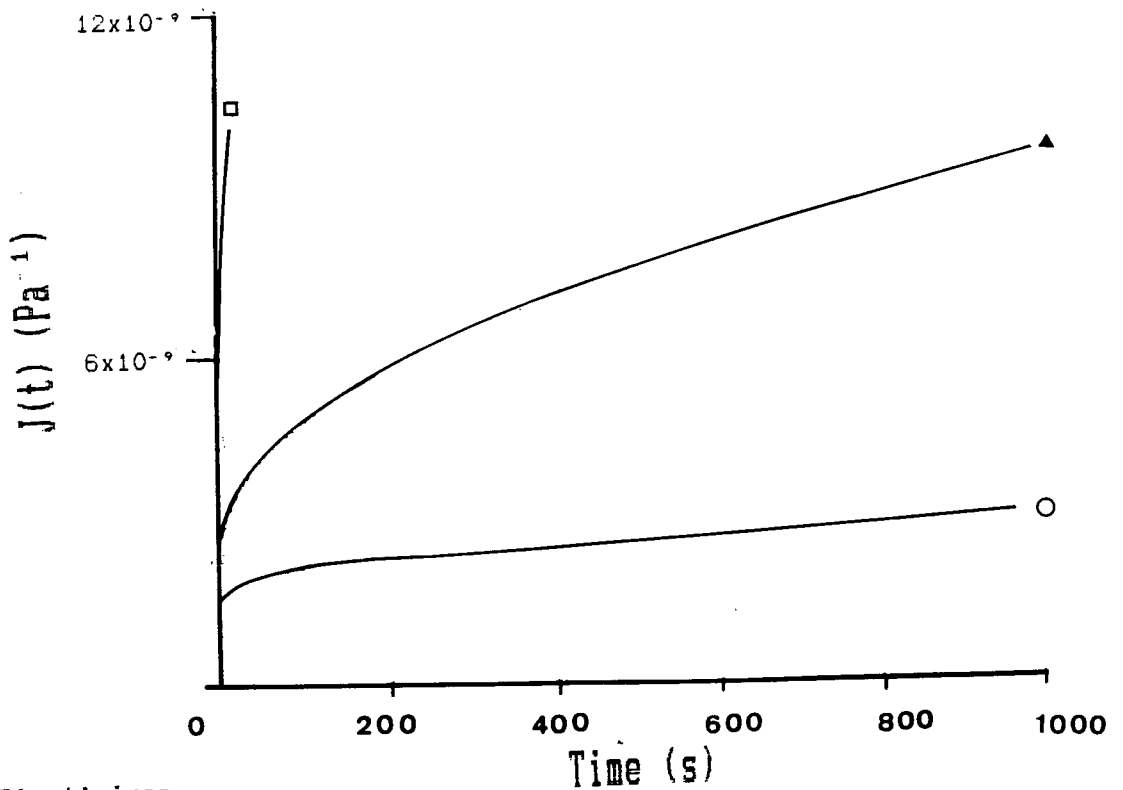
PVP films equilibrated at 59.5% RH and containing 10%w/w or greater of PEG 200 were readily and rapidly deformed. The rate of deformation was so rapid that the maximum indentation depth measurable was exceeded within the test duration, even when using only a 1g indenting load. Consequently, for these plasticized PVP samples only, a test duration of 50 seconds was used. While it was accepted that the results would not be strictly comparable with those obtained over the longer test period, it was felt that useful information would still be obtained.

Figure 4.10 Influence of Plasticizer Content on the Creep Compliance of PVP Films

(a) 22.5% RH



(b) 59.5% RH

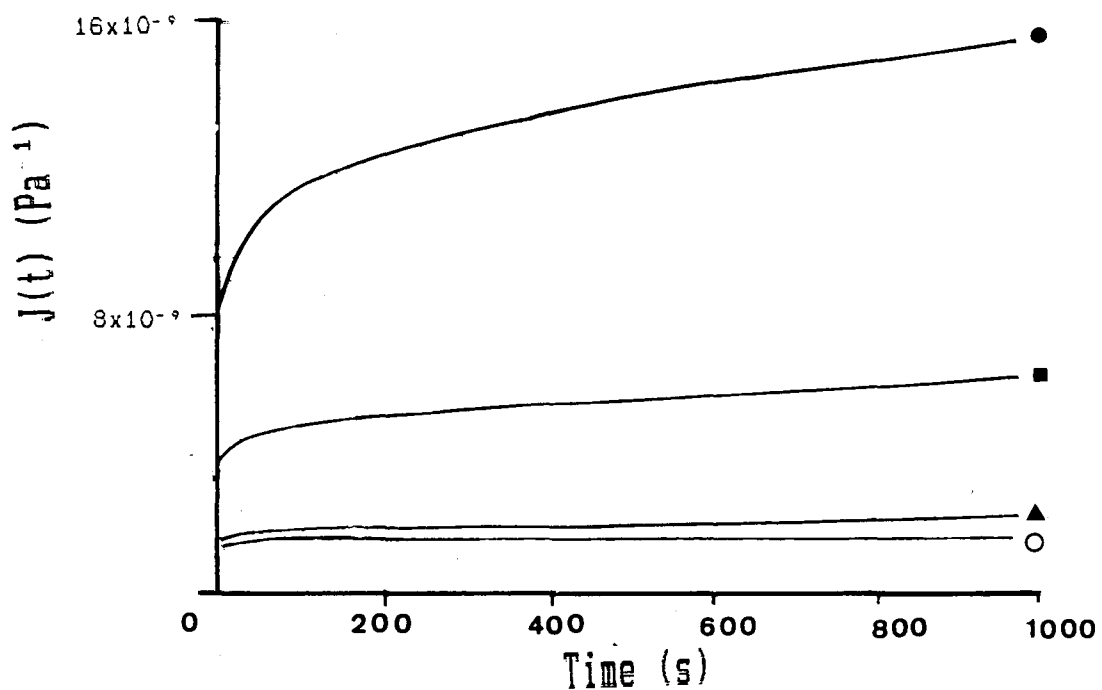


Plasticizer

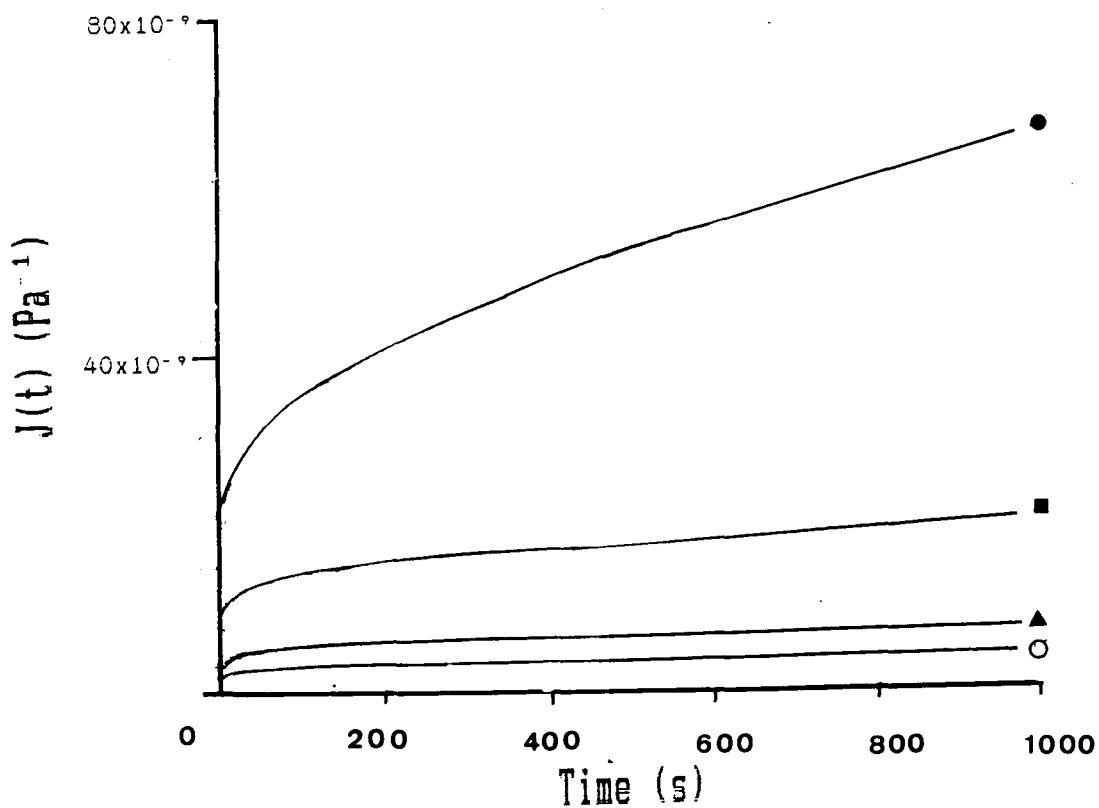
PEG 200 0% w/w ○ PEG 200 5% w/w ▲ PEG 200 10% w/w ■ PEG 200 15 %w/w

Figure 4.11 Influence of Plasticizer Content on the Creep Compliance of HPMC Films

(a) 22.5% RH



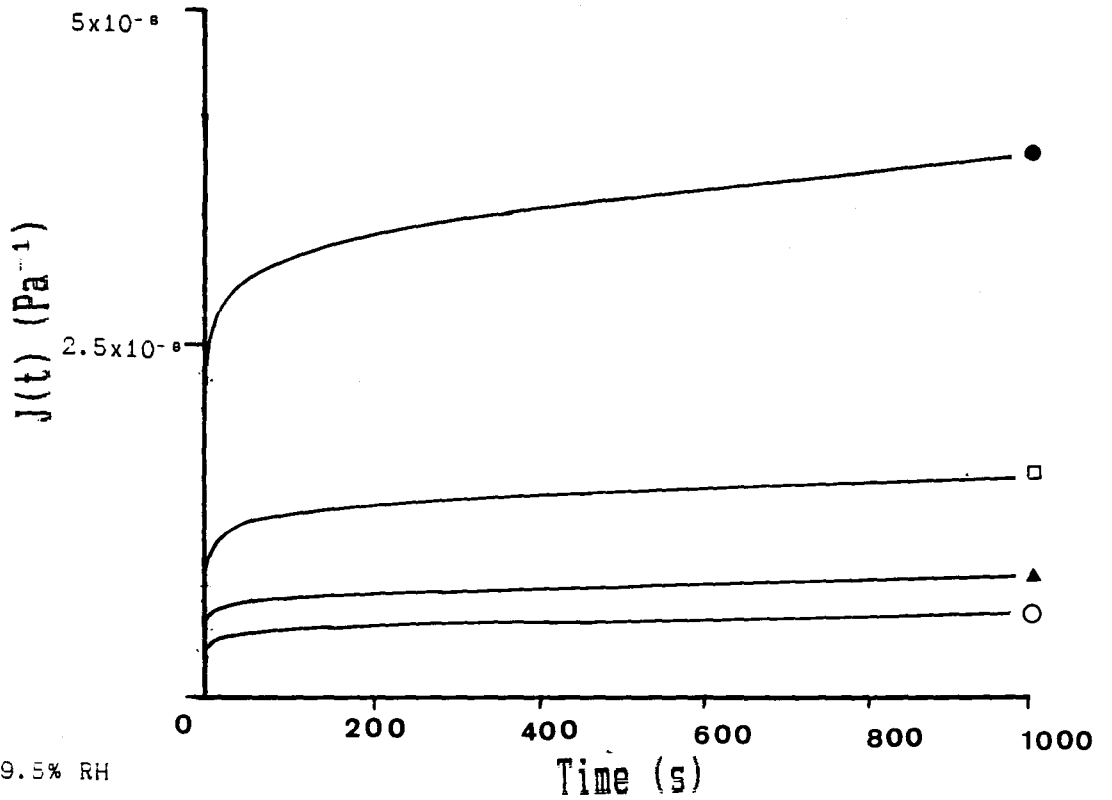
(b) 59.5% RH



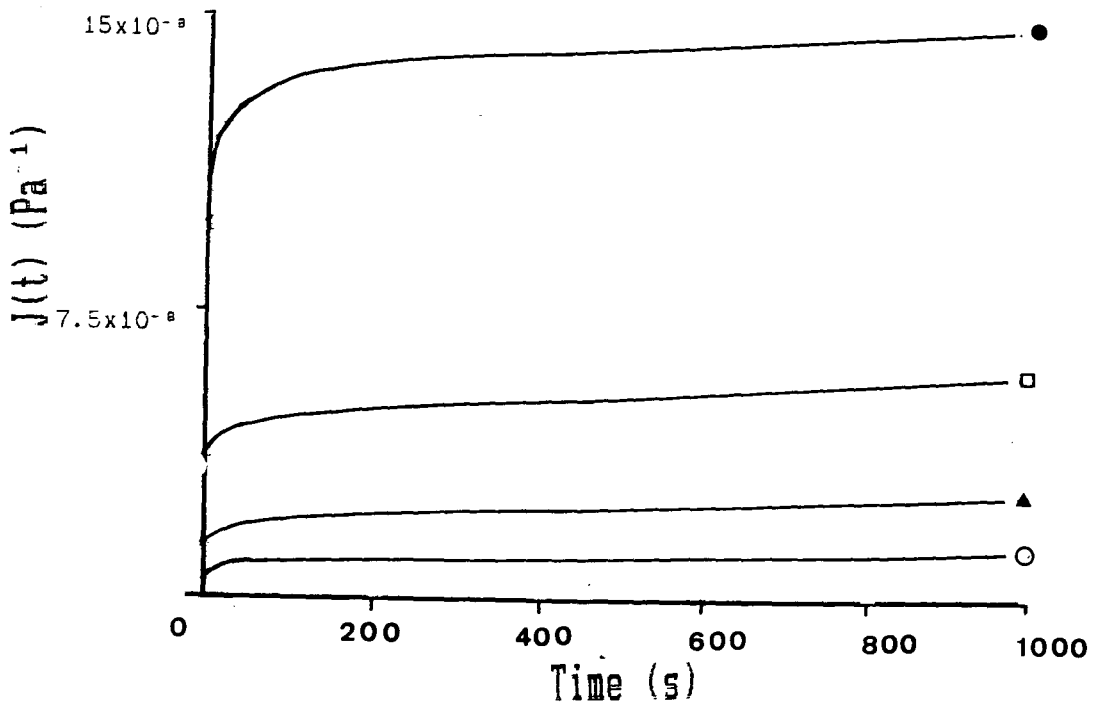
PEG 200 0% w/w ○ PEG 200 10% w/w ▲ PEG 200 20% w/w ■ PEG 200 30 %w/w ●

Figure 4.12 Influence of Plasticizer Content on the Creep Compliance of Starch 1500 Films

(a) 22.5% RH



(b) 59.5% RH



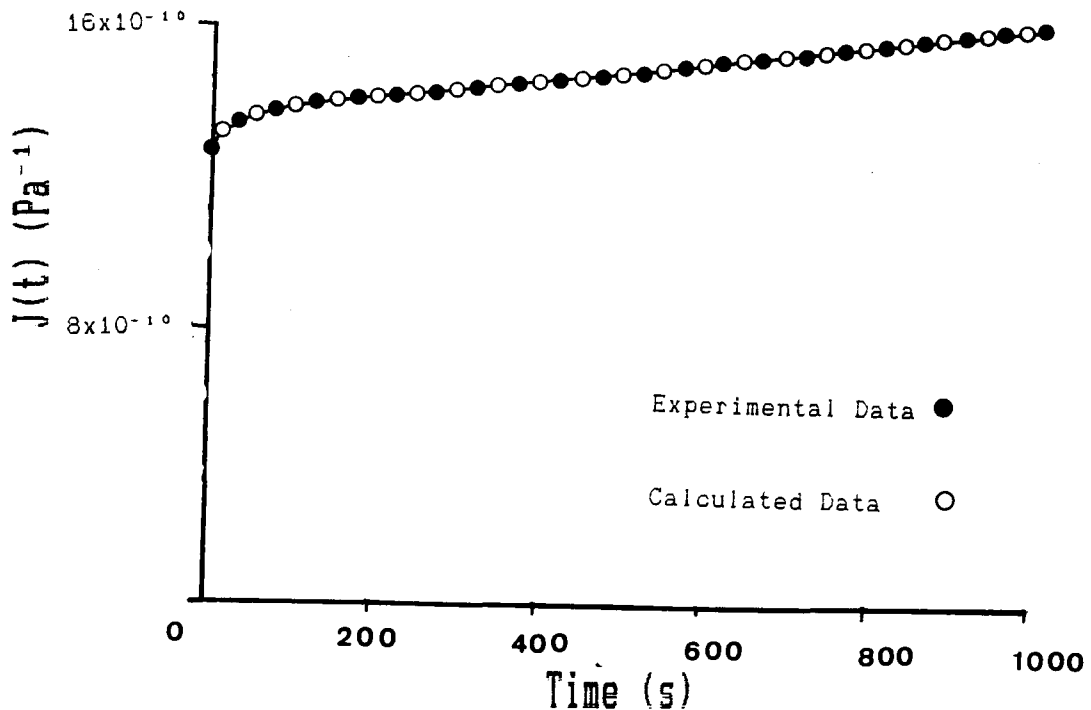
Plasticizer

Glycerol 0% w/w ○ Glycerol 10% w/w ▲ Glycerol 20% w/w ■ Glycerol 30% w/w ●

4.3.3 Discrete Mechanical Analysis

Prior to the application of discrete mechanical analysis, some creep profiles were recorded over a five kilosecond duration for PVP, HPMC and Starch 1500 films equilibrated at 22.5% and 59.5% RH. The resultant data indicated that the creep compliance curves tended to linearity within a test period of one kilosecond. Consequently, quantitative mechanical parameters were derived from indentations carried out over one kilosecond. Regression coefficients for the late linear portion of the creep compliance curve (determined within the time period 950 - 1000 seconds) were highly significant ($p < 0.1$). Validation of the analysis (effectively, a test of the assumption that the behaviour observed was linear viscoelastic) was performed by reconstruction of creep curves using the derived discrete mechanical parameters. Warburton and Barry (1968) suggested that if derived data agree within 2% of the experimental data the analysis may be accepted. The extent of agreement between derived and experimental data typically obtained in the present work is demonstrated in Fig. 4.13.

Figure 4.13 Superimposition of Experimental and Reconstituted Creep Curves



Superimposition of experimental and reconstituted curves substantiated the application of a linear viscoelastic model to characterise creep phenomena of polymeric films used here. Subsequently, all data was validated in this manner before accepting the derived parameters. Deviation of the reconstituted data from the experimental data was generally due to errors in assessing the point at which the data no longer supported the existence of a further Voigt unit. Recalculation of results omitting the last apparent Voigt unit invariable resulted in an acceptable fit of the data. As a general rule it was observed that resolution of distinct Voigt units was impossible where the retardation times differed by less than a factor of ten. The reciprocal of the late linear slope gave the uncoupled Newtonian viscosity (η_0) of the material. J_0 (and consequently G_0) were determined from the value of creep compliance at time $(t) = 0.5s$. This was determined experimentally as the duration required for pneumatic application of the indenting load. In practice instantaneous load application was an unattainable ideal and J_0 would contain some contribution from viscoelastic compliance.

Discrete mechanical parameters for unplasticized films of Starch 1500, PVP, and HPMC equilibrated at various relative humidities are given in Tables 4.3, 4.4 and 4.5 respectively. Corresponding parameters for the plasticized films are reported in Tables 4.6 to 4.11. Recorded parameters were the mean of not less than four replicate indentations. Coefficients of variation were within the range 10% to 20%, which was regarded as acceptable considering the sensitivity of the method used to generate the creep curves. Inspection of the data presented in Tables 4.3 to 4.8 showed that increased moisture content and plasticization both had significant effects on the elasticity, viscoelasticity, and plasticity of the polymer films. The nature and magnitude of these effects is discussed in the following sections.

Table 4.3 Effects of Storage Humidity on Discrete Mechanical Properties of Starch 1500 Films

Storage Humidity % RH	0	22.5	59.5
G_0 (Pa)	2.994×10^8	2.932×10^8	1.426×10^8
J_0 (Pa ⁻¹)	3.338×10^{-9}	3.409×10^{-9}	7.009×10^{-9}
J_1 (Pa ⁻¹)	2.902×10^{-10}	3.847×10^{-10}	5.660×10^{-10}
J_2 (Pa ⁻¹)	2.013×10^{-10}	0.888×10^{-9}	2.633×10^{-9}
J_3 (Pa ⁻¹)		4.658×10^{-10}	0.899×10^{-9}
τ_1 (s)	37.6	257.0	94.3
τ_2 (s)	5.1	31.5	27.0
τ_3 (s)		3.1	2.0
η_0 (Pa s)	6.370×10^{12}	8.262×10^{11}	5.235×10^{11}
η_1 (Pa s)	1.298×10^{11}	6.679×10^{11}	1.663×10^{11}
η_2 (Pa s)	2.552×10^{10}	3.549×10^9	1.165×10^{10}
η_3 (Pa s)		6.710×10^9	2.175×10^9

Table 4.4 Effects of Storage Humidity on Discrete Mechanical Properties of PVP Films

Storage Humidity % RH	0	22.5	59.5
G_0 (Pa)	9.322×10^8	8.827×10^8	5.913×10^8
J_0 (Pa ⁻¹)	1.062×10^{-9}	1.132×10^{-9}	1.689×10^{-9}
J_1 (Pa ⁻¹)	1.628×10^{-10}	1.203×10^{-10}	3.433×10^{-10}
J_2 (Pa ⁻¹)		0.913×10^{-10}	2.449×10^{-10}
J_3 (Pa ⁻¹)			1.536×10^{-10}
τ_1 (s)	24.5	36.9	67.3
τ_2 (s)		4.4	9.8
τ_3 (s)			2.1
η_0 (Pa s)	$> 10^{15}$	4.100×10^{12}	1.032×10^{12}
η_1 (Pa s)	1.659×10^{11}	3.107×10^{11}	1.977×10^{11}
η_2 (Pa s)		4.802×10^{10}	3.980×10^{10}
η_3 (Pa s)			1.341×10^{10}

Table 4.5 Effects of Storage Humidity on Discrete Mechanical Properties of HPMC Films

Storage Humidity % RH	0	22.5	59.5
G_0 (Pa)	7.581×10^8	6.855×10^8	5.377×10^8
J_0 (Pa^{-1})	1.318×10^{-9}	1.458×10^{-9}	1.840×10^{-9}
J_1 (Pa^{-1})	1.614×10^{-10}	1.289×10^{-10}	6.399×10^{-10}
J_2 (Pa^{-1})			4.005×10^{-10}
J_3 (Pa^{-1})			2.364×10^{-10}
τ_1 (s)	39.56	22.03	291.05
τ_2 (s)			37.92
τ_3 (s)			3.45
η_0 (Pa s)	$> 10^{15}$	4.675×10^{12}	9.138×10^{11}
η_1 (Pa s)	1.977×10^{11}	1.707×10^{11}	4.533×10^{11}
η_2 (Pa s)			9.466×10^{10}
η_3 (Pa s)			1.461×10^{10}

Table 4.6 Effects of Plasticizer Concentration on Discrete Mechanical Properties of Starch 1500 Films (22.5% RH)

Glycerol % w/w.	0	10	20	30
G_0 (Pa)	2.932×10^8	1.785×10^8	9.314×10^8	4.358×10^7
J_0 (Pa^{-1})	3.409×10^{-9}	5.600×10^{-9}	8.140×10^{-9}	2.293×10^{-8}
J_1 (Pa^{-1})	3.847×10^{-10}	4.885×10^{-10}	1.883×10^{-9}	2.980×10^{-9}
J_2 (Pa^{-1})	8.880×10^{-10}	9.200×10^{-10}	1.646×10^{-9}	4.071×10^{-9}
J_3 (Pa^{-1})	4.658×10^{-10}	3.540×10^{-10}	2.243×10^{-9}	3.540×10^{-9}
τ_1 (s)	257.0	140.0	90.5	179.8
τ_2 (s)	31.5	37.0	15.5	35.0
τ_3 (s)	3.1	2.1	2.8	8.1
η_0 (Pa s)	8.262×10^{11}	6.624×10^{11}	4.152×10^{11}	1.524×10^{11}
η_1 (Pa s)	3.549×10^{11}	1.920×10^{11}	4.802×10^{10}	6.031×10^{10}
η_2 (Pa s)	3.549×10^{10}	3.283×10^{10}	9.324×10^9	9.334×10^9
η_3 (Pa s)	6.717×10^9	5.960×10^9	1.334×10^9	2.300×10^9

Table 4.7 Effects of Plasticizer Concentration on Discrete Mechanical Properties of Starch 1500 Films (59.5% RH)

Glycerol % w/w.	0	10	20	30
G_0 (Pa)	1.426×10^6	6.645×10^7	2.669×10^7	9.943×10^6
J_0 (Pa ⁻¹)	7.009×10^{-9}	1.504×10^{-8}	3.745×10^{-8}	1.005×10^{-7}
J_1 (Pa ⁻¹)	5.664×10^{-10}	1.486×10^{-9}	5.009×10^{-9}	2.251×10^{-8}
J_2 (Pa ⁻¹)	2.315×10^{-9}	3.462×10^{-9}	3.982×10^{-9}	1.593×10^{-8}
J_3 (Pa ⁻¹)	8.990×10^{-10}	1.681×10^{-9}	2.520×10^{-9}	
τ_1 (s)	94.3	107.0	72.9	55.6
τ_2 (s)	27.0	22.1	15.7	4.5
τ_3 (s)	2.0	1.3	5.7	
η_0 (Pa s)	5.235×10^{11}	1.622×10^{11}	8.750×10^{10}	8.064×10^{10}
η_1 (Pa s)	1.663×10^{11}	7.196×10^{10}	1.454×10^{10}	2.524×10^9
η_2 (Pa s)	1.165×10^{10}	6.382×10^9	3.942×10^9	2.830×10^8
η_3 (Pa s)	2.223×10^9	8.146×10^8	2.271×10^8	

Table 4.8 Effects of Plasticizer Concentration on Discrete Mechanical Properties of PVP Films (22.5% RH)

PEG 200 % w/w.	0	5	10	15
G_0 (Pa)	8.827×10^6	8.070×10^6	5.334×10^6	3.997×10^6
J_0 (Pa ⁻¹)	1.132×10^{-9}	1.239×10^{-9}	1.876×10^{-9}	2.500×10^{-9}
J_1 (Pa ⁻¹)	1.203×10^{-10}	1.983×10^{-10}	4.375×10^{-10}	6.145×10^{-10}
J_2 (Pa ⁻¹)	9.130×10^{-11}	7.780×10^{-11}	2.080×10^{-10}	2.138×10^{-10}
J_3 (Pa ⁻¹)				2.107×10^{-10}
τ_1 (s)	36.9	30.0	64.9	91.4
τ_2 (s)	4.4	3.4	5.9	19.9
τ_3 (s)				5.7
η_0 (Pa s)	4.100×10^{12}	3.442×10^{12}	1.021×10^{12}	5.550×10^{11}
η_1 (Pa s)	3.107×10^{11}	1.511×10^{11}	1.454×10^{11}	1.487×10^{11}
η_2 (Pa s)	4.802×10^{10}	4.378×10^{10}	3.531×10^{10}	9.347×10^{10}
η_3 (Pa s)				2.727×10^{10}

Table 4.9 Effects of Plasticizer Concentration on Discrete Mechanical Properties of PVP Films (59.5% RH)

PEG 200 (% w/w)	0	5	10*	15*
(. Indentations carried out over 50 seconds)				
G_0 (Pa)	5.913×10^8	3.916×10^8	2.842×10^8	2.842×10^8
J_0 (Pa^{-1})	1.689×10^{-9}	2.552×10^{-9}	3.540×10^{-9}	3.540×10^{-7}
J_1 (Pa^{-1})	3.433×10^{-10}	2.657×10^{-10}	5.976×10^{-10}	5.815×10^{-10}
J_2 (Pa^{-1})	2.449×10^{-10}	8.150×10^{-10}	1.448×10^{-9}	5.571×10^{-7}
J_3 (Pa^{-1})	1.536×10^{-10}	4.044×10^{-10}		
τ_1 (s)	67.3	215.3	18.7	7.7
τ_2 (s)	9.8	22.4	1.5	1.4
τ_3 (s)	2.0	4.2		
η_0 (Pa s)	1.032×10^{12}	2.460×10^{11}	3.317×10^9	1.408×10^8
η_1 (Pa s)	1.977×10^{11}	8.101×10^{10}	3.131×10^9	1.320×10^7
η_2 (Pa s)	3.983×10^{10}	2.750×10^{10}	1.021×10^9	2.466×10^6
η_3 (Pa s)	1.341×10^{10}	3.317×10^9		

Table 4.10 Effects of Plasticizer Concentration on Discrete Mechanical Properties of HPMC Films (22.5% RH)

PEG 200 (% w/w)	0	10	20	30
G_0 (Pa)	6.855×10^8	6.207×10^8	2.604×10^8	1.204×10^8
J_0 (Pa^{-1})	1.458×10^{-9}	1.607×10^{-9}	3.830×10^{-9}	8.290×10^{-9}
J_1 (Pa^{-1})	1.289×10^{-10}	2.590×10^{-10}	5.954×10^{-10}	2.753×10^{-9}
J_2 (Pa^{-1})		1.862×10^{-10}	4.918×10^{-10}	1.321×10^{-9}
J_3 (Pa^{-1})			4.043×10^{-10}	1.280×10^{-9}
τ_1 (s)	22.0	128.8	241.4	219.9
τ_2 (s)		15.7	29.2	36.5
τ_3 (s)			4.9	7.5
η_0 (Pa s)	4.675×10^{12}	3.968×10^{12}	7.019×10^{11}	2.872×10^{11}
η_1 (Pa s)	1.707×10^{11}	4.546×10^{11}	4.055×10^{11}	7.987×10^{10}
η_2 (Pa s)		8.474×10^{10}	5.942×10^{10}	2.759×10^{10}
η_3 (Pa s)			1.219×10^{10}	5.833×10^9

Table 4.11 Effects of Plasticizer Concentration on Discrete Mechanical Properties of HPMC Films (59.5% RH)

PEG 200 (% w/w)	0	10	20	30
G_0 (Pa)	5.377×10^8	3.231×10^8	1.245×10^8	5.802×10^7
J_0 (Pa ⁻¹)	1.859×10^{-9}	3.095×10^{-9}	8.032×10^{-9}	1.723×10^{-8}
J_1 (Pa ⁻¹)	6.437×10^{-10}	1.159×10^{-9}	2.131×10^{-9}	1.011×10^{-8}
J_2 (Pa ⁻¹)	4.005×10^{-10}	1.015×10^{-9}	1.789×10^{-9}	5.143×10^{-9}
J_3 (Pa ⁻¹)	2.364×10^{-10}		1.669×10^{-9}	2.897×10^{-9}
J_4 (Pa ⁻¹)				1.612×10^{-9}
τ_1 (s)	291.0	102.7	126.9	235.3
τ_2 (s)	37.9	9.6	27.7	27.9
τ_3 (s)	3.4		4.8	4.0
τ_4 (s)				1.1
η_0 (Pa s)	9.138×10^{11}	5.988×10^{11}	1.768×10^{11}	3.944×10^{10}
η_1 (Pa s)	4.533×10^{11}	8.857×10^{10}	5.956×10^{10}	2.326×10^{10}
η_2 (Pa s)	9.466×10^{10}	9.442×10^9	1.550×10^{10}	5.240×10^9
η_3 (Pa s)	1.461×10^{10}		2.875×10^9	1.387×10^9
η_4 (Pa s)				6.823×10^8

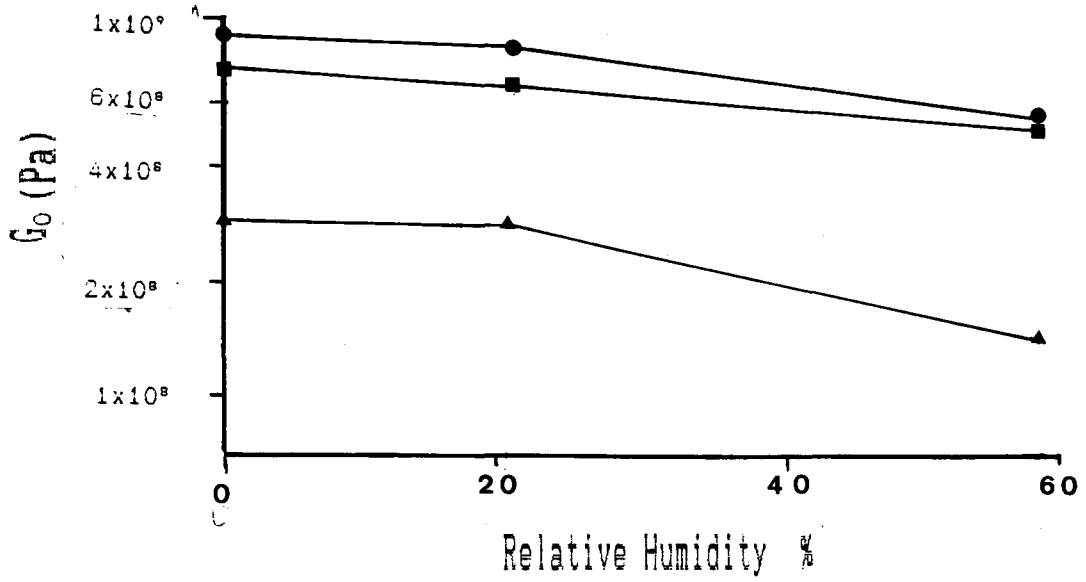
4.3.3.1 The Influence of Moisture Content on Polymer Plasticity and Elasticity

The influence of storage humidity on rigidity modulus G_0 and Newtonian viscosity η_0 for the three polymers is summarised by Figs. 4.14a and 4.14b respectively. Since changes in rigidity modulus and plastic viscosity may cover several orders of magnitude the data was represented logarithmically.

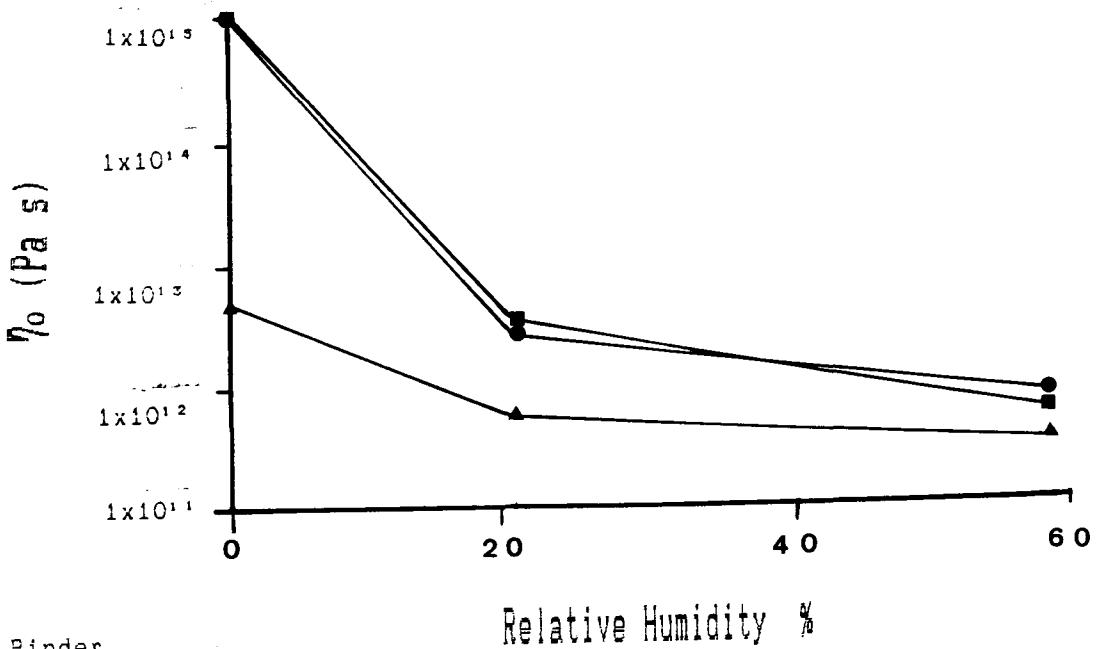
For all the polymers examined, increased moisture content resulted in a decrease in the measured rigidity modulus (Fig. 14a). For unplasticized binders the rank order for the magnitude of the modulus was PVP > HPMC > Starch 1500 irrespective of the storage humidity. PVP was most resistant to deformation whilst Starch 1500 was most readily deformed. A similar rank correlation for Young's modulus was observed in Chapter three (section 3.4.1). Comparison of the moduli reported

Figure 4.14 Influence of Moisture Content on Polymer Elasticity and Plasticity

(a) Rigidity Modulus G_0



(b) Newtonian Viscosity η_0



Binder

PVP ● HPMC ■ Starch 1500 ▲

in Tables 4.3, 4.4 and 4.5 with the Young's moduli in Table 3.3 of the previous chapter revealed a considerable difference in magnitude, however. Young's moduli obtained from tensile tests were of the order of two to five times greater than the rigidity moduli obtained from the instantaneous elastic indentation. Moduli differences most probably arose as a consequence of the different mode of deformation induced by the respective test methods. Thus, Young's modulus was obtained from deformation in tension whereas the rigidity modulus G , was obtained from deformation in shear. These results indicate that the polymers examined in the present work deform more readily in shear than in tension. Since Hookean elasticity is ideally instantaneous, differences in the initial rate of strain imposed by the two test methods should not influence the value of the moduli obtained. In practice, some strain-rate dependence (albeit small) would be inevitable due to the finite time over which stress was applied, and the finite time required for any mechanical deformation.

In parallel with the decreased stiffness of the polymers, increased moisture content also resulted in a reduction in plastic viscosity η_p . (Fig. 14b). Regression of the late-linear portion of the creep curve for PVP and HPMC films equilibrated at 0% RH yielded Newtonian viscosities greater than 10^{15} Pa s. The regression coefficients for the analyses were not significant, however, confirming that compliance had attained a time-independent equilibrium value. The sorption of moisture by equilibration at 22.5% RH or 59.5% RH was, therefore, responsible for the induction of significant plastic deformation. Viscosities for PVP and HPMC films were generally of a similar magnitude. Starch 1500 films, however, had lower viscosities than observed for the other polymers at all conditioning humidities. These results indicated that Starch 1500 was more easily deformed in a plastic manner, however, the application of stress was also associated with greater elastic strain.

The absence of plasticity noted for PVP and HPMC films equilibrated at 0% RH, was consistent with the mechanical properties of amorphous polymers at temperatures well below their glass transition. The behaviour of Starch 1500 under similar conditions suggested, however, that flow in the crystalline domains may account for the observed plasticity at very low moisture content.

4.3.3.2 The Influence of Plasticizer Content on Polymer Elasticity and Plasticity

The effect of plasticizer content on the rigidity modulus G_0 and Newtonian viscosity η_0 for the three polymers is summarised by Figs. 4.15a and 4.15b respectively. Incorporation of increasing levels of PEG 200 in HPMC and PVP or glycerol in Starch 1500 resulted in a progressive decrease both in the modulus and the apparent viscosity. The influence of increased plasticizer content was thus analogous to the influence of increased moisture sorption (section 4.3.3.1). The figures also showed that plasticized films equilibrated at 59.5% RH were both softer and more ductile than those equilibrated at 22.5% RH. Sorbed moisture and the plasticizer inclusion therefore acted in concert to modify the mechanical properties of the polymer matrix.

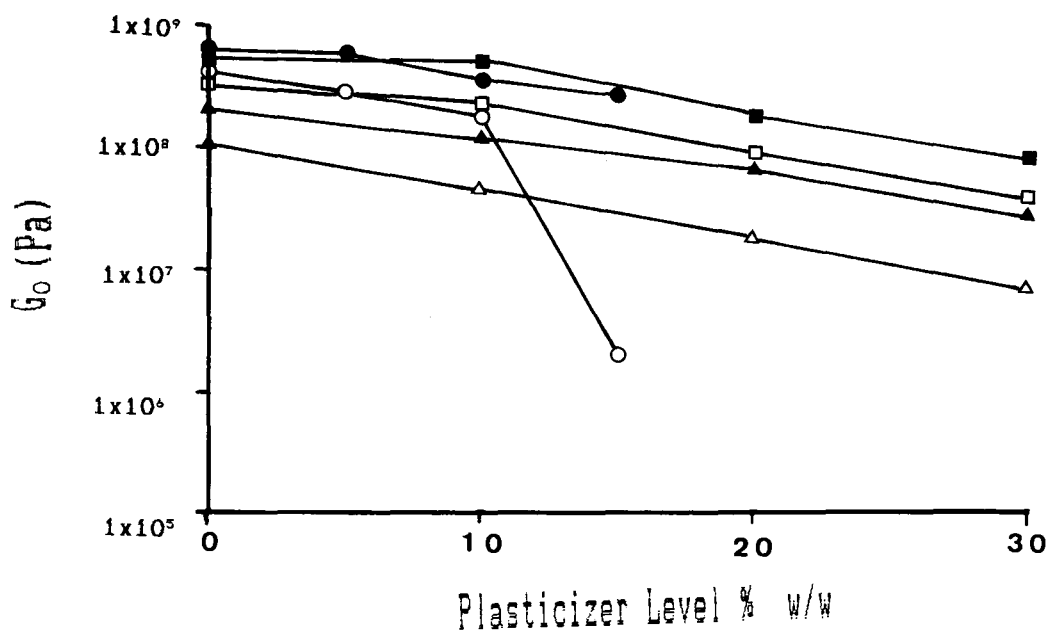
At equivalent plasticizer content and conditioning humidity, the rank order for plasticized binders generally reflected the rank order for unplasticized binders. Thus, plasticized Starch 1500 films were generally softer and more plastic than the corresponding PVP or HPMC films. There was, however, an exception to this. Incorporation of PEG 200 in PVP films equilibrated at 59.5% RH resulted in a sharp decrease both in rigidity and plasticity around the 10% to 15% inclusion level. The magnitude of the changes were of the order of several log reductions. Gross changes in the viscoelastic properties of polymers are commonly observed around the temperature of the glass transition. It appeared that the inclusion of a highly compatible plasticizer coupled with PVP's affinity for water resulted in a glass transition temperature at or below ambient. The absence of a similar trend for HPMC and Starch 1500 reflected the lower extent of polymer-plasticizer compatibility and also the lower moisture affinity of those polymer formers.

4.3.3.3 The Influence of Moisture Content and Plasticizer Content on Viscoelastic Deformation

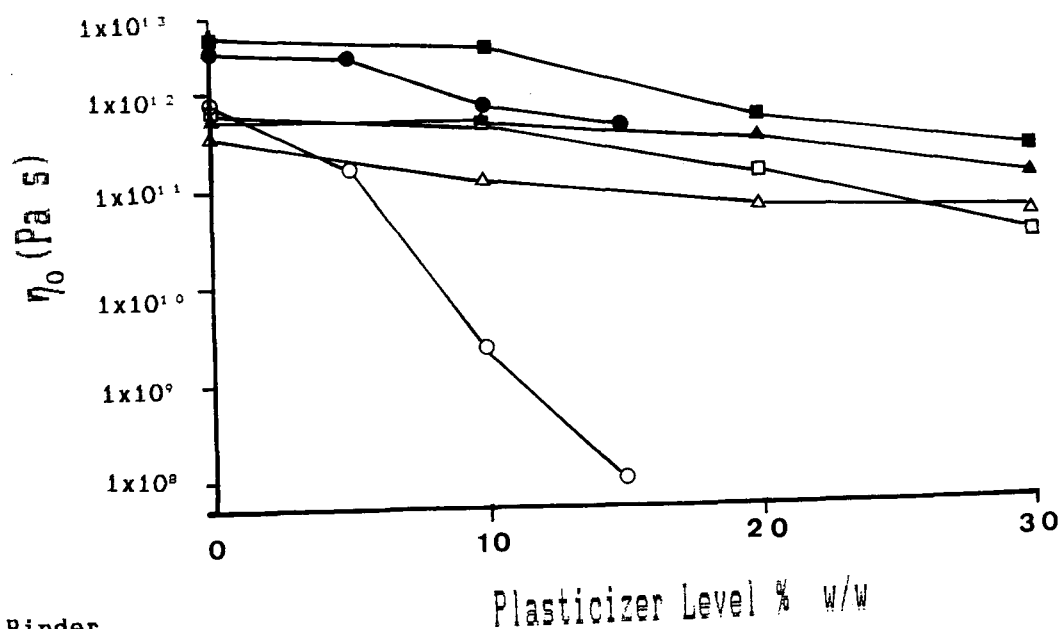
An increase in either the moisture content or the plasticizer content of the polymers, resulted in significant changes in the constitution of the discrete spectral analysis (Tables 4.6 - 4.11). Generally, although there were exceptions, an increase in moisture or

Figure 4.15 Influence of Plasticizer Content on Polymer Elasticity and Plasticity

(a) Rigidity Modulus G_0



(b) Newtonian Viscosity η_0



Binder

PVP (22.5% RH) ● HPMC (22.5% RH) ■ Starch 1500 (22.5% RH) ▲
 PVP (59.5% RH) ○ HPMC (59.5% RH) □ Starch 1500 (59.5% RH) △

plasticizer levels resulted in an increase in the number of resolved Voigt units. Unplasticized films equilibrated at 0% RH were adequately modelled by very simple discrete spectra. In the case of PVP and HPMC the observed behaviour was described by a Hookean spring in series with a single Voigt unit. Starch 1500 required the addition of a viscous dashpot to characterise the continuing increase in creep compliance with time due to plastic flow. In the latter case, the mechanical behaviour was modelled by a generalised viscoelastic model consisting of a Maxwell and a Voigt unit in series. Moisture sorption by equilibration at either 22.5% RH or 59.5% RH produced a number of changes in the discrete spectra. The induction of plasticity in both PVP and HPMC at the higher humidities required the addition of a viscous dashpot to model non-recoverable deformation, such that these polymers were also described by a generalised viscoelastic model. Starch 1500 generally exhibited a more complex viscoelastic behaviour than either PVP or HPMC, requiring a greater number of constituent Voigt units to model its mechanical properties. This probably resulted from the greater heterogeneity of starch systems, particularly with respect to the presence of crystallinity.

In addition to the influences on uncoupled elastic and plastic components (discussed in sections 4.3.3.1 and 4.3.3.2), increased moisture or plasticizer content generally resulted in an increase in the number of Voigt units required to model the retarded elastic deformation. This indicated that both increased moisture content and plasticization facilitated deformations which were distinctly different at the molecular level. Numerical values assigned to the constituent Voigt units enabled the changes to be quantified, although they were of little fundamental significance. An exception to the general rule was observed for PVP films equilibrated at 59.5% RH. In these films, increasing the plasticizer level from 10% to 15% PEG 200 resulted in a decrease in the number of resolved Voigt units. While these results may be atypical since they were derived from very short indentation profiles, the magnitude of the changes indicated that the plasticized polymer was close to its glass transition point. It might be expected that, as a polymer passes through the glass transition point to behave as an ideal viscous fluid, the number of Voigt units required would diminish as the discrete spectrum degenerates to a single dashpot.

Examination of discrete mechanical parameters characterising the viscoelastic region revealed a number of features. As Voigt units increased from $i = 1$ to $i = n$ (where n is the maximum number of Voigt units required) the apparent viscosity η_i and the retardation time τ_i of the respective Voigt units decreased. There was no consistent trend for the respective compliance contribution J_i , however. At short times, the apparent viscosity (or internal friction), was small compared with the apparent rigidity modulus G_i (the reciprocal of J_i). Thus, deformation at short times was predominantly elastic in nature and strain recovery on removal of the indenting load would be rapid. The corollary to this is that at zero time the observed mechanical properties would be those of unretarded (Hookean) spring, with infinitesimal retardation time.

Comparison of the numerical constants for equivalent Voigt units, (i.e. first Voigt, second Voigt, etc.) for a polymer with increased moisture or plasticizer content did not reveal any consistent trends. This was not surprising for a number of reasons. Firstly, it would be unlikely for polymer deformations or conformation changes to progress in an ideally continual manner. Quantum-type changes would be more probable since deformations which were prohibited or frozen at low moisture or plasticizer concentration may be facilitated at higher concentrations where polymer segmental free volume was greater. Evidence to support this concept may be found in the thermomechanical properties of polymers.

In addition to the true glass transition temperature, some polymers may exhibit characteristic thermomechanical transitions at lower temperatures. These are associated with increased segmental mobility over limited regions of the polymer chain, for example, within side chain substituents (branched polymers), within amorphous regions (partially crystalline polymers) or between entanglement couplings. Okhamafe and York (1988) suggested that this may be analogous to the loss of tertiary or secondary structure in thermally treated proteins. The latter workers showed that PVA and HPMC each undergo at least two distinct thermal transitions. Other workers (Abdul-Razzak, 1980; Majeed, 1984 and Mochun, 1984) have also reported low temperature thermomechanical transitions in HPMC films. Since plasticization reduces the true glass transition temperature (by increasing free

volume) then, by analogy, the necessary temperature for other thermomechanical transitions may similarly be lowered. Consequently, plasticization may facilitate mechanical transitions at room temperature which are prohibited in the absence of plasticizer.

4.3.4 Continuous Spectral Analysis

Continuous retardation spectra were constructed by means of a BASIC program written to perform the second-order approximation discussed in section 4.3.1.2. The source data in each case was a representative creep compliance versus time curve. The resulting spectrum was plotted as the magnitude of the distribution function (L) versus the natural log of time. Retardation times in the continuous spectrum were obtained from the elapsed time divided by two (section 4.3.1.2). Interpretation of the continuous retardation spectra was necessarily more complicated than for the discrete case, and a simple mechanistic interpretation was not possible. Nevertheless, a number of general observations could be made regarding the influence of moisture sorption and plasticization.

4.3.4.1 Continuous Retardation Spectra of Unplasticized Binders

Continuous spectra for unplasticized PVP, HPMC and Starch 1500, equilibrated at 0% RH, 22.5% RH and 59.5% RH are shown in Figs. 4.16, 4.17 and 4.18. Maxima in the spectra represent concentrations of retardation processes (which must be similar at the molecular level) as measured by their contribution to the overall creep compliance. Thus, shifts in the position of maxima indicated fundamental changes in the nature of the retardation process at the molecular level. The heights of maxima within a spectrum represent the relative number of retardation processes having retardation times around the peak. Retardation spectra for unplasticized films equilibrated at 0% RH were simple. HPMC and PVP exhibited a single peak, whereas two peaks were resolved for Starch 1500. Equilibration of the films at higher relative humidities resulted in a number of changes in the form of the retardation spectrum.

Figure 4.16 Influence of Moisture on the Continuous Retardation Spectrum of PVP

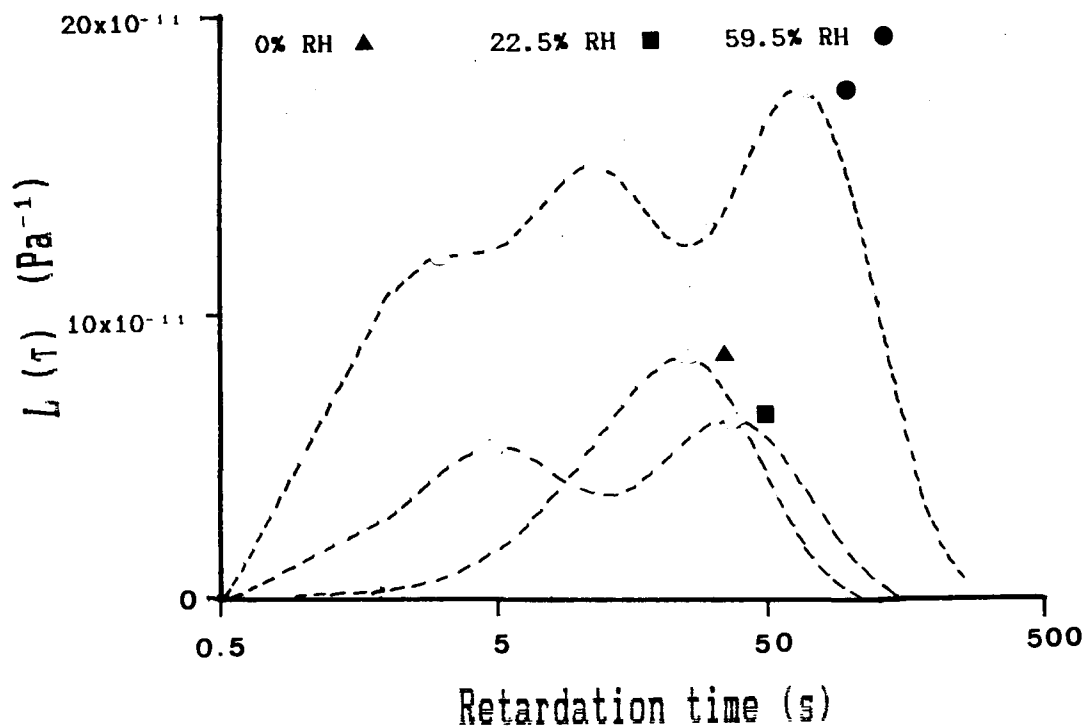


Figure 4.17 Influence of Moisture on the Continuous Retardation Spectrum of HPMC

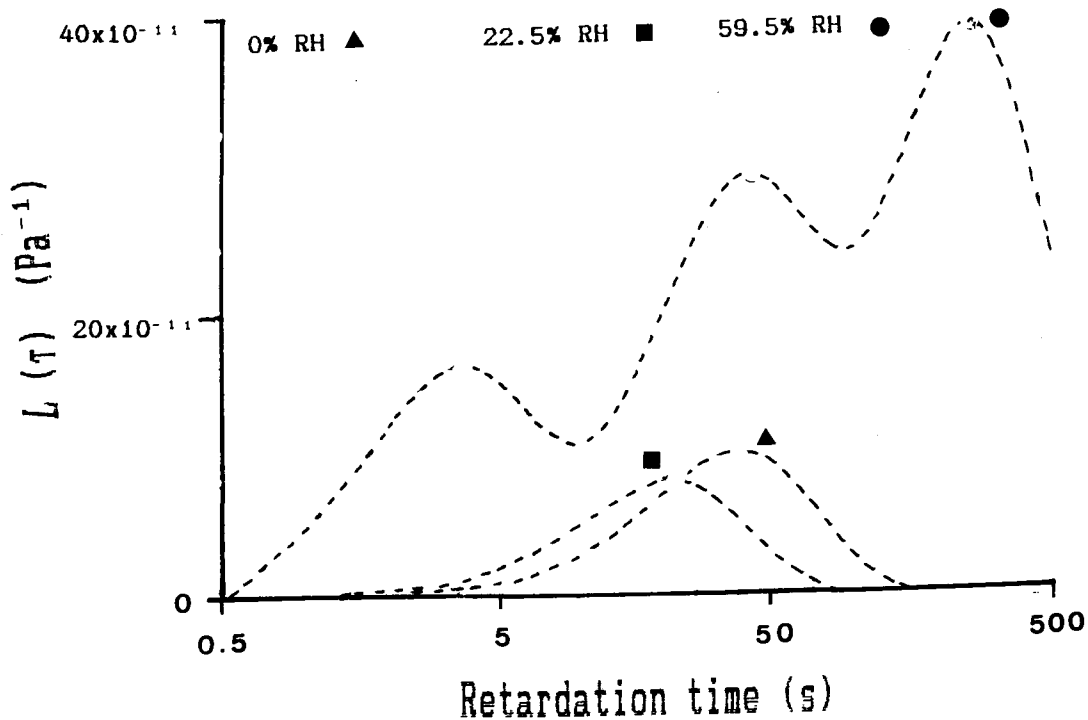
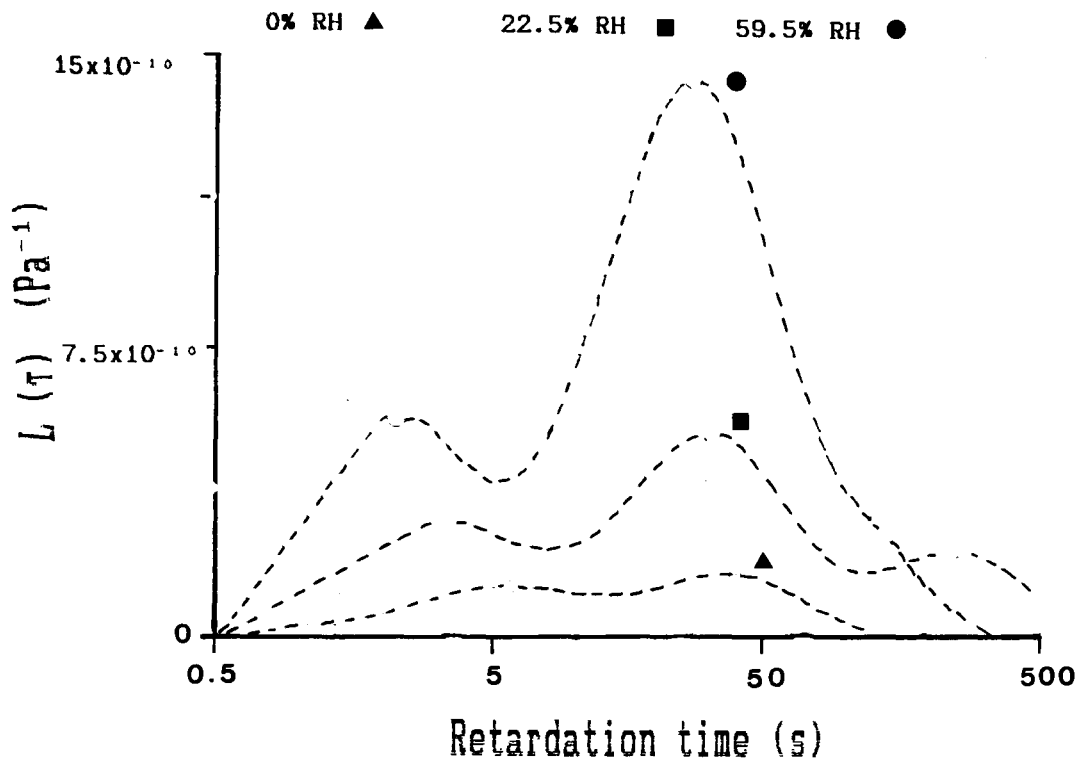


Figure 4.18 Influence of Moisture on the Continuous Retardation Spectrum of Starch 1500



The changes were qualitatively the same, irrespective of the polymer, examined and are summarised, in general terms, as:

- broadening of the spectrum
- resolution of a greater number of retardation concentrations (peaks in the spectrum)
- increase in the height of the spectrum

A broadening of the retardation spectrum was common to all three polymers as the conditioning humidity was raised from 0% RH to 59.5% RH. This showed that viscoelastic deformation of films containing increased moisture levels involved processes with a greater spread of retardation times than observed for the dried films. There was also an increase in the number of maxima in the continuous spectrum. Although there was some shift on the time axis, all curves for the same polymer retained one peak of similar retardation time. This

implied that, in each case, there was at least one fundamentally similar association or interaction at the molecular level contributing to the retardation phenomena. The appearance of more than one distinct maxima, however, implied that the sorption of moisture resulted in the enabling of some fundamentally different translations at the molecular level. Films equilibrated at 58% RH exhibited three retardation maxima, with one peak at shorter retardation time, and one peak at longer retardation time than the common peak. The appearance of a peak at longer times indicated that at higher moisture content, viscous deformations which were otherwise prohibited were enabled or "unfrozen". The resolution of a peak of characteristically shorter retardation time implied that some element of deformation which was coupled, i.e. subject to viscous retardation, became uncoupled at higher moisture content and hence less time-dependent.

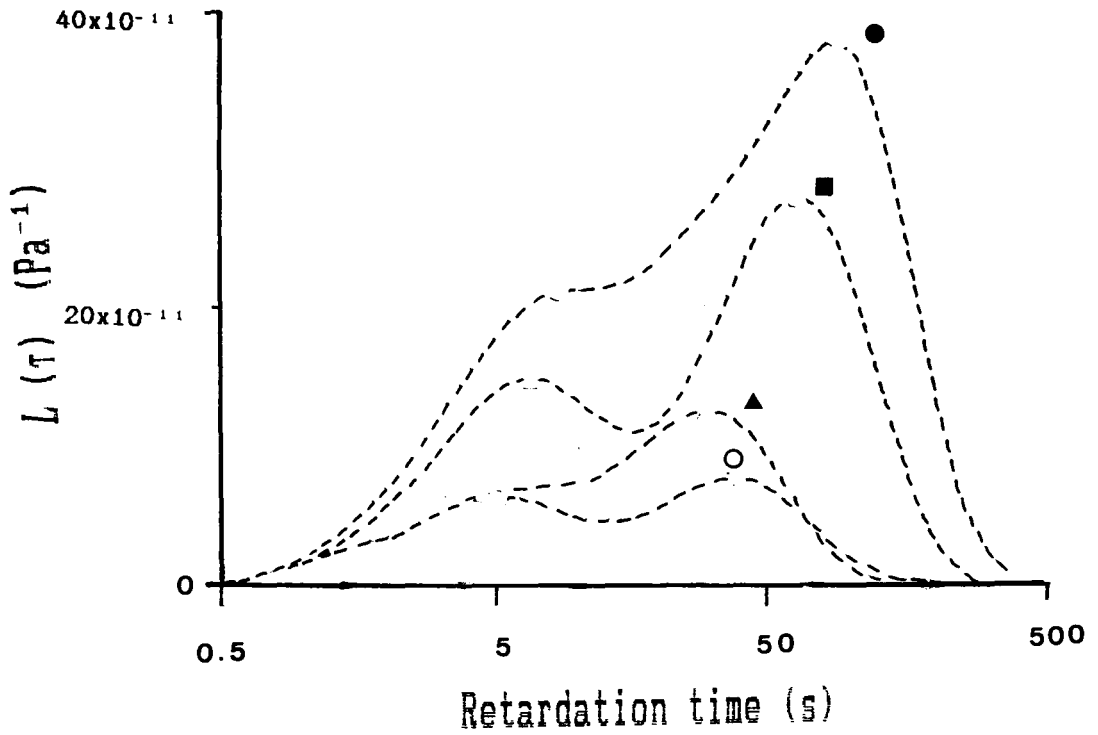
There was a general increase in spectra height with increasing moisture content. This was consistent with a loss of rigidity and general softening of the polymeric matrix. At the molecular level, this may be explained by an overall reduction in the number of interactions contributing to retardation. At infinitely long time the distribution function (L) should vanish when the polymer either attains a constant equilibrium compliance or the polymer reaches steady state (Newtonian) flow. The tendency of the spectra to zero at about 1000 seconds duration (earlier for unplasticized films) confirmed that this was the case.

4.3.4.2 The Effects of Plasticization on Continuous Retardation Spectra

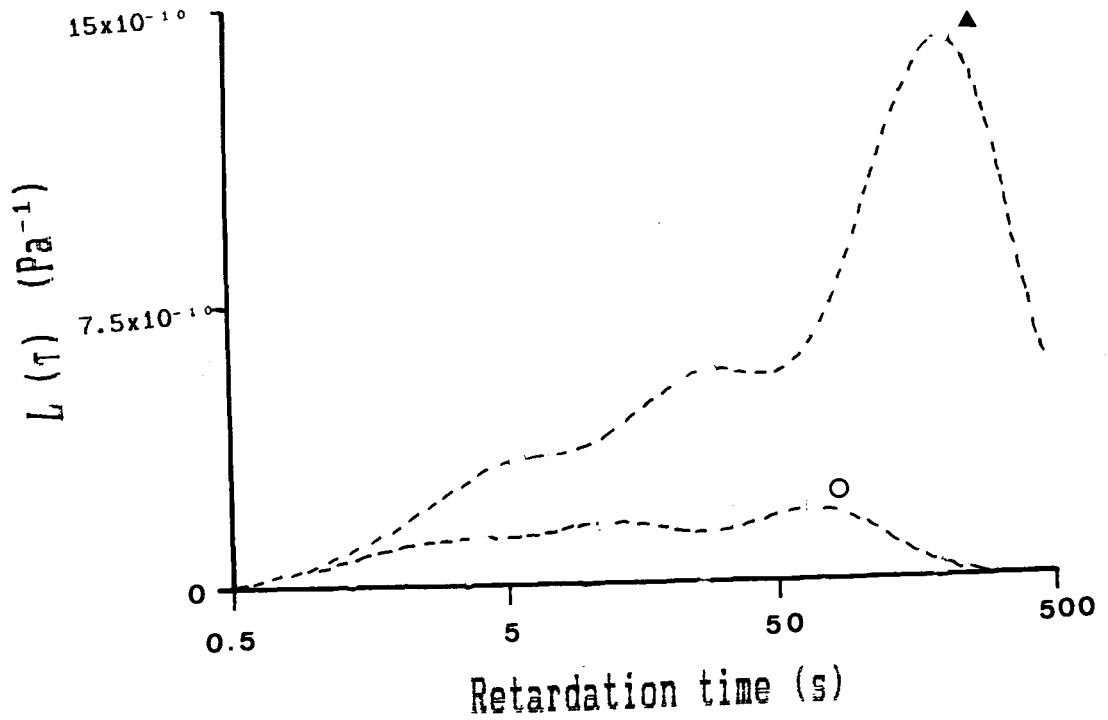
The continuous spectra for plasticized binders, equilibrated at either 22.5% RH or 59.5% RH, are shown in Figs. 4.19a-b, 4.20a-b and 4.21a-b. The spectrum obtained for the unplasticized binder was also included, for comparison. At 59.5% RH continuous spectra for PVP films were derived only for the 5% PEG 200 level. Creep curves at the higher plasticizer levels were recorded over too short a time period for meaningful analysis.

Figure 4.19 Influence of Plasticizer Content on the Continuous Retardation Spectrum of PVP

(a) 22.5% RH



(b) 59.5% RH

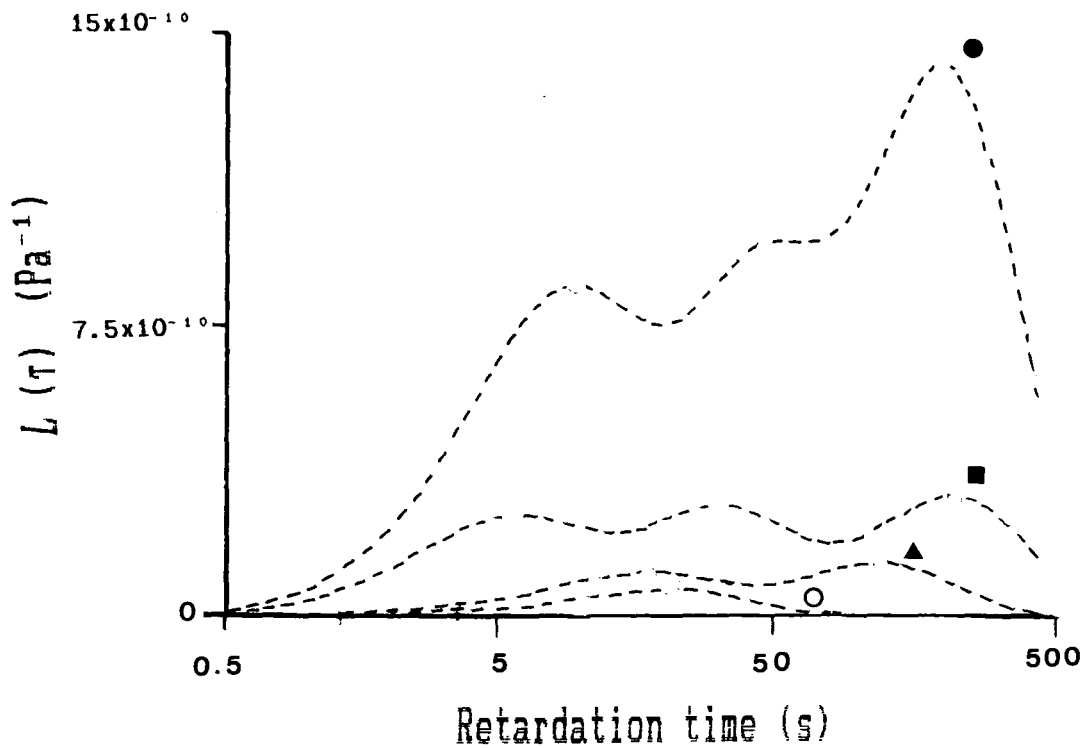


Plasticizer

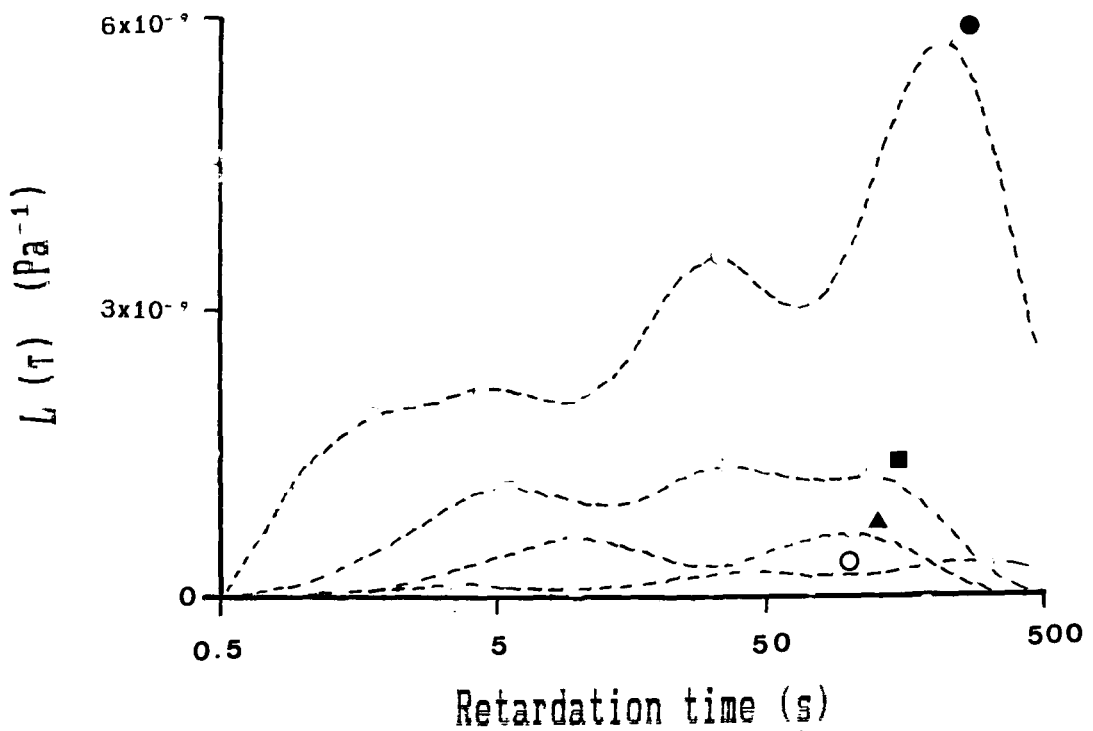
PEG 200 0% w/w ○ PEG 200 5% w/w ▲ PEG 200 10% w/w ■ PEG 200 15% w/w ●

Figure 4.20 Influence of Plasticizer Content on the Continuous Retardation Spectrum of HPMC

(a) 22.5% RH



(b) 59.5% RH

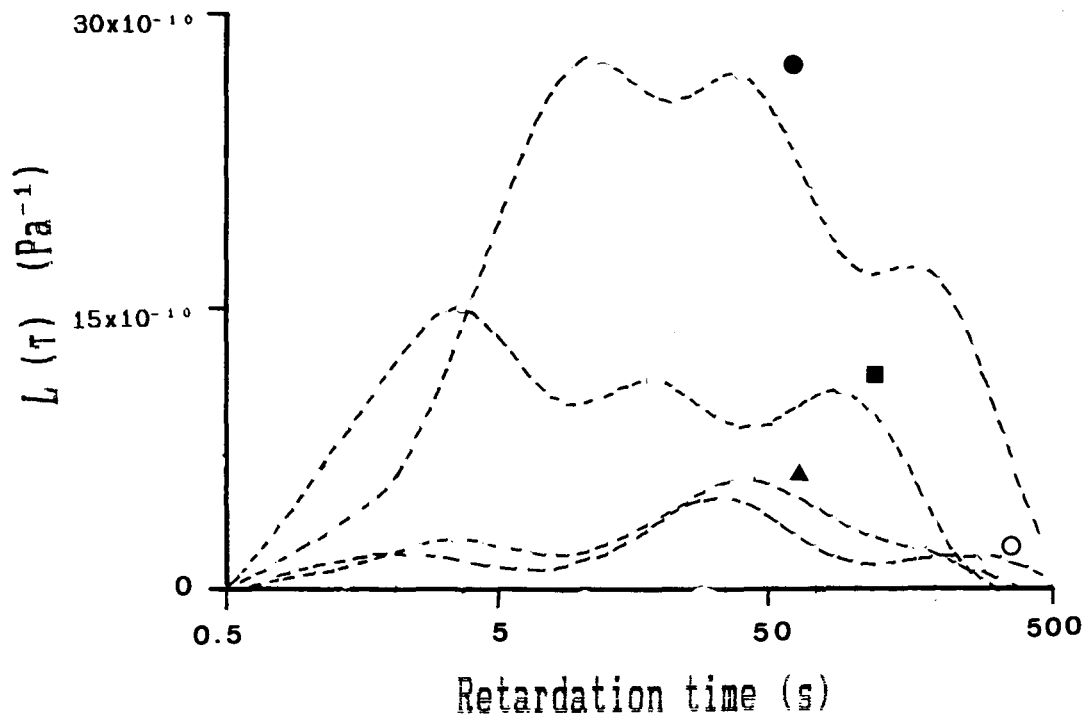


Plasticizer

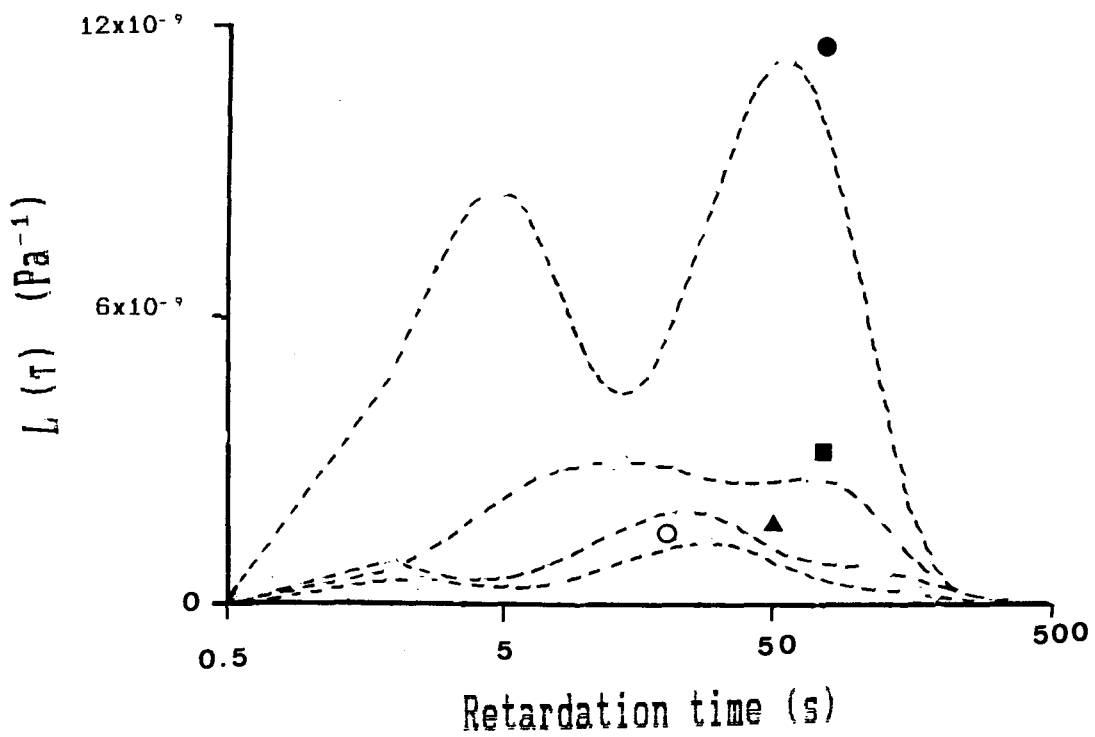
PEG 200 0% w/w ○ PEG 200 10% w/w ▲ PEG 200 20% w/w ■ PEG 200 30 %w/w ●

Figure 4.21 Influence of Plasticizer Content on the Continuous Retardation Spectrum of Starch 1500

(a) 22.5% RH



(b) 59.5% RH



Plasticizer

Glycerol 0% w/w ○ Glycerol 10% w/w ▲ Glycerol 20% w/w ■ Glycerol 30% w/w ●

In many respects, the effect of increasing plasticizer level was analogous to the effect of increased moisture content in the previous section. Thus, inclusion of increasing amounts of PEG 200 (in HPMC and PVP) or glycerol (in Starch 1500) resulted in an increase in the height of spectra, changes in the number of retardation maxima, and shifts in peak positions. Although the observed trends were generally similar for all three binders, some binder dependent differences were observed. For PVP and HPMC, increasing plasticizer content was generally associated with an increase in the number of retardation maxima in the spectra. At 22.5% R.H the spectra for Starch 1500 films exhibited three maxima irrespective of the glycerol content. At 59.5% RH, however, spectra for films containing 20% or 30% glycerol inclusion had only two maxima.

At the lowest levels of plasticizer inclusion (10% by weight in HPMC and Starch 1500; 5% by weight in PVP) the characteristic shape of retardation spectra were similar to those obtained for the unplasticized films. This indicated that the processes determining viscoelastic retardation were essentially identical at the molecular level. Further increase in plasticizer level resulted in changes both in the relative height of spectra and in the retardation times of the maxima. This was consistent with fundamental changes in the retardation process at the molecular level.

The relative height of maxima in the spectra generally increased with longer time, particularly as the level of plasticizer was increased. This behaviour was most noticeable for PVP and HPMC (Figs. 4.19a and 4.20a). There were exceptions, however. Spectra obtained for Starch 1500 films containing 20% or more of glycerol (Fig. 21a) exhibited higher maxima at shorter retardation times. The greater significance of processes having short retardation time in the overall viscoelastic strain of starch films, may reflect some influence of the crystalline component of the polymer matrix.

Differences in the form of the retardation spectra recorded at 59.5% RH reflected the relative moisture affinity of the polymers. HPMC had the lowest affinity for moisture. Spectra for plasticized HPMC films equilibrated at the higher humidity were increased in height, although peaks were located at similar times. This indicated that interactions

contributing to retardation remained similar in fundamental nature, although the number of interactions were reduced. This was not evident for PVP or Starch 1500. For the latter polymers, equilibration at the higher humidity resulted both in increased spectra height and changes in the distribution and concentration of retardation processes. Of the binders examined, PVP was observed to have the greatest affinity for moisture. Data on discrete mechanical properties of plasticized PVP films (section 4.3.3) indicated that gross mechanical changes occurred with the inclusion of 10% or more of PEG 200 and equilibration at 59.5% RH. This would involve significant changes in retardation processes at the molecular level. The spectrum obtained for PVP containing 5% PEG 200 at 59.5% RH was, thus, greatly different from that obtained at the lower conditioning humidity. Starch 1500 had an intermediate moisture affinity and, in the presence of only 10% glycerol, showed a similar retardation distribution to that observed for the film equilibrated at 22.5% RH. At 20% glycerol inclusion or higher, there were significant shifts in the positions of retardation maxima along with the loss of one peak. These shifts indicate significant changes in the fundamental mechanisms contributing to retardation.

4.4 Discussion

4.4.1 Mechanistic Interpretation of Viscoelastic Phenomena

Simple mechanical models produced by combining Hookean springs and Newtonian dashpots provide a useful macroscopic representation of the elastic and viscous properties of real materials. The components of the discrete spectrum are, however, an arbitrary set of parameters. The retardation time is a product of a compliance and its associated or "coupled" viscosity; any number of compliance-viscosity products may give rise to the same retardation time. A particular system may be adequately described by several equivalent models (Kuhn, 1947; Alfrey, 1948). Thus, such models give no insight into the fundamental processes occurring at the molecular level. Alfrey and Gurnee (1956) suggested that the individual elements may be qualitatively identified with general processes at the molecular level in the following manner. The rigidity modulus G_0 is analogous to the instantaneous elasticity of the polymer matrix and is associated with bond stretching. The

viscoelastic region (modelled by Voigt units connected in series), is associated with elongation and orientation of the polymer chains which involve the breaking and reforming of secondary bonds. The retardation time may then be regarded as the time required to break and reform secondary bonds or, alternatively, as the time required for polymer chains to attain their new equilibrium orientations. Since different types of secondary bond may be involved (or different equilibrium orientations), the processes involved do not occur at the same rate and a spectrum of retardation times exists. Treatment of creep compliance data by mechanical analysis has the effect of grouping similar retardation times (rate-dependent processes) into average values. After sufficient time (when all Voigt units have become fully extended) further deformation occurs by viscous flow, modelled by the residual dashpot. At the molecular level, this can be visualised as the slippage of polymer chains past each other.

Mechanistic and thermodynamic theories, discussed in Chapter 3, provide complimentary interpretations of plasticizer activity and efficiency. But neither concept addresses the time-dependent nature of deformation in polymers. Previously (section 3.4.1) some analogies were drawn between the effect of plasticization and the effect of increased environmental temperature on the observed tensile properties of a polymer. Similar considerations can be advanced to understand the influence of moisture sorption and plasticization on time-dependent aspects of polymer deformation.

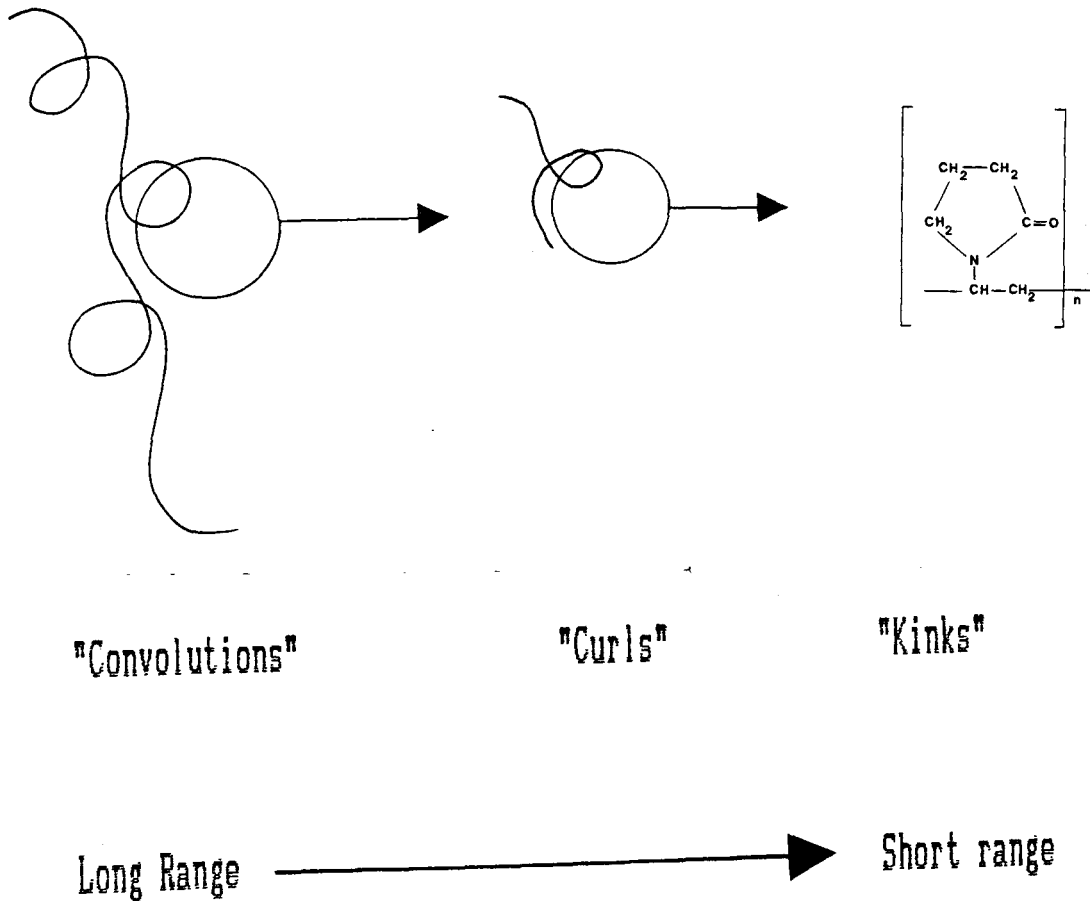
4.4.2 Thermal Properties of Polymers - Dependence of Viscoelastic Behaviour on Temperature

Ferry (1961) suggested that a single polymer chain could be regarded as a flexible threadlike molecule occupying a finite volume, the shape and conformation being determined by the thermal energy of the molecule. In order to understand polymer relationships and their influence on mechanical properties it is necessary to consider:

- gross long range polymer chain relationships,
- more local relationships at a more detailed scale
- monomer relations in the polymer backbone and bond orientation at a molecular level

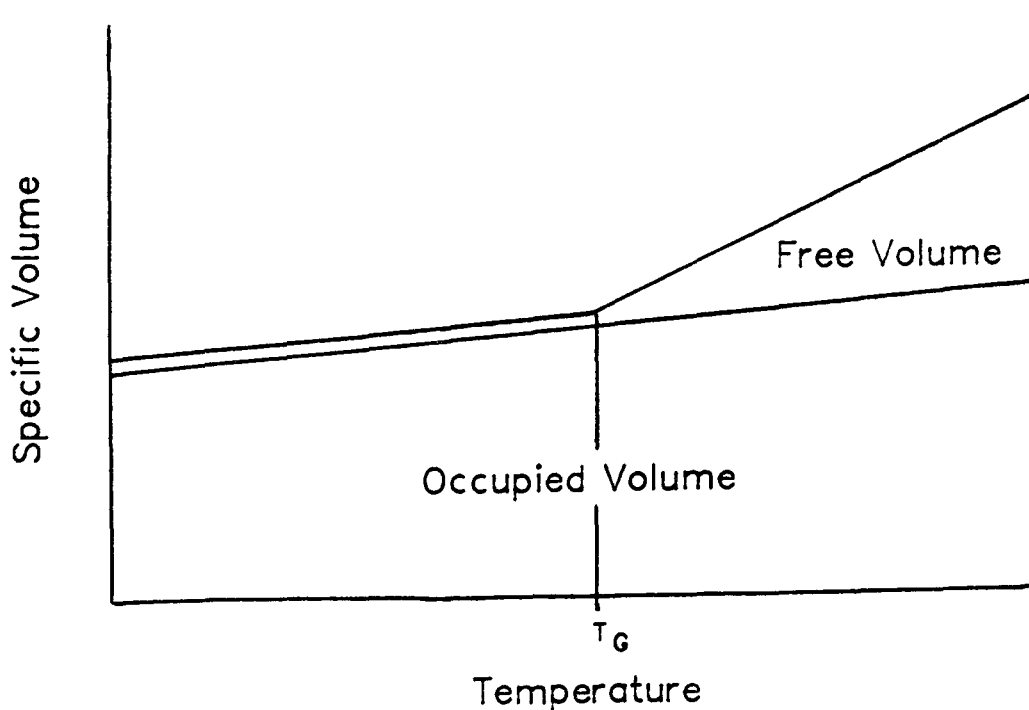
Alfrey (1948) has referred to these spatial relationships as kinks, curls and convolutions as viewed over a progressively longer range. This concept, as it could be applied to one of the polymers (PVP) used in the present work, is illustrated in Figure 4.22. Rearrangements at the local level, i.e. within kinks, are rapid since they involve only local atomic translation and stretching or bending of covalent bonds. Longer range rearrangements are potentially much slower.

Figure 4.22 Model Spatial Relationships for PVP



Amorphous polymers are characterised by a glass transition temperature, (T_g), below which thermal motions essentially cease and long range conformational readjustments are severely restricted (Ferry, 1961). The glass transition is defined as the point at which the thermal expansion coefficient (α) undergoes a discontinuity. Above T_g , α has the magnitude normally associated with a liquid, i.e. $6-10 \times 10^{-4} \text{ }^\circ\text{C}^{-1}$. A decrease in temperature is accompanied by a collapse in free volume, made possible by conformational adjustment. Eventually free volume is reduced such that further changes can occur only slowly or are even prohibited. Free volume then no longer decreases and further contraction in total volume is much less. The thermal expansion coefficient is then of the order $1 - 3 \times 10^{-4} \text{ }^\circ\text{C}^{-1}$. The interrelationship between free volume, occupied volume, and total specific volume over a range of temperatures is shown diagrammatically in Figure 4.23.

Figure 4.23 The Relationship Between Free volume, Occupied Volume, and Specific Volume (after Ferry, 1961)



At the molecular level, free volume can be visualised as "holes" of the order of molecular (monomeric) dimensions or small voids associated with packing irregularity. A fall in temperature is associated with a collapse in free volume. At lower temperatures further temperature reduction is associated with solid-like volume contraction and free volume is small but almost constant.

The appearance of a glass transition results from a reduction of molecular mobility as temperature falls. The concept therefore arises that chain mobility at any temperature depends primarily on the free volume remaining. Hence shear deformation can be expressed in terms of a free volume parameter rather than temperature. The retardation times which constitute the viscoelastic spectrum decrease rapidly with increased temperature (Ferry, 1961). This reflects the increase in free volume and resultant decrease in apparent viscosity of polymer chain mobility.

4.4.3 Thermal Properties of Polymers - Correlation with Viscoelastic Properties of Plasticized Binders

As noted previously (section 3.4.1), all the polymers used in the present work are amorphous to a greater or lesser degree and therefore exhibit glass transition points. The essentially rigid-glassy behaviour of the unplasticized polymers can therefore be interpreted in terms of grossly restricted free volume. In the case of Starch 1500, modulus enhancement by pseudo-crystalline domains may also be significant since the restriction of polymeric motion associated with highly ordered crystalline regions is analogous to crosslinking or entanglement coupling (Mark, 1965). In the absence of moisture or plasticizer mediated effects, shear deformations will be restricted mainly to bond stretching between adjacent monomeric subunits. Discrete mechanical analysis and continual spectral analysis showed, however, that the measured creep behaviour was not ideally elastic. PVP and HPMC films equilibrated at 0% RH exhibited retarded elasticity characteristic of an anelastic material. Under the same test conditions, Starch 1500 films also exhibited plastic flow. Since starches are highly crystalline, this may be due to non-recoverable deformation in the crystalline slip planes.

The influence of sorbed moisture or inclusion of a plasticizer on the viscoelastic properties of hydrophilic polymers can be interpreted in terms of free volume. In mechanistic terms, sorbed water or plasticizer molecules act simply as diluents, increasing the physical separation of polymer chains. This is analogous to the influence of increased environmental temperature on free volume. For the polymers studied in the present work, there is substantial evidence to indicate that sorption of water markedly decreases the glass transition temperature and, by inference, increases polymer free volume (Tan and Challa (1976); Entwistle and Rowe (1978); Okhamafe and York (1984); Eith et al., (1986)). Published literature on the influence of potential plasticizers on thermomechanical properties of the polymers is less extensive. However, PEGs including PEG 200 have been shown to lower the glass transition temperature of HPMC (Entwistle and Rowe (1978); Abdul Razzak (1980)). Similar results have been observed for PEG-plasticized PVP films (Forrest, 1987) but analogous observations for starch-glycerol systems have not been reported. It seems reasonable to assume that a diluent molecule (glycerol) interposed between adjacent starch chains in the amorphous regions would increase the free volume although crystalline domains would be unaffected.

As noted previously (section 4.4.2) retardation times which constitute the viscoelastic spectrum decrease rapidly with increased temperature. Since this is directly attributable to the increase in free volume a similar correlation would be expected for increasing moisture or plasticizer content. The experimental results, however, showed deviations from this general rule. The continuous retardation showed that increased moisture and plasticizer content in some cases induced processes of longer retardation time than reported at lower levels. This apparent anomaly can be accounted for in two ways. Firstly, at low moisture or plasticizer content where free volume is severely restricted, it might not prove possible to discriminate between viscoelasticity of long retardation times and apparent Newtonian flow. Secondly, increasing moisture or plasticizer content may facilitate molecular translations (with characteristic retardation times) which were previously inhibited or "frozen" at the same temperature.

At the glass transition temperature, mechanical properties of polymers change by many orders of magnitude as the physical state is

change by many orders of magnitude as the physical state is transformed from a viscoelastic solid to a viscous rubber or fluid state. In the present work this gross change in the magnitude of G_0 and η_0 was only seen for PVP films containing 15% PEG 200 at 59.5% RH. This behavior was not observed for HPMC or Starch 1500 despite higher plasticizer loadings. The difference can be explained by the higher affinity of PVP for moisture and greater polymer-plasticizer compatibility. The decrease in the number of Voigt units required to model the behaviour of PVP films containing 10% or 15% PEG 200 at 59.5% RH, compared with similar PEG loadings at the lower humidity, may be a mechanistic manifestation of the transition from a viscoelastic solid to a viscous fluid. In the transition from elastic glass to viscous plastic a polymer will inevitably pass through a maxima in the number of Voigt units required to model the intervening viscoelasticity.

4.5 Conclusions

Plasticizer or moisture induced changes in the characteristic shape of tensile stress-strain curves noted in the previous chapter, implied qualitative changes in the viscoelastic nature of PVP, HPMC and Starch 1500 tablet binders. By the use of creep rheological methods, a detailed and quantitative study of time-dependent deformation of these binders was possible. The results confirmed the empirical classifications of viscoelasticity derived from tensile stress-strain relationships. Time-dependent deformation in the systems examined conformed to a linear viscoelastic model. Hence, it was possible to resolve the discrete components of viscoelastic deformation and, to quantify the influence of sorbed moisture and plasticizer upon them.

The design and installation of the ICI micro-indenter enabled the determination of creep profiles for binder samples equilibrated at 0% RH. It was therefore possible to evaluate mechanical properties with the minimum interference from sorbed moisture. This was not possible for tensile properties investigated in the previous chapter. Unplasticized binders equilibrated at 0% RH were predominantly elastic in nature, exhibiting large values for the instantaneous shear moduli. All three binders exhibited some degree of retarded elastic deformation, however. Starch 1500, in addition, showed evidence of

limited but finite plastic flow which was probably due to slippage in crystalline domains of the polymer matrix. The relative magnitude of the elastic, viscoelastic and plastic components of deformation indicated that all three binders could be classified as glassy-brittle materials. This was consistent with the anticipated properties of a polymer held at a temperature more than 100°C below that of its glass transition point.

For unplasticized films equilibrated at 22.5% or 59.5% RH, comparison of elastic moduli derived from tensile tests (Chapter 3) and indentation tests showed some similarities. The rank order of the moduli was the same irrespective of the test method, indicating that PVP was the binder most resistant to deformation whilst Starch 1500 was most readily deformed. Young's moduli obtained from tensile tests were considerably greater than rigidity moduli obtained from indentation tests. This observation indicated that the binders deformed more readily in shear than in tension.

Increased moisture content or the incorporation of a plasticizer resulted in binders which were both softer and more easily deformed. The reduction in rigidity modulus (analogous to the reduction in Young's modulus in the previous chapter) resulted in greater instantaneous elastic strain per unit stress. A greater proportion of the overall induced strain was of a time-dependent nature, however. This comprised both retarded elasticity and non-recoverable (plastic) deformation. In all the polymers examined, an increase in either moisture content or plasticizer content was associated with a reduction in the apparent Newtonian viscosity of plastic deformation. This provided a direct and quantifiable evaluation of polymer plasticity. An increase in moisture content or plasticizer content also resulted in greater viscoelastic compliance. Changes in moisture and plasticizer content also resulted in changes in characteristic retardation times (or shifts in position of retardation maxima). This indicated that there were changes in the fundamental nature of mechanisms involved in retarded elastic strain, not simply changes in numbers of mechanisms of similar retardation times.

The creep test enabled fundamental material properties such as elasticity, viscoelasticity and plasticity, to be discretely resolved

and quantified under controlled conditions. Thus, valid comparisons could be made between binder films of differing moisture content and plasticizer content. This demonstrated that, when evaluating the tableting performance of a polymeric binder, the presence of moisture or a potential plasticizer must be considered. It is highly probable that the performance of the same binder may differ markedly if tested under conditions which give rise to different tensile or viscoelastic characteristics. By inclusion of a suitable plasticizer and/or moisture control, the potential exists to modify binder properties in a controllable manner. Where the binder is incorporated into a granulate by wet massing, modification of the binder mechanical properties may influence:

- the properties of the tablets formed by compression
- the way in which a granulate deforms in response to applied compressive stress

Consequently, the influence of binder plasticity on the tablettability of some model substrates forms the subject of the following chapters. Work reported addresses the influence of binder mechanical properties on the mechanical properties of tablets and also on the nature of deformation occurring during the compaction process.

CHAPTER FIVE

GRANULATION AND TABLETTING STUDIES

CHAPTER FIVE

GRANULATION AND TABLETTING STUDIES

5.1 Granulation

Granulation is carried out as a component of many industrial processes to improve powder handling characteristics. In the production of pharmaceutical tablets, granulation is often used to improve the tableting properties of drugs. Broadly, granulation may be classified into "dry methods" such as precompression or slugging (e.g. Khan and Musikabhumma, 1981) and agglomerative phase of comminution (APOC) (Ho and Hersey, 1979), and "wet methods" such as pan granulation (e.g. Ahmed and Pilpel, 1967), spray drying (e.g. Seager, 1977), fluidized bed granulation (e.g. Aulton and Banks, 1981) and massing and screening (e.g. Jaiyeoba and Spring, 1979).

Wet granulation methods are by far the most common in the pharmaceutical industry and are carried out by massing the blended powders with a liquid granulating agent. The granulating agent alone may be sufficient to achieve aggregation of soluble drugs and excipients. But more often a binder (usually an adhesive polymer) is incorporated as a solution the granulating liquid. Where enhanced compressibility is the aim, the incorporation of a binder is the norm.

Mechanisms of granulation and factors which influence the process and the product have been extensively reviewed (Pilpel, 1969; Record, 1980; Kristensen and Schaefer, 1987) and are considered briefly here.

5.1.1 Theories of Aggregation and Bonding

Mechanisms which can mediate particulate agglomeration either in the dry state or in the wet state have been reviewed by Rumpf (1958). They have classified as: molecular forces (i.e. valency bonding, Van der Waal's forces, electrostatic attraction and magnetic forces), frictional forces and mechanical interlocking, and liquid or solid

bridges formed between adjacent particles. Valency forces act only over molecular dimensions and hence do not contribute to bonding between macroscopic particles. Van der Waal's forces can act at displacements up to about 100nm (Rumpf, 1962) and although weak in comparison with gravitational forces, may contribute to bonding in fine powders ($< 50\mu\text{m}$) or when compaction results in low interparticulate separation. Electrostatic forces may be important in the initial aggregation of very fine powders ($< 2\mu\text{m}$) but Barlow (1968) considered that their contribution to final granule strength would be minimal.

Interlocking of irregular particles may contribute to interparticulate bonding especially if close proximity is achieved, for example, during compression. Elevated temperature due to friction at the points of contact may facilitate molecular diffusion with the resultant formation of solid bridges. Under conditions of tablet compression the applied force is transmitted across point contacts of small area. Resultant pressures are correspondingly high and can result in frictional melting (asperity melting) with an increase in contact area and recrystallization bonding on cooling (Britten and Pilpel, 1978). In wet granulation deposition of material (binder or soluble excipient) dissolved in the binding agent, on drying, forms solid bridges.

The influence of liquids on bonding in a particulate system depends on the nature of the liquid, the amount of liquid, and its distribution. For freely mobile liquids Newitt and Conway-Jones (1958) described three distinct states of a powder bed according to the extent to which interparticulate voids were filled with liquid. The states, termed pendular, funicular, and capillary, represent a progressive increase in liquid void filling with associated changes in capillary forces and strength of the aggregate. Barlow (1968) noted a fourth, droplet or suspension, state in which only surface tension holds the particles together.

In wet granulation, aggregation is initiated by the formation of liquid bridges between adjacent particles. A number of studies have shown that bridge development, and hence granule growth and properties, are dependent on the base material, physical properties of

the granulating solution, and also on processing variables.

5.1.2 The Granulating Liquid

The volume of granulating liquid has long been recognised as one of the most important variables in successful wet-massed granulation. Early research concentrated on variations in the granulating liquid volume and its influence on granule growth. More recent work has addressed the influence of physicochemical properties (surface tension, contact angle, and viscosity) of the granulating liquid on granulation.

Detailed studies on the mechanisms of wet aggregation were first reported by Newitt and Conway-Jones (1958). By studying the pan granulation of sand using a systematic variation in the volume of granulation liquid, they found that formation of coherent granules occurred only as the liquid saturation approached the capillary state. Kapur and Fuerstenau (1964) using a pulverised limestone also found that granules could only be formed over a narrow range of liquid contents. Capes and Dankwert (1965) studied the pan-granulation of a number of uniformly sized sands. Using water as the binding agent their conclusions were similar to those of Newitt and Conway-Jones, in that significant granule formation and growth only occurred as the capillary state was approached. Where aqueous solutions of ethyl alcohol were used as the granulating agent, the lowered surface tension resulted in reduced capillary cohesion. Sands which had granulated satisfactorily with water no longer formed aggregates of sufficient strength for granulation to occur.

Ganderton and Hunter (1971) attempted to relate granulation theory to pharmaceutical practice. They compared granules produced by pan granulation with those formed by wet-massing and screening for a cohesive powder and a non-cohesive powder (calcium phosphate and lactose respectively). For massing and screening, as in pan granulation, a minimum amount of liquid was required for aggregation and the formation of coherent granules. An increase in liquid above the minimum resulted in greater densification of lactose but had less effect on calcium phosphate where consolidation appeared to be dependent on the shear force imparted by the mixer. With both

substrates, an increase in granulating liquid resulted in greater mass cohesion and the elimination of fines.

Determination of optimum granulating liquid volume and duration of massing (granulation endpoint control) has attracted considerable attention. Techniques have been developed to enable measurement of wet-mass rheology directly via torque transducers (Rogerson et al, 1976; Schildcrout, 1984, Lindberg, 1984) or indirectly via power consumption of the granulator (Luenberger et al. 1979; Ritala et al, 1986).

Luenberger et al., (1979) observed that mixer power consumption during granulation could be divided into five phases, each related to the amount of granulating liquid added. It was demonstrated that the stepwise change in power consumption could be satisfactorily interpreted on the basis of the development of cohesive liquid bridges between solid particles (Newitt and Conway-Jones, 1958). The granulation models of Luenberger et al., (1979) and Luenberger, (1982) indicate that granulating liquid requirement will be dependent on the porosity of the powder bed. The practical relevance of this was demonstrated by the results of Duchene et al., (1982). For both a water soluble substrate and an insoluble substrate, the quantity of granulating liquid necessary to achieve satisfactory massing was dependent on the degree of densification provided by the granulator used. Thus, the granulating fluid requirement using a high densification extruder was significantly lower than for a high speed mixer-granulator or a planetary mixer. Fluidized-bed granulation, providing the least mechanical densification, correspondingly required the greatest volume of granulating liquid for agglomeration to occur.

5.1.3 Processing Factors

The dependence of granule formation and properties on a series of interacting processing factors was recognised by Ganderton and Hunter (1971). Subsequent work has demonstrated that granule growth rate, size, size distribution and porosity may be affected by:

- mixer design (Hunter and Ganderton, 1973; Duchene et al., 1982)
- duration of massing, (Ganderton and Hunter, 1971; Chalmers

- and Elworthy, 1976; Holm et al., 1984)
- sieve aperture sizes, (Osewa and Nasipuri, 1983)
 - binder solution factors and the nature and rate of solution addition (Holm et al., 1983; Wells and Walker, 1983; Jaegerskou et al., 1984; Ritala et al., 1986)

5.1.4 Binders

The process may be influenced by the nature of an included binder (Healey et al., 1972) and by solution factors such as viscosity, surface tension, substrate wetting and binder concentration. Wells and Walker (1983) demonstrated the importance of secondary binding effects. i.e dissolution of drug or excipient in the granulating solution with subsequent redeposition on drying, in wet-massed granulation. Using an aspirin-based formulation they showed that drug solubility in, and wetting by, the granulating solvent was more significant in the granulation process than was granulating solvent viscosity. They also concluded, however, that problems may be encountered in the homogeneous distribution of very viscous binder solutions. A linear relationship was found between the binder solution surface tension and granule bulk density.

Spring and Femi-Oyewo (1982) reported that the inclusion of surfactants in aqueous granulating solutions of PVP resulted in a reduction in mean granule size. Wells and Walker (1983), however, noted that improved substrate wettability tended to increase granule growth. Ritala et al., (1986) investigated the influence of binder type and concentration on the growth of dicalcium phosphate aggregates granulated by wet-massing in a high shear mixer. Increasing the concentration of binder solutions had only a minimal effect on granule growth. The binders Kollidon K90 (a PVP) and Protein S (a hydrolysed gelatin) promoted granule growth in contrast with Kollidon VA64 (a vinyl pyrrolidone/vinyl acetate copolymer) or various grades of HPMC. Kollidon K90 and Protein S also produced granules of lower intragranular porosity than the other binders at equivalent binder solution volumes. The correspondingly higher liquid saturation of the wet mass was considered responsible for enhanced granule growth and increased work required to shear the wetted mass during granulation.

5.2 The Effect of Binders on Physical Properties of Granules and Tablets

In addition to their effects on mechanisms of granulation and the size distribution of granulates, binders may also influence the physical and mechanical properties of granules and tablets.

5.2.1 Granule Properties

The use of low pressure mercury intrusion techniques has enabled the study of intragranular porosity (Strickland et al., 1956). Fugiwara et al., (1966) showed that the mean intragranular pore size was decreased with increased levels of a binding agent and also with decreased initial particle size. Healey et al., (1972) noted that the surface tension of the binder solution also influenced granule porosity. In a subsequent paper (Healey et al., 1973) they showed that compact porosity was dependent only on compaction pressure and binder type. The pressure applied during compaction eliminated effects due to intragranular porosity and granule strength, except at very low compaction pressures. Krycer et al., (1982b) demonstrated that an increase in intragranular porosity resulted in an increase in bonding, by increasing interparticulate friction during compression. They suggested that the energy of compaction was utilised most effectively to yield strong tablets, if the granule contained a good binder and had a high intragranular porosity. Jaegerskou et al., (1984) observed that densification of water-soluble and water-insoluble substances, in a high-speed mixer, was controlled primarily by the amount of binder solution added and by the mixer impellor speed.

A number of studies have shown that increased binder concentration increases granule crushing strength and decreases granule friability (Jarosz and Parrott, 1982; Cutt, 1983). This has been considered to be due to increases in the area of bonding and/or the number of bonds formed. Cutt (1983) also demonstrated the significance binder-substrate adhesion in determining the mechanical properties of granules. Reading and Spring (1984b) found, however, that there was no correlation between the bond strength of binders (determined using a glass butt joint test) and the strength of sand granules prepared with the binders. The mechanical properties of granules have also been

shown to vary with the nature of the binder used (Shotton and Edwards, 1974; Doelker and Shotton, 1977; Cutt, 1983). There is, however, no universal relationship between granule strength and the strength of tablets formed by the compression of those granules. Thus, Doelker and Shotton (1977) found that for paracetamol the softest granules yielded the strongest compacts, whereas the reverse relationship was true for dicalcium phosphate.

5.2.2 Tablet Properties

The method of granulation affects densification and binder distribution which, in turn, influence the physico-mechanical properties of compressed tablets. These properties are important since they determine the ability of the tablet to withstand abrasion and impact shock and remain as a coherent unit dose throughout subsequent handling operations.

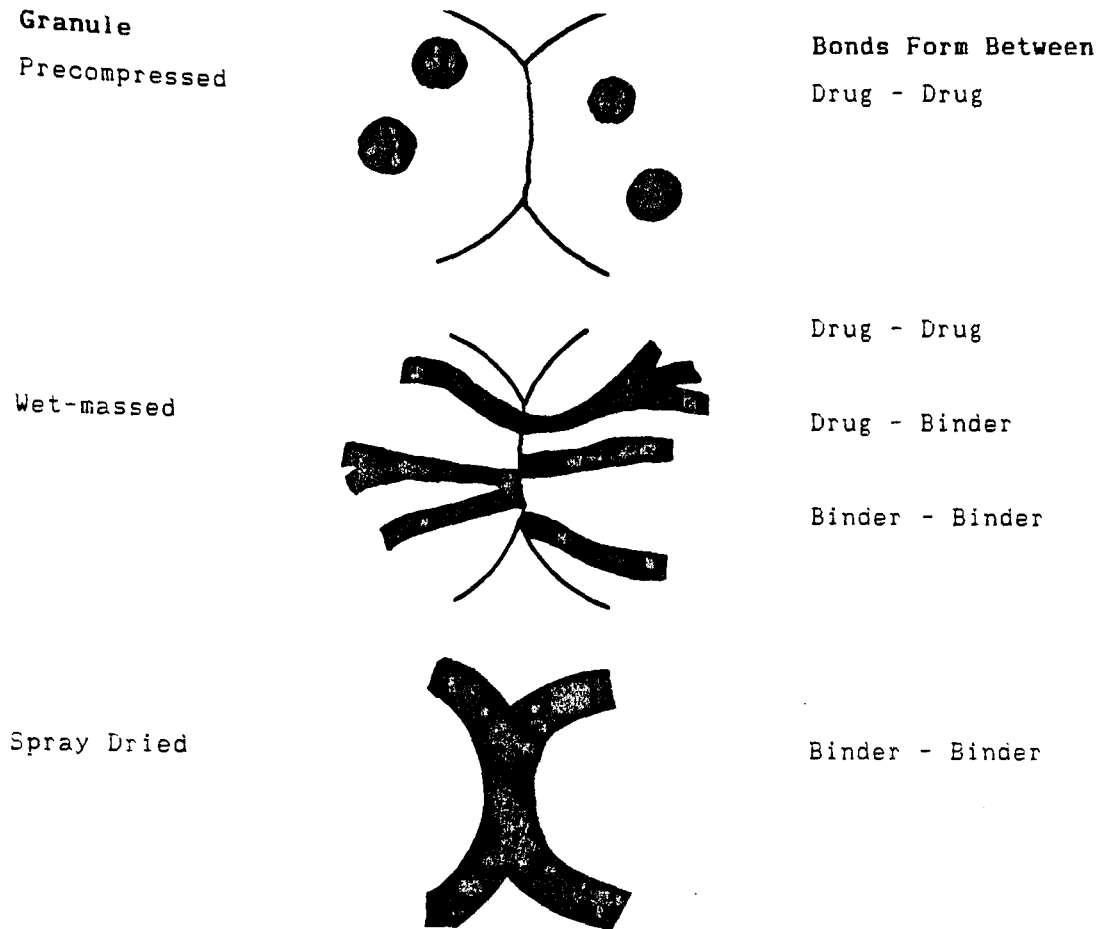
5.2.2.1 Tablet Strength

A number of methods have been used to assess the mechanical strength of tablets. Krycer et al. (1982a) have suggested that a useful means of evaluating energy utilisation in the production of strong tablets is to plot tablet strength against the work exerted on the lower punch on first compaction (LPW1). The mechanical strength of tablets has variously been described by crushing strength, hardness (Aulton, 1977) tensile strength (Newton and Fell, 1971) and work-of-failure (Rees and Rue, 1978).

5.2.2.2 Granulation Method

Rue et al. (1980) showed that tablets produced by spray-dried granulation of paracetamol were stronger than those produced from wet-massed granules or roller compacted granules. This was explained by preferential concentration of binder at the surface of spray dried granules (Figure 5.1) compared with other methods of granule production. Increasing binder concentration had little effect on tablet strength until compaction pressure was raised to the point where capping occurred. Similar results were obtained by Ragnarson and Sjorgren (1982).

Figure 5.1 Influence of Granulation Method on Binder Distribution and Intergranular Bonding (after Rue et al., 1980)



Tablets of a high dose drug prepared from granules produced by fluidized-bed granulation were stronger than those produced from conventional wet-massed granules. For other materials, increasing binder concentration has been associated with an increase in the strength of resultant tablets (Esezobo and Ambujan, 1982; Jarosz and Parrott, 1982; Cutt, 1983).

5.2.2.3 Binder Type

Many studies have examined the influence of binder type on the strength of tablets (for example, Kurrup and Pilpel, 1978; Chowan and Chow, 1981a; Reading, 1983; Cutt 1983). Alderborn and Nystrom (1984) examined the effect of a gelatin binder on the radial and axial tensile strengths of paracetamol tablets. They observed that increasing the binder level from 2% to 4% had little effect on the

radial strength, but greatly increased the axial strength. This was associated with a decrease in the capping tendency of the formulation. They concluded that low values of the isotropy ratio (the ratio of axial strength to radial strength) were indicative of incipient capping. Esezobo and Pilpel (1974a) and Chohan and Chow (1981b) noted that the strength of compacts was also dependent on the granule moisture content before compression. The latter workers found that, although the crushing strength of compacts was dependent on binder type at low moisture contents, differences were less significant at higher moisture contents.

Inconsistencies between studies can, to a large extent, be explained by differences in experimental protocols. The degree of variability is not surprising, however, since tablet strength may be dependent on adhesion and/or cohesion between drug, excipient and binder. The rank adhesion for a series of binders will inevitably vary depending on the nature of the substrate and the extent of adhesive-substrate compatibility (Iyengar and Erickson, 1967; Barton, 1962).

5.2.2.4 Tablet Friability and Work of Failure

In many cases the absolute crushing strength of a formulated tablet will be of secondary consideration to its ability to withstand impact attrition or friabrasion. Tablet friability ultimately determines the bulk handling properties of tablet formulation. The appearance of loose powder or tablet debris implies a physically fragile tablet and, where the tablet is a dispensed product, may contribute to problems in patient compliance.

Although several techniques have been developed for assessing friability, the Roche Friabilator has generally been accepted as the industry standard. The value of the apparatus lies in the fact that it provides a numerical measurement (a percentage loss of tablet weight) indicating the resistance of compressed tablets to abrasion and repeated impact shock. The extent of use of friability testing has been reviewed by Wollish and Miodozieniec (1982). They emphasised that no general relationship could be determined between tablet friability and tablet crushing strength and that the crushing strength of a tablet was in no way a reliable indicator of its ability to

withstand abrasion.

Rue (1980) has proposed that compliance with a toughness test would ensure resistance to failure for all formulations under given conditions of stress. Toughness or work of failure is determined from the integrated area of the force-displacement curve during diametral compression testing and has the units of energy expended. Studies on some direct compression excipient (Rees and Rue, 1978) showed that materials such as Emcompress which consolidate by brittle failure formed tablets of low toughness. Conversely, plastically deforming materials such as Elcema produced tablets of a high toughness. A rank order correlation between resistance to impact attrition and toughness was found for tablets of equal tensile strength. Rees et al. (1977) showed a good linear correlation between toughness and impact resistance for a wide range of tablet formulations, suggesting that toughness was a more reliable indication of a tablets resistance to damage than tensile strength alone.

Rue et al., (1980) carried out toughness tests on paracetamol tablets compressed from granules prepared by roller compaction, spray drying, and by wet-massing. The toughness and fracture deformation of tablets compressed from spray dried granules were greater than those of the wet-massed tablets which in turn, were greater than those of the roller compacted tablets. The results suggested that the differences in tablet properties were due to the different distribution of binder in the granules which altered the plastic deformation of the different granules during compaction. Stress relaxation studies substantiated this. Later studies have shown that binder film formation (Krycer et al., 1983) and binder plasticity (Wells et al., 1982) are major factors in determining the resistance of a compact to impact attrition.

5.3 Materials and Methods

It is clear from the preceeding section that at present there exists no definitive model for the prediction of optimum granule properties in relation to the production of coherent tablets. Satisfactory

granular morphology alone is no guarantee of good tablettability. Perhaps the best general definition of a "good granulate" is one which processes satisfactorily to produce acceptable tablets. Implicit in such a definition are the requirements for homogeneity, flowability, stability, compressibility and the required drug release profile. Consequently, in the present chapter, the granulation process has not been investigated per se but has been regarded as the means by which binders of varying degrees of plasticity may be incorporated into free-flowing aggregates of a substrate material. Regard has been paid, however, to the observations of previous workers with a view to minimising extraneous variables and establishing a rigidly standardised and reproducible granulation method.

5.3.1 Materials

Since the objective was to examine the influence of binder plasticity on compressibility and the resultant mechanical properties of tablets it was necessary to choose model substrates which would emphasise binder-mediated effects. Previous workers have utilised sand (Reading, 1983) or glass ballotini (Cutt, 1983) as model substrates of low intrinsic plasticity and virtual aqueous insolubility. These materials are, however, untypical of drug substances or tableting excipients. For the present work it was decided to select substrates of pharmaceutical significance which would be representative of materials refractory with regard to tablettability. The inclusion of a binder with the view to modifying tablettability in such cases typifies a common formulation situation.

5.3.1.1 Model Substrates

The substrates selected were:

paracetamol (fine powder, Hoechst)

dicalcium phosphate (anhydrous, Albright and Wilson)

These materials were selected to exhibit deformation behaviour under compression consistent with tablettability problems. Thus, dicalcium phosphate is known to deform by brittle fragmentation; resultant compacts, although resistant to crushing, may however be susceptible to impact attrition or friabration. Paracetamol also consolidates by

fragmentation although there is evidence for some plastic flow. Paracetamol undergoes considerable elastic strain compared with dicalcium phosphate and the elastic strain recovery during decompression has been associated with the manifestation of many compression problems especially lamination and capping.

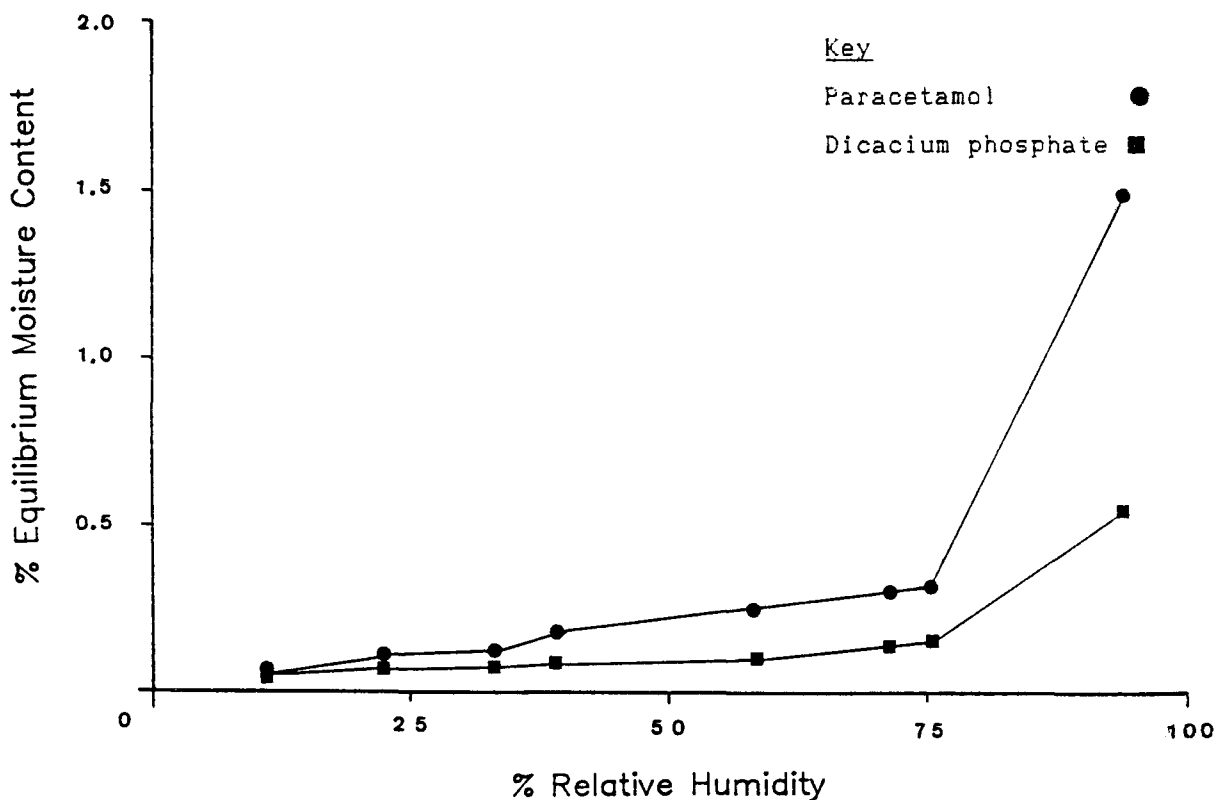
Several factors make these materials particularly suitable model compounds:

- they are well characterised materials of wide pharmaceutical usage
- plastic flow is not a major contribution to their deformation
- they have low intrinsic aqueous solubility minimising the influence of secondary binding on granule formation and strength
- their equilibrium moisture uptakes are low and change little over a wide range of relative humidities, consequently, storage humidity can, therefore, be used to control moisture content of incorporated binders with minimal substrate effects

There exists the disadvantage that both substrates exhibit a small but finite aqueous solubility. Dissolution of substrate in the granulating liquid and recrystallization in the binder film on drying will alter binder properties. Such effects tend to decrease the plasticity of polymeric binders (Reading and Spring, 1984b) and thus may serve to emphasise potential benefits of binder plasticization.

Substrates were used as received from the suppliers. Moisture contents before use as determined by infra-red drying were 0.21% and <0.1% for paracetamol and dicalcium phosphate respectively. The equilibrium moisture contents for the substrates used (determined over a range of relative humidities by the methods of Callaghan et al., 1982) are shown in Fig. 5.2.

Figure 5.2 Equilibrium Moisture Contents for Paracetamol and Dicalcium Phosphate



5.3.1.2 Binders and Plasticizers

The polymeric binders used were PVP, HPMC and Starch 1500 as described previously in Chapter 2. Sucrose was also used as a binder in this study as an example of a non-film former, binding by means of crystalline bridges. Being a low molecular weight crystalline monomer, sucrose is not amenable to plasticization. Unlike the polymers, sucrose would not be expected to exhibit significant viscoelastic deformation but has been characterised as a hard material of high elastic modulus (Aulton et al., 1974; 1976).

The performance of the polymeric binders was also evaluated after the inclusion of a plasticizer. Plasticizers and plasticization levels were those used in Chapters 3 and 4. PEG 200 was employed as the plasticizer for PVP and HPMC at levels of 0-15% w/w and 0-30 % w/w respectively. Starch 1500 was plasticized using glycerol at levels of 0-30% w/w.

5.3.2 Methods

5.3.2.1 Granulation Method

Granules were prepared by wet granulation using a novel massing technique. Laboratory and pilot scale granulations have tended to be performed using planetary or waltzing-gate type mixers such as the Kenwood Chef[®] foodmixer. But factory scale granulations are more and more frequently performed in high speed, high shear, mixer-granulators such as the Diosna, Fielder or Lödige-type equipment. The high shear of the latter apparatus can, to a great extent, overcome problems of localised overwetting and poor distribution of viscous binder solutions. In the present work a food processor (Kenwood Gourmet[®], model A535, Thorn EMI, Havant, Hants, U.K) was utilised in an attempt to simulate high shear granulation conditions. The basic unit shown in Fig. 5.3 consists of a perspex mixing bowl with a power unit driving a central clockwise rotating spindle. Mixing and shearing were achieved using a modified mixing paddle with four blades set at 90 degrees and mounted on the spindle. Paddle rotation was variable between 500rpm and 1500rpm. This was confirmed using a revolution counter. An interlocked perspex lid with integral port for liquid addition sealed the mixer vessel during processing.

Figure 5.3 Kenwood Gourmet[®] Model A535 Food Processor



The basic formula for the granulations is given in Table 5.1. A standard charge size of 250g was adequate for paracetamol formulations although a charge size of 350g was necessary for the denser dicalcium phosphate. Binders were incorporated at a fixed level of 2.5% by weight with respect to the substrate, using 62.5g of a 10% w/w aqueous binder solution for paracetamol or 73g of a 12% w/w aqueous binder solution for dicalcium phosphate. The difference in binder concentrations was necessitated by the granulating liquid volume requirements of the two substrates. This was determined by initial granulation studies using water alone as the granulating agent.

Table 5.1 Basic Granule Formula

Substrate	250g paracetamol 350g dicalcium phosphate
Binder	2.5% by weight with respect to substrate
Plasticizer	0 - 30% w/w in the plasticized binder film.

The plasticizers, where incorporated, were added to the granulating solution to give levels of 0-30% w/w (PEG 200 in HPMC and glycerol in Starch 1500) or 0-15% w/w (PEG 200 in PVP) in the final polymer-plasticizer film matrix. As a control, granulations were also carried out using an aqueous solution of PEG 200 to give a final PEG concentration of 1.03% w/w in the dry granule. This was equivalent to the maximum plasticizer loading used in the studies. i.e. 30% w/w in the plasticized binder film. This was done to investigate potential effects due to the liquid plasticizer in the absence of binder. Granulating solutions were added in eight equal aliquots over a period of eight minutes with the mixer rotor running at 1000rpm. At two minute intervals mixing was stopped and any adherent wet mass scraped from the mixer sides back into the bulk mass. Massing was continued for a further two minutes after the final addition of granulating solution. In common with industrial scale high-speed mixer-granulators, discrete granules were formed during the wet-massing

phase. Wet-screening via a 2mm aperture sieve using an Erweka oscillating sieve was necessary only to break up large loose agglomerates and did not contribute specifically to granule formation. Damp granules were thinly spread onto paper-lined trays and dried under forced convection at ambient temperature to a moisture content of about 0.5% w/w (as determined by infra-red drying using a Mettler moisture balance). Dried granules were rescreened via a 1.4mm aperture sieve and stored in airtight containers until required.

5.3.2.2 Granule Size Distribution

Granule size distributions were determined by sieve analysis. About 50g of the granules was placed on a nest of 200mm brass test sieves (Endecott, London, UK) with sieve apertures decreasing from 1200 μ m to 125 μ m. Fractionation was performed on a sieve shaker (Fritsch Analysette, Pascal Engineering, Crawley, UK) for five minutes. The duration and amplitude (setting 4) was determined experimentally to be sufficient for the fractionation of granules containing binder without excessive damage to the granules. Granules formed by wet-massing, in the absence of any binder, showed evidence of attrition and friabration even at shorter durations.

The granular fraction retained on each sieve was weighed and the results expressed as percentage weight retained. Determinations were performed in duplicate for each batch of granules and the mean used to calculate the cumulative percentage oversize. Size distributions were represented by plots of the cumulative percentage oversize probit against the log of the sieve aperture. Geometric average granule sizes were obtained graphically from the 50% cumulative weight oversize.

5.3.2.3 Granule Bulk Densities

The initial poured bulk density and the limiting tapped bulk densities of the granulates was determined using a graduated tapped-densitometer. An accurately weighed mass of granule (about 40g for paracetamol granulates or 90g for dicalcium phosphate granulates) was carefully transferred via a funnel to the volumetric cylinder of the densitometer. The volume of the initial loosely packed bed was recorded and the bulk density determined thus:

$$\text{Poured bulk density} = \frac{\text{mass of sample}}{\text{poured bulk volume}} \quad (5.2)$$

(gcm^{-3})

The volumetric cylinder was then positioned within a guideway over a rotating cam which progressively lifted the cylinder then allowed it to fall suddenly through a height of 25mm. The cam rotation speed was adjusted to give repeated taps at a frequency of one every two seconds. The test granulated was thus subjected to a periodic tamping which was continued until no further decrease in bed height was observed (usually after 500 to 600 taps). The limiting tapped bulk volume was then recorded and the limiting tapped bulk density calculated:

$$\text{Limiting tapped bulk density} = \frac{\text{mass of sample}}{\text{Limiting tapped bulk volume}} \quad (5.3)$$

(gcm^{-3})

The limiting consolidation achieved was expressed as percentage in a manner analogous to Carr's compressibility index (Carr, 1965).

5.3.2.4 Tabletting

Tablets were prepared using the 250 - 1000 μm sieve fraction. This range was selected to remove ungranulated fines and oversized granules which could lead to poor diefill uniformity. Granules were lubricated by blending with 0.5% w/w magnesium stearate in a Turbula mixer (Glen Creston, Stanmore, Middlesex, UK) for five minutes. Blends were conditioned at either 22.5% RH or 59.5% RH at 20°C prior to compression. Compression was carried out on a single punch reciprocating tablet press (Manesty F2, Manesty Machines, Speke, Liverpool, UK). A piezoelectric load washer fitted in the upper punch holder, with output to an storage oscilloscope, enabled the monitoring of upper punch force.

Tablets were compressed with a nominal weight of 250mg using 8mm diameter flat-faced tooling at a compaction rate of 42 tablets per minute. Compaction pressures of 150MPa, 250MPa and 350MPa were applied. Compressed tablets were stored at the same relative humidity as the parent granulate for two weeks before testing to largely eliminate time-dependent stress/strain recovery effects.

5.3.2.5 Determination of Tablet Physical Properties

Crushing strength of the tablets was determined from the mean of ten samples using a Schleuniger-2E "hardness" (sic) tester (Copley, Nottingham, UK) with the plattens padded to assist failure in diametral tension. Tensile strengths (TS), for those tablets observed to fail in tension, were calculated from the crushing strengths using the relationship of Newton and Fell (1970):

$$TS \text{ (MPa)} = \frac{2P}{\pi dt} \quad (5.4)$$

where P was the crushing strength (N), d was the diameter (mm) and t was the thickness (mm) of the test tablet.

Friability was assessed using a Roche Friabilator (Pharma Test, PTF-R). Ten tablets, initially dedusted, were weighed and the percentage weight loss determined after friabration for 12 minutes at a rotation speed of 25 rpm. Silica gel discs were mounted in the friabilator drum, to prevent weight gain due to moisture sorption during testing for those tablets compressed and stored at 22.5% RH.

5.3.2.6 Tablet Toughness

Apparent tablet toughness was determined by numerical integration of the force-displacement curve obtained during a diametral compression test. Testing was carried out using a CT-40 compression tester (Engineering Systems, Nottingham, UK) operating at a compression rate of 2mm min⁻¹. The compression load cell output was input to the Y-axis of a flatbed chart recorder (Bryan Southern, UK) running at a chart speed of 5mm s⁻¹. For tablets observed to fail in diametral tension, the applied force increased linearly with displacement up to the point of failure.

5.4 Results and Discussion

5.4.1 Granule Properties

5.4.1.1 Reproducibility of the Granulation Method

Reproducibility of the wet-massing procedure was studied by preparing four replicate batches of the two substrates using unplasticized HPMC as the binding agent. Granular morphology, characterised by the size distribution and bulk densities, was determined for each batch of granules. The results, shown in Table 5.2 indicate that satisfactory reproducibility was obtained using the granulation method based on the Kenwood Gourmet food processor. Single granulation batches were prepared and used for all subsequent granulation and tableting studies.

Table 5.2 Reproducibility of the Granulation Method for HPMC Granulations. (4 replicates)

Sieve Aperture μm	Mean % Oversize by weight (%rsd)			
	Paracetamol		Dicalcium Phosphate	
1200	7.6	(8.7)	7.4	(10.6)
1000	11.3	(7.5)	9.3	(9.6)
710	25.6	(4.7)	22.6	(2.0)
500	28.6	(5.2)	30.4	(6.4)
350	17.6	(10.4)	20.1	(5.0)
250	6.9	(6.7)	7.7	(3.2)
125	1.8	(35.7)	2.1	(19.9)
<125	0.5	(50.2)	0.4	(70.0)
Geometric mean granule diameter (μm)	660.9	(6.0)	630.9	(8.9)
Poured bulk density (g cm^{-3})	0.436	(1.6)	0.862	(1.0)
Limiting tapped bulk density (g cm^{-3})	0.509	(1.5)	1.016	(0.6)

5.4.1.2 Granulation with Water Alone

It was possible to granulate both paracetamol and dicalcium phosphate with water alone and in both cases some granular integrity was retained after drying and screening. In the case of paracetamol 62.5g of water was required to satisfactorily mass a 250g charge size; with dicalcium phosphate 73g of water was needed to mass a 350g charge. The difference in water requirement is a consequence both of the charge mass and the extent of packing during the granulation process. The resultant granules were weak. Consequently, considerable friabration was evident during screening after drying and during sieve analysis. This loss of granule integrity illustrated the limited extent of secondary-binding in granules of paracetamol and dicalcium phosphate prepared by aqueous wet-massing.

5.4.1.3 The Effect of Binding Agents on Granule Properties

Particle size distributions for the granulations, shown in Figs. 5.4 and 5.5 for paracetamol and dicalcium phosphate respectively, were dependent on binder type. The higher proportion of fines recorded for simple aqueous-massed dicalcium phosphate when compared with aqueous-massed paracetamol reflects the higher aqueous solubility of paracetamol with a resultant increase in granule integrity as a result of solid bridging.

Incorporation of a binding agent resulted in a much greater proportion of larger granules and a reduction in fines. Plots of cumulative percent oversize (by weight) probit against log sieve aperture (Figs. 5.4 and 5.5) were approximately linear with polymeric binders, but not with water or sucrose due to the tendency to mechanical failure in the latter cases. Slopes of the plots were steeper for the polymeric binders than for water or sucrose indicating narrower granule size distributions in the former case. Differences in the slopes between polymeric binders were not significant either for paracetamol or for dicalcium phosphate.

The influence of binder type on mean granule size is given in Table 5.3. Massing with water alone produced the smallest mean granule size both with paracetamol and with dicalcium phosphate.

Figure 5.4 Influence of Binder Type on Size Distribution of Paracetamol Granules

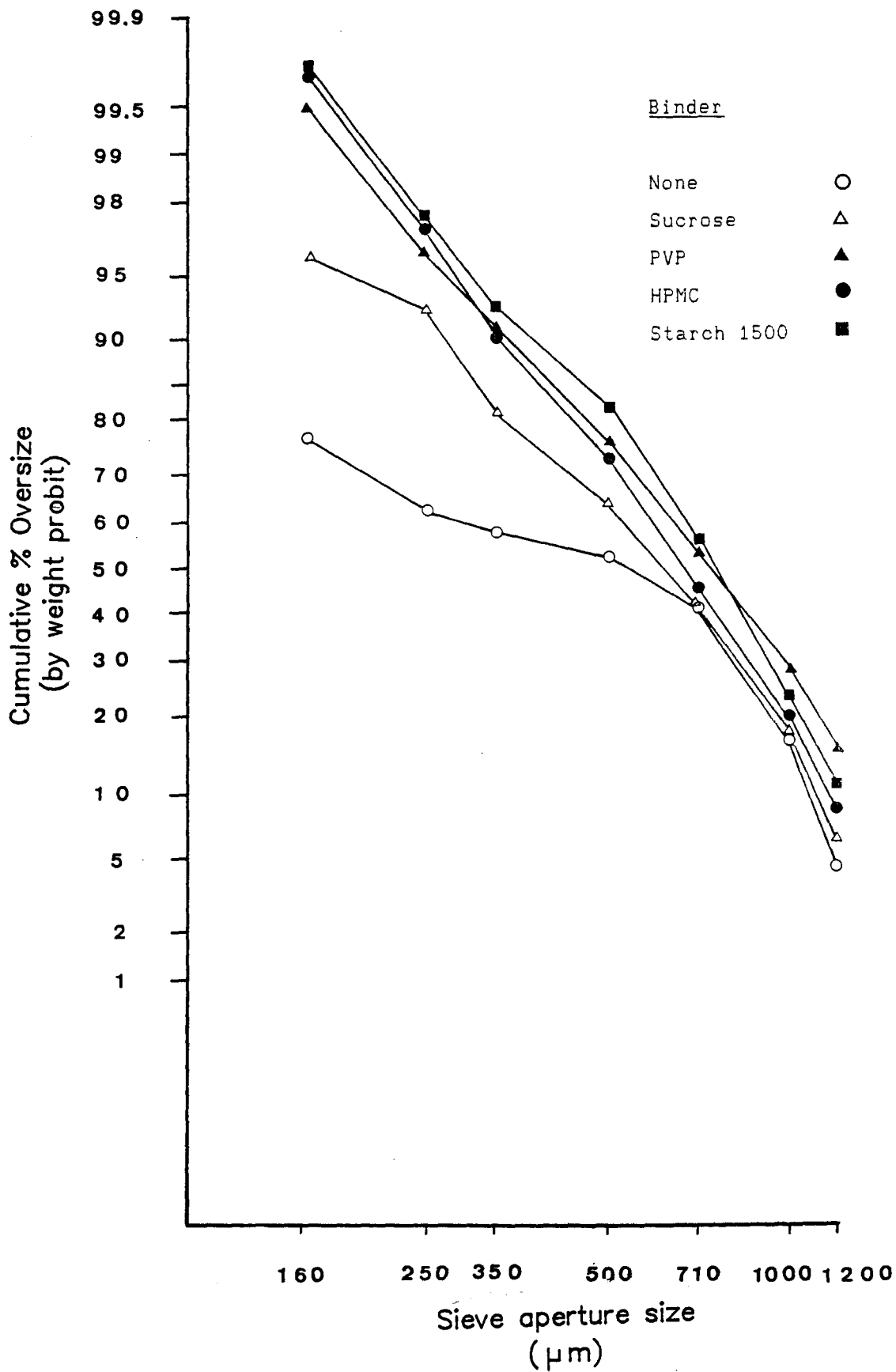


Figure 5.5 Influence of Binder Type on Size Distribution of Dicalcium Phosphate Granules

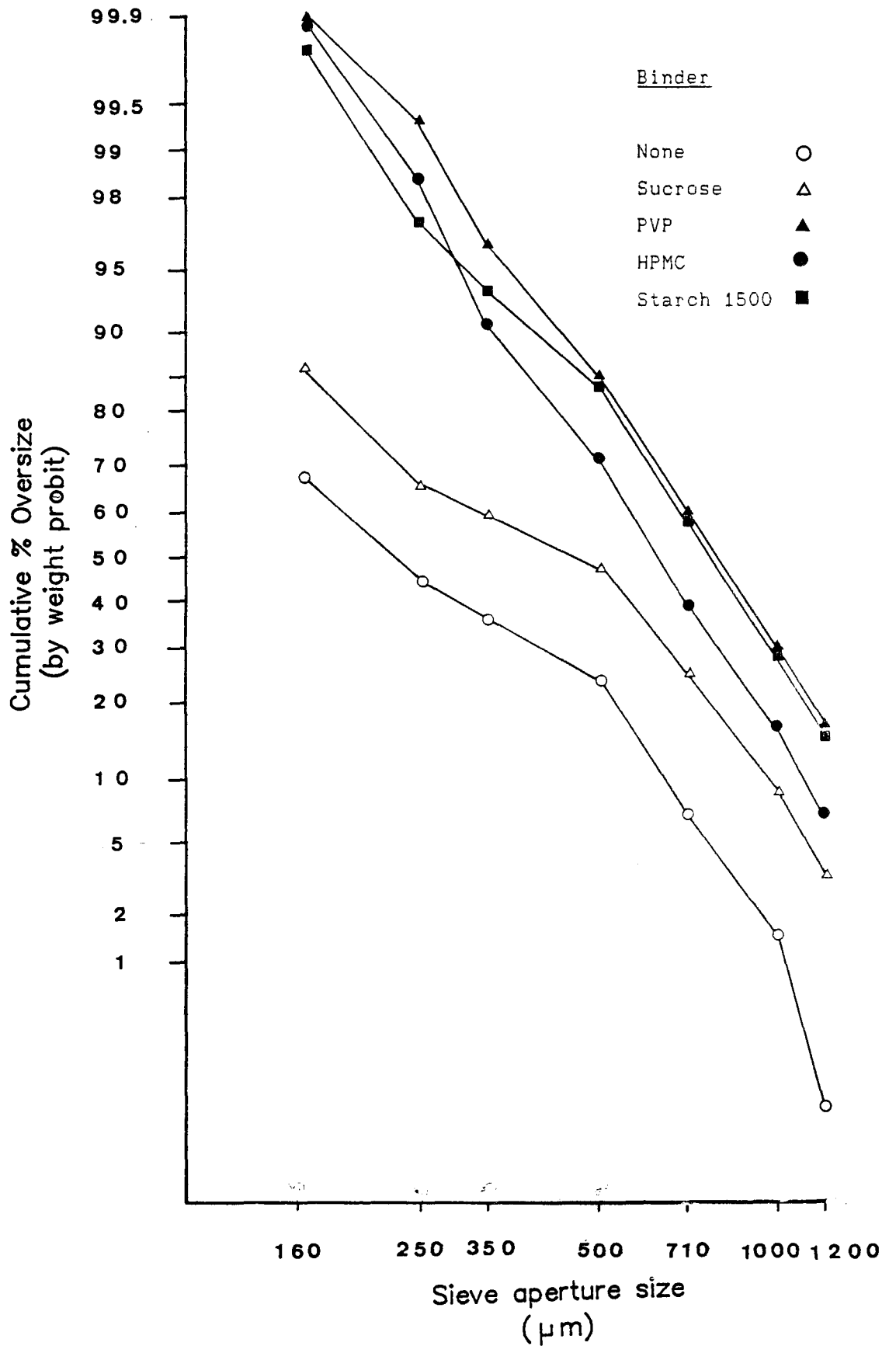


Table 5.3 The Influence of Binder Type on Mean Granule Size

Binder	Geometric Mean Granule Diameter By Weight (50% probit) μm	
	Paracetamol	Dicalcium Phosphate
Water	530.8	223.8
+ 1.03% PEG 200	540.2	218.7
Sucrose	616.5	455.8
HPMC	660.9	630.9
+ 30% PEG 200	670.5	641.0
PVP	724.4	783.6
+ 15% PEG 200	735.3	770.0
Starch 1500	741.3	766.8
+ 30% Glycerol	724.4	755.5

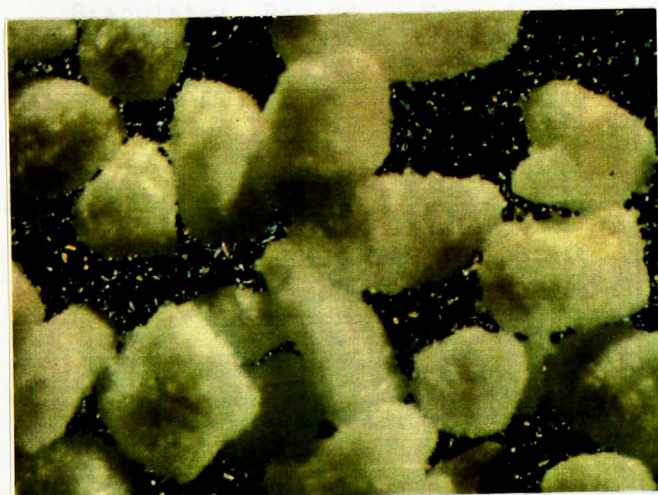
Granulations prepared by massing with sucrose were significantly larger but still had a high proportion of fines. Of the granulation prepared with the polymeric binders, those containing HPMC consistently had a smaller mean diameter than those prepared with PVP or Starch 1500. The proportion of fines, which was very low, was similar for all three polymeric binders. PVP-massed granulations exhibited a higher proportion of large granules than the other binders.

The incorporation of a plasticizer (PEG 200 for HPMC or PVP and glycerol for Starch 1500) in the granulating solutions produced no significant change in the size distribution. Mean granule diameters given in Table 5.3 for granulates containing the maximum level of plasticizers illustrate the lack of influence of plasticizer. Likewise, the incorporation of PEG 200 in the absence of binder had no effect on the mean granule size compared with granules prepared by massing with water alone. Whilst PEG 200 could act as a cosolvent for paracetamol, and increase the probability of secondary binding, the magnitude of the effect was insignificant in this case.

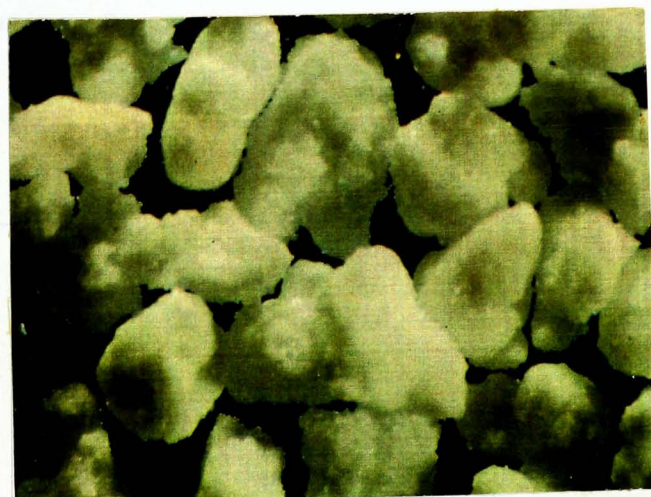
5.4.1.4 Granule Morphology

Figures 5.6a-d illustrate the morphology of paracetamol and dicalcium phosphate granules manufactured by wet-massing. Photomicrographs were taken of granules from the $>500\mu\text{m}$ $<750\mu\text{m}$ sieve fraction for granules prepared by massing with water alone (Figs. 5.6a and c) or with HPMC as binder (Figs. 5.6b and d). The presence of friabraded fines is evident for paracetamol granules prepared by massing with water alone (Fig. 5.6a). Incorporation of a binder resulted in the virtual elimination of fines as shown by the photomicrograph (Fig. 5.6b) and confirmed by the granule size distributions.

Figure 5.6 Granular Morphology $>500\mu\text{m}$ $<750\mu\text{m}$ Sieve Fraction



a. Paracetamol Granules
(binder : water)



b. Paracetamol Granules
(binder: HPMC)



c. Dicalcium Phosphate Granules
(binder: water)



d. Dicalcium Phosphate Granules
(binder: HPMC)

Granule morphology, i.e. shape, size distribution and rugosity, may influence granule handling properties such as packing and flowability. Bulk densities, loose packed and limiting tapped, and the percentage compressibility for the granulates are given in Table 5.4. The presence of plasticizer in the binder had no significant influence on granule bulk properties as can be seen by comparing results for granules prepared with plasticized binder and unplasticized binder. The influence of granulation on bulk properties was, however, dependent on the substrate and on the nature of the binder used.

Table 5.4 Bulk Densities and For Test Granulates

Granulate/ Binder	Paracetamol			Dicalcium phoshate		
	Poured bulk density gcm ⁻³	Tapped bulk density gcm ⁻³	Consolidation %	Poured bulk density gcm ⁻³	Tapped bulk density gcm ⁻³	Consolidation %
Water	0.406	0.600	32.33	1.301	1.705	23.69
+ 1.03% PEG 200	0.408	0.605	32.56	1.295	1.700	23.82
Sucrose	0.407	0.557	26.93	1.022	1.358	24.74
PVP	0.448	0.529	15.31	0.905	1.076	15.94
+ 15% PEG 200	0.445	0.535	16.82	0.895	1.060	15.56
HPMC	0.436	0.509	14.34	0.862	1.016	15.15
+ 30% PEG 200	0.431	0.506	14.82	0.854	1.015	15.86
Starch 1500	0.440	0.508	13.38	0.849	1.010	15.94
+ 30% glycerol	0.438	0.505	13.26	0.845	1.008	16.17

Paracetamol granulates prepared with water or with sucrose as binder had a lower poured bulk density than those prepared with any of the polymeric binders. Limiting tapped bulk densities were, however,

considerably higher. In contrast dicalcium phosphate granulated with water or with sucrose as binder had a higher poured bulk density and a much higher limiting tapped bulk density than granulates prepared with the polymeric binders. The large values for the percentage consolidation recorded in Table 5.4 indicated that granulates of dicalcium phosphate and paracetamol massed with water or with sucrose as binder were cohesive with consequential poor flowability. This can be attributed to the high proportion of fines present.

Both the poured bulk and the tapped bulk densities of granules prepared with PVP were higher than for granules prepared with HPMC or Starch 1500. This trend was evident both for paracetamol and dicalcium phosphate. Percentage consolidation for all granules prepared using the polymeric binders were significantly lower than those for water or sucrose. Flowability of these granules would, therefore, be considerably better than for granules prepared without a binder or with sucrose as the binder.

5.4.1.5 Granule Moisture Content

Table 5.5 shows the equilibrium moisture contents for the test granulates conditioned at 22.5% RH and 59.5% RH. Moisture contents were determined by drying to constant weight in a vacuum oven at 30°C over phosphorus pentoxide. The relatively low drying temperature was selected to minimise potential loss of any plasticizer present. The volatility of both PEG 200 and glycerol is, however, low.

The results were calculated from five replicate granule samples of about 2g mass, accurately weighed. The moisture contents of the simple aqueous-massed granules was low reflecting the low equilibrium moisture uptake of the base substrates. Where a binder was included, the equilibrium moisture content of the granules clearly reflected the relative moisture affinity of the binder used. The rank order for granule moisture content thus followed the rank order for binder moisture content shown in the equilibrium moisture content profiles for binder alone shown earlier in Fig. 3.4. The influence of plasticizer inclusion on the equilibrium moisture content was less evident, probably because the highest plasticizer level used only contributed 1.03% of the total granule mass.

Table 5.5 Equilibrium Moisture Contents of Test Granulates

Binder / Plasticizer System	Equilibrium Moisture content (%)			
	Paracetamol		Dicalcium Phosphate	
	22.5% RH	59.5% RH	22.5% RH	59.5% RH
Water	0.10	0.25	< 0.10	0.15
+ 1% PEG 200	0.18	0.33	0.15	0.27
Sucrose	0.10	0.29	0.13	0.19
PVP				
+ 0% PEG 200	0.34	0.92	0.30	0.83
+ 5% PEG 200	0.32	0.93	0.28	0.79
+ 10% PEG 200	0.29	0.90	0.31	0.82
+ 15% PEG 200	0.38	0.99	0.33	0.87
HPMC				
+ 0% PEG 200	0.16	0.46	0.15	0.37
+ 10% PEG 200	0.18	0.39	0.15	0.30
+ 20% PEG 200	0.15	0.45	0.12	0.35
+ 30% PEG 200	0.18	0.49	0.20	0.44
Starch 1500				
+ 0% Glycerol	0.26	0.62	0.24	0.52
+ 10% Glycerol	0.25	0.59	0.20	0.52
+ 20% Glycerol	0.31	0.67	0.29	0.67
+ 30% Glycerol	0.39	0.91	0.41	0.82

Generally it appeared that the inclusion of plasticizer produced little change in the granule moisture content. The plasticizers used, i.e. PEG 200 and glycerol, are themselves relatively hygroscopic and might be expected to increase moisture sorption into the granulate. However, the potential for interaction between plasticizer and polymer may lead to mutual masking of potential binding sites for water. Okhamafe and York (1984) demonstrated a decreased moisture affinity

for HPMC with increasing content of PEG 400 up to a level of 15% of PEG. Above 15%, PEG 400 inclusion resulted in an increase in moisture uptake. Whilst the inclusion of PEG 200 in HPMC and PVP granulates showed no significant trends, incorporation of glycerol in Starch 1500 granulates indicated a small consistent shift to higher moisture contents. This trend may reflect the limited compatibility of Starch 1500 and glycerol such that free glycerol existing within the binder film is available to bind moisture within the film. Glycerol has been described as a "humectant plasticizer" for starch films (Davidson, 1983).

5.4.2 Tablet Properties

Properties of the tablets produced by compression of the test granulates are given in Tables 5.6 to 5.9. Results are presented as friability (percentage weight loss) and as diametral tensile strength (MPa). Where any tablets failed completely, i.e. capped or laminated during the friability test, friability was recorded as 100%. Tablets capping or laminating on ejection from the die were recorded as laminators and were not subjected to the diametral crushing test. Standard deviations for tensile strength (mean of ten determinations) were in the range 0.10 to 0.15 MPa giving coefficients of variation as high as 20% for the weakest tablets and as low as 5% for the strongest tablets. Generally coefficients of variation were around 10%. Weight uniformity for tablets formed from granules containing the polymeric binders was excellent (coefficients of variation were all less than 3%) reflecting the flowability of these granules. Variability was greater for water and sucrose massed granulates but still fell within the British Pharmacopoeia limits for weight uniformity.

Examination of the results indicated that the behaviour observed was dependent on the nature of the substrate, the nature of the binder, the moisture content of the granulate, and the level of plasticizer. A number of consistent trends were identified, and these are discussed in the following sections.

Table 5.6 Effect of Conditioning Humidity and Plasticization on Tablet Properties (water and sucrose binder)

Binder + Plasticizer	Compaction Pressure (MPa)					
	150		250		350	
	%F	TS	%F	TS	%F	TS
Paracetamol						
Water						
22.5% RH	Lamination	Lamination	Lamination	Lamination	Lamination	Lamination
59.5% RH	Lamination	Lamination	Lamination	Lamination	Lamination	Lamination
Water + 1% PEG 200						
22.5% RH	Lamination	Lamination	Lamination	Lamination	Lamination	Lamination
Sucrose						
22.5% RH	Lamination	Lamination	Lamination	Lamination	Lamination	Lamination
59.5% RH	5.38	1.29	Lamination	Lamination	Lamination	Lamination
Dicalcium phosphate						
Water						
22.5% RH	100	0.44	7.14	1.19	4.23	1.87
59.5% RH	100	0.78	6.76	1.29	4.18	1.97
Water + 1% PEG 200						
22.5% RH	100	0.51	6.21	1.21	3.95	1.96
Sucrose						
22.5% RH	100	0.46	100	0.94	3.79	1.60
59.5% RH	100	0.72	100	0.99	3.89	1.61

Notes:

%F = Friability (% weight loss)

TS = Diametral tensile strength

Lamination refers to lamination or capping occurring on ejection

100% Friability refers to lamination or capping during testing

Table 5.7 Effect of Conditioning Humidity and Plasticization on Tablet Properties (PVP binder)

Binder + Plasticizer	Compaction Pressure (MPa)					
	150		250		350	
	%F	TS	%F	TS	%F	TS
Paracetamol						
22.5% RH						
PVP + 0% PEG 200	2.32	1.34	Lamination	Lamination		
+ 5% PEG 200	2.30	1.72	Lamination	Lamination		
+ 10% PEG 200	1.95	2.06	1.96	2.41	2.10	2.66
+ 15% PEG 200	1.73	2.00	1.72	2.66	1.98	3.12
59.5% RH						
PVP + 0% PEG 200	2.23	1.74	2.35	2.40	2.40	2.94
+ 5% PEG 200	1.76	2.11	1.94	2.62	2.22	3.10
+ 10% PEG 200	1.73	2.24	1.74	2.64	1.74	3.27
+ 15% PEG 200	1.42	2.07	1.55	2.60	1.64	3.09
Dicalcium phosphate						
22.5% RH						
PVP + 0% PEG 200	2.75	1.36	1.82	2.31	1.40	3.32
+ 5% PEG 200	2.63	1.28	1.91	2.03	1.28	3.00
+ 10% PEG 200	2.34	1.21	1.90	1.82	1.29	2.89
+ 15% PEG 200	1.63	1.05	1.54	1.74	1.16	2.69
59.5% RH						
PVP + 0% PEG 200	2.32	1.48	1.52	2.22	1.14	3.29
+ 5% PEG 200	1.91	1.33	1.65	2.08	1.23	3.04
+ 10% PEG 200	1.96	1.25	1.53	1.91	1.20	2.92
+ 15% PEG 200	1.45	1.09	1.27	1.71	1.01	2.90

Notes: %F = Friability (% weight loss)
 TS = Diametral tensile strength
 Lamination refers to lamination or capping occurring on ejection

Table 5.9 Effect of Conditioning Humidity and Plasticization on Tablet Properties (HPMC binder)

Binder + Plasticizer	Compaction Pressure (MPa)					
	150		250		350	
	%F	TS	%F	TS	%F	TS
Paracetamol						
22.5% RH						
HPMC + 0% PEG 200	3.12	1.41	3.44	1.99	Lamination	
+ 10% PEG 200	2.80	1.54	2.87	2.06	Lamination	
+ 20% PEG 200	1.95	1.20	1.92	1.68	2.24	1.98
+ 30% PEG 200	1.91	1.09	1.89	1.47	2.10	1.82
59.5% RH						
HPMC + 0% PEG 200	2.89	1.52	1.88	2.00	2.98	1.95
+ 10% PEG 200	2.45	1.29	2.48	1.80	2.14	2.23
+ 20% PEG 200	1.85	1.33	1.84	1.67	2.09	1.90
+ 30% PEG 200	1.67	1.12	1.65	1.37	1.74	1.57
Dicalcium phosphate						
22.5% RH						
HPMC + 0% PEG 200	5.36	0.87	3.93	1.50	2.67	2.30
+ 10% PEG 200	5.37	0.91	3.16	1.59	2.35	2.19
+ 20% PEG 200	4.56	0.80	3.14	1.35	2.29	1.94
+ 30% PEG 200	4.37	0.62	3.14	1.13	2.23	1.62
59.5% RH						
HPMC + 0% PEG 200	5.37	1.29	3.50	1.90	2.36	3.10
+ 10% PEG 200	5.17	1.25	3.78	1.88	2.04	3.01
+ 20% PEG 200	4.00	1.09	2.87	1.69	2.02	2.14
+ 30% PEG 200	3.08	1.00	2.53	1.24	1.69	1.89

Notes: %F = Friability (% weight loss)
 TS = Diametral tensile strength
 Lamination refers to lamination or capping occurring on ejection

Table 5.9 Effect of Conditioning Humidity and Plasticization on Tablet Properties. (Starch 1500 binder)

Binder + Plasticizer	Compaction Pressure (MPa)					
	150		250		350	
	%F	TS	%F	TS	%F	TS
Paracetamol						
22.5% RH						
Starch 1500 + 0% Glycerol	Lamination		Lamination		Lamination	
+ 10% Glycerol	Lamination		Lamination		Lamination	
+ 20% Glycerol	3.19	1.45	Lamination		Lamination	
+ 30% Glycerol	2.72	1.23	3.03	1.52	Lamination	
59.5% RH						
Starch 1500 + 0% Glycerol	Lamination		Lamination		Lamination	
+ 10% Glycerol	3.55	1.33	Lamination		Lamination	
+ 20% Glycerol	3.17	1.35	3.57	1.56	Lamination	
+ 30% Glycerol	2.69	1.18	2.81	1.39	2.97	1.30
Dicalcium phosphate						
22.5% RH						
Starch 1500 + 0% Glycerol	3.35	1.47	2.19	2.48	1.48	3.78
+ 10% Glycerol	2.89	1.39	1.97	2.35	1.50	3.44
+ 20% Glycerol	2.81	1.33	2.09	2.07	1.44	3.31
+ 30% Glycerol	2.22	1.12	1.56	2.03	1.23	2.77
59.5% RH						
Starch 1500 + 0% Glycerol	3.01	1.90	2.11	3.25	1.46	4.43
+ 10% Glycerol	3.06	1.90	1.74	3.11	1.44	4.00
+ 20% Glycerol	2.61	1.36	1.63	2.03	1.22	3.16
+ 30% Glycerol	1.95	1.01	1.42	2.01	1.09	2.68

Notes: %F = Friability (% weight loss)
 TS = Diametral tensile strength
 Lamination refers to lamination or capping occurring on ejection

5.4.2.1 Substrate-Dependent Differences

Differences between the compression behaviour of dicalcium phosphate and paracetamol was evident from the results shown in Table 5.6. Paracetamol granulated with water alone (or with the inclusion of 1.03% PEG 200) failed to form coherent tablets at the compaction pressures investigated. All tablets failed by lamination or capping on ejection from the die due to the disruptive effects of elastic strain recovery. Increasing the moisture content of the granulate by equilibration at 59.5% RH rather than 22.5% RH had no beneficial effect and lamination was observed as before. Dicalcium phosphate, in contrast, formed tablets within the range of compaction pressures investigated. As tensile strength increased with compaction pressure, so the friability was decreased. Inclusion of 1.03% PEG 200 in dicalcium phosphate granules or increasing the granulate moisture content by equilibration at 59.5% RH resulted in a small increase in tablet tensile strength and a decrease in friability. In the latter case the presence of small amounts of liquid, either PEG 200 or sorbed water, probably acted to smooth out surface microrugosity on particle surfaces. The true area of interparticulate contact would therefore be increased and the effective interparticulate separation decreased (Rumpf, 1958). These factors result in increased van der Waal's forces at equivalent compaction pressures with concurrent increase in compact strength and reduced friability.

5.4.2.2 Binder-Dependent Differences

Binder-dependent differences in compression behaviour for the two substrates was evident from the results presented in Tables 5.6 to 5.9. Paracetamol granulated with sucrose or Starch 1500 failed to form satisfactory tablets irrespective of the granule moisture content. Granulations prepared by wet-massing with HPMC and equilibrated at 22.5% RH formed satisfactory tablets without capping or lamination at compaction pressures up to 250MPa but laminated above this. PVP-massed granulates also formed coherent tablets at pressures up to 150MPa but higher compaction pressures induced lamination. Equilibration of HPMC and PVP granulations at 59.5% RH produced several significant changes in compaction performance. In both cases the pressure at which lamination occurred was elevated such that

coherent tablets were formed at all pressure in the range 150MPa to 350MPa. At equivalent compaction pressures the higher moisture content granulations gave tablets of a higher tensile strength and a lower friability compared with lower moisture content granules. The tensile strength of paracetamol granulations forming tablets increased with increased compaction up to the limit where lamination occurred. Friability, however, also increased with increased compaction pressure.

Figures 5.7a and 5.7b show the influence of the different binders on the tensile strength and friability respectively of dicalcium phosphate tablets produced from granules equilibrated at 22.5% RH. Incorporation of the crystalline non-film-forming binder sucrose resulted in tablets which were weaker and more friable than those produced by massing with water alone. The polymeric binders, however, produced tablets of a significantly greater tensile strength and enhanced resistance to friabrasion. Increased compaction pressures resulted in an increase in tablet strength and a decrease in friability. The inverse relationship between tensile strength and friability observed for dicalcium phosphate granulates was in contrast to the relationship seen with paracetamol granulates. An apparent dependence of friability on the tablet strength was also implied by the rank correlation of the polymeric binders. Thus Starch 1500-massed and PVP-massed granulations yielded tablets of greater strength than HPMC-massed granulations. Tablets containing HPMC as binder were also significantly more friable.

Trends for the compression characteristics of dicalcium phosphate granulates equilibrated at 59.5% RH were essentially the same as those at 22.5% RH. Tablets formed using sucrose as the binder were weaker and more friable than those prepared by massing with water alone. Tablets containing HPMC as binder were weaker and considerable more friable than those tablets containing PVP or Starch 1500 as binder. Tensile strengths at the higher conditioning humidity were, however, greater and friabilities were correspondingly lower.

Figure 5.7a The Effect of Binder Type on the Tensile Strength
of Dicalcium Phosphate Tablets (22.5% RH)

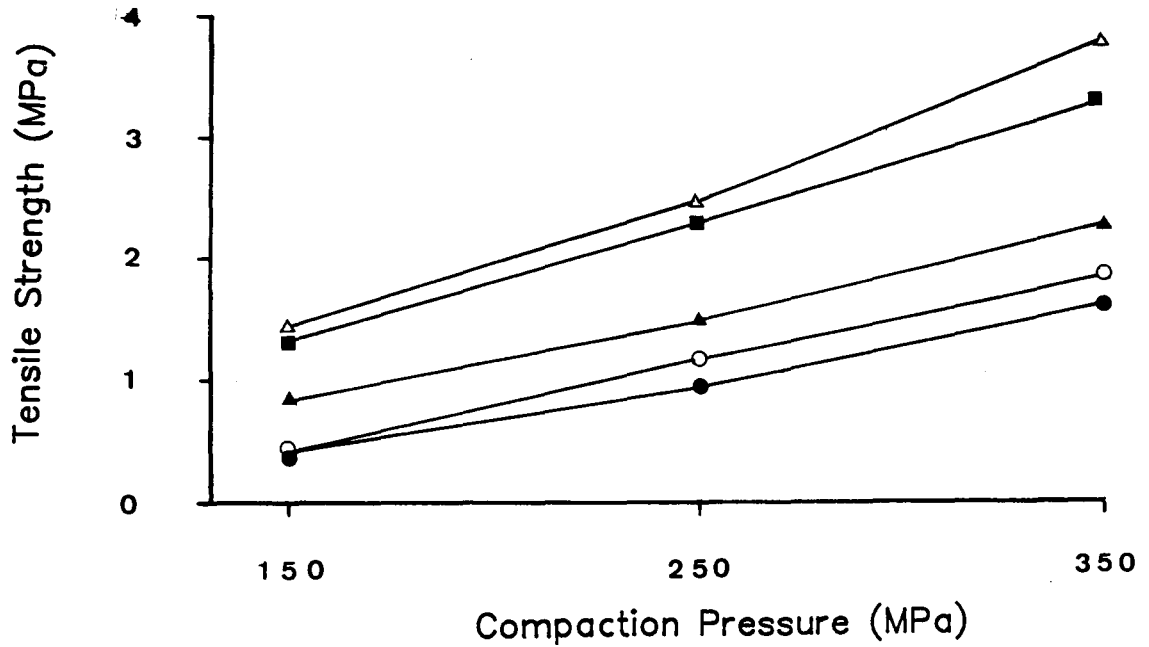
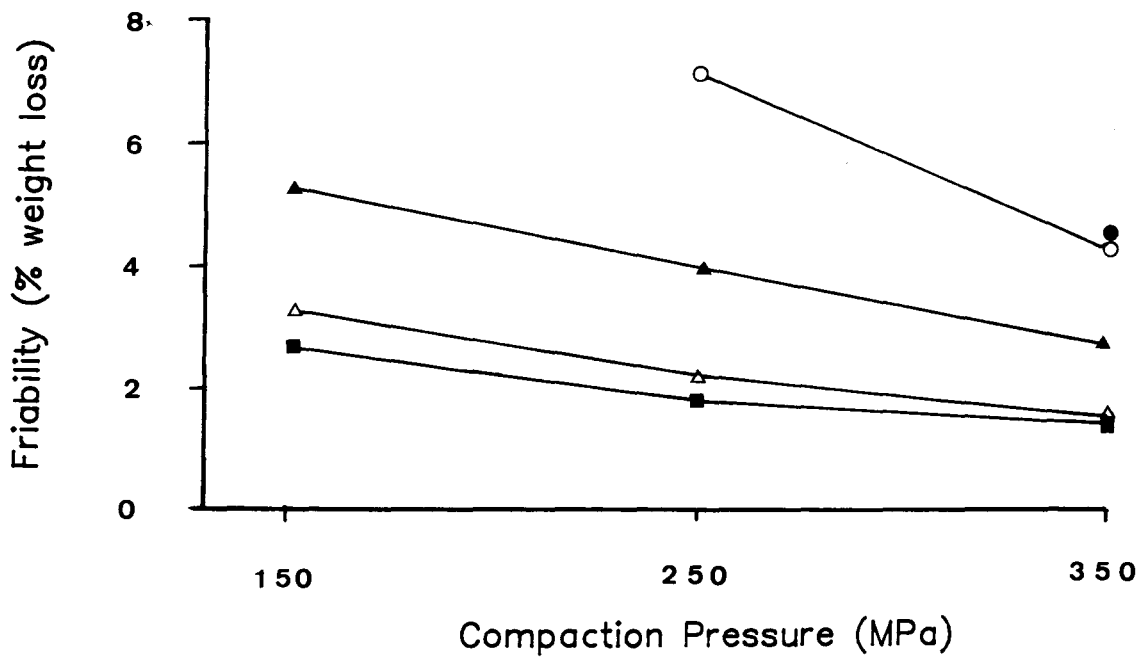


Figure 5.7b The Effect of Binder Type on the Friability
of Dicalcium Phosphate Tablets (22.5% RH)



Binder Type

None ○

Sucrose ●

PVP ■

HPMC ▲

Starch 1500 △

5.4.2.3 The Effect of Binder Plasticization

Inclusion of a plasticizer in the polymeric binder systems resulted in significant changes in the tablettability of the system. In the case of dicalcium phosphate tablets, plasticization of the polymeric binder resulted in tablets which were significantly weaker than those prepared with the unmodified binder. An increase in the level of plasticizer incorporated produced a corresponding decrease in the tensile strength of the tablets produced at all compaction pressures. The trend is illustrated in Fig. 5.8a for dicalcium phosphate-HPMC formulations. Results given in Tables 5.7 and 5.9 show that this behaviour was also exhibited by tablets prepared with plasticized PVP and plasticized Starch 1500 respectively. Results for the friability of the tablets, however, indicated that although binder plasticization produced weaker tablets the tablets were more resistant to friabrasion. This trend, which was consistent for the three polymeric binders, is shown for the dicalcium phosphate-HPMC systems in Fig. 5.9b. Tablets prepared from granules equilibrated at 59.5% RH generally had a greater tensile strength than those prepared from granules equilibrated at 22.5% RH and friability was correspondingly lower.

With paracetamol formulations, plasticization of the polymeric binders produced several significant changes. The most important of these was to facilitate the production of coherent compacts at compaction pressures where, in the absence of plasticizer, lamination had occurred. This was most significant for PVP (Table 5.8) and Starch 1500 (Table 5.10) systems but was also apparent for HPMC (Table 5.9) granulations. With PVP as the binder, increasing plasticizer levels resulted in an increase in the tablet tensile strength for granules conditioned at both storage humidities. An increase in tablet strength was also evident for HPMC at a plasticizer level of 10% by weight. At higher levels, however, tablet strength decreased with plasticizer content as shown in Fig. 5.9a. Plasticizer-mediated increases in tablet diametral tensile strength were not evident with Starch 1500 although satisfactory tablets were only formed at high plasticizer levels. Increased plasticizer level was also associated with a decrease in paracetamol tablet friability for all the polymeric binders, as illustrated for the HPMC-massed granulations in Fig. 5.9b.

Figure 5.8a The Effect of Plasticizer Concentration on the Tensile Strength of Dicalcium Phosphate Tablets Containing HPMC as Binder (22.5% RH)

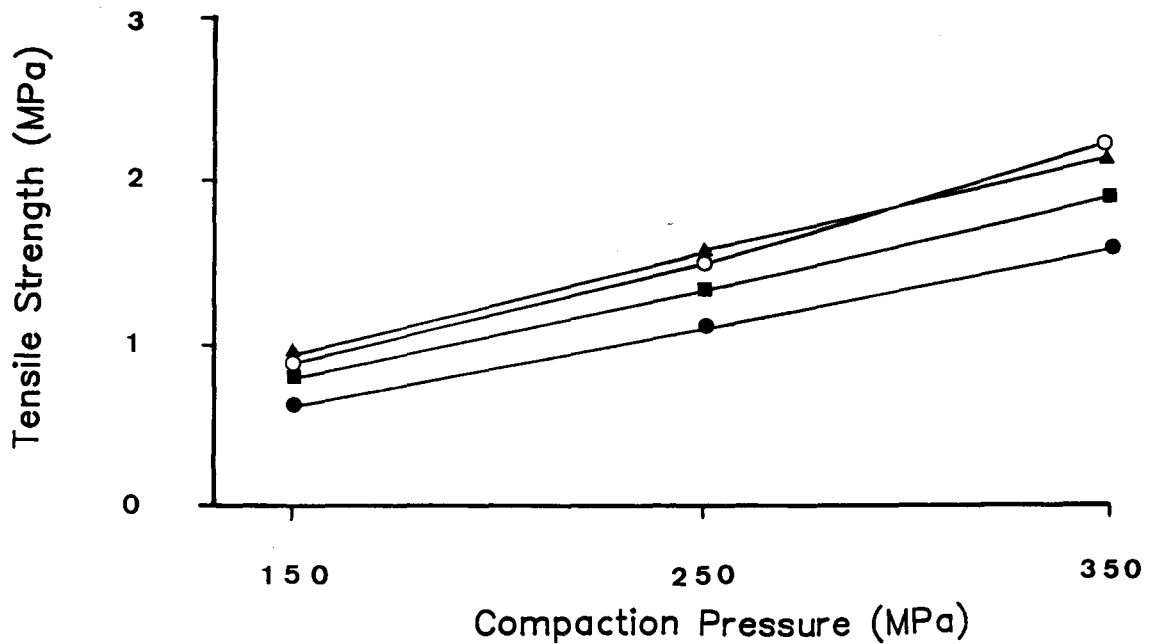
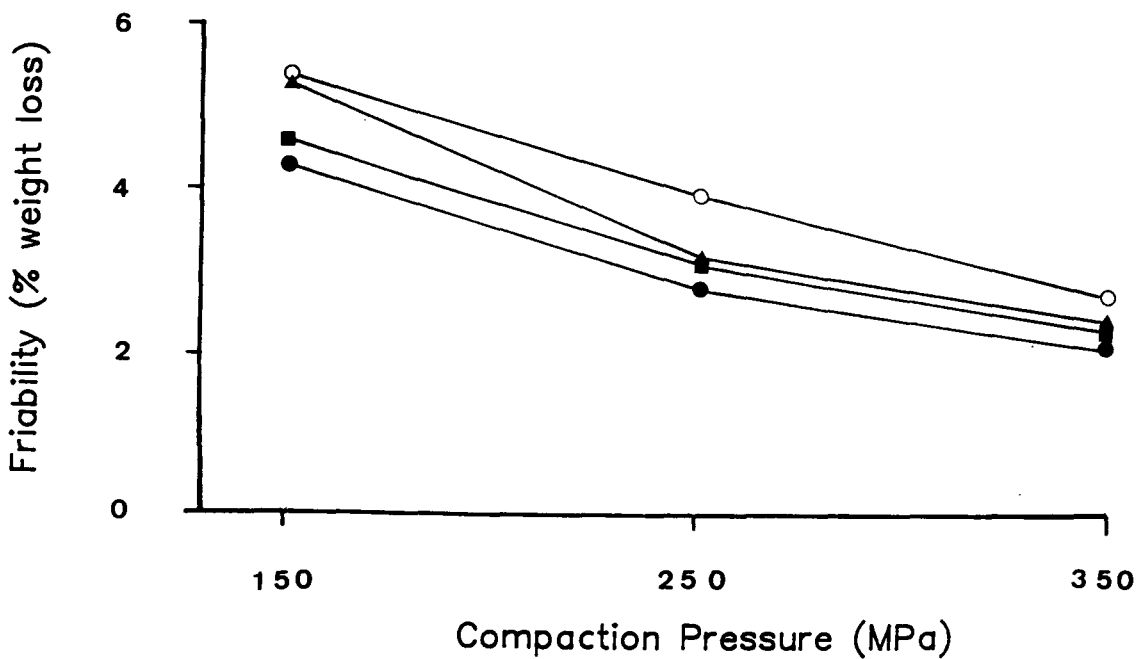


Figure 5.8b The Effect of Plasticizer Concentration on the Friability of Dicalcium Phosphate Tablets Containing HPMC as Binder (22.5% R.H)



Plasticizer Level

PEG 200 0% w/w ○
 PEG 200 20% w/w ■

PEG 200 10% w/w ▲
 PEG 200 30% w/w ●

Figure 5.9a The Effect of Plasticizer Concentration on the Tensile Strength of Paracetamol Tablets Containing HPMC as Binder (22.5% RH)

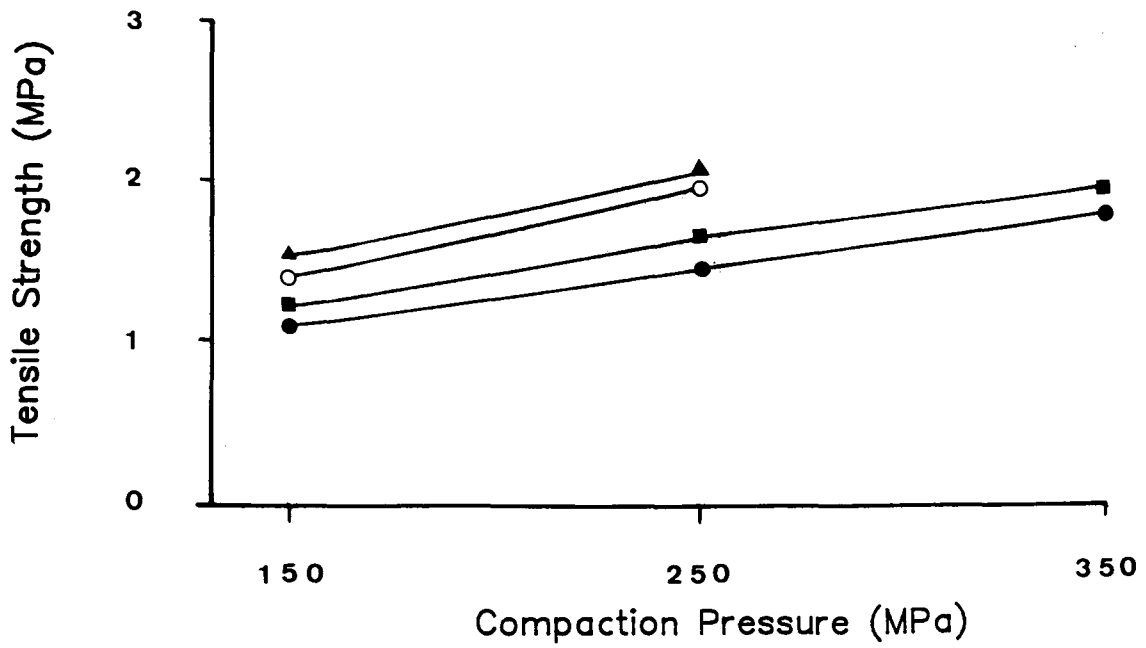
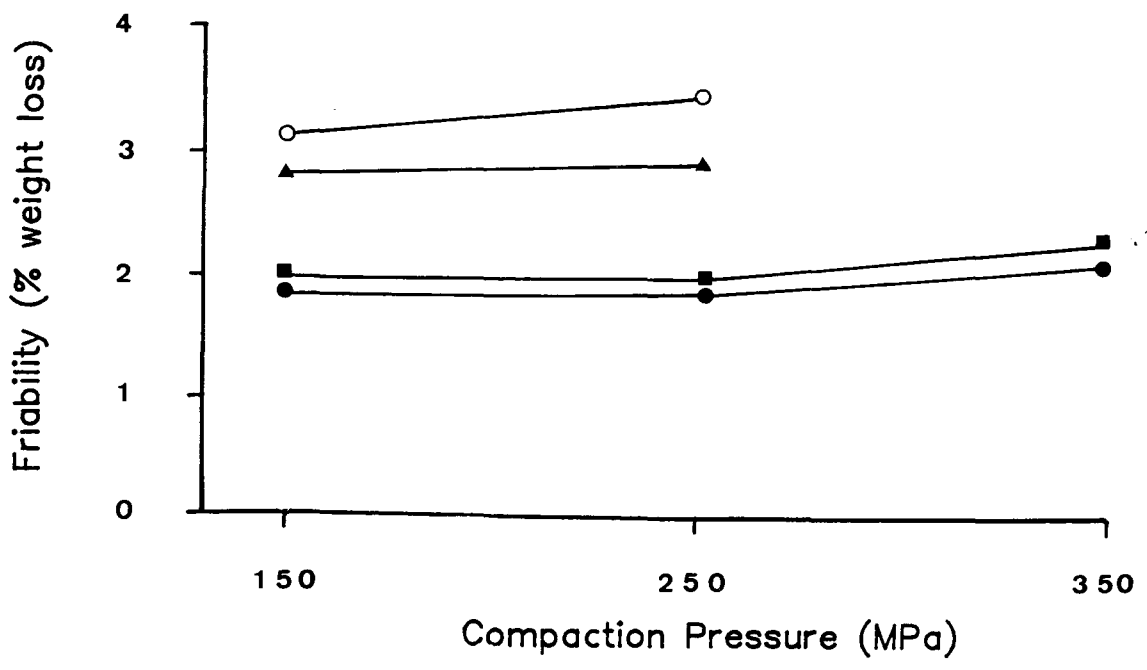


Figure 5.9b The Effect of Plasticizer Concentration on the Friability of Paracetamol Tablets Containing HPMC as Binder (22.5% RH)



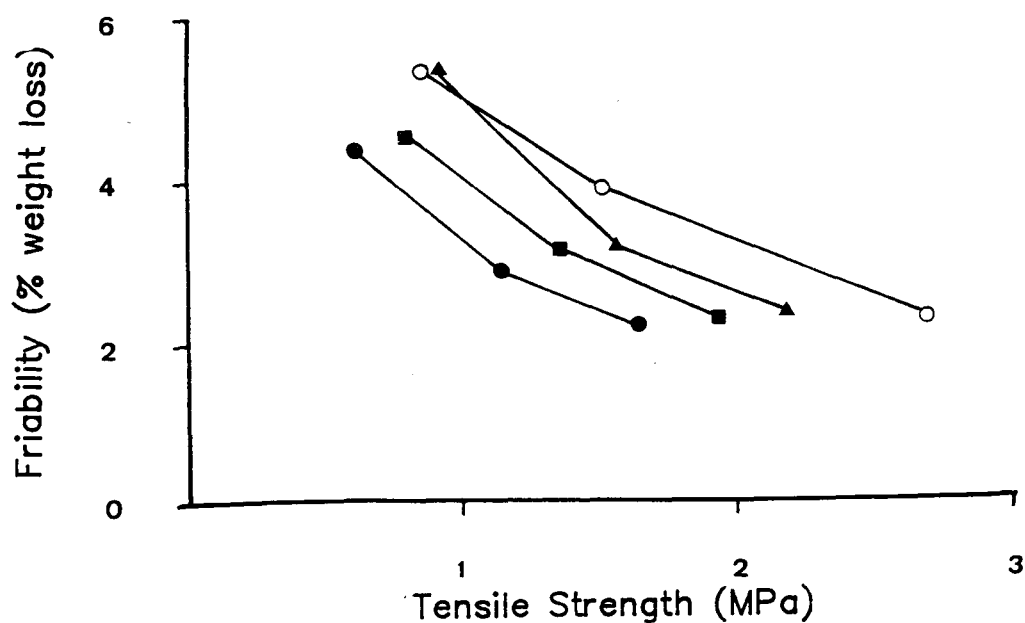
Plasticizer Level

- | | |
|-------------------|-------------------|
| PEG 200 0% w/w ○ | PEG 200 10% w/w ▲ |
| PEG 200 20% w/w ■ | PEG 200 30% w/w ● |

Equilibration of the paracetamol granulates at 59.5% RH resulted in an increase in capping pressure and a decrease in friability, when compared with granulates conditioned at the lower humidity. Effects on the tensile strengths were relatively small and did not follow a consistent trend. The trends observed with increasing plasticizer level generally paralleled those observed at the lower humidity, however.

Figures 5.10 and 5.11 show friability plotted against tablet tensile strength for dicalcium phosphate-HPMC systems and for paracetamol-HPMC systems. These profiles confirm that plasticizer-induced tablet weakness was not associated with an increased friability.

Figure 5.10 Effect of Plasticizer Concentration on Friability Versus Tensile Strength Profiles For Dicalcium Phosphate Containing HPMC as Binder (22.5% RH)



Plasticizer Level

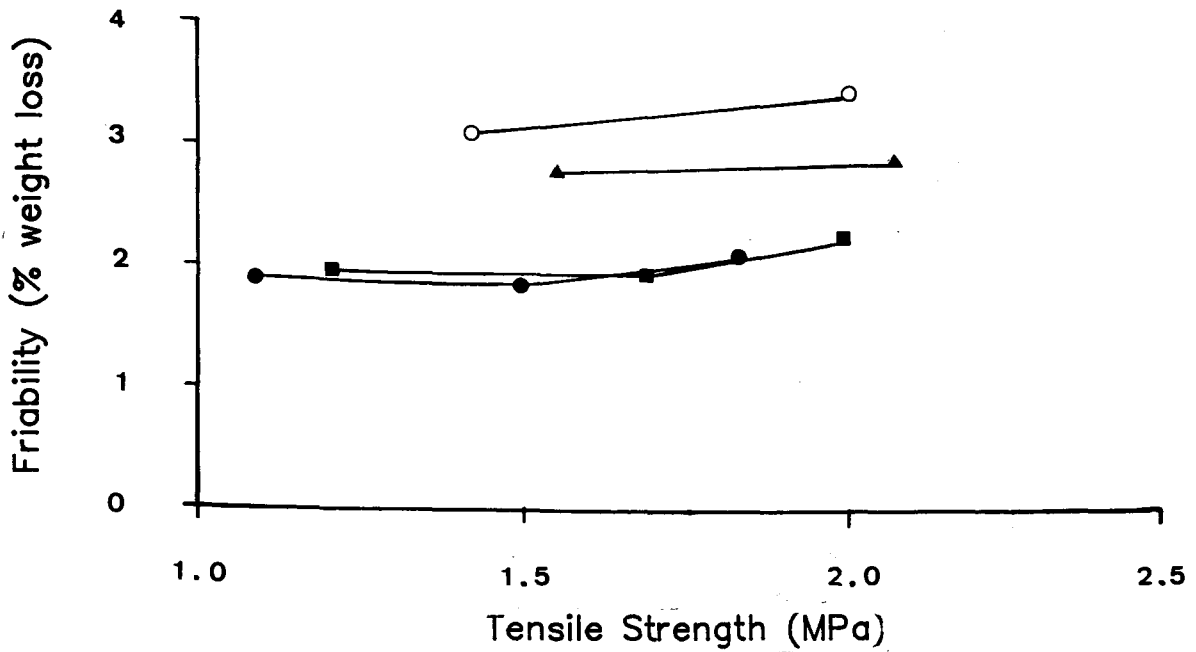
PEG 200 0% w/w ○

PEG 200 10% w/w ▲

PEG 200 20% w/w ■

PEG 200 30% w/w ●

Figure 5.11 Effect of Plasticizer Concentration on Friability Versus Tensile Strength Profiles For Paracetamol Containing HPMC as Binder (22.5% RH)



Plasticizer Level

PEG 200 0% w/w ○

PEG 200 10% w/w ▲

PEG 200 20% w/w ■

PEG 200 30% w/w ●

At equivalent tensile strengths tablets prepared with the plasticized binders were more resistant to impact shock and friabrasion. At any plasticizer level, the friability of dicalcium phosphate tablets decreased with increased tablet strength. With paracetamol, however, this trend was not evident. Friability was either independent of tablet tensile strength or showed a tendency to increase. The latter factor probably represents an increased contribution of debonding elastic strain recovery in paracetamol tablets formed at higher compaction pressures.

5.4.2.4 The Effect of a Low Efficiency Plasticizer

Results shown in Table 5.11 confirmed that the effects observed were due to binder plasticity, rather than a non-specific effect resulting from the inclusion of a low-volatility liquid in the granule formulation.

Table 5.11 The Effect of a Low Efficiency Plasticizer on Tablet Properties (HPMC binder, 22.5% R.H)

Binder + Plasticizer	Compaction Pressure (MPa)					
	150		250		350	
	%F	TS	%F	TS	%F	TS
Paracetamol (22.5% RH)						
+ 20% PEG 200	1.95	1.20	1.92	1.68	2.24	1.98
+ 20% PEG 600	2.80	1.01	2.78	1.34	Laminates	
Dicalcium phosphate (22.5% RH)						
+ 20% PEG 200	4.56	0.80	3.14	1.35	2.29	1.94
+ 20% PEG 600	5.28	0.96	3.80	1.48	2.56	2.79

Notes: %F = Friability (% weight loss)

TS = Diametral tensile strength

PEG 600 had previously been demonstrated to be an inferior plasticizer for HPMC. The effect of PEG 600 inclusion of the properties of the resultant tablets was consistent with reduced binder plasticity. Thus, the inclusion of PEG 600 resulted in paracetamol tablets which were weaker, more friable and with a lower capping pressure than similar tablets prepared using PEG 200 as plasticizer. Dicalcium phosphate tablets prepared with PEG 600 were, in contrast, stronger yet more friable than those prepared with PEG 200.

5.4.2.5 Discussion

A comparison of the tensile strength results for dicalcium phosphate granules equilibrated at 22.5% RH and 59.5% RH appeared, at first inspection, to be anomalous. The higher moisture content of granules equilibrated at 59.5% RH was associated with an increased tensile strength. Moisture sorption has previously been shown to increase

binder plasticity (Chapters three and four). This is associated with decreased tablet tensile strength (Figure 5.8a). Changes in tensile strength due to moisture uptake/loss by re-equilibrium during the storage period between tableting and testing could be discounted, since the compressed tablets were stored at the same relative humidity as the parent granules. The moisture-induced strength increase was most evident for unplasticized binders and at low plasticizer levels. At the higher plasticizer levels the effect was not significant or was absent. The effect was most evident for HPMC granulates, less for Starch 1500 granulates and was virtually eliminated for PVP. Thus, the effect was most significant for binders having the lowest affinity for moisture.

An explanation for the observed effects may be found by considering factors affecting the tensile strength of a tablet and the influence moisture may have on these factors. Within a tablet formed from a granular system containing a polymeric binder, forces contributing to the strength of the compact may be cohesive or adhesive, i.e. acting between identical materials or non-identical materials. At the interface of a substrate particle and the binder film, adhesive forces operate whereas within the binder itself cohesive forces operate. During the tensile testing of a tablet, failure may occur at the adhesive interface or within the cohesive binder film. The tensile strength of the tablet will depend on the weaker of the two. The area over which the bonding force is exerted will also affect the resultant tablet strength.

The presence of moisture in the system will influence both adhesion and cohesion. At the adhesive interface sorbed moisture will act to reduce microrugosity, decrease interparticle separation and increase the true area of contact, with the result that the magnitude of van der Waal's attractive forces is increased. Moisture associated with the polymeric binder, however, results in a decrease in the cohesion of the binder matrix. This is demonstrated by the fall in binder film tensile strength (Chapter three). For unplasticized binders of low moisture affinity, binder cohesion would be high and adhesion might prove to be the limiting factor in the tensile strength of a tablet. Moisture-mediated increase in van der Waal's forces would therefore increase tablet tensile strength. In the case of highly plasticized

binders, binder cohesion would be lower and might be sufficiently low to be the limiting factor in the determination of tablet tensile strength. The ability of sorbed water to plasticize the binding agent and thus further decrease cohesion would then result in tablets of a lower tensile strength. The same considerations also apply to the influence of moisture on the tableting properties of the paracetamol granulates.

Tableting results presented in this chapter show some agreement with the observations of earlier workers. A number of differences exist, however, both in the nature of the effect and in its interpretation. The ability of binder plasticization to increase the strength and capping pressure of paracetamol tablets, substantiates earlier reports (Wells et al., 1982; Krycer et al., 1983). The present work has shown, however, that an optimum level of binder plasticity exists with respect to the tablet strength. Wells et al., (1982) found that while binder plasticization decreased the friability of paracetamol tablets, the magnitude of the effect was independent of plasticizer concentration. This is in contrast with the present observations.

Wells et al., (1982) suggested that the reduction in dicalcium phosphate compact strength with increasing plasticizer level, was due to increased binder deformation at the expense of substrate fragmentation. While this could be true, it is an unsatisfactory explanation of the phenomena observed here. Dicalcium phosphate compacts prepared without binder (where fragmentation during compression would presumably be greatest) were observed to be much weaker than those containing a polymeric binder. Plastic deformation of binder during compression generates a much greater area of true contact between particles, resulting in stronger tablets than those prepared without binder. Doelker and Shotton (1977) have shown, however, that the strength of dicalcium phosphate tablets is also determined by the strength of their granules. Since weaker binders yield weaker granules (Reading, 1983), the reduction in binder strength resulting from plasticization accounts for the fall in compact strength with increased plasticizer levels.

The effect of binder plasticity on the strength of paracetamol tablets has some similarities with the observations of Doelker and Shotton

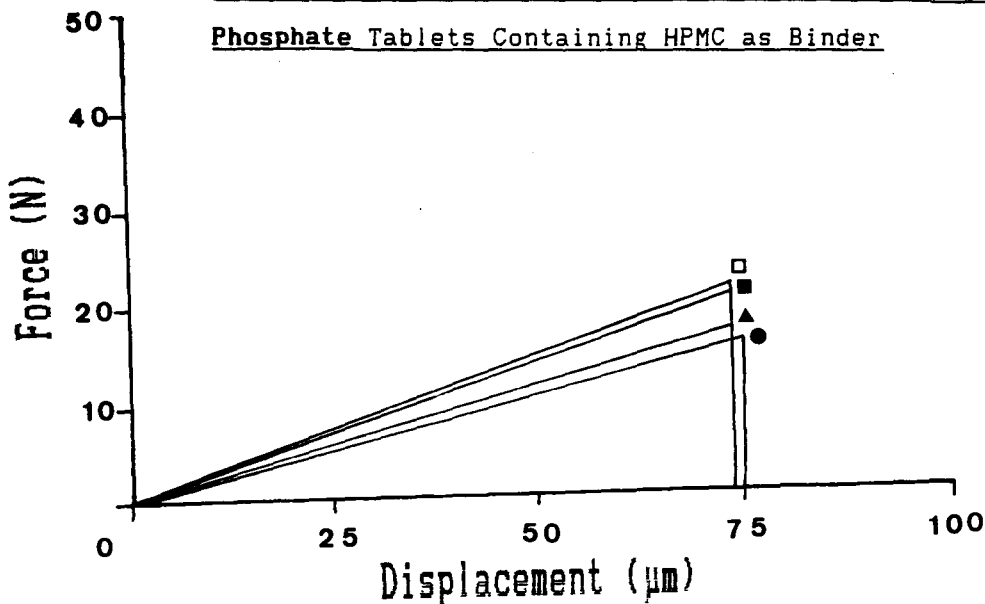
(1977). The latter workers noted that binders yielding the weakest granules gave rise to the strongest tablets of paracetamol. In an analogous manner plasticization, with its resultant weakening of the binder matrix, was associated with an increase in paracetamol tablet strength and a decrease in capping pressure. A significant observation of the present work was the existence of an optimum level of binder plasticization for the paracetamol tablets. Above this level, increasing binder plasticity was associated with decreased tablet strength as observed for dicalcium phosphate tablets. This behaviour suggests that the fundamental behaviour of the binder is essentially the same irrespective of the substrate material. At low levels of binder plasticity, however, the debonding effect of elastic strain recovery in materials like paracetamol is the dominant factor in determining tablet strength. But, when the binder is sufficiently plastic to ensure the persistence of a coherent tablet, then binder strength will directly determine tablet strength.

5.4.3 Tablet Work of Failure - Correlation with Friability

The influence of plasticizer inclusion on the tensile strength and friability of tablets was observed to be qualitatively similar irrespective of the binder used. In an attempt to further interpret these effects, the influence of binder plasticity on tablet toughness or apparent work of failure, was investigated. Tablets formed from the substrates (paracetamol and dicalcium phosphate) granulated with HPMC plasticized with PEG 200 were employed as the model system. The apparent work of failure was determined by integration of the area beneath the diametral compression force versus platten displacement curve (Rees and Rue, 1978). Church and Kennerley (1984) noted that this was not strictly correct since the measurement of deformation should be unidirectional with the failure stress and not perpendicular to it. Nevertheless information of a quantitative nature is obtained.

All plots obtained, irrespective of substrate or plasticizer level showed a linear increase in strain with increasing application of load up to the point of failure. There was no evidence of further plastic flow or of yield in the deformation of the test tablets. This is illustrated for tablets compressed at 150MPa in Figs. 5.12a and b for dicalcium phosphate and paracetamol respectively.

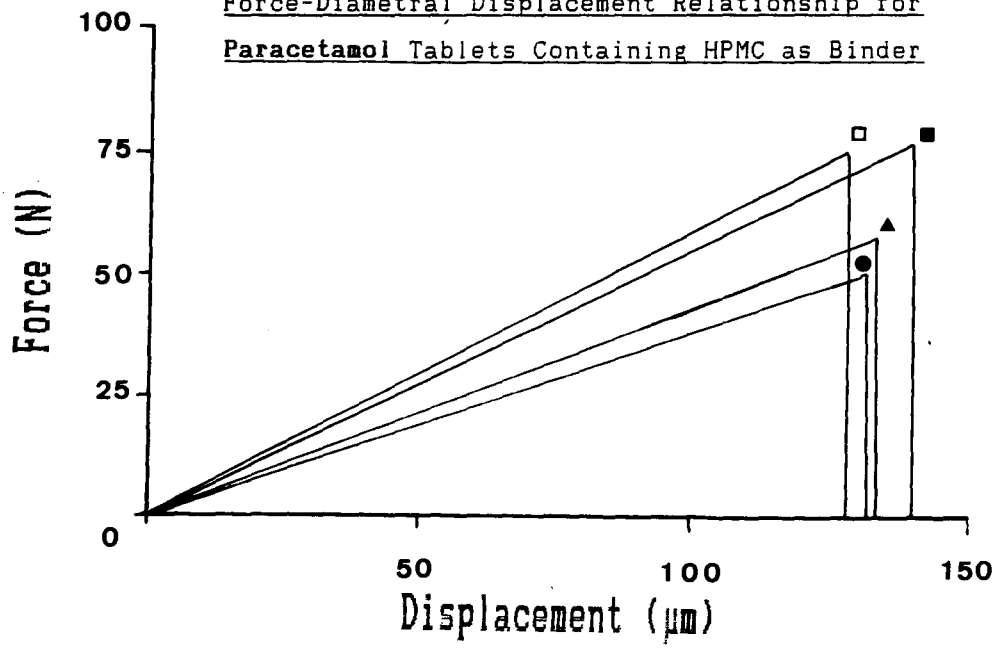
Figure 5.12a Effect of Plasticizer Concentration on the Force-Diametral Displacement Relationship for Dicalcium Phosphate Tablets Containing HPMC as Binder



Plasticizer Concentration

- | | | | |
|-----------------|---|-----------------|---|
| PEG 200 0% w/w | □ | PEG 200 10% w/w | ■ |
| PEG 200 20% w/w | ▲ | PEG 200 30% w/w | ● |

Figure 5.12b Effect of Plasticizer Concentration on the Force-Diametral Displacement Relationship for Paracetamol Tablets Containing HPMC as Binder



Plasticizer Concentration

- | | | | |
|-----------------|---|-----------------|---|
| PEG 200 0% w/w | □ | PEG 200 10% w/w | ■ |
| PEG 200 20% w/w | ▲ | PEG 200 30% w/w | ● |

Church and Kennerley (1984), using a four point bending test, reported similar results for a range of materials irrespective of the nature of deformation during compression.

Results presented in Table 5.11 shows that increased binder plasticity did not result in an increase in tablet toughness for the dicalcium phosphate granules.

Table 5.11 Effect of Conditioning Humidity and Plasticization on Tablet Work of Failure (HPMC Granulates)

		Compaction Pressure (MPa)		
		150	250	350
		Work of Failure (mJ)		
Paracetamol				
22.5% RH				
	+ PEG 200 0%	48.54	81.23	Laminates
	+ PEG 200 10%	53.50	94.32	Laminates
	+ PEG 200 20%	38.45	49.98	65.43
	+ PEG 200 30%	28.44	46.78	49.05
59.5% RH				
	+ PEG 200 0%	54.44	83.40	82.51
	+ PEG 200 10%	48.25	77.65	75.30
	+ PEG 200 20%	39.10	50.10	69.55
	+ PEG 200 30%	36.09	49.02	63.75
Dicalcium phosphate				
22.5% RH				
	+ PEG 200 0%	7.97	15.00	28.56
	+ PEG 200 10%	7.40	13.13	19.40
	+ PEG 200 20%	6.34	10.79	20.28
	+ PEG 200 30%	5.47	9.56	16.14
59.5% RH				
	+ PEG 200 0%	8.19	17.06	35.50
	+ PEG 200 10%	7.98	16.54	30.50
	+ PEG 200 20%	7.75	13.10	26.05
	+ PEG 200 30%	7.54	12.68	19.06

The work of failure of a tablet is a product of tensile strength and of diametral deformation. The reduction in tablet strength, associated with increasing plasticizer content, had a predominant influence on the observed toughness which consequently decreased. In contrast, binder plasticization in paracetamol granulations facilitated an increase in tablet tensile strength and consequently an increase in toughness. Higher plasticizer concentrations which resulted in a decreased tensile strength, however, reduced the apparent toughness. At the higher relative humidity, small increases in work of failure reflected the increase in tablet strength. In all cases, tablets prepared at the higher compaction pressures showed an increase in toughness. This resulted primarily from increased tensile strength and, to a lesser degree, increased diametral displacement at failure. In contrast to the observations of Rees and Rue (1978b), the resistance of the tablets to impact attrition did not correlate with the work expended in causing diametral failure.

All formulations examined exhibited different tensile strengths and different diametral deformations. However, since the diametral strain was observed to increase linearly with applied load, it was possible to compare data directly by calculating a diametral modulus, defined as the slope of the force-displacement plot during diametral compression. Table 5.12 shows that, irrespective of compaction pressure, increasing plasticizer concentration resulted in a lower modulus both for dicalcium phosphate and paracetamol tablet. In contrast, the modulus increased with increasing compaction pressure.

The apparent diametral moduli presented in Table 5.13 represents the diametral stiffness of the formed tablets. It is unlikely that the process of compaction would affect the stiffness of primary substrate particles (although the potential for work-hardening cannot be entirely ignored). It is suggested therefore, that the measured modulus is dependent on two factors. Firstly, the degree of interparticle bonding which occurs during compression and secondly, the mechanical properties of the binder matrix.

Table 5.12 Effect of Conditioning Humidity and Plasticization on the Apparent Diametral Modulus (HPMC Granulates)

Compaction Pressure (MPa)	150	250	350
	Apparent Diametral Modulus (MNm ⁻¹)		
Paracetamol			
22.5% RH			
+ PEG 200 0%	0.59	0.66	Laminates
+ PEG 200 10%	0.55	0.62	Laminates
+ PEG 200 20%	0.43	0.54	0.54
+ PEG 200 30%	0.38	0.51	0.50
59.5% RH			
+ PEG 200 0%	0.56	0.61	0.64
+ PEG 200 10%	0.53	0.58	0.62
+ PEG 200 20%	0.44	0.53	0.51
+ PEG 200 30%	0.35	0.51	0.52
Dicalcium phosphate			
22.5% RH			
+ PEG 200 0%	0.29	0.41	0.51
+ PEG 200 10%	0.28	0.40	0.48
+ PEG 200 20%	0.23	0.37	0.48
+ PEG 200 30%	0.21	0.29	0.39
59.5% RH			
+ PEG 200 0%	0.28	0.40	0.51
+ PEG 200 10%	0.29	0.39	0.47
+ PEG 200 20%	0.22	0.38	0.47
+ PEG 200 30%	0.21	0.28	0.39

In the absence of disruptive elastic decompression effects, the former factor is enhanced by increased compaction pressures resulting in compacts of increased stiffness. Incorporation of a plasticizer, however, reduces the stiffness of polymeric binders (see Chapters three and four). It might be expected that, under certain conditions,

increased binder plasticity may contribute to greater densification and bonding with a resultant increase in compact stiffness. There is some evidence that this occurs for tablets formed at the higher relative humidity.

These results indicate that tablet friability cannot be correlated directly with any single mechanical property of the tablet. The results strongly indicate that resistance to friabrasion is dependent on a balance between strength and stiffness. At low compaction pressures and high plasticizer levels, a low tablet stiffness enables impact to be translated into elastic strain (which may be recovered without bond rupture as illustrated by the influence of binder plasticity on paracetamol capping). At high compaction pressures, increased inter-particulate bond strength evidenced by increased tablet tensile strength, facilitates resistance to impact despite increased compact stiffness. This is less evident for paracetamol, however, because of the greater extent of debonding elastic strain at higher compaction pressures. An analogy may be drawn between the impact resistance of three model materials as indicated in Table 5.13.

Table 5.13 The Influence of Strength and Stiffness on the Impact Resistance of Three Model Materials

Material	Stiffness	Strength	Impact Resistance
Glass	HIGH	LOW	LOW
Steel	HIGH	HIGH	HIGH
Rubber	LOW	LOW	HIGH

If a brittle material is subjected to stress, as a result of a lack of ductility, localised stress concentrations will occur at the site of imperfections or flaws (Griffith, 1920). The magnitude of the

stress will depend on the severity of the flaws and their orientation with respect to the applied stress. When the stress exceeds a critical value for the material, fracture will be initiated and will propagate through the specimen to give failure. Thus, materials such as glass fail readily under impact due to both a low ductility and a low critical failure stress. Similarly, tablets of low ductility and low tensile strength are friable. Materials such as steel, which may have a low degree of ductility, show a much greater resistance to impact due to the high critical failure stress, i.e. an inherent greater strength. Likewise, in the absence of debonding elastic strain recovery, stronger tablets produced at higher compaction pressures show reduced friability despite an increased stiffness. Rubbery materials, although weak, also show a high resistance to impact damage since the impact stress is readily dissipated by elastic strain. Highly plasticized tablet binders reduce tablet friability in a similar manner, since they confer rubbery extensibility in addition to reducing the tensile strength of the tablet.

5.5 Conclusions

The use of the modified Kenwood Gourmet food processor gave good reproducibility for granulation by wet-massing. Production of highly regular granules with a tight size distribution in situ demonstrates that the mixer acted as satisfactory model for a high speed mixer-granulator. Binder-dependent differences in granular morphology were detected but the inclusion of a plasticizer did not result in any further changes. This was explained by the limited effect that the binder inclusion would have on the physical properties of the granulating solution. PEG 200 is a known co-solvent for paracetamol in aqueous systems but, at the level used here, differences in granular morphology due to increased secondary binding (Wells and Walker, 1983) were not detected.

The properties of tablets formed from granulated dicalcium phosphate or paracetamol were found to be dependent, not only on the nature of the substrate material, but also on the plasticity of the binder. Sucrose, included as a crystalline non-film forming control, exhibited very poor binder characteristics for both substrates.

Plasticizer inclusion had significant effects on the mechanical properties of both paracetamol and dicalcium phosphate tablets prepared with polymeric binders. The nature of the effect was, however, substrate dependent. Thus, increasing binder plasticity invariably resulted in a decrease in the tensile strength of dicalcium phosphate tablets. In contrast, increasing binder plasticity could increase the strength of paracetamol tablets, although an optimum was observed above which tensile strength fell. A significant effect of binder plasticization was to facilitate the production of coherent tablets at compaction pressures which, in the absence of plasticizer caused lamination or capping. Further increase in binder plasticity results in the elevation of capping pressure.

Although some binder dependent differences in tablet properties were observed, the effects of binder plasticization were qualitatively similar. This implies that the effects of binder plasticization are mediated via a common physico-mechanical mechanism.

For both dicalcium phosphate and paracetamol tablets, friability was reduced with increasing binder plasticity. This occurred irrespective of whether the tensile strength of the tablet was increased or decreased. This increase in resistance to impact attrition was not simply related to an increase in the work of failure (a measure of the toughness) of the tablets. A model concept to explain the observed friability in terms of a balance between tablet stiffness and tensile strength was proposed.

The effect of increased binder moisture content on the properties of paracetamol tablets was consistent with increased binder ductility. The results for dicalcium phosphate were more ambiguous in terms of tablet crushing strength, although friability was still reduced. Results for dicalcium phosphate could be explained by a moisture-mediated increase in tablet hardness. Within a tablet, moisture may influence polymeric binder cohesion (via its plasticizer effect) and binder-substrate adhesion (by smoothing micro-rugosity to increase bonding area). Discrimination between cohesive tablet failure and adhesive tablet failure was not attempted in the present work. However, it is probable that the net effect on tablet strength will reflect the weaker of the two.

Inclusion of a plasticizer (PEG 200) in the absence of a polymeric binder produced no significant benefits in the properties of resultant tablet (where formed) compared with tablets produced from granules massed with water alone. This constitutes evidence that the influence of the plasticizer is mediated through its influence on the mechanical properties of the binder film. Further evidence that the effects observed reflect binder plasticity, is given by the data presented for control granulations containing a plasticizer of lower efficiency. In the case of paracetamol granulations, tensile strength enhancement and friability decrease were either absent or diminished. In the case of dicalcium phosphate granulations, the resultant tablets were stronger (reflecting the greater strength of the binder film) but resistance to friabrasion was lower.

While binder plasticization clearly does not produce significant effects on granule morphology, there are significant effects on the mechanical properties of the tablets. This must reflect the manner in which the granule responds to compressive stress. Consequently, the influence of binder plasticity on the consolidation, plasticity and elasticity of granulates is investigated in the following chapter.

CHAPTER SIX

COMPRESSION STUDIES

CHAPTER SIX

COMPRESSION STUDIES

6.1 Introduction

The previous chapter reported on the influence of binder and binder plasticity on the physico-mechanical properties of compressed tablets formed from some model granulates. The properties of the tablet will be determined by the deformation and bonding/debonding characteristics of the granulate during compression. Methods for evaluating the deformation behaviour of compressed materials have been reviewed in section 1.2. Frequently, the methods may not be entirely representative of the situation occurring during a real tableting process. Nevertheless, they offer the potential for controlled evaluation of the effect of formulation and process variables on compression behaviour. In the present chapter, a number of techniques have been employed to investigate the effects of binder and binder plasticity on the consolidation, plasticity, and elasticity of model granulates. Compression was carried out using a punch and die set mounted between the plattens of a hydraulic testing machine. The sophisticated control systems of the press enabled accurate control and determination of applied load and upper punch displacement.

6.2 Materials and Methods

6.2.1 Materials

Substrates for the compression studies were paracetamol and dicalcium phoshate. The rationale for their selection was described in Chapter five. The composition, manufacture and conditioning of the test granulates was identical to that described in section 5.3. Granules were prepared either in the absence of a binding agent by wet-massing in the absence of a binder (with water alone or with a solution of PEG 200), or by wet-massing with a binding agent, i.e. HPMC, PVP, Starch 1500 or sucrose. Granules containing PEG 200-plasticized HPMC or PVP and glycerol-plasticized Starch 1500 were prepared to study the influence of binder plasticity on compression behaviour.

6.2.2 Methods

6.2.2.1 The Mayes Press

A Mayes Universal Hydraulic Testing Machine (W. H. Mayes (Windsor) Ltd) was used to study the compaction characteristics of the model granulates. Although not a purpose-built compaction simulator as described, for example, by Hunter et al. (1976), the Mayes press has a number of features which make it particularly useful for compaction studies. Operation of the Mayes Press (Fig. 6.1) was possible in two modes:

- Ram displacement control to maintain constant strain
- Load control to maintain constant stress

Figure 6.1 The Mayes Press



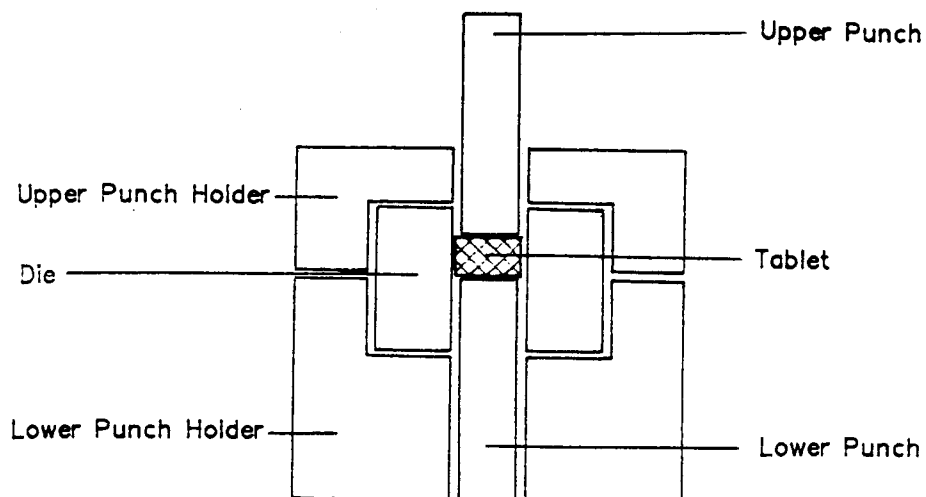
In ram control, strain rates of up to 1000mm min^{-1} were achievable. The ram displacement was monitored by an internal displacement transducer with a minimum stroke of 20mm and a resolution of 0.1%. The analogue output of 0 to -10 volts at full scale could be conditioned using an inverting operational amplifier and attenuated to a level suitable for digitising and logging via the analogue port of the BBC microcomputer. Data logging using the BBC microcomputer has been discussed previously in Chapter Four. Calibration of the displacement transducer was carried out using slip gauges, accurate to $\pm 5\mu\text{m}$, in the range 0 to 20mm. The regression of digital output against displacement was linear (regression coefficient $r > 0.999$) and intercepted at the origin.

In load control loading rates of up to 500kNmin^{-1} were obtainable. Using a 50kN crosshead mounted loadcell (warranted to A1 standard, B.S. 1610, 1957) the maximum load could be attained in 6 seconds. The analogue signal from the loadcell, 0 to -10 volts at full scale, could be conditioned using an inverting operational amplifier and attenuated to a level suitable for digitising and logging via the analogue port of the BBC microcomputer. With load control selected, a feedback loop to the ram servo mechanism enabled a constant load to be applied to the test specimen thus compensating for stress-relaxation which may occur due to time-dependent deformations.

6.2.2.2 The Punch and Die Set

A punch and die set using 10mm round flat-faced punches (I. Holland Ltd, Nottingham) were used in this work (Fig. 6.2). Punch faces and the internal bore of the die were polished prior to use and periodically between runs as necessary. The punches and die were enclosed in a separate aluminium holder which acted to correctly locate punches within the die and to ensure that top punch penetration was normal to the die. The complete assembly was positioned between the ram and the loadcell of the Mayes press. During a compression event the top punch force was monitored by the crosshead loadcell whilst displacement was gauged by the displacement transducer.

Figure 6.2 The Punch and Die Set



6.2.2.3 Consolidation of Granules During Compression

Granules were prepared and conditioned as described previously in Chapter five. Enough material (400mg for paracetamol granulates and 700mg for dicalcium phosphate granulates) to give a compact approximately 4mm thick at theoretical zero porosity was poured into the bottom punch and die assembly and the top punch inserted. Granulates were used unlubricated but in all cases the die bore and punch faces were pre-lubricated using a suspension of magnesium stearate 5% w/v in carbon tetrachloride. The complete assembly was positioned in its holder between the ram and loadcell plattens of the Mayes press.

For the study of consolidation a final upper punch force of 30kN (approximately 380MPa) was programmed in load control at a loading rate of either 500kN min⁻¹ or 50kN min⁻¹ giving theoretical loading times of 3.6 seconds and 36.0 seconds respectively. Granulates were subjected to a pre-load of 1MPa prior to running a compression event in order to provide an unambiguous starting reference. Analogue outputs from the loadcell and the external displacement transducer were conditioned and logged into ADC channels 0 and 1 respectively of

the BBC microcomputer. Software written for data logging with the ICI micro-indenter (Chapter Four) was modified for this purpose. Analogue signals could be sampled and digitised sequentially every 10ms enabling a maximum of 50 load-displacement coordinates to be captured per second. To record a compaction event, the Mayes press was set into compression mode and the output from the loadcell monitored by a software procedure. Data logging continued either until the preset maximum axial load was reached or for a predetermined holding time after reaching maximum load (to investigate consolidation at constant stress). Captured data was then written to disc for analysis.

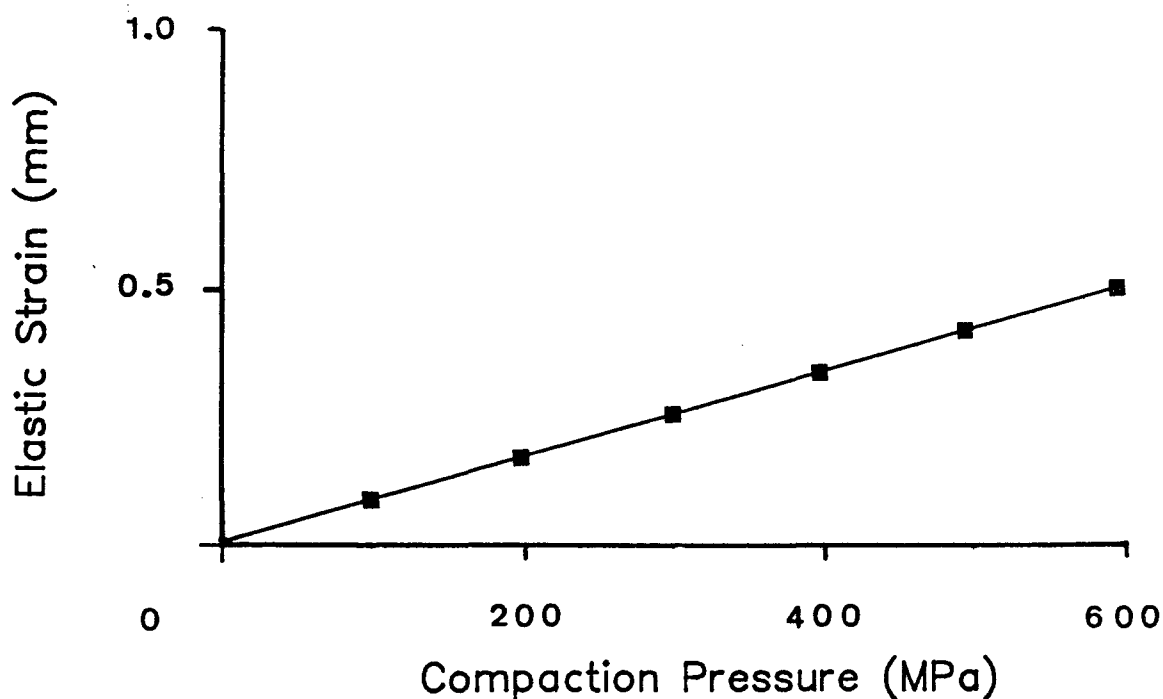
Methods for the study of consolidation have been discussed in a previous section (1.2.2). In the present work force-displacement data captured by microcomputer was analysed using the relationship between compressive pressure and relative density proposed by Heckel (1961). The Heckel approach has some limitations but is widely used and allows quantification of various modes of deformation. By comparing tablet densities at equivalent pressures, the relative deformability of different granulates can be compared. In addition the relative densification can be regarded as an indirect measure of bonding area, since the true area of interparticulate contact will increase as the relative density approaches unity.

The tendency of paracetamol granulations to cap or laminate in the absence of binder or under conditions of low binder plasticity lead to problems in the accurate measurement of post-compression compact dimensions. Heckel plots were consequently derived from tablet dimensions determined under compression (this was adopted as the convention for dicalcium phosphate also for consistency). Fell and Newton (1971) have indicated that the measurement of compact dimensions under pressure will include a contribution due to elastic deformation. This gives an increased value for the derived Heckel function $\ln(1/1-D)$ resulting in a lower mean yield pressure than would be obtained from the dimensions of ejected compacts.

Procedures written into the data logging software enabled rapid conversion of captured parameters to the form of the Heckel relationship. The thickness of a compact at any time during a compaction event was evaluated from the logged ram displacement of

the Mayes press after correction for the elastic deformation of the test rig (Fig. 6.3). Thus, using software constants for the die diameter and the mass of granule in the die, the apparent density was obtained. The relative density D in the Heckel equation is the apparent compact density at any given pressure divided by the solid density at zero porosity. In the absence of facilities for accurate pycnometry it was assumed that the density of compacts compressed for 30 seconds at 50kN (636MPa) was equal to the true solid density. Compressive pressure was obtained from the logged axial force and the punch face area.

Figure 6.3 Elastic Deformation of the Test Rig



6.2.2.4 Stress-relaxation

The stress-relaxation of a material stressed under conditions of constant strain is a function of purely plastic flow without interference from viscoelastic (retarded elastic) strain. Stress-relaxation of compressed granulates was investigated under constant strain using the Mayes press in ram control mode. Granules were prepared and conditioned as before, and a granule mass sufficient to give a compact 4.0mm thick at theoretical zero porosity was employed to enable comparison of equivalent bulk of materials. Granulates were used unlubricated but in all cases the die bore and punch faces were pre-lubricated using a suspension of magnesium stearate 5% w/v in carbon tetrachloride.

The ram displacement was programmed to achieve the required maximum upper punch pressure at strain rates of either 1000mm min⁻¹ or 100mm min⁻¹. To record a compaction event, the Mayes press was set into compression mode and the output from the loadcell monitored by a software procedure. The first detectable load in excess of 1MPa initiated logging of axial force and time. Compression was automatically halted at the preset upper punch pressure and the decay in axial force was recorded for a further 100 seconds. Captured data was then written to disc for analysis.

Data captured by the BBC microcomputer was converted to residual stress-elapsed time profiles. The relaxation of the empty punch and die set compressed between the ram platten and crosshead loadcell to a peak stress of 150MPa was also recorded. The decay in axial stress with time was small, i.e. of the order of 2 - 3% after 100s, indicating the relative mechanical stiffness of the Mayes press-punch and die set. Nevertheless, stress-relaxation data for the test granulates was corrected for the relaxation of the test rig before data analysis.

6.2.2.5 Elastic Strain Recovery

Axial elastic strain recovery was determined within the die immediately after decompression. Granules were prepared and conditioned as before, and a granule mass sufficient to give a compact

4.0mm thick at theoretical zero porosity was employed to enable comparison of equivalent bulk of materials. Granulates were used unlubricated but in all cases the die bore and punch faces were pre-lubricated using a suspension of magnesium stearate 5% w/v in carbon tetrachloride.

The ram displacement was programmed to give a maximum upper punch pressure of 150MPa at a strain rate of either 1000mm min⁻¹ or 100mm min⁻¹. To record a compaction event, the Mayes press was set into compression mode and the output from the loadcell and displacement transducer logged by the BBC microcomputer. Release of the compaction load was initiated manually as soon as the maximum upper punch pressure had been achieved. In all cases, the dwell period between achieving maximum pressure and release of pressure was less than one second. The axial elastic recovery of the tablet was determined from the upper punch displacement when the upper punch pressure had decayed to a reference value of 1MPa.

Data captured by the BBC microcomputer were reduced to the form of compaction pressure-displacement profiles which were stored on disc. Using a software procedure, the tablet thickness at 150MPa compaction pressure was evaluated from the displacement data. Similarly, the tablet thickness after axial elastic strain recovery was evaluated when the upper punch pressure had decayed to a reference value of 1MPa. Displacement data was corrected for deformation and recovery of the test rig to give accurate tablet thicknesses.

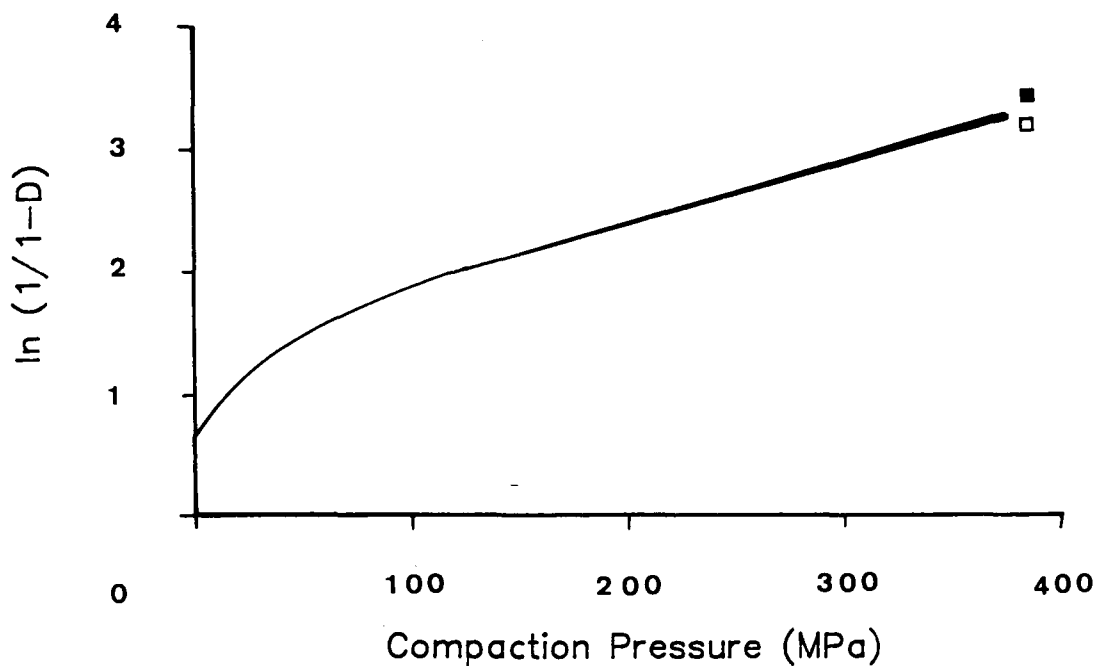
6.3 Results and Discussion

6.3.1 Pressure - Volume Relationships

6.3.1.1 Consolidation of the Substrates

The relationship between compaction pressure and $\ln 1/(1-D)$ for dicalcium phosphate and paracetamol granulates prepared by wet-massing in the absence of a binder is shown in Figs. 6.4 and 6.5 respectively.

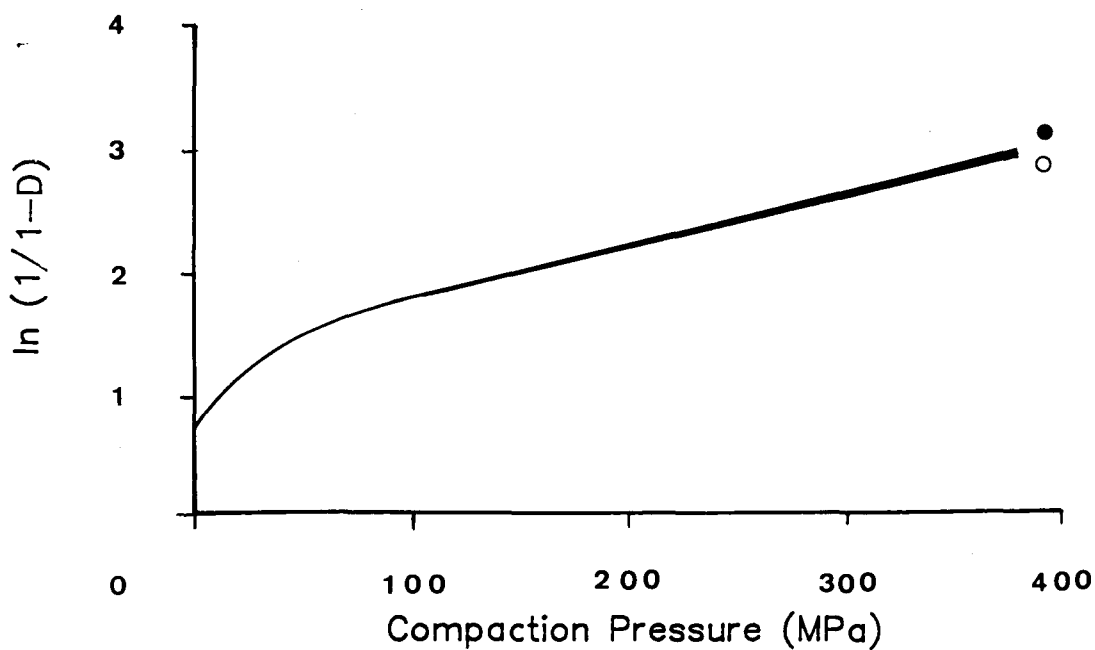
Figure 6.4 Consolidation of Paracetamol Granulates



Relative Humidity

22.5 % ■ 59.5% □

Figure 6.5 Consolidation of Dicalcium Phosphate Granulates



Relative Humidity

22.5 % ● 59.5% ○

Heckel (1961 a) proposed that non-linearity of the plots at low pressures was due to particulate rearrangement achieving closer packing in the absence of bonding. For both substrates the presence of an initial non-linear region suggested that densification at low loads involved rearrangement. But, since granules prepared without a binder were weak and friable, densification in the non-linear part of the Heckel plot was also associated with concurrent granule failure at low pressures. At pressures above about 50MPa for dicalcium phosphate and about 100MPa for paracetamol the plots tended to linearity.

Analysis of the Heckel plots allows the determination of a number of parameters which characterise the consolidation process. The reproducibility of the system used and the accuracy of data analysis was checked by performing 10 replicate compression cycles on a dicalcium phosphate granulate wet-massed in the absence of binder and equilibrated at 22.5% RH. Using a loading rate of 500kN min⁻¹ the derived constants P_v , D_A and D_0 with their respective coefficients of variation were 234.9 MPa (1.58%), 0.734 (1.05%) and 0.672 (2.93%). The initial relative density D_0 of the granule bed was determined after the application of a pre-load of 1 MPa. This provided an unambiguous initial reference point.

For all granulations investigated, best linearity was achieved within the pressure range 150MPa to 300MPa. Regression analysis on data points within these limits was highly significant ($R > 0.999$) in all cases. The low values for the coefficients of variation and the coincidence of replicate Heckel plots reflect the confidence in the experimental procedure and in the method of analysis. Subsequently, Heckel parameters for all other granulates were determined from three replicate experiments. The calculated Heckel parameters for the consolidation of paracetamol and dicalcium phosphate granulates are reported in Tables 6.1 and 6.2 respectively.

For both substrates, Heckel profiles were essentially unaffected by the conditioning humidity. For dicalcium phosphate a small increase in densification seen at the higher humidity was due mainly to an increase in the rearrangement phase of consolidation. This was evident from the higher value of the intercept A_w and the resultant increase in D_0 (Table 6.2).

Table 6.1 Heckel Parameters for the Consolidation of Paracetamol

Relative Humidity %	Loading Rate (kN min ⁻¹)	K _H x 10 ³ (MPa ⁻¹)	P _V (MPa)	A _H	D ₀	D _A	D _B
22.5	500	5.152	194.0	1.367	0.626	0.745	0.119
	50	5.200	192.3	1.355	0.621	0.742	0.121
+ 1.03% PEG 200							
	500	5.047	198.1	1.402	0.628	0.753	0.125
59.5	500	5.224	192.8	1.400	0.627	0.754	0.127

Table 6.2 Heckel Parameters for the Consolidation of Dicalcium Phosphate

Relative Humidity %	Loading Rate (kN min ⁻¹)	K _H x 10 ³ (MPa ⁻¹)	P _V (MPa)	A _H	D ₀	D _A	D _B
22.5	500	4.257	234.9	1.327	0.672	0.734	0.062
	50	4.344	233.7	1.327	0.674	0.734	0.060
+ 1.03% PEG 200							
	500	4.221	236.9	1.387	0.675	0.750	0.075
59.5	500	4.323	233.3	1.383	0.670	0.746	0.076

This can attributed to a lubricant activity of sorbed moisture at low compaction pressures. Paracetamol also showed evidence of a lubricant mediated increase in densification however a small decrease in the mean yield pressure P_V also contributed to densification at the higher humidity (Table 6.1). The low dependence of compression properties with respect to storage humidity reflects the low equilibrium moisture contents of dicalcium phosphate and paracetamol over the relative humidity range considered. This substantiates the choice of these

materials as suitable models for the investigation of binder effects on compression with minimal moisture mediated substrate effects.

The inclusion of 1.03% PEG 200 in the granules also had little effect on the consolidation characteristics of granules prepared without a binding agent. Both paracetamol and dicalcium phosphate exhibited a small increase in densification at low pressure, probably due to a lubricant effect. The mean yield pressure was slightly greater than for granules prepared without the PEG 200 and this may reflect a hydrodynamic resistance to consolidation at higher pressures.

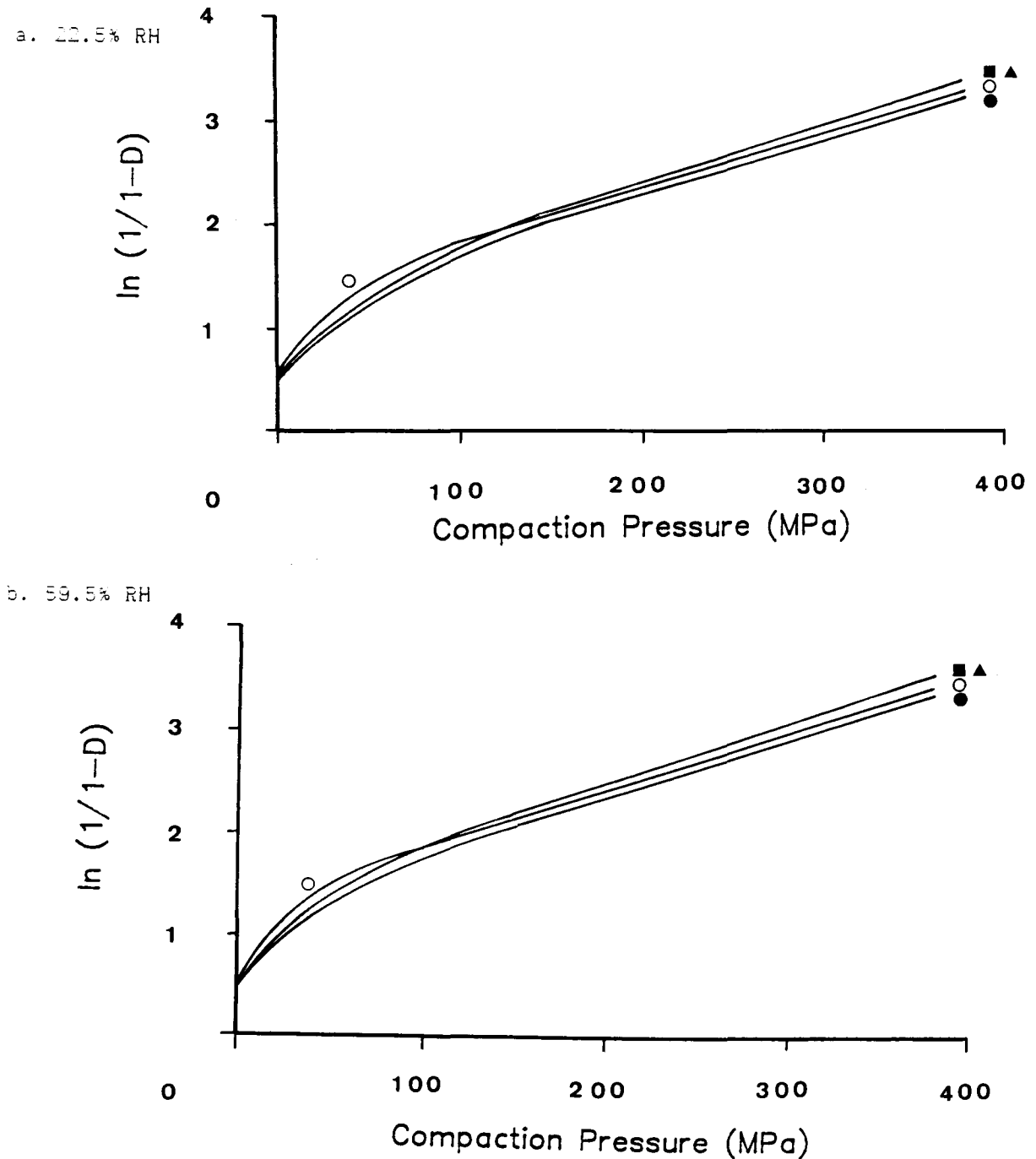
The yield pressure for dicalcium phosphate (234.9 MPa at 22.5% RH) was greater than for paracetamol (194.0 MPa at 22.5% RH) probably reflecting a greater intrinsic hardness of the inorganic material. The yield pressure for the paracetamol granules reported here is considerably higher than previously reported for paracetamol powder. Humbert-Droz et al., (1983) reported a yield pressure of 79MPa whilst Roberts and Rowe (1985) reported an approximate value of 110MPa. Different compression protocols inevitably will give different yield pressures. The main difference can be attributed to the fact that granular paracetamol densifies to a greater extent by rearrangement and crushing. Linearity of the Heckel plot is not therefore encountered until higher pressures where further densification is impeded by a low compact porosity.

The original work of Heckel (1961a) used post-compression compact dimensions for the evaluation of relative density. His compactions were carried out on deformable metal powders of high elastic modulus and consequently fragmentation and elastic strain were probably negligible. Non-linear Heckel plots may have resulted with granulates used here had compact dimensions been determined after decompression. Slow viscoelastic strain recovery, in addition to elastic strain recovery, may introduce a degree of time-dependency in the form of Heckel plots determined from post-compression compact dimensions. The suggestion of Rees and Rue (1978) that differences in Heckel plots obtained at different contact times should be due only to plastic deformation may not therefore be correct.

6.3.1.2 The Effect of Granulation with a Binder
On Granule Consolidation

Heckel consolidation profiles for paracetamol and dicalcium phosphate granulated with each binder system are shown in Figs. 6.6 and 6.7 respectively.

Figure 6.6 The Effect of Binder Type on the Consolidation of Paracetamol



Binder Type

Sucrose ○

Starch 1500 ●

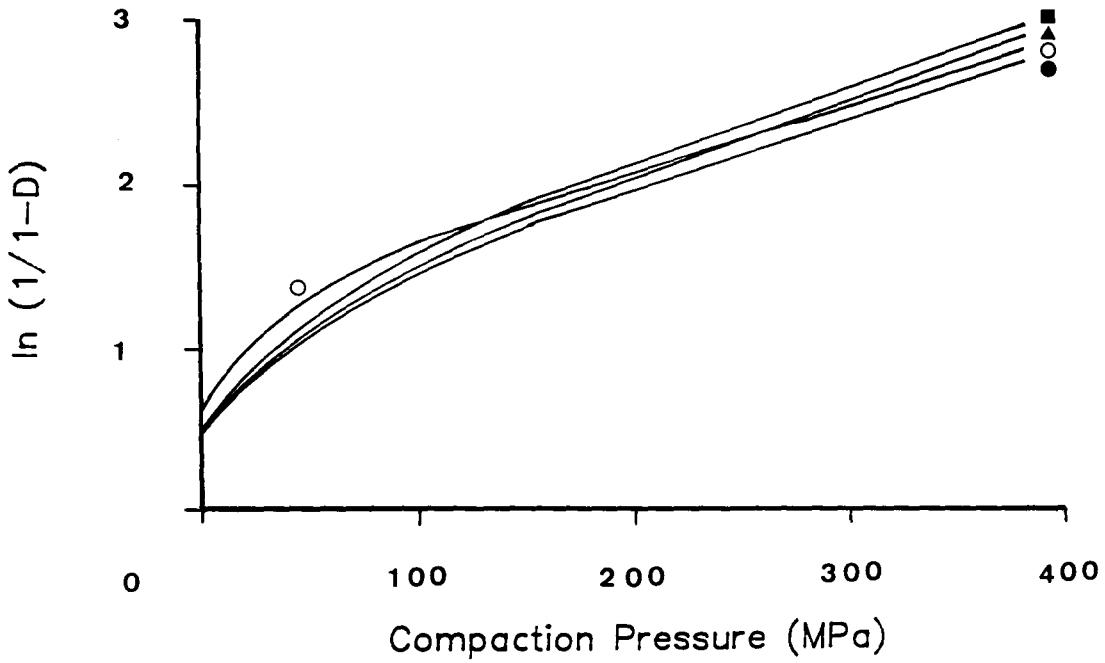
PVP ■

HPMC ▲

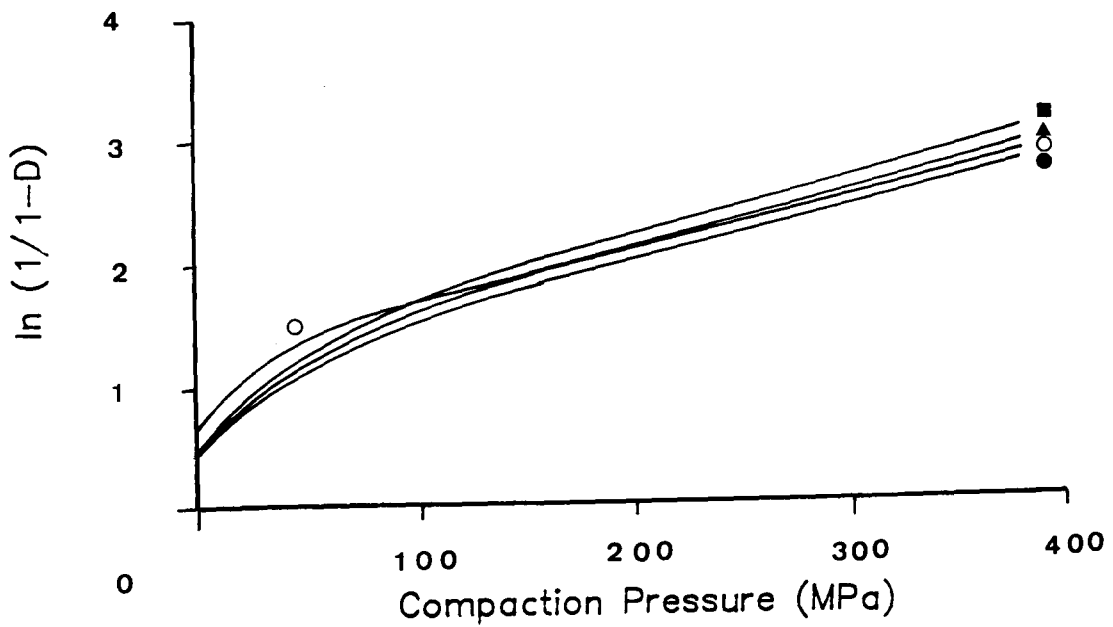
Figure 6.7

The Effect of Binder Type on the Consolidation of Dicalcium Phosphate

a. 22.5% RH



b. 59.5% RH



Binder Type

Sucrose ○

Starch 1500 ●

PVP ■

HPMC ▲

In all cases a compaction rate of 500 kN min⁻¹ was used. Comparison with the Heckel plots derived for the substrates alone (Figs. 6.4 and 6.5) show several features. The curved phase of the Heckel plots, indicative of consolidation by rearrangement, was greater for all granulates containing a binder than for the simple aqueous massed substrates. Relative densities of binder containing granulates were lower than those of the substrates at low compaction pressures. At higher pressures, binder-containing granules were densified to a greater extent. This indicates that although the extent of the close packing and rearrangement phase was increased, binder induced granule strength meant that higher pressures were required to facilitate the process. This was particularly marked for the polymeric binders, but less so for sucrose granulates where granule friability facilitated greater densification at low compaction pressures. Above about 150MPa the Heckel plots tended to linearity. At a conditioning humidity of 22.5% RH the rank order for increase in relative density on compression of the granulates was:

HPMC > PVP > sucrose > Starch 1500

Constants characterising consolidation which were derived from the Heckel plots are given in Tables 6.3 and 6.4.

Table 6.3 The Effect of Binder Type on the Consolidation of Paracetamol

Binder	Relative Humidity %	$K_H \times 10^3$ (MPa ⁻¹)	P_V (MPa)	A_H	D_0	D_A	D_B
Sucrose	22.5	5.552	180.1	1.279	0.561	0.721	0.160
PVP	22.5	5.618	178.0	1.199	0.515	0.698	0.183
HPMC	22.5	5.638	177.3	1.239	0.525	0.710	0.185
Starch 1500	22.5	5.534	180.7	1.220	0.537	0.704	0.167
Sucrose	59.5	5.580	179.2	1.303	0.561	0.728	0.167
PVP	59.5	5.925	168.9	1.298	0.515	0.726	0.211
HPMC	59.5	5.735	173.8	1.356	0.525	0.742	0.217
Starch 1500	59.5	5.636	177.4	1.237	0.537	0.709	0.172

Table 6.4 The Effect of Binder Type on the Consolidation of Dicalcium Phosphate

Binder	Relative Humidity %	$K_w \times 10^3$ (MPa ⁻¹)	P_v (MPa)	A_w	D_0	D_A	D_B
Sucrose	22.5	4.266	234.5	1.222	0.623	0.705	0.082
PVP	22.5	4.583	218.2	1.128	0.489	0.676	0.187
HPMC	22.5	4.649	215.1	1.201	0.526	0.699	0.173
Starch 1500	22.5	4.441	226.6	1.099	0.499	0.666	0.167
Sucrose	59.5	4.281	233.5	1.253	0.627	0.714	0.087
PVP	59.5	4.644	215.3	1.194	0.489	0.697	0.208
HPMC	59.5	4.665	214.8	1.237	0.526	0.710	0.184
Starch 1500	59.5	4.476	223.4	1.133	0.499	0.678	0.179

Comparison of the initial bed density D_0 for the granulates and for the substrates alone (Tables 6.1 and 6.2) demonstrated the greater inter-granular porosity of granules prepared using a binder. This was most marked with the polymeric binders. Granules prepared with sucrose, being weak and friable, exhibited lower porosities although still greater than for granules prepared in the absence of binder. Granulation with a binder resulted in lower mean yield pressures (P_v) than that of the base substrate alone.

With the exception of sucrose granulates, the rank order for ease of densification was reflected both by the rank order of decrease in P_v and in the rank order of increase in the intercept A_w . The term A_w is a constant of the Heckel treatment of consolidation data and does not represent any fundamental material property. However an increase in the constant A_w (and hence D_A) in this work was generally indicative of greater granule rearrangement and granule deformation in the curved region of the Heckel plot. The consolidation parameters D_A and D_0 taken in isolation appeared to be of little value in interpretation of compressibility. The derived function D_B , however, proved to be

discriminatory of the influence of binders on granule deformation/rearrangement in the curved portion of the Heckel plot. These results suggest that the influence of the binder on compression properties is mediated via two mechanisms:

- crushing or plastic deformation of the original granules, determined by binder-mediated granule strength
- further reduction of void volume within granules by rearrangement of individual particles and binder extrusion, determined by the bulk plasticity of the binder-substrate matrix

The effect of granulation was also investigated after equilibrating the granulates at 59.5% RH in order to assess the effects of moisture sorption on binder dependent compression properties. Comparison with corresponding plots at 22.5% RH show that densification at the higher humidity was significantly greater for granules prepared with polymeric binders but not for those prepared with sucrose. Moisture sorption on the substrates alone was not responsible for the greater densification (section 6.3.1.1) consequently the greater densification represents the ability of sorbed moisture to plasticize hydrophilic polymeric binders. Similar effects would not be expected with crystalline sucrose unless the moisture tension was sufficiently high enough to cause dissolution at crystal surfaces.

Compression parameters for Heckel plots obtained at the higher humidity are included in Tables 6.3 and 6.4. At the higher relative humidity the initial bed density D_0 (determined under a pre-load of 1 MPa) was observed to be slightly higher for granulates containing polymeric binders. Since granule morphology would be unaltered at the higher humidity changes in packing density would not be expected. The increase in D_0 represented increased granule ductility at low load. D_b values at the higher humidity were consequently calculated using D_0 determined from granules equilibrated at 22.5% RH. This had the advantage that any densification occurring during application of pre-load was included in the term D_b . Increased D_b values recorded at the higher relative humidity therefore were an accurate reflection of increased densification during the curved portion of the Heckel plot. Compression parameters recorded for the higher relative humidity reflect increased binder plasticity for the polymeric binders and the

ability to confer increased plasticity to the binder-substrate matrix. Yield pressures determined at the higher humidity were correspondingly lower.

The interpretation of the effect of moisture sorption on the properties granulates containing different polymeric binders is complicated by different binder affinities for water (Chapter three, Fig. 3.4). However, from the equilibrium moisture uptake curves it can be seen that by comparing PVP and Starch 1500 granulates equilibrated at 22.5% RH with HPMC granulates equilibrated at 59.5% RH a comparison can be made under conditions of similar moisture content in the binders. Examination of the relevant Heckel parameters show that under conditions of similar moisture content HPMC clearly confers greater granule plasticity than PVP or Starch 1500. Greater densification seen in PVP granulates equilibrated at 59.5% RH is a consequence of the higher affinity of PVP for sorbed moisture and the consequent increase in binder plasticity. Similar results were reported by Cutt (1983).

Chowan and Chow (1981a and 1981b) also studied the compression behaviour of granulations made with different binders. Whilst the technique used here is not strictly comparable with their method (they used post-ejection compact dimensions to calculate relative densities used in the derivation of the Heckel plots) some comparisons can be made. In contrast with the earlier study, Heckel plots obtained in the present work did not show a biphasic linearity. Chowan and Chow (1981a and 1981b) observed that non-linearity of their Heckel plots ceased at relatively low compaction pressures (<50MPa) and a break in the linear portion of the Heckel plots occurred at a pressure range of 120MPa to 190MPa. They attributed this to the incompressibility of free moisture within the granulates at high compaction pressures. The second linear phase reported by Chowan and Chow (1981a and 1981b) corresponds closely with the pressure range for linearity observed in the present work. The initial linear phase reported by these workers forms part of the curved phase of Heckel plots reported here and as such has been interpreted as indicative of rearrangement and granule failure rather than plastic flow. Differences may be related to the method of deriving the relative density of the compact and also to the loss of resolution when preparing Heckel plots from a limited number

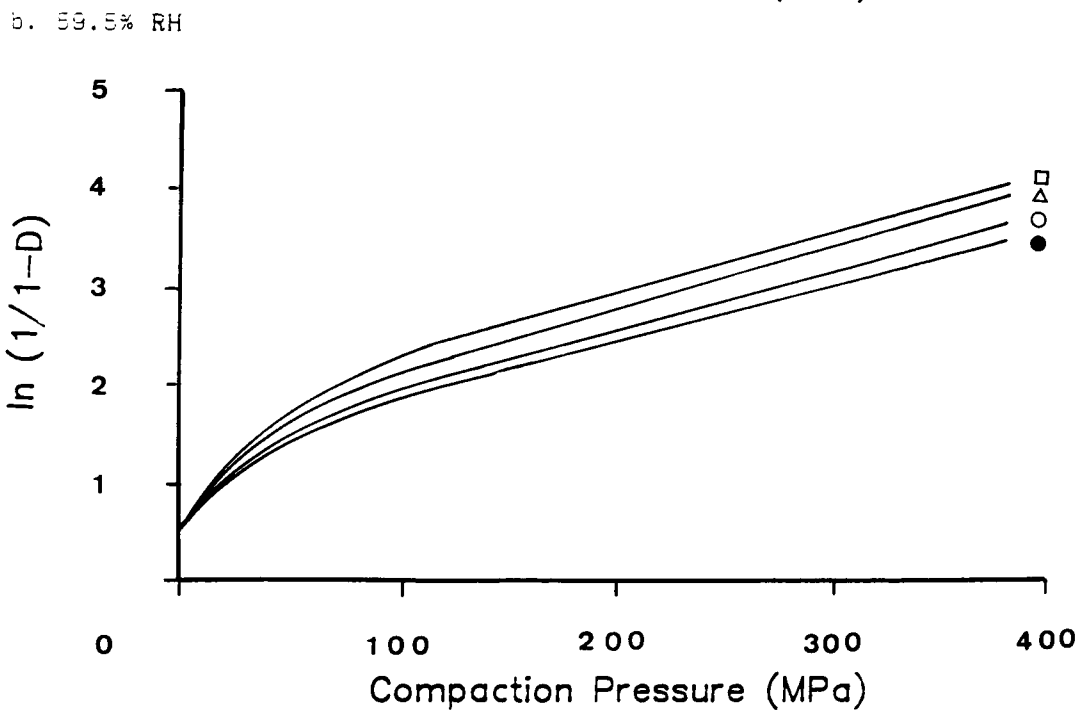
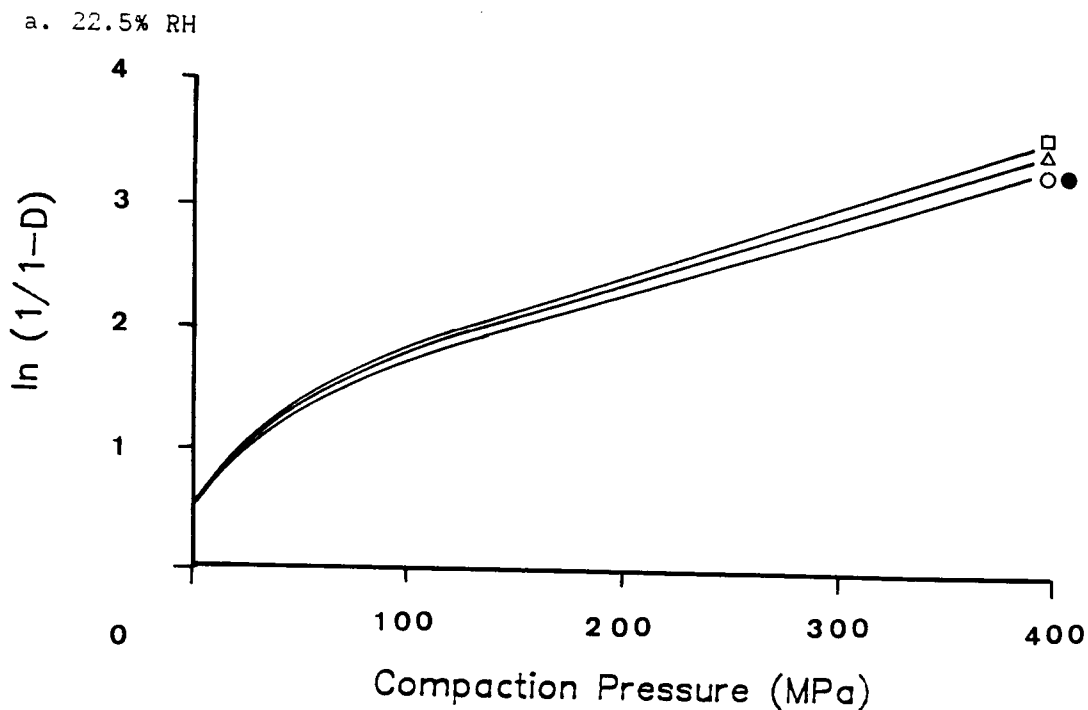
of points rather than from the continuous plot achieved using computer logging. Despite differences in the forms of the Heckel plots, general conclusions for the rank correlation of the binders with respect to densification are similar. Both the present work and the earlier studies indicate ease of densification for sucrose granulates under low compaction pressures. Further, both studies suggest that, at higher moisture contents, PVP-containing granules are more compressible than granules containing other binders.

6.3.1.3 The Effect of Binder Plasticization On Granule Consolidation

The effect of binder plasticization on the consolidation of binder-massed granules, equilibrated at 22.5% RH and 59.5% RH, is shown in Figs. 6.8 to 6.10 for paracetamol and 6.11 to 6.13 for dicalcium phosphate. For both substrates, increased plasticizer content in the polymeric binder resulted in increased densification of the compressed granules. For granules equilibrated at the higher relative humidity, there was a further increase in densification due to the concerted activity of sorbed moisture and plasticizer.

Heckel parameters derived for the above plots are given in Table 6.5 for paracetamol granulates and Table 6.6 for dicalcium phosphate granulates. Irrespective of the polymeric binder used, increased binder plasticity at low pressure was reflected by an increase in the intercept A_w and an increased degree of densification occurring in the rearrangement phase D_s . An increase in plasticizer-mediated binder ductility was accompanied by an increase in the initial granule bed density under the 1MPa pre-load, indicative of granule deformation at very low load. Particle size analysis and bulk density determinations (Chapter three) indicated that this was not due to any influence of plasticizer content on granule morphology or packing. D_s values recorded in the tables were therefore calculated using D_0 for the unplasticized binder. Increasing D_s values with increased plasticizer content consequently reflect the total influence of binder plasticity on densification during the initial curved portion of the Heckel plot.

Figure 6.8 The Effect of Plasticizer Concentration on the Consolidation of PVP-Massed Paracetamol

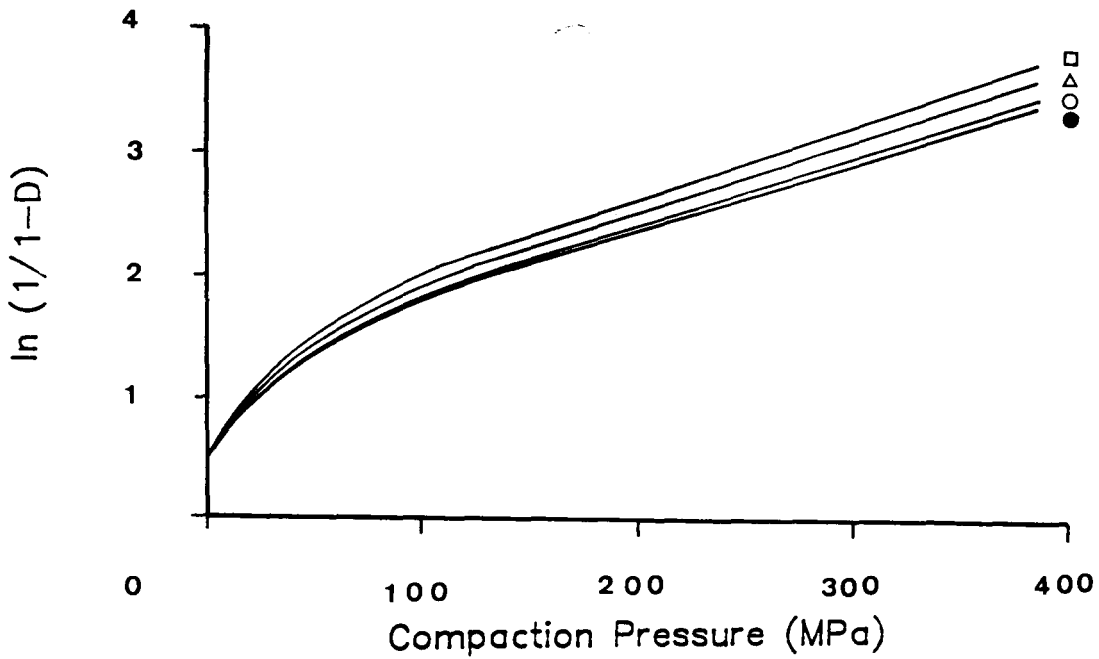


Plasticizer level

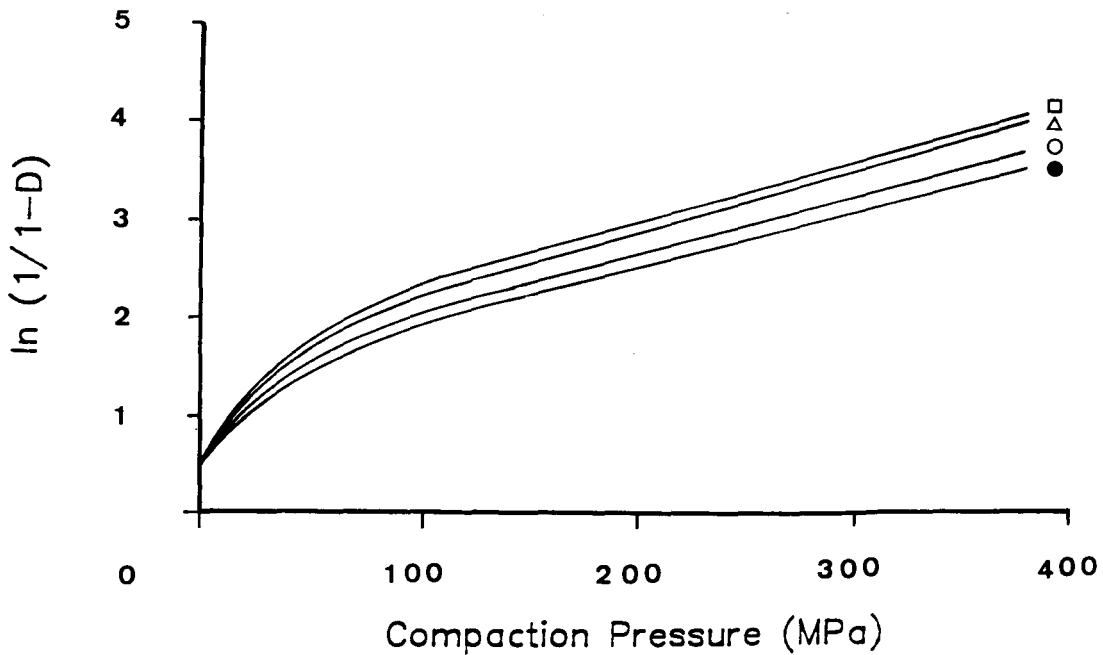
● PEG 200 0% w/w ○ PEG 200 5% w/w △ PEG 200 10% w/w □ PEG 200 15% w/w

Figure 6.9 The Effect of Plasticizer Concentration on the Consolidation of HPMC-Massed Paracetamol

a. 22.5% RH



b. 59.5% RH

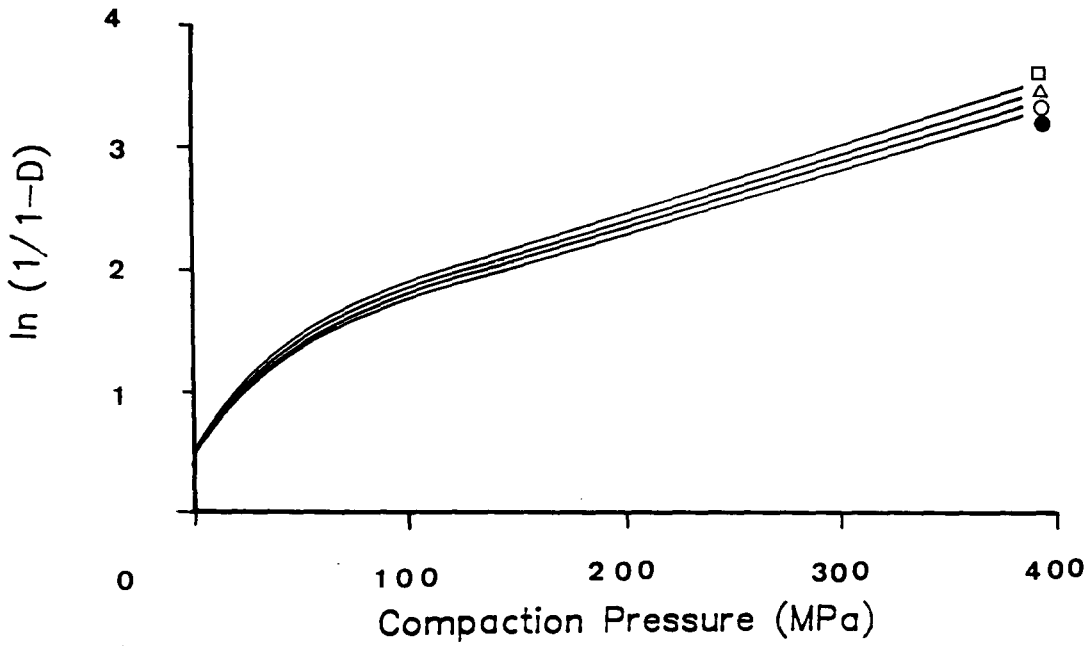


Plasticizer level

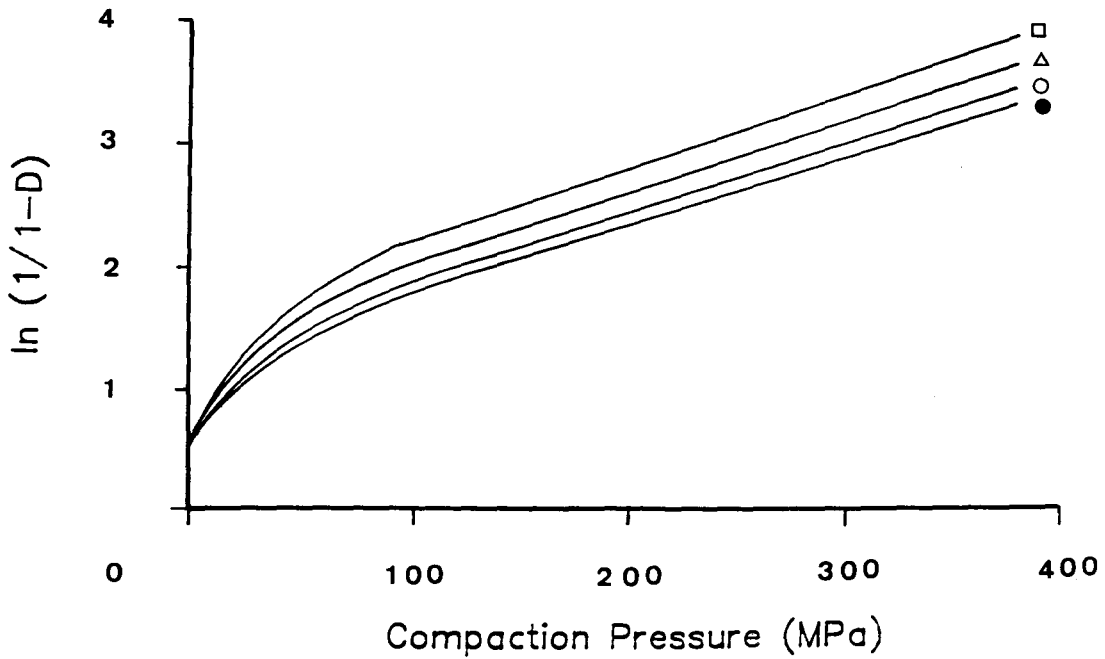
● PEG 200 0% w/w ○ PEG 200 10% w/w △ PEG 200 20% w/w □ PEG 200 30% w/w

Figure 6.10 The Effect of Plasticizer Concentration on the Consolidation of Starch 1500-Massed Paracetamol

a. 22.5% RH



b. 59.5% RH

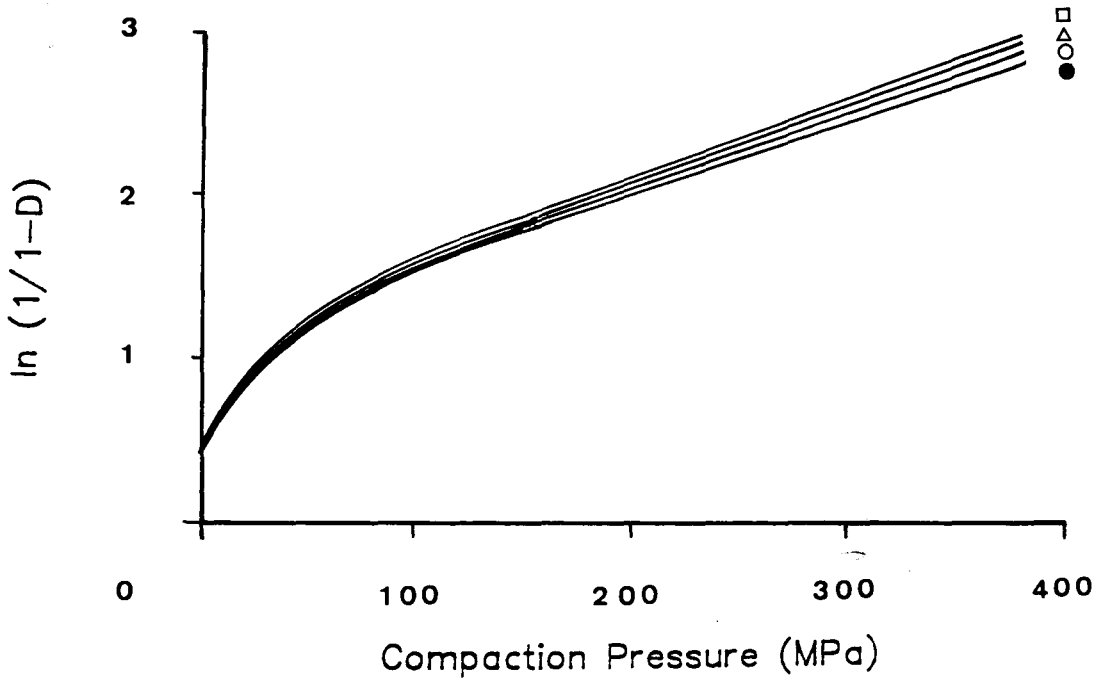


Plasticizer level

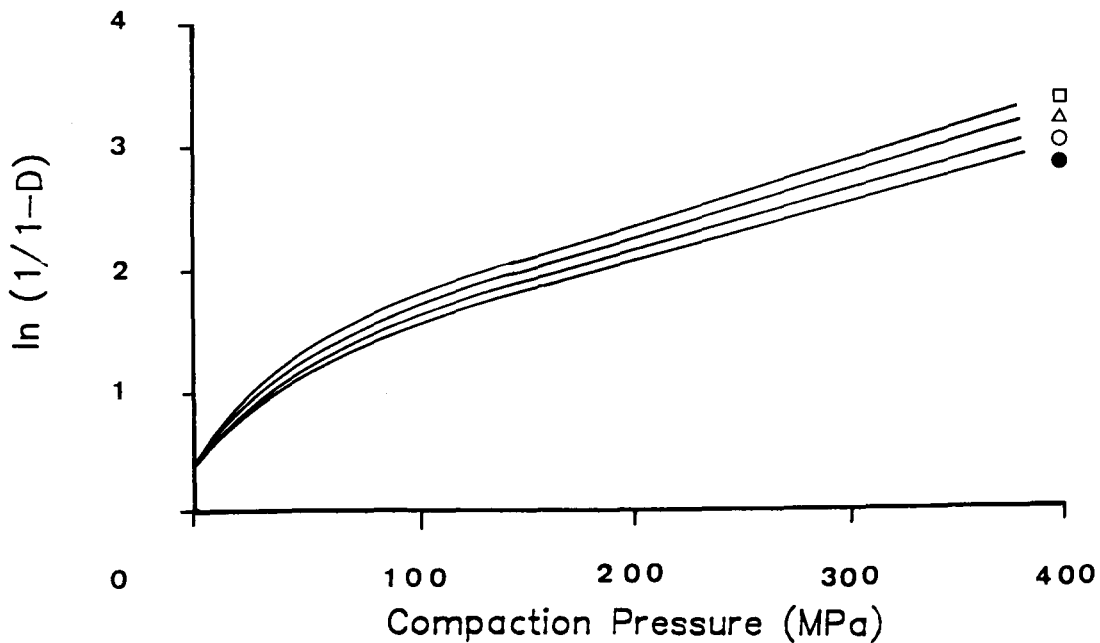
● Glycerol 0% w/w ○ Glycerol 10% w/w △ Glycerol 20% w/w □ Glycerol 30% w/w

Figure 6.11 The Effect of Plasticizer Concentration on the Consolidation of PVP-Massed Dicalcium Phosphate

a. 22.5% RH



b. 59.5% RH

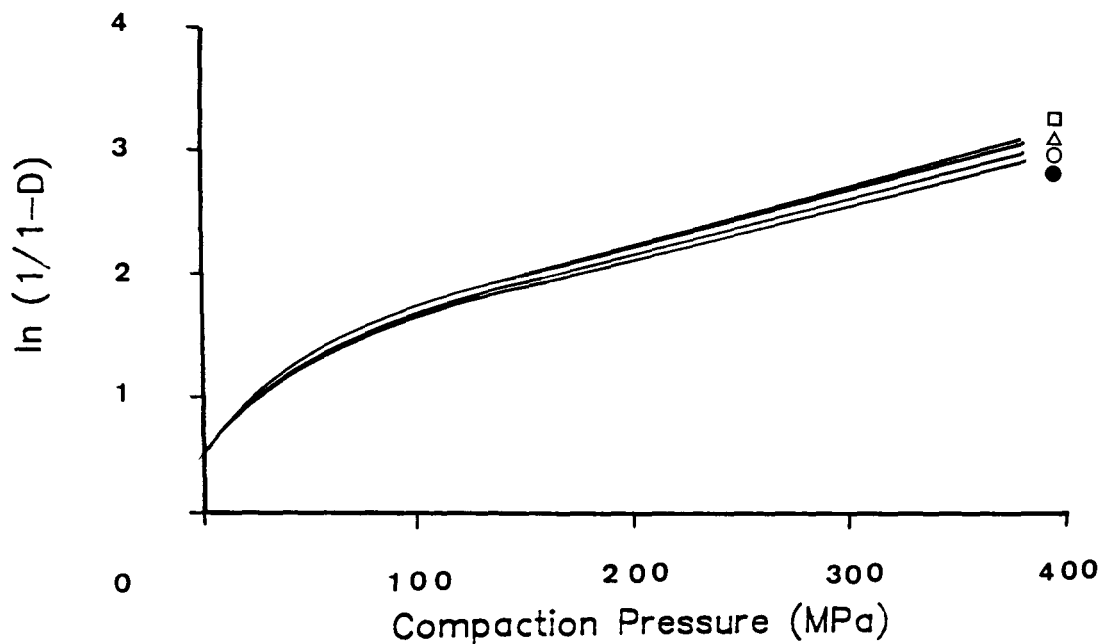


Plasticizer level

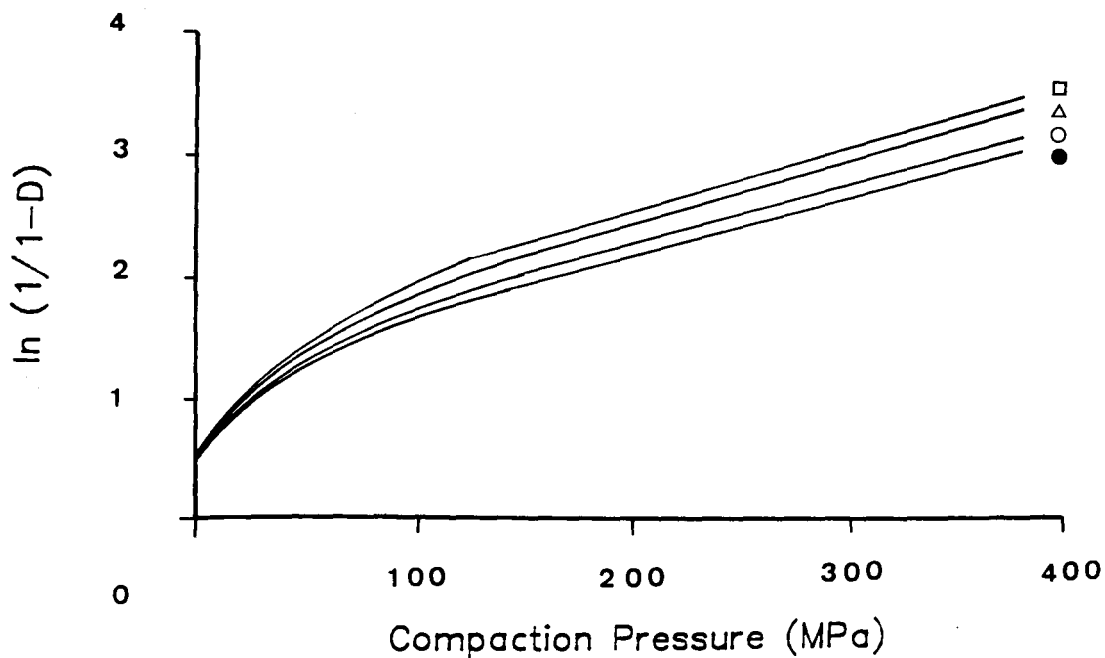
● PEG 200 0% w/w ○ PEG 200 5% w/w △ PEG 200 10% w/w □ PEG 200 15% w/w

Figure 6.12 The Effect of Plasticizer Concentration on the Consolidation of HPMC-Massed Dicalcium Phosphate

a. 22.5% RH



b. 59.5% RH

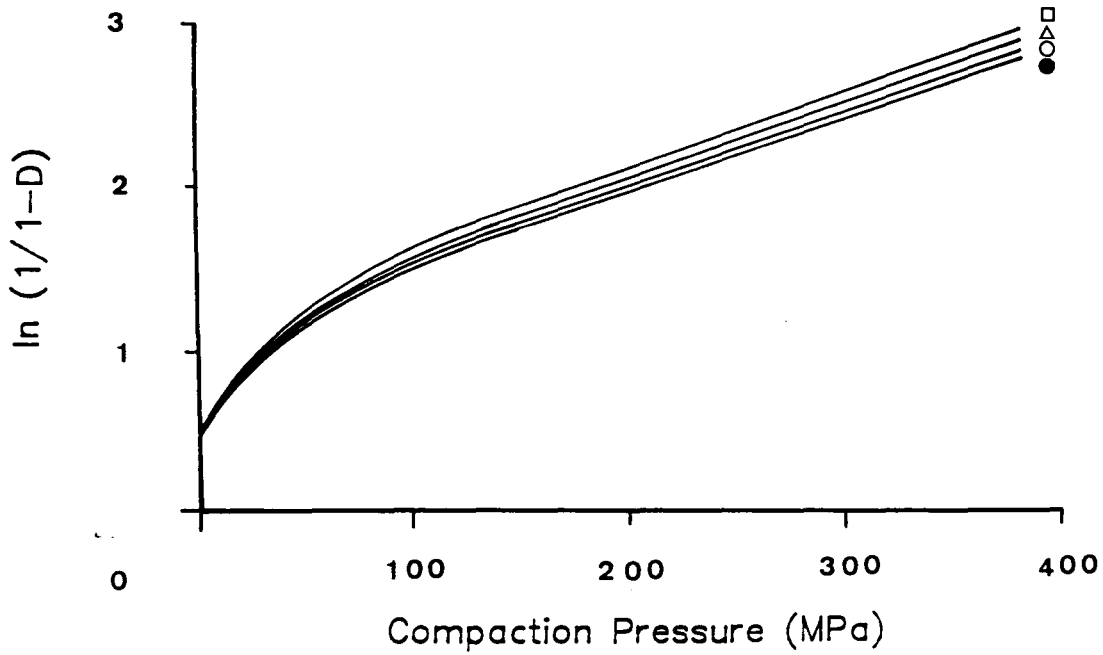


Plasticizer level

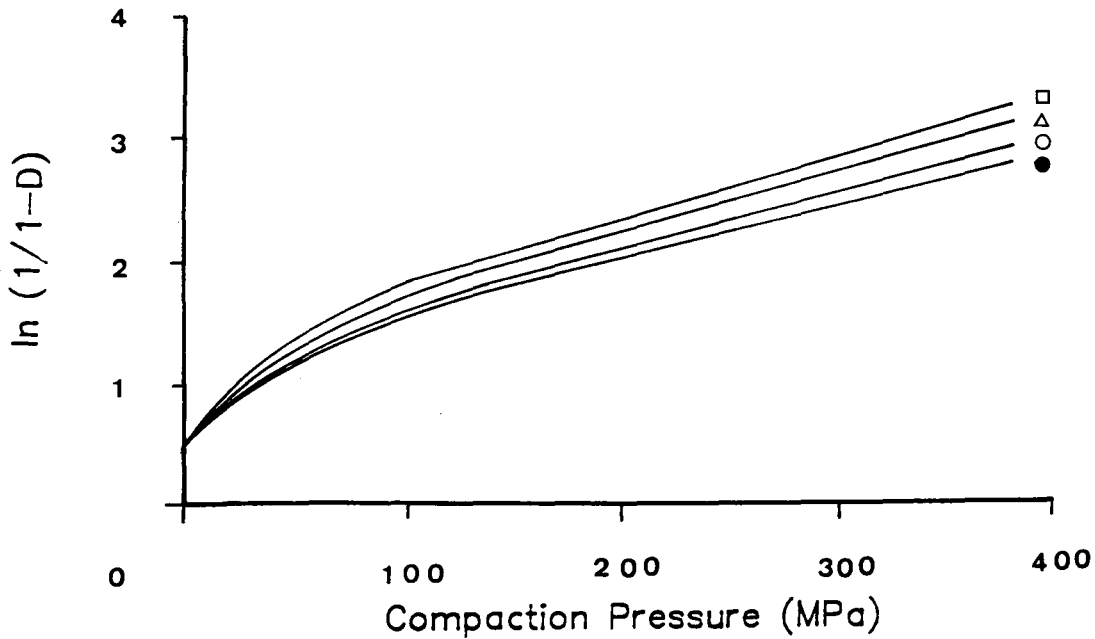
● PEG 200 0% w/w ○ PEG 200 10% w/w △ PEG 200 20% w/w □ PEG 200 30% w/w

Figure 6.13 The Effect of Plasticizer Concentration on the Consolidation of Starch 1500-Massed Dicalcium Phosphate

a. 22.5% RH



b. 59.5% RH



Plasticizer level

● Glycerol 0% w/w ○ Glycerol 10% w/w △ Glycerol 20% w/w □ Glycerol 30% w/w

Table 6.5 The Effect of Plasticizer Concentration on the Consolidation of Paracetamol

Binder	Plasticizer Level	$K_H \times 10^3$ (%)	P_V (MPa)	A_H	D_0	D_A	D_B
22.5% RH							
PVP	0	5.618	178.0	1.199	0.515	0.698	0.183
+ PEG 200	5	5.552	180.1	1.216	0.515	0.703	0.188
+ PEG 200	10	5.747	174.0	1.213	0.515	0.702	0.187
+ PEG 200	15	5.903	169.4	1.246	0.515	0.712	0.197
HPMC	0	5.638	177.3	1.239	0.525	0.710	0.185
+ PEG 200	10	5.691	175.7	1.246	0.525	0.712	0.187
+ PEG 200	20	5.807	172.2	1.384	0.525	0.749	0.224
+ PEG 200	30	5.979	167.2	1.421	0.525	0.758	0.233
Starch 1500	0	5.534	180.7	1.220	0.537	0.704	0.167
+ Glycerol	10	5.571	179.5	1.260	0.537	0.716	0.179
+ Glycerol	20	5.665	176.5	1.272	0.537	0.719	0.182
+ Glycerol	30	5.773	173.2	1.310	0.537	0.753	0.198
59.5% RH							
PVP	0	5.925	168.9	1.298	0.515	0.726	0.211
+ PEG 200	5	6.093	164.1	1.398	0.515	0.753	0.238
+ PEG 200	10	6.493	154.0	1.523	0.515	0.782	0.267
+ PEG 200	15	6.313	158.4	1.692	0.515	0.816	0.301
HPMC	0	5.735	173.8	1.356	0.525	0.742	0.217
+ PEG 200	10	5.927	168.7	1.435	0.525	0.762	0.237
+ PEG 200	20	6.361	157.2	1.604	0.525	0.799	0.274
+ PEG 200	30	6.127	163.2	1.737	0.525	0.824	0.299
Starch 1500	0	5.636	177.4	1.237	0.537	0.709	0.172
+ Glycerol	10	5.763	173.5	1.294	0.537	0.726	0.189
+ Glycerol	20	6.042	165.5	1.394	0.537	0.752	0.215
+ Glycerol	30	6.064	164.9	1.584	0.537	0.795	0.258

Table 6.7 The Effect of Plasticizer Concentration on the Consolidation of Dicalcium Phosphate (22.5% RH)

Binder	Plasticizer Level	$K_H \times 10^3$ (MPa ⁻¹)	P_v (MPa)	A_H	D_0	D_A	D_B
22.5% RH							
PVP	0	4.583	218.2	1.128	0.489	0.676	0.187
+ PEG 200	5	4.737	211.1	1.143	0.489	0.681	0.192
+ PEG 200	10	4.770	209.6	1.152	0.489	0.684	0.195
+ PEG 200	15	4.793	208.8	1.165	0.489	0.688	0.199
HPMC	0	4.649	215.1	1.201	0.526	0.699	0.173
+ PEG 200	10	4.664	214.4	1.200	0.526	0.698	0.172
+ PEG 200	20	4.803	208.2	1.207	0.526	0.700	0.174
+ PEG 200	30	4.805	208.1	1.231	0.526	0.708	0.182
Starch 1500	0	4.441	226.6	1.099	0.499	0.666	0.167
+ Glycerol	10	4.522	221.1	1.098	0.499	0.666	0.167
+ Glycerol	20	4.694	213.0	1.106	0.499	0.669	0.170
+ Glycerol	30	4.703	212.6	1.151	0.499	0.683	0.184
59.5% RH							
PVP	0	4.644	215.3	1.194	0.489	0.696	0.207
+ PEG 200	5	4.782	209.1	1.234	0.489	0.708	0.219
+ PEG 200	10	5.151	194.1	1.294	0.489	0.726	0.237
+ PEG 200	15	5.202	192.2	1.362	0.489	0.744	0.255
HPMC	0	4.665	214.8	1.237	0.526	0.710	0.184
+ PEG 200	10	4.826	207.2	1.294	0.526	0.726	0.200
+ PEG 200	20	5.257	190.2	1.386	0.526	0.750	0.224
+ PEG 200	30	5.178	193.1	1.491	0.526	0.775	0.249
Starch 1500	0	4.476	223.4	1.133	0.499	0.678	0.179
+ Glycerol	10	4.564	219.1	1.190	0.499	0.696	0.197
+ Glycerol	20	4.909	203.7	1.269	0.499	0.719	0.220
+ Glycerol	30	5.083	196.7	1.324	0.499	0.734	0.235

Increasing the concentration of plasticizer in the polymeric binders generally resulted in an increased slope for the linear part of the Heckel plot corresponding to lower mean yield pressure P_v . However, for granules equilibrated at 59.5% RH there appeared to be a limiting plasticizer level above which the yield pressure did not decrease or even increased. The latter behaviour resulted from the higher degree of densification occurring at lower pressures with highly plasticized binders. The reduced porosity of the compact consequently restricted further reduction in yield pressure.

Shifts to greater relative densities at equivalent compressive pressures have been reported by other workers in response to an increase in the binder content in the wet-massed granules (Nelson et al., 1957; Kurup and Pilpel, 1978; Cutt, 1983). The reverse trend was reported, however, by Esezobo and Pilpel (1977a) who suggested that binder-induced granule rigidity opposed consolidation. These observations suggest that the influence of a binder on the densification of a compressed granule mass is determined by three factors:

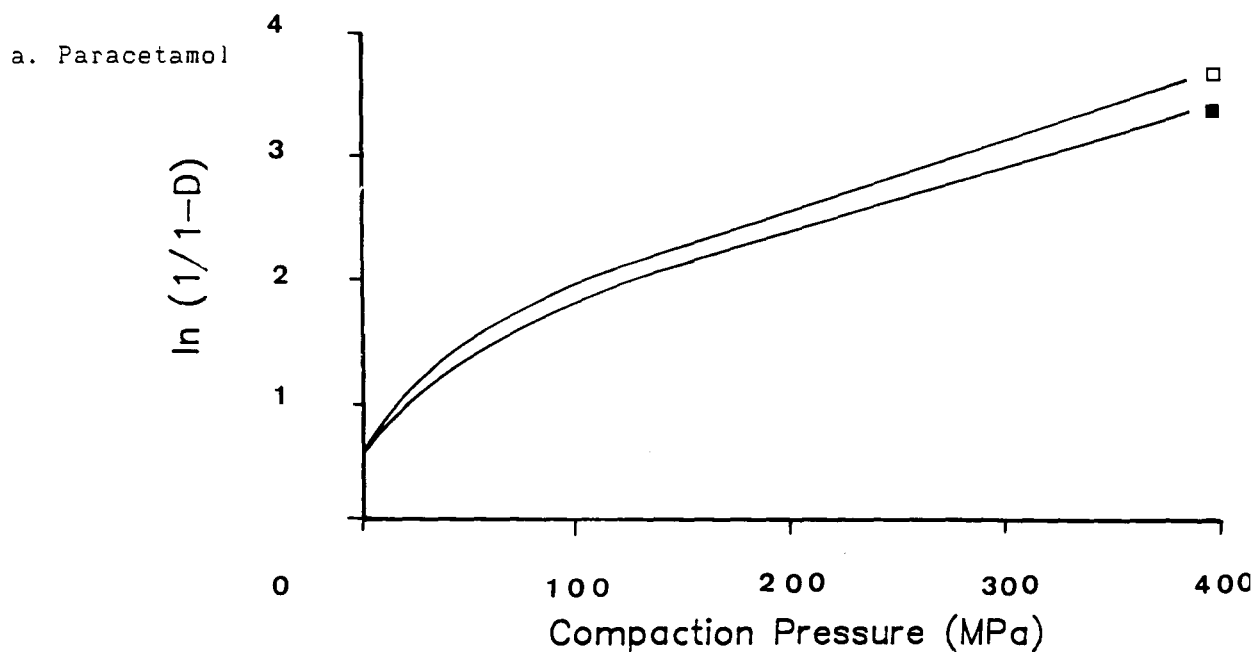
- the plasticity of the binder
- the relative proportion of the compact which can deform plastically (or binder level)
- the initial strength of the granules

Binder level was maintained at a constant level in the present studies, thus eliminating the second factor above as a variable. Increased densification due to the inclusion of a plasticizer, therefore, reflects binder plasticity and granule strength. The increased densification observed at low pressures results from granule weakening as a consequence of binder film weakening. This is consistent with a reduction in the tensile strength of cast binder films on plasticization (Chapter three). Increased densification at higher pressures reflects the ease of deformation of plasticized binders. The deformability of the substrate materials themselves (paracetamol or dicalcium phosphate) would not be altered specifically. However, the increased ductility of the plastic binder would facilitate easier consolidation of substrate particles within the binder-substrate matrix and greater plastic extrusion of binder into void spaces.

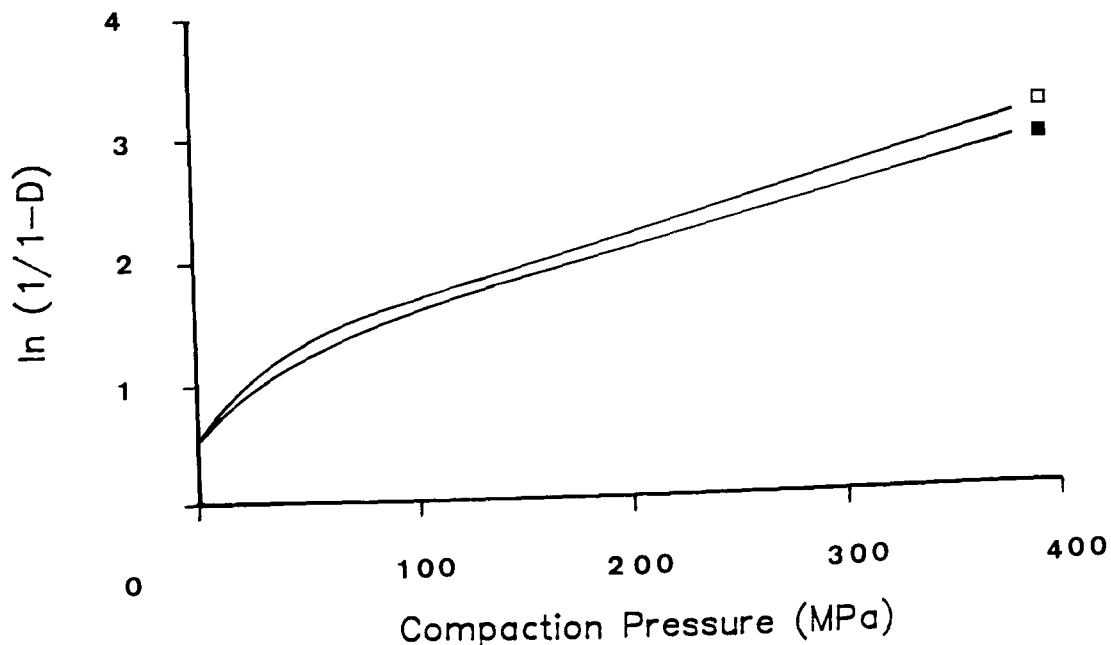
6.3.1.4 The Effect of a Low Efficiency Plasticizer

Figure 6.14 shows the densification characteristics of paracetamol and dicalcium phosphate granulates containing HPMC as the binder and either 20% PEG 200 or 20% PEG 600 as plasticizer.

Figure 6.14 The Effect of a Low Efficiency Plasticizer on Heckel Parameters (22.5% RH)



b. Dicalcium Phosphate



Plasticizer

PEG 200 20% w/w □

PEG 600 20% w/w ■

For both substrates, greater densification occurred when PEG 200 was utilised as the plasticizer. PEG 600 exhibits lower compatibility and efficiency than PEG 200 when used as a plasticizer for HPMC. The reduced densification observed using PEG 600 supports the contention that the plasticizer-mediated increase in densification was due specifically to increased binder plasticity.

The Heckel parameters shown in Table 6.7 indicated that the lower densification observed with PEG 600 was a consequence of two factors. Firstly, increased resistance to rearrangement and crushing at low pressures (lower D_b) and secondly, a lower bulk plasticity (higher mean yield pressure). This corresponds with the higher tensile strength and lower ductility of PEG 600 plasticized HPMC films (confering greater granule strength) compared with PEG 200 plasticized HPMC films.

Table 6.7 The Effect of Plasticizer Type on Heckel Parameters (22.5 %RH)

Binder	Plasticizer	$K_H \times 10^3$ (MPa ⁻¹)	P_v (MPa)	A_H	D_0	D_A	D_B
Paracetamol							
HPMC	PEG 200	5.807	172.2	1.384	0.525	0.749	0.224
	PEG 600	5.497	181.9	1.290	0.520	0.725	0.205
Dicalcium phosphate							
HPMC	PEG 200	4.803	208.2	1.207	0.526	0.700	0.174
	PEG 600	4.595	217.6	1.177	0.522	0.692	0.170

6.3.2 Time-Dependent Densification

6.3.2.1 Time-Dependent Densification of the Substrates

The densification of dicalcium phosphate used "as received" has been shown by several studies to be independent of time (Rees and Rue,

1978; Celik, 1983; Roberts and Rowe, 1985), characteristic of a material consolidating by brittle fragmentation. Evidence for the deformation mode of paracetamol is conflicting (Doelker and Shotton, 1977) suggesting that there is a degree of plastic flow and some brittle behaviour (Humbert-Droz et al., 1983). The ability of paracetamol to undergo considerable elastic strain does not seem to be in doubt. Roberts and Rowe (1985) concluded that mixed behaviour was probably the case for paracetamol. Since previous studies have utilised ungranulated material it was relevant for the present study to examine the influence of wet-massing on the potential for time-dependent deformation in dicalcium phosphate and paracetamol granulates.

Heckel plots were determined for dicalcium phosphate and paracetamol granulates at a slow loading rate of 50kN min^{-1} effectively increasing the total contact time to achieve peak pressure by a factor of ten over the original loading rate of 500kN min^{-1} . Resultant Heckel plots were coincident with the original plots obtained at 500kN min^{-1} and shown previously in Figs. 6.4 and 6.5. Derived constants for consolidation under different loading rates were reported for comparison in Tables 6.1 and 6.2.

The time-independent nature of consolidation of a dicalcium phosphate granulate, prepared by wet-massing with water alone, was confirmed by the coincidence of Heckel plots determined at the two different loading rates. Constants derived from the respective plots (Table 6.2) showed little difference either in the extent of rearrangement (D_b) or in the yield pressure P_y . In the case of paracetamol compression at the slower loading rate resulted in a very small decrease in yield pressure which was not significant in terms of the Heckel plot.

One feature of the Mayes press operated in load control, was that it was possible to maintain a constant stress on the test granulate. Using this feature, paracetamol and dicalcium phosphate granulates, compressed at a loading rate of 500kN min^{-1} , were subjected to a 10 second holding time while maintaining a constant peak upper punch pressure (380MPa). During this period, the displacement of the upper punch was monitored to determine whether any further densification

occured. Neither substrate was observed to undergo further densification under constant stress conditions, however. These observations are similar to those of Celik (1984) who observed that the materials Paracetamol DC (a direct compression form of paracetamol) and Emcompress (a direct compression form of dicalcium phosphate) did not exhibit further densification during prolonged compression at constant stress. These results and the limited dependence of P_v on loading rate suggests that fragmentation is the predominant mode of deformation for granulated paracetamol and dicalcium phosphate.

6.3.2.2 The Effect of Binder and Binder Plasticity on Time-Dependent Densification

The reduction in the mean yield pressure resulting from the inclusion of a binding agent suggested that the presence of binder induced plasticity in the granulates. The degree of densification in a plastic granular mass should, therefore, be influenced by the duration of compression and holding time under constant stress. In order to test this, Heckel plots were constructed for plasticized and unplasticized HPMC-massed paracetamol and dicalcium phosphate granulates at a slow loading rate of 50kN min^{-1} . A comparison of the resultant Heckel plots with those obtained at 500kN min^{-1} loading rate is shown in Figs. 6.15 and 6.16. Derived constants for consolidation under the two different loading rates are given in Tables 6.8 and 6.9.

In contrast with the granules prepared without a binder, the binder-massed granules exhibited time-dependent consolidation. Granules compressed at the slower loading rate achieved greater relative density at equivalent pressures compared with the higher loading rate. This phenomena was observed with both substrates. The extent of time-dependent densification was greater for those granules conditioned by equilibration at 59.5% RH compared with those conditioned at 22.5% RH and also for those granules with plasticized binder. Examination of the Heckel plots given in Figs. 6.15 and 6.16 showed a feature that was absent for plots of the substrates granulated in the absence of a binder.

Figure 6.15 Effect of Loading Rate on Heckel Parameters for the Consolidation of HPMC-massed Paracetamol Granulates

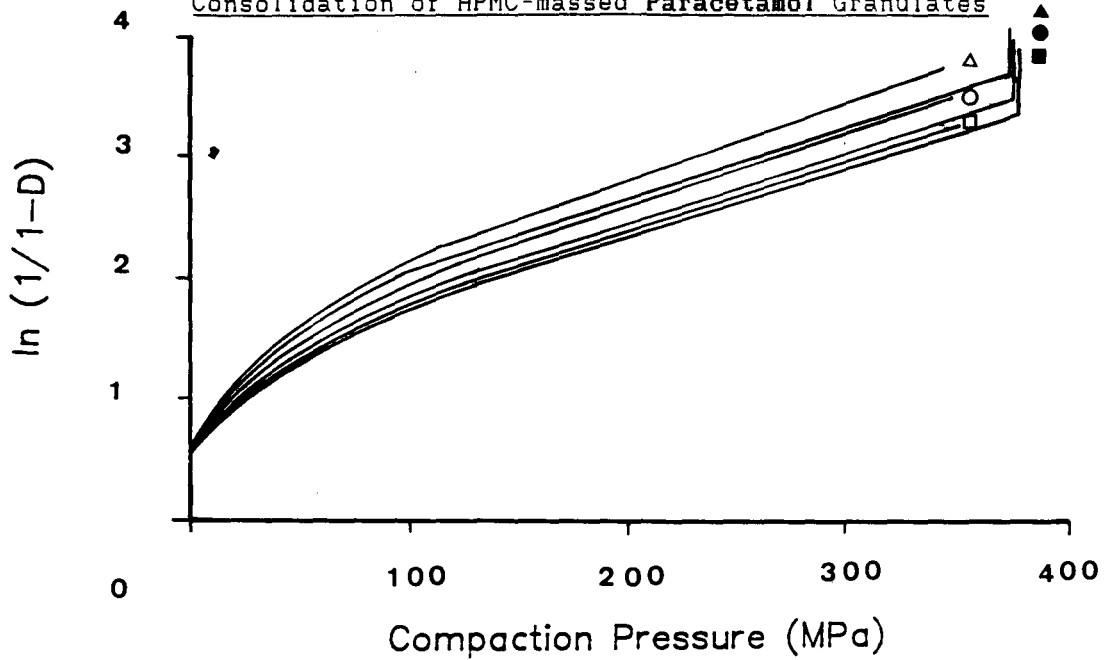
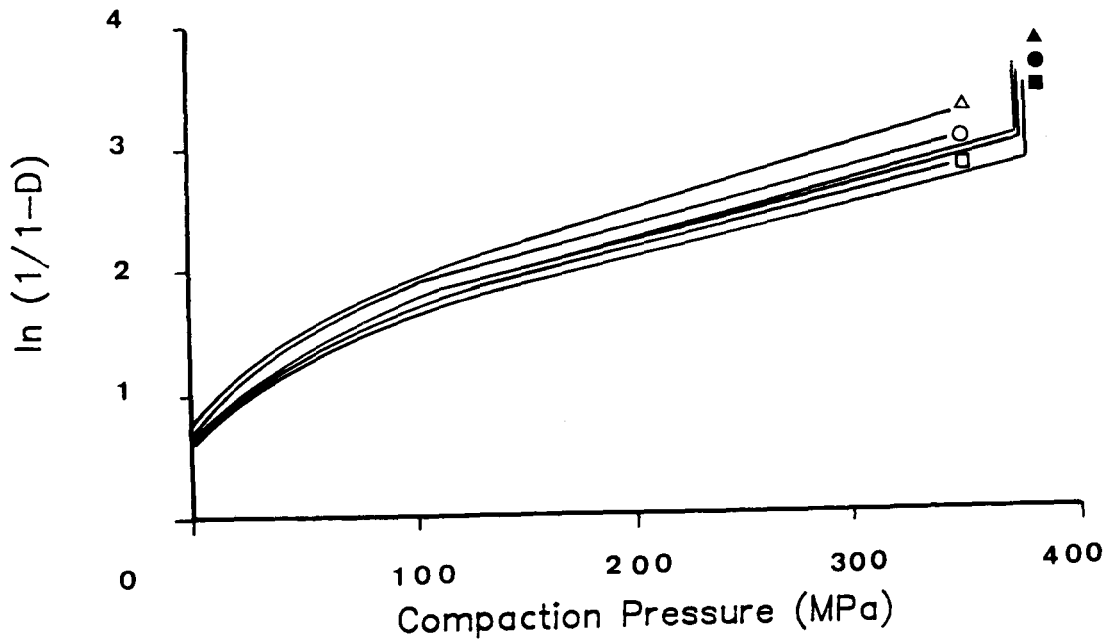


Figure 6.16 Effect of Loading Rate on Heckel Parameters for the Consolidation of HPMC-massed Dicalcium Phosphate Granulates



Key to Figs 6.15 & 6.16

- 22.5% RH, 500 kN min⁻¹, 10s holding time
- 22.5% RH, 50 kN min⁻¹
- ▲ 22.5% RH, 500 kN min⁻¹, 10s holding time, PEG 200 30% w/w
- △ 22.5% RH, 50 kN min⁻¹, PEG 200 30% w/w
- 59.5% RH, 500 kN min⁻¹, 10s holding time
- 59.5% RH, 50 kN min⁻¹

Table 6.8 Effect of Loading Rate on Heckel Parameters for the Consolidation of HPMC-massed Paracetamol Granulates

Relative Humidity %	Loading Rate (kN min ⁻¹)	K _H x 10 ³ (MPa ⁻¹)	P _V (MPa)	A _H	D ₀	D _A	D _B
22.5	500	5.638	177.3	1.239	0.525	0.710	0.185
	50	5.721	174.8	1.297	0.525	0.726	0.201
(+ 30% PEG 200)	500	5.979	167.2	1.421	0.525	0.758	0.233
	50	6.464	154.7	1.482	0.525	0.773	0.248
59.5	500	5.735	173.8	1.356	0.525	0.742	0.217
	50	5.977	167.3	1.397	0.525	0.752	0.227

Table 6.9 Effect of Loading Rate on Heckel Parameters for the Consolidation of HPMC-massed Dicalcium Phosphate Granulates

Relative Humidity %	Loading Rate (kN min ⁻¹)	K _H x 10 ³ (MPa ⁻¹)	P _V (MPa)	A _H	D ₀	D _A	D _B
22.5	500	4.649	215.1	1.201	0.526	0.699	0.173
	50	4.686	213.4	1.214	0.526	0.703	0.177
(+ 30% PEG 200)	500	4.805	208.1	1.231	0.526	0.708	0.182
	50	5.178	193.1	1.456	0.526	0.767	0.241
59.5	500	4.665	214.8	1.237	0.526	0.710	0.184
	50	4.760	210.0	1.432	0.526	0.761	0.235

This was an increase in densification without further increase in compaction pressure during a 10 second holding time for granules compressed at a loading rate of 500kN min⁻¹. This appeared as the vertical portion of the Heckel plots. The consolidation observed

during constant stress conditions must be due to time-dependent plastic or viscoelastic flow.

Comparison of the Heckel parameters derived for the two different loading rates indicated that increased densification resulted both from increased consolidation at lower pressures and decreased yield pressure. The induction of time-dependent densification supports the premise that the presence of a plastic binder induces plasticity within a non-plastic substrate material. However, similar behaviour could also be attributed to retarded elastic deformation which, unlike plastic deformation, is recoverable with time.

These observations are similar to those of Rees and Rue (1978a) who obtained divergent Heckel plots for Elcema and Sta-Rx when these material were held for different dwell times. Emcompress tablets did not exhibit this behaviour. Celik (1984) observed that materials known to deform plastically, e.g. Starch 1500 and Avicel PH-101 densified to a greater extent at slower compression rates. Roberts and Rowe (1985, 1986), using a compaction simulator, studied the effect of punch velocity on the compaction of a variety of materials. For materials known to deform plastically, e.g. maize starch and polymeric materials, there was an increase in yield pressure with punch velocity. This they attributed to either a change from ductile to brittle behaviour or to a decrease in the amount of plastic deformation due to the time dependent nature of plastic flow. For materials known to consolidate by fragmentation, e.g. magnesium and calcium carbonate, there was no increase in yield pressure with increasing punch velocity. They proposed a strain rate sensitivity (SRS) index defined as:

$$\text{SRS} = \frac{P_{v_2} - P_{v_1}}{P_{v_2}} \times 100 \quad (6.1)$$

where P_{v_1} was the measured yield pressure at an upper punch strain rate of 0.033mm s^{-1} and P_{v_2} was the measured yield pressure at an upper punch strain rate of 300mm s^{-1} . Plastically deforming materials exhibited higher values for SRS than brittle fragmentary materials. Analogous values for loading rate sensitivity (LRS), substituting yield pressures obtained at 50kN min^{-1} and 500kN min^{-1} for P_{v_1} and P_{v_2} respectively, are given in Table 6.10 for a number of

granulations examined in the present work. It can be seen from this data that the substrates granulated in the absence of binder exhibit negligible loading rate sensitivity.

Table 6.10 Loading Rate Sensitivity (LRS) of Paracetamol and Dicalcium Phosphate granulates

Granulate	Relative Humidity %	Loading Rate Sensitivity (defined in Section 6.3.3.2)
Paracetamol		
no binder	22.5	0.8
HPMC-massed	22.5	1.4
	59.5	3.7
HPMC-massed + 30% PEG 200	22.5	7.5
Dicalcium Phosphate		
no binder	22.5	0.5
HPMC-massed	22.5	0.8
	59.5	2.2
HPMC-massed + 30% PEG 200	22.5	7.2

The presence of a polymeric binder and, more significantly, the increase in binder plasticity either by plasticization or moisture sorption greatly increases loading rate sensitivity. This is in agreement with the observations of Roberts and Rowe (1985,1986). More recently Danjo et al., (1989) concluded, on the basis of slow, single-sided compression studies using a simple hydraulic press, that Heckel plots were independent of die fill, die diameter and punch speed. They only evaluated one material however (Ditab, a direct compression dicalcium phosphate) at punch strain rates of 5.4mm s^{-1} to 41.8mm s^{-1} . The general validity of their conclusions, particularly with respect to the influence of punch speed on the form of Heckel plots for plastic materials, must be questioned.

6.3.3 Stress-Relaxation Studies

Stress-relaxation studies on the granulates, prepared and conditioned as described previously in section 5.3, were carried out using the Mayes press in ram-control mode. This was in contrast to the load-control mode used for the Heckel studies. The reason for this difference of approach was that ram-control enabled constant strain conditions to be maintained (via a servo feedback loop). This is a prerequisite for meaningful stress-relaxation data to be generated. Many previous studies of stress-relaxation have employed hand operated presses, simple hydraulic presses or commercial tablet presses. Lack of mechanical stiffness or the presence of overload springs results in considerable difficulty in assuring constant strain when using such equipment. This problem has been reiterated by Armstrong (1989).

In the present work, compressions (not less than three replicates in each case) were performed to peak upper punch pressures of either 150MPa or 250MPa. Huckle (1965) indicated the importance of employing a range of strain rates when comparing the stress-relaxation of different materials. Consequently, strain rates of 1000mm min^{-1} and 100mm min^{-1} were used to investigate the effect of loading time on relaxation. Data (pairs of stress-time co-ordinates at 0.1 second intervals) were captured and digitised using the BBC microcomputer interfaced to the Mayes press. Data logging was initiated as soon as the first stress above 1MPa was detected. Immediately that the required peak stress was attained, the ram of the Mayes press was automatically halted and a constant strain maintained whilst recording any decay in axial stress. The time from first stress detection to peak stress was observed to fall between 0.2 and 0.3 seconds at a strain rate of 1000mm min^{-1} and 2.8 to 3.5 seconds at a strain rate of 100mm min^{-1} .

Initial tests carried out without any granule in the die showed that relaxation of the test rig alone was small but finite. Consequently stress-relaxation profiles for the granulates were corrected to yield the relaxation of the granulate alone as a function of time. Data obtained for the granulates used in this study indicated that stress-relaxation was incomplete after 100 seconds. Preliminary investigations showed that the relaxation phenomena recorded could not

be adequately represented by the Maxwell model as employed by David and Augsburger (1977). This was not unexpected in view of the stress distribution and density anomalies which occur during the compaction of a granular material. The application of the Maxwell model assumes that the plastic flow facilitating stress-relaxation is analogous to the finite flow of a single Newtonian fluid in a dashpot. It seems highly unlikely that the plasticity of a heterogeneous system, such as a granulate, could be characterised in terms a single parameter. Stress relaxation in the bulk solid, at intergranular interfaces, or within any binder may all exhibit different characteristic viscosities.

In the present work stress-relaxation data was presented as the percentage residual axial stress plotted against log time. A semi-log representation facilitated expansion of the early time relaxation and allowed visual comparison of material properties immediately after halting compression. Stress relaxation was also characterised in terms of the stress decay after 100 seconds at constant strain expressed as a percentage of the maximum applied upper punch stress.

6.3.3.1 Stress-Relaxation of the Tablet Substrates

The predominant deformations under compressive stress for paracetamol and dicalcium phosphate have been reported as elasticity and brittle failure respectively. Ideally both types of deformation are independant of time although elastic strain is recoverable unlike brittle failure. Heckel plots determined at two different loading rates (section 6.3.2) supported the general model of time-independent deformation both for paracetamol and dicalcium phosphate granulates prepared by wet-massed granulation in the absence of a binder. The stress-relaxation behaviour reported in Tables 6.11 and 6.12 and illustrated by Figs. 6.17 and 6.18 indicated, however, that simple wet-massed granulates of both materials exhibited some plastic deformation. For both substrates, visual examination of the stress-relaxation plots suggested that the relaxation phenomena was essentially biphasic. The initial relaxation phase, which contributed the greater part of the total relaxation, was rapid and complete by about 3 seconds. This was followed by a much slower, protracted relaxation which was not completed after 100 seconds.

Table 6.11 Stress-Relaxation of Paracetamol Granulates

Strain Rate (mm min ⁻¹)	1000		100
Peak Compaction	150	250	150
Pressure (MPa)			

Percentage Stress Decay at Constant Strain			
22.5% RH	8.9	5.3	1.5
+ 1.03% PEG 200	8.3	-	-
59.5% RH	8.8	-	-
+ 1.03% PEG 200	7.9	-	-

Table 6.12 Stress-Relaxation of Dicalcium Phosphate Granulates

Strain Rate (mm min ⁻¹)	1000		100
Peak Compaction	150	250	150
Pressure (MPa)			

Percentage Stress Decay at Constant Strain			
22.5% RH	11.2	8.9	2.2
+ 1.03% PEG 200	10.5	-	-
59.5% RH	12.0	-	-
+ 1.03% PEG 200	11.3	-	-

Figure 6.17 Stress-Relaxation of Paracetamol Granulates

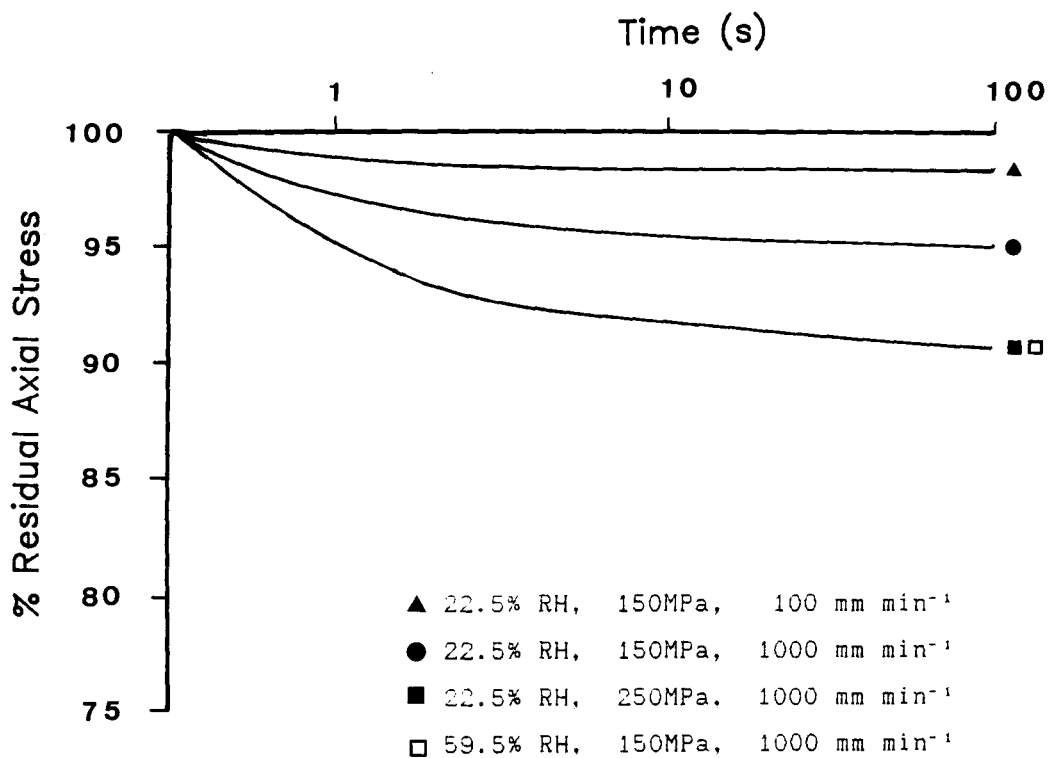
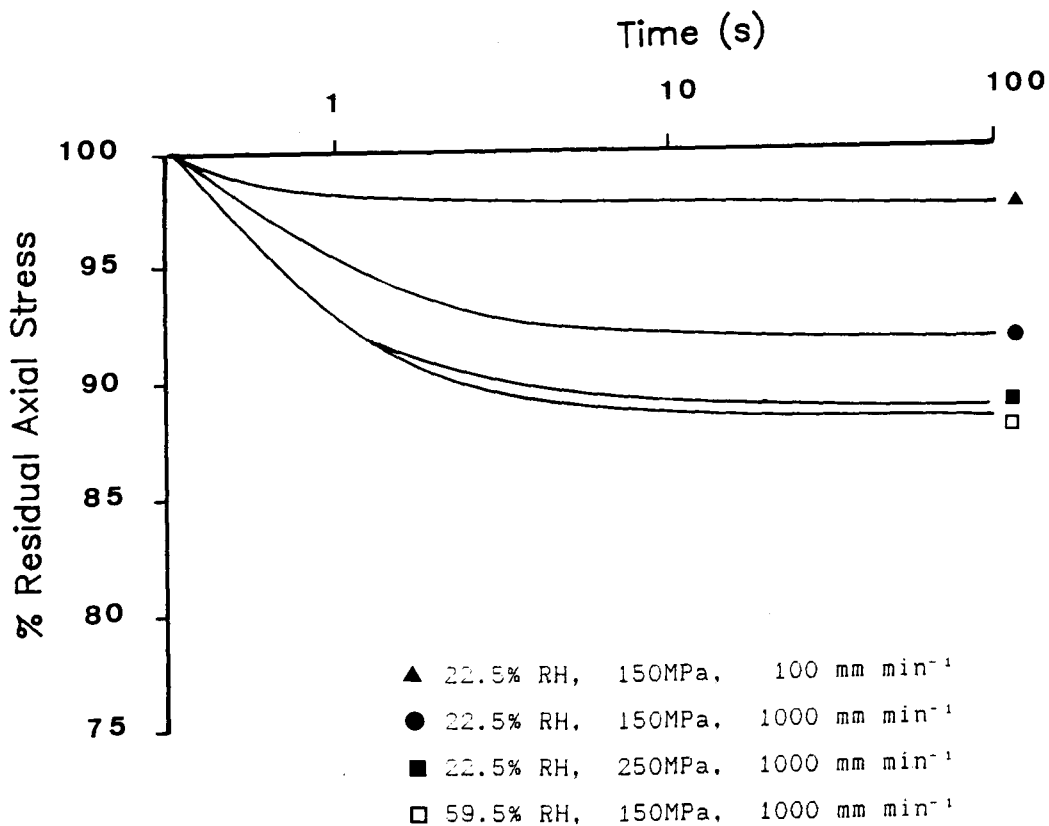


Figure 6.18 Stress-Relaxation of Dicalcium Phosphate Granulates



Comparison of Figs. 6.17 and 6.18 suggested that the initial relaxation rate for dicalcium phosphate was greater than that for paracetamol while at longer times, the converse was true.

Hiestand et al., (1977) noted that brittle materials exhibit a slower and reduced total relaxation compared with plastic materials. The initial relaxation rate for paracetamol was slower than for the brittle dicalcium phosphate and the magnitude of relaxation was less after 100 seconds. The slow and limited ability to deform plastically contributes to the tableting problems encountered with paracetamol.

Under identical test conditions (150MPa peak stress and 1000mm min⁻¹ strain rate) the extent of stress-relaxation was not significantly affected by increasing the conditioning humidity from 22.5% RH to 59.5% RH. This reflected the low affinity for moisture exhibited by paracetamol and dicalcium phosphate. In contrast, incorporation of 1.03% w/w PEG 200 into the granule resulted in a small but consistent decrease in stress-relaxation. Rees and Rue (1978) observed that the presence of a lubricant (magnesium stearate) decreased the stress-relaxation of some excipients. In the present work, it seems that PEG 200 also acted as a lubricant, reducing localised high stress concentrations from which relaxation would tend to occur.

Increasing the peak compaction pressure from 150MPa to 250MPa resulted in an apparent decrease in the rate and extent of stress-relaxation of paracetamol and dicalcium phosphate. After 100 seconds, the percentage stress-relaxation of the former was reduced from 8.9% (13.3MPa) to 5.3% (13.2MPa) while that of the latter was reduced from 11.2% (16.7MPa) to 8.9% (22.3MPa). The actual stress dissipated (in MPa) during the constant strain period was, however, unchanged for paracetamol and actually increased for dicalcium phosphate. The differences observed between the relative (percentage) and absolute stress dissipated indicates that stress-relaxation data must be evaluated with some caution. Cook and Summers (1986) also observed that the relaxation characteristics of some compressed single and multicomponent systems varied with the maximum upper punch pressure applied. They observed that the relaxation of mixture was more complex than an additive function of the properties of the individual components. Compression to a higher initial peak stress will increase

densification and reduce the void space available for further plastic deformation within the confines of the die. The higher initial stress may, however, facilitate greater plastic deformation where this is not grossly restricted by excessive confinement.

Reducing the loading strain rate from 1000mm min^{-1} to 100mm min^{-1} reduced the stress-relaxation of paracetamol and dicalcium phosphate granulates both as a percentage of the peak stress (150MPa) and in terms of the actual stress dissipated. For both substrates, residual plasticity was almost eliminated. The reduction in stress-relaxation observed at the lower strain rate may reflect decreased voidage available for further plastic deformation. A further possibility is that the propensity for plastic deformation was dissipated during the longer loading phase of compression. The latter factor was probably most significant since the duration of loading at the slower strain rate was very similar to the duration of the initial rapid stress-relaxation phase noted above.

6.3.3.2 The Effect of Granulation with a Binder on Stress-Relaxation

Tables 6.13 and 6.14 show the stress-relaxation characteristics of paracetamol and dicalcium phosphate granulates manufactured by wet-massing with a binder. The data was calculated as the mean percentage stress decay after 100s holding time at constant strain. Granules were conditioned prior to testing by equilibration at either 22.5% RH or 59.5% RH and were compressed at a strain rate of 1000mm min^{-1} to a peak compaction pressure of either 150MPa or 250MPa. Testing on granules equilibrated at 22.5% RH was also repeated at the lower strain rate of 100mm/min to investigate the influence of deformation during loading on the stress-relaxation. Representative stress-relaxation curves for the binder-massed granulates are shown in Figures 6.19 and 6.20 for paracetamol and dicalcium phosphate respectively.

Table 6.13 Effect of Binder Type on the Stress-Relaxation of Paracetamol Granulates

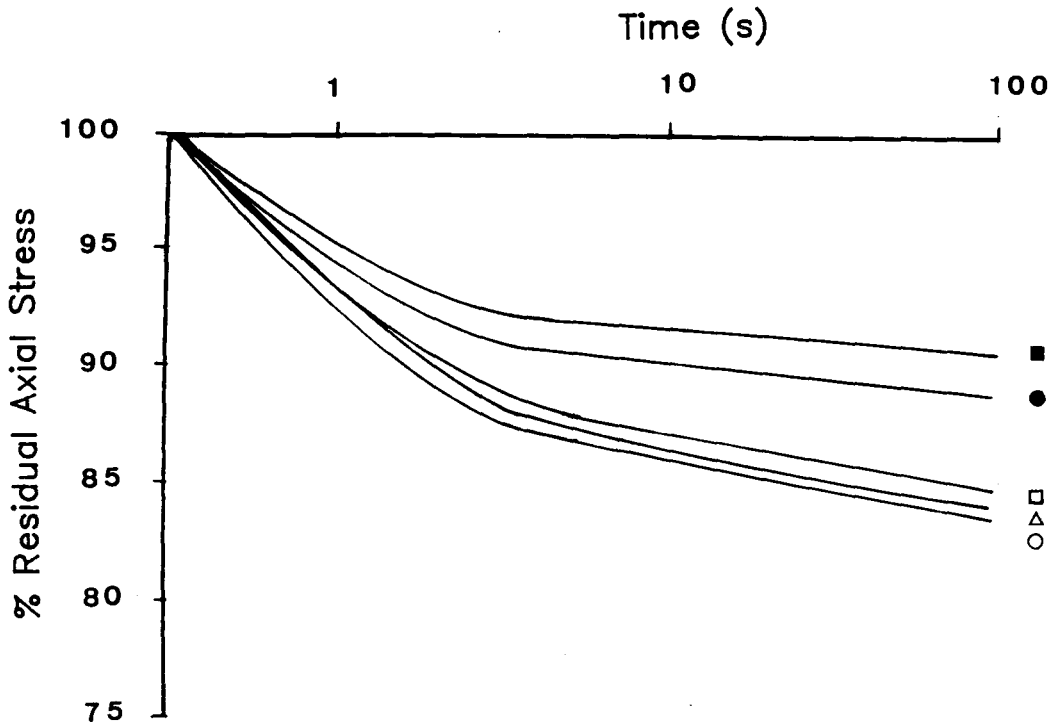
Strain Rate (mm min ⁻¹)	1000		100
Peak Compaction Pressure (MPa)	150	250	150
22.5% RH			
	Percentage Stress Decay at Constant Strain		
No Binder	8.9	5.3	0.5
Sucrose	12.2	9.1	1.6
PVP	14.5	11.8	2.4
HPMC	16.5	12.6	3.0
Starch 1500	15.6	12.5	2.9
59.5% RH			
No Binder	8.8	-	-
Sucrose	14.4	-	-
PVP	20.0	-	-
HPMC	18.8	-	-
Starch 1500	17.5	-	-

Table 6.14 Effect of Binder Type on the Stress-Relaxation of Dicalcium Phosphate Granulates

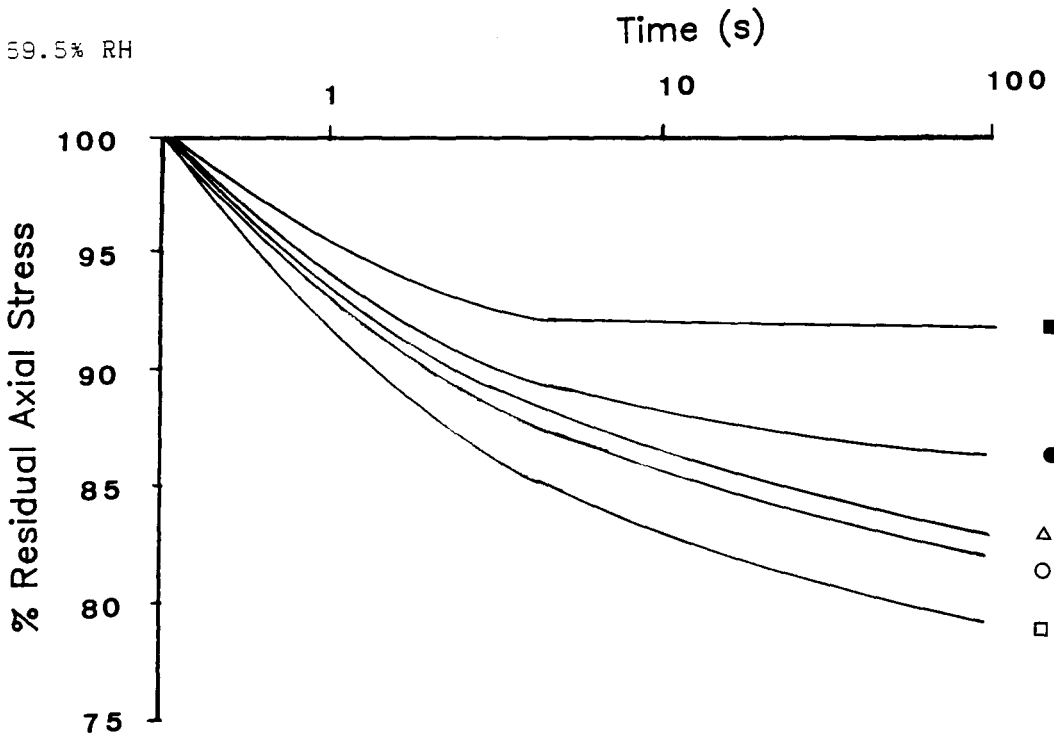
Strain Rate (mm min ⁻¹)	1000		100
Peak Compaction Pressure (MPa)	150	250	150
22.5% RH			
	Percentage Stress Decay at Constant Strain		
No Binder	11.2	8.9	2.2
Sucrose	11.9	8.9	2.1
PVP	12.0	9.5	3.3
HPMC	14.0	10.4	3.2
Starch 1500	13.7	10.3	5.2
59.5% RH			
No Binder	12.0	-	-
Sucrose	12.6	-	-
PVP	16.7	-	-
HPMC	16.3	-	-
Starch 1500	15.8	-	-

Figure 6.19 Effect of Binder Type on the Stress-Relaxation of Paracetamol

a. 22.5% RH



b. 59.5% RH

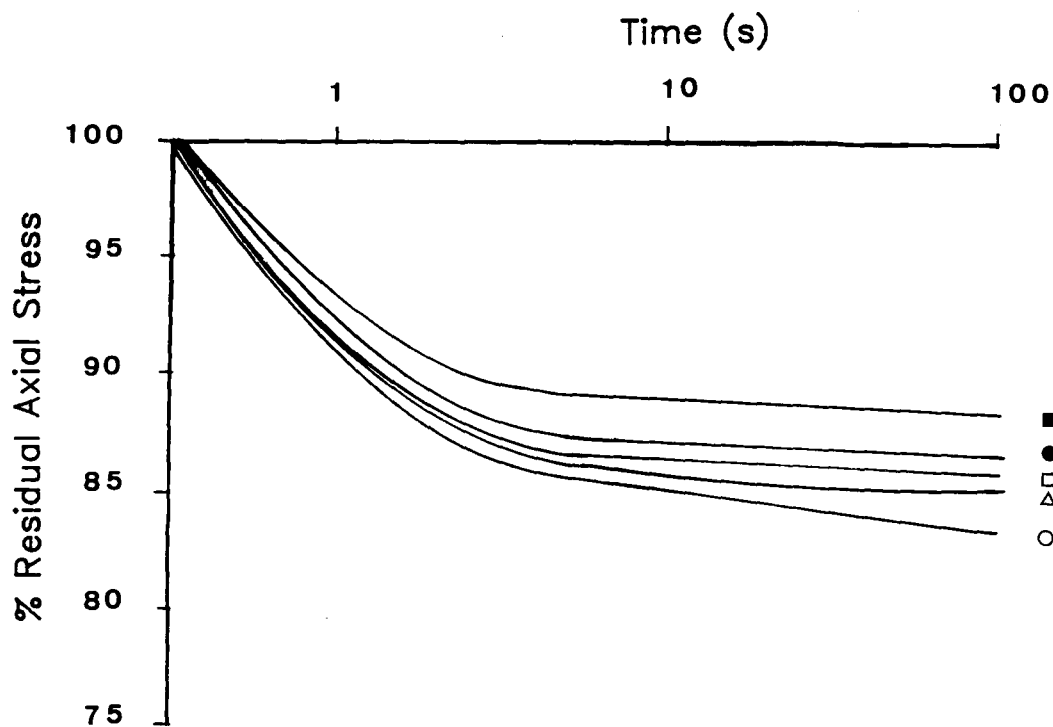


Binder

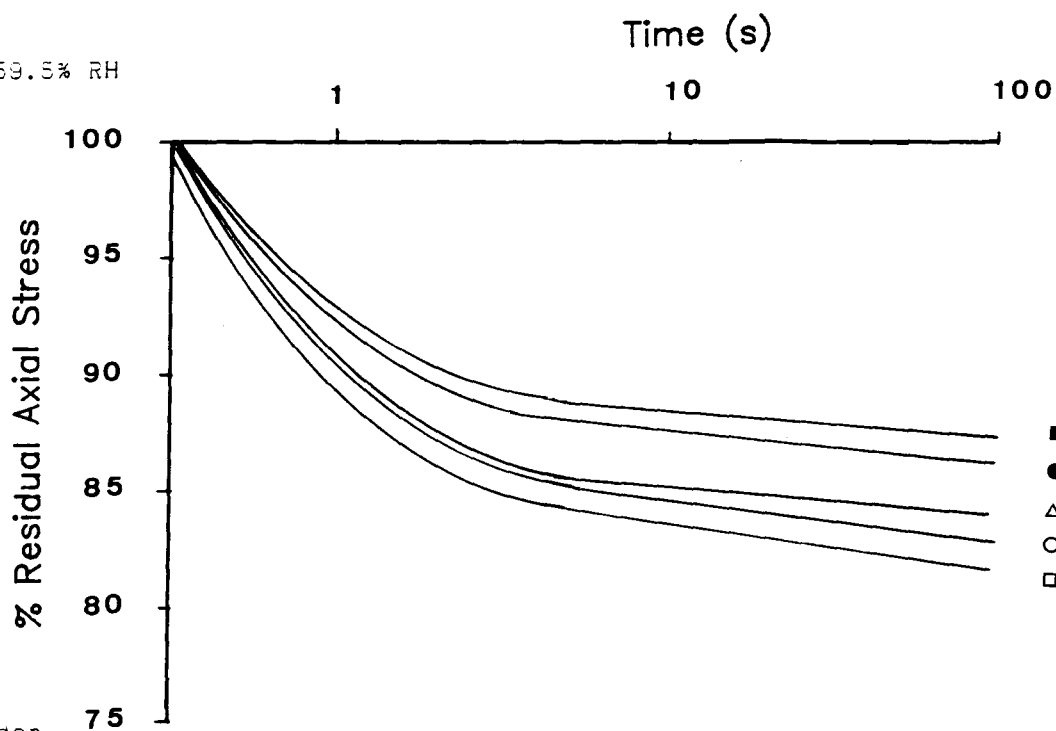
None ■ Sucrose ● PVP □ HPMC ○ Starch 1500 △

Figure 6.20 Effect of Binder Type on the Stress-Relaxation of Dicalcium Phosphate Granulates

a. 22.5% RH



b. 59.5% RH



Binder

None ■ Sucrose ● PVP □ HPMC ○ Starch 1500 △

The presence of a binder, irrespective of type, resulted in a greater stress-relaxation than observed for the substrates alone (section 6.3.1.2). Earlier studies (section 6.3.1.1) demonstrated that at low compaction pressures, granules (of paracetamol or dicalcium phosphate) prepared without a binder densified readily. The presence of a binder, however, resulted in greater granular integrity and initial resistance to consolidation. At a compaction pressure of 150MPa, the increase in stress-relaxation due to the presence of a binding agent might reflect a greater proportion of void spaces to accommodate further plastic flow. Stress relaxation studies were therefore repeated at 250MPa peak compaction pressure where granules prepared with a binding agent exhibited greater densification. Comparison of the results (Tables 6.13 and 6.14) with those for the substrates alone (Tables 6.11 and 6.12) confirmed that the binder induced plasticity was real and not simply a voidage effect. The percentage stress-relaxation observed at 250MPa was, however, lower than observed at 150MPa.

The rate and extent of stress-relaxation was dependent on the binder type and on the conditioning humidity. For granules conditioned at 22.5% RH the rank order for stress-relaxation was:

HPMC > Starch 1500 > PVP > sucrose

Conditioning the granulates at 59.5% RH resulted in increases in the rate and extent of stress-relaxation and also a change in the rank order thus:

PVP > HPMC > Starch 1500 > sucrose

Sucrose, a brittle crystalline material, was the least effective binder in terms of plasticity enhancement for both substrates. For granules conditioned at 22.5% RH, PVP was only marginally better, consistent with its brittle glassy nature when dry and unplasticized.

The change in stress-relaxation rank order observed at the higher humidity reflected the relative moisture affinity of the binders and the ability of sorbed moisture to plasticize hydrophilic polymers. In an earlier section (6.3.1.2) it was noted that an increase in conditioning humidity was associated with increased granule densification at equivalent compaction pressures. This would be

expected to reduce propensity for further plastic deformation on account of the reduced residual voidage. The results of this section indicate, however, that binder dependent differences in stress-relaxation were not determined simply by the extent of consolidation.

Stress-relaxation profiles for the binder-massed granulates (Figs. 6.20 and 6.21) exhibited a biphasic character similar to those for the substrates alone. Visual inspection indicated that the initial relaxation rate of dicalcium phosphate granulates was greater than that of paracetamol granulates. In contrast, the second relaxation phase was slower and more limited in extent for the dicalcium phosphate granules than for the paracetamol granules.

Differences in the form of the stress-relaxation profile reflected differences in the fundamental mechanical nature of paracetamol and dicalcium phosphate. In its simplest form, stress-relaxation can be modelled by the Maxwell unit, i.e. a spring and dashpot in series. Elastic strain, stored during the loading phase of compression, provides the driving force for any subsequent plastic deformation at constant strain. Differences in the nature of stress-relaxation observed for paracetamol and dicalcium phosphate in the present work can be ascribed to the mechanical characteristics of their respective spring and dashpot analogues.

Reducing the loading strain rate from 1000mm min^{-1} to 100mm min^{-1} reduced the percentage stress-relaxation of both paracetamol and dicalcium phosphate granulates. This was due to the greater extent of plastic deformation and densification occurring during the longer loading phase. The presence of a binder did, however, result in greater residual plasticity than observed for the substrates alone.

6.3.3.3 The Effect of Binder Plasticity on Stress-Relaxation

Tables 6.15 and 6.16 show the stress-relaxation characteristics of paracetamol and dicalcium phosphate respectively when granulated with plasticized binders. A peak stress of 150MPa was used in all cases.

Table 6.15 Effect of Plasticizer Concentration on the Stress-Relaxation of Paracetamol Granulates

Relative humidity		22.5%		59.5%
Strain Rate (mm min ⁻¹)		1000	100	1000
Percentage Stress Decay at Constant Strain				
Plasticizer Level %				
PVP	0	14.5	2.9	20.0
+ PEG 200	5	16.3	3.5	21.0
+ PEG 200	10	17.5	5.6	22.6
+ PEG 200	15	21.1	8.7	27.2
HPMC	0	16.5	3.0	18.8
+ PEG 200	10	22.0	5.0	25.5
+ PEG 200	20	35.6	12.4	33.4
+ PEG 200	30	46.1	18.4	35.8
Starch 1500	0	15.6	2.4	17.5
+ Glycerol	10	16.5	3.7	19.1
+ Glycerol	20	18.5	5.3	23.3
+ Glycerol	30	24.2	7.5	26.7

Granules were conditioned prior to testing by equilibration at either 22.5% RH or 59.5% RH and were compressed at a strain rate of 1000mm min⁻¹. Testing on granules equilibrated at 22.5% RH was repeated at a lower strain rate of 100mm min⁻¹ to investigate the influence of deformation during loading on the stress-relaxation.

Table 6.16 Effect of Plasticizer Concentration on the Stress-Relaxation of Dicalcium Phosphate Granulates

Relative humidity		22.5%		59.5%
Strain Rate (mm min ⁻¹)		1000	100	1000
Percentage Stress Decay at Constant Strain				
Plasticizer Level %				
PVP	0	12.0	3.3	16.7
+ PEG 200	5	13.5	3.9	19.3
+ PEG 200	10	15.8	5.8	21.6
+ PEG 200	15	17.5	6.5	24.8
HPMC	0	14.0	3.2	16.3
+ PEG 200	10	15.1	3.8	17.2
+ PEG 200	20	16.8	5.5	19.4
+ PEG 200	30	20.5	6.4	25.4
Starch 1500	0	13.7	5.2	15.8
+ Glycerol	10	13.8	5.5	19.0
+ Glycerol	20	16.1	6.0	20.7
+ Glycerol	30	19.5	6.9	23.8

Plasticization of the polymeric binders resulted in an increase in both the rate and magnitude of stress-relaxation under constant strain compared with the unplasticized binders. This was observed regardless of the binder type or the granule substrate. The rate and extent of relaxation was observed to increase with the level of plasticizer. These results are illustrated for granules conditioned at 22.5% R.H. and compressed at a strain rate of 1000mm min⁻¹ in Figs. 6.21 to 6.26. The stress-relaxation of granules conditioned at the higher relative humidity was generally greater than observed for the lower humidity. This reflected the additional plasticizing activity of the sorbed moisture on the polymeric binders. An exception to this trend was noted in the behaviour of paracetamol granulated with plasticized HPMC (Table 6.15).

Figure 6.21 Effect of Plasticizer Concentration on the Stress-Relaxation of HPMC-massed Paracetamol Granulates

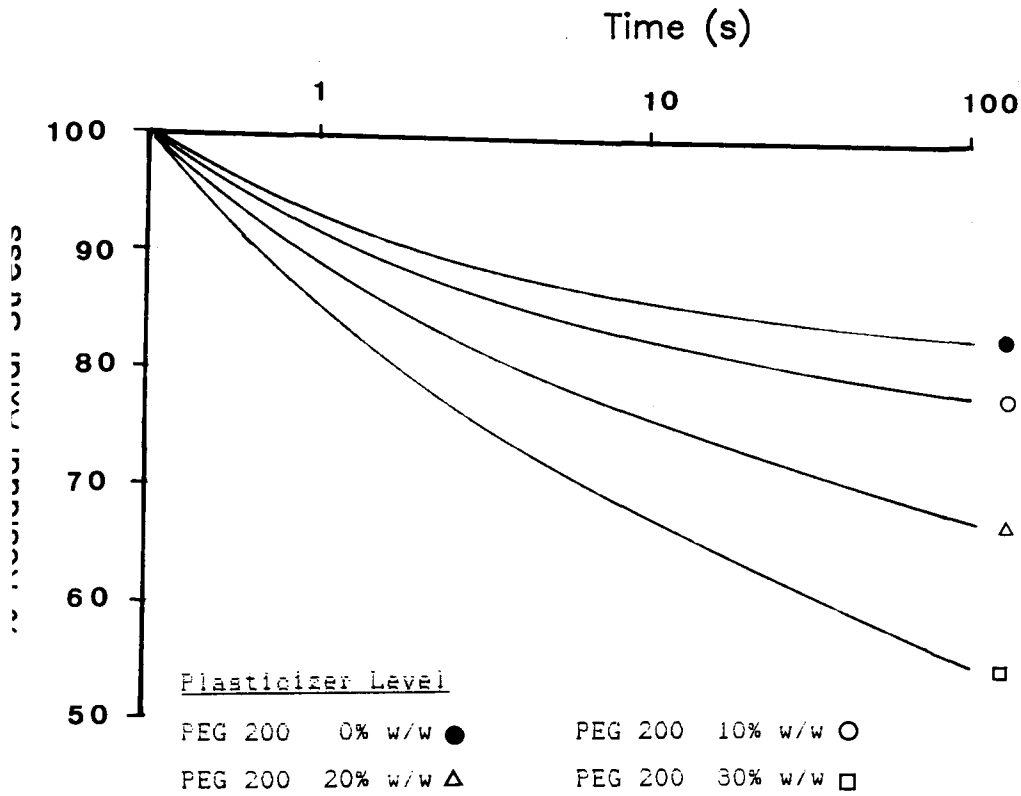


Figure 6.22 Effect of Plasticizer Concentration on the Stress-Relaxation of HPMC-massed Dicalcium Phosphate Granulates

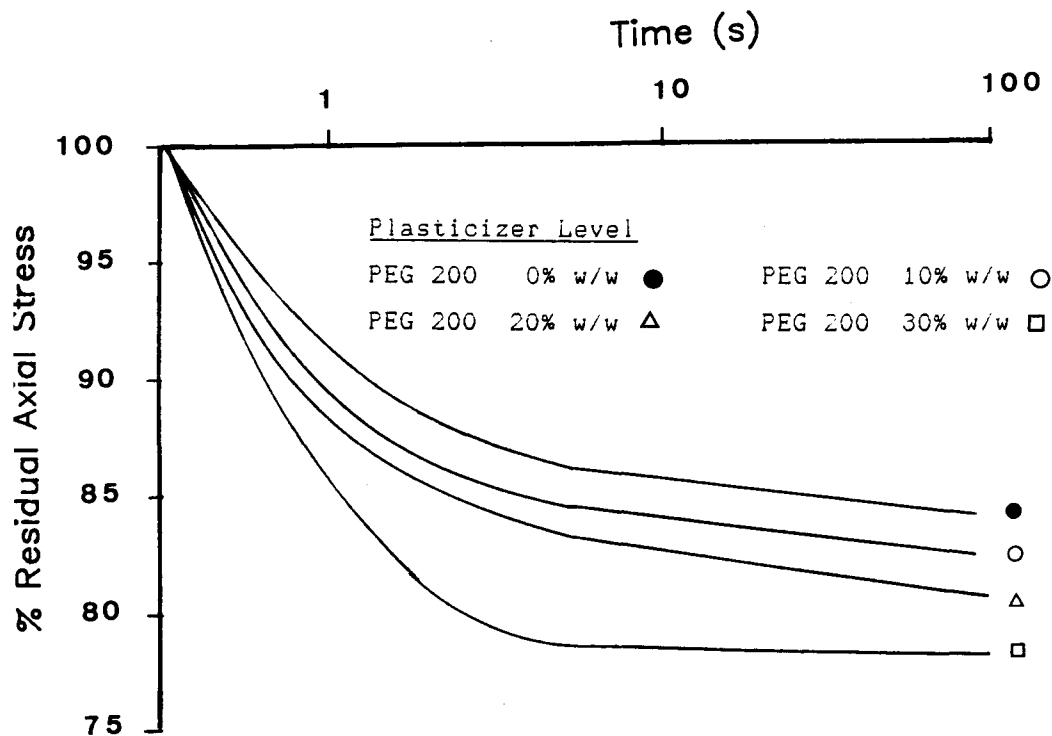


Figure 6.23 Effect of Plasticizer Concentration on the Stress-Relaxation of PVP-massed Paracetamol Granulates

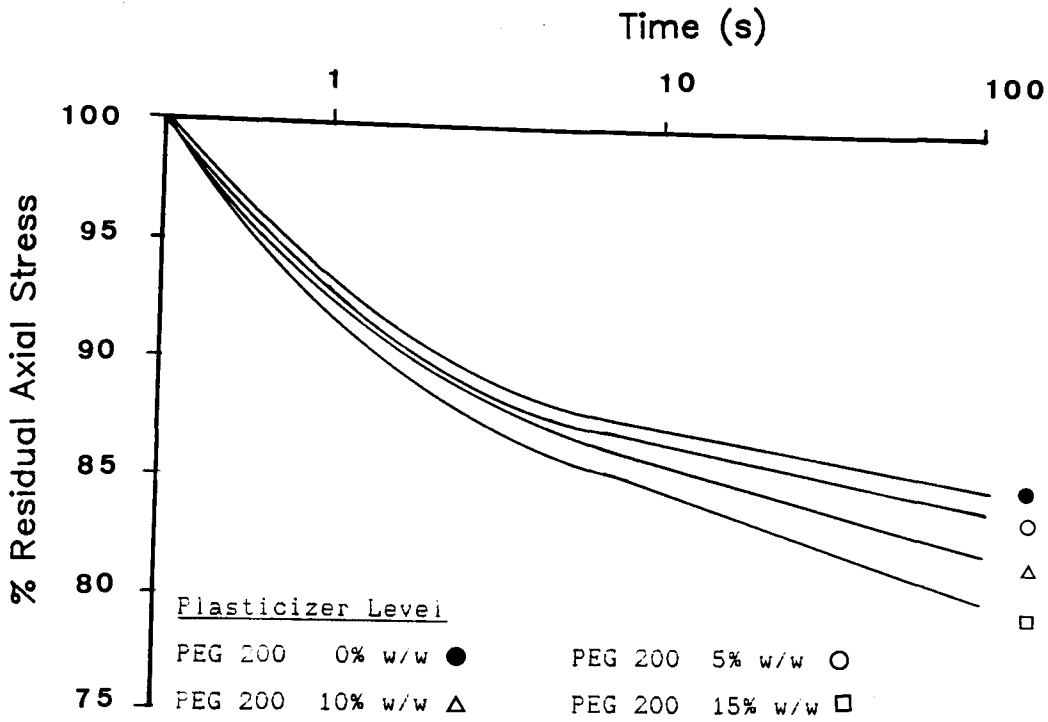


Figure 6.24 Effect of Plasticizer Concentration on the Stress-Relaxation of PVP-massed Dicalcium Phosphate Granulates

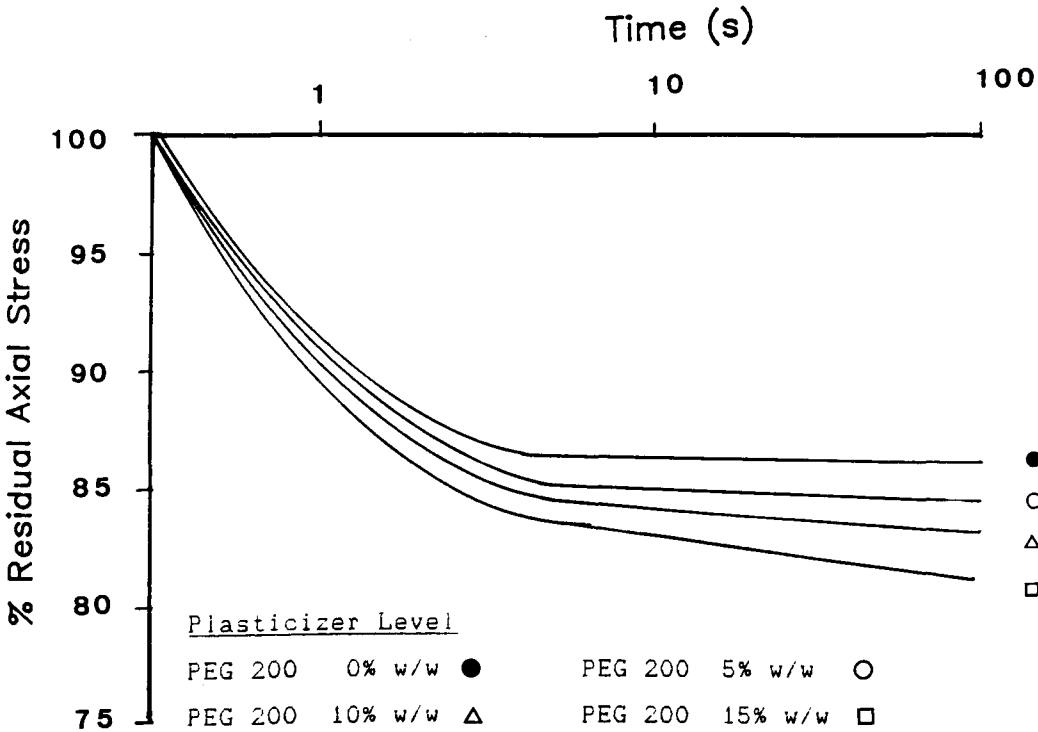


Figure 6.25 Effect of Plasticizer Concentration on the Stress-Relaxation of Starch 1500-massed Paracetamol Granulates

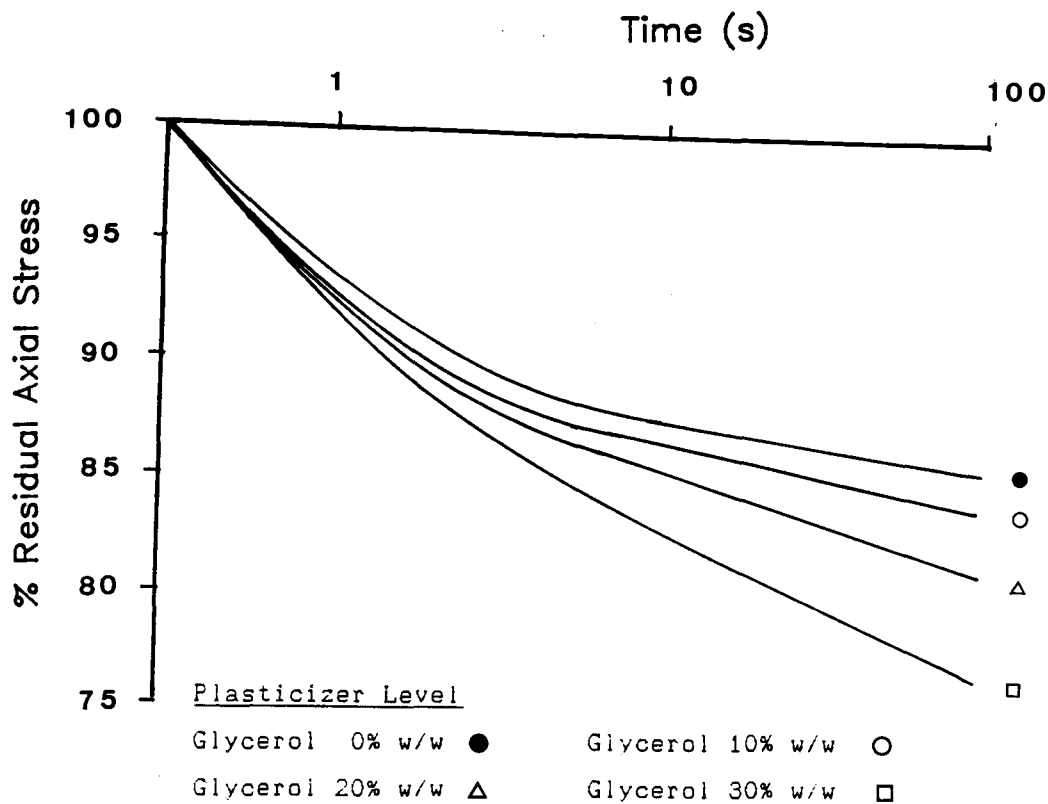
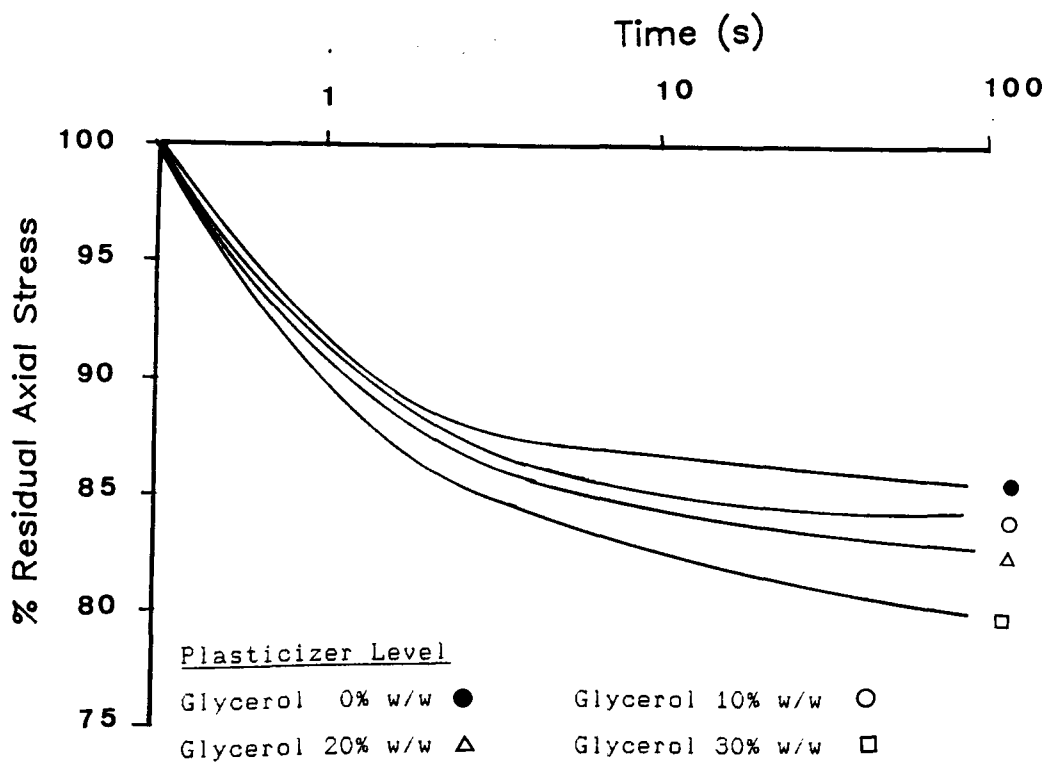


Figure 6.26 Effect of Plasticizer Concentration on the Stress-Relaxation of Starch 1500-massed Dicalcium Phosphate Granulates



At the 20% and 30% levels of plasticizer inclusion, the percentage stress decay after 100 seconds was lower for granules conditioned at 59.5% RH than for those at 22.5% RH. In the latter cases it was concluded that the extent of plastic deformation during compression and the degree of densification achieved, limited the potential for further stress-relaxation. Similar behaviour during the compression of damp polymeric binder powders has been noted by Cutt (1983).

Granules compressed at a strain rate of 100mm min^{-1} exhibited slower and reduced stress-relaxation compared with those compressed at 1000mm min^{-1} . All granulates compressed at the slower rate nevertheless had a finite capacity for stress-relaxation and this was increased at higher plasticizer levels both for the paracetamol granulates and for the dicalcium phosphate granulates. The dependence of the measured stress-relaxation on the initial strain rate reflected two interdependent factors. Firstly, the extent of plastic deformation occurring during the loading phase of compression and secondly, the residual void space available to accommodate stress-relaxation. Slower initial strain rates resulted in greater plastic deformation during compression (with concurrent stress-relaxation) and greater densification at the holding strain. Both these factors limited the potential for further stress-relaxation.

6.3.3.4 The Effect of a Low Efficiency Plasticizer on Stress-Relaxation

The presence of a liquid inclusion in a granulate may act as a lubricant, aiding densification and opposing subsequent stress-relaxation. The results presented in section 6.3.1.1 suggested that PEG 200 and sorbed moisture could, in the absence of a binder, behave in this way. Subsequent results indicated, however, that in the presence of a polymeric binder, moisture sorption or a plasticizer mediated their activity via effects on the plasticity of the polymer. As a further check to exclude non-specific effects on stress-relaxation, a comparison of the stress-relaxation of HPMC-massed granulates containing either PEG 200 or PEG 600 (the latter demonstrated to be an inferior plasticizer) was carried out.

In both cases a peak compaction pressure of 150MPa was used with a strain rate of 1000mm min⁻¹.

The results shown in Table 6.17 demonstrate that for both substrates, the incorporation of the inferior plasticizer resulted in reduced stress-relaxation after 100 seconds. In the event that the plasticizer activity resulted from a non-specific liquid film effect, the observed stress-relaxation would be similar for PEG 200 and PEG 600. The results, however, confirmed that the effect of plasticizer inclusion on stress-relaxation was mediated through an effect on binder plasticity.

Table 6.17 Effect of Plasticizer Type on the Stress-Relaxation of HPMC-Massed Granulates (22.5% RH)

Percentage Stress Decay at Constant Strain				
Plasticizer		PEG 200	PEG 600	
Substrate	Plasticizer			
	Level %			
	Paracetamol	0	16.5	11.7
		10	22.0	17.9
	20	35.6	24.3	
	30	46.1	31.2	
Dicalcium Phosphate		0	14.0	12.5
		10	15.1	14.5
		20	16.8	13.2
		30	20.5	16.9

6.4 Elastic Strain Recovery

The elastic recovery of compressed materials has been assessed by a number of methods and at various times post-compression as noted in section 1.2.6. In many cases, the measured response would have included some viscoelastic strain recovery as well as the ideally instantaneous elastic response. In the present work, axial elastic strain recovery (ER) was determined within the die immediately after decompression, using the ram displacement transducer of the Mayes Press. ER was defined thus:

$$ER = [(H_0 - H_p) / H_p] \times 100\% \quad (6.2)$$

where H_p was the tablet thickness at a specified maximum upper punch pressure P_{MAX} , and H_0 was the tablet thickness after decompression within the die after minimal holding time.

Percentage elastic recovery for dicalcium phosphate granulates and for paracetamol granulates, equilibrated at either 22.5% RH or 59.5% RH, was determined using a loading rate of 1000mm min^{-1} and a maximum upper punch pressure of 150MPa. For selected granulates, the influence of a longer contact time on elastic recovery was investigated by using a slower loading rate of 100mm min^{-1} . Release of the compaction load was initiated manually as soon as the maximum upper punch pressure had been achieved. In all cases, the dwell period between achieving maximum pressure and release of pressure was less than one second. Decompression occurred within about 100ms and consequently the axial recovery of the compact (logged automatically as soon as compaction force had decayed to a reference of 1MPa) reflected elastic strain with minimal influence of viscoelasticity. Percentage strain recoveries determined as the mean of three runs are given in Table 6.18.

Differences in the elasticity of the base substrates, dicalcium phosphate and paracetamol, were obvious. In the absence of binder elastic strain recoveries for granules conditioned at 22.5% RH were 3.3% for dicalcium phosphate compared with 12.7% for paracetamol. The relative magnitude of the respective strain recoveries indicated that dicalcium phosphate formed relatively stiff tablets of high modulus. Paracetamol, in contrast, formed tablets of lower modulus.

Table 6.18 Percentage Post-Compression Elastic Strain Recovery
for Paracetamol and Dicalcium Phosphate Granulates

	Dicalcium phosphate			Paracetamol			
	22.5% RH	59.5% RH		22.5% RH	59.5% RH		
Loading	1000	100	1000	1000	100	1000	
Rate mm min ⁻¹							
Binder	Plasticizer						
	Level % w/w						
None	3.3	3.3	3.7	12.7	12.2	13.0	
Sucrose	3.4	3.5	3.5	11.8	10.3	10.3	
PVP	0	3.6	3.6	4.0	7.5	7.3	9.1
+ PEG 200	5	3.8	3.2	3.3	7.3	7.0	8.8
+ PEG 200	10	3.7	3.6	3.4	7.5	7.0	9.5
+ PEG 200	15	4.0	2.9	2.9	7.8	6.5	9.5
HPMC	0	3.6	3.5	3.7	8.3	8.1	9.8
+ PEG 200	10	3.9	3.3	3.3	8.8	8.2	8.5
+ PEG 200	20	4.2	3.5	3.5	9.6	8.0	9.1
+ PEG 200	30	4.1	3.5	3.4	9.5	7.3	9.2
Starch 1500	0	3.7	3.6	3.8	10.6	10.3	8.6
+ Glycerol	10	4.1	3.0	3.3	10.4	9.9	9.3
+ Glycerol	20	3.6	3.5	3.6	8.4	7.8	9.7
+ Glycerol	30	4.0	3.1	3.3	8.4	7.4	9.3

The magnitude of elastic strain recovery for paracetamol correlated with the poor tablettability of this material noted in Chapter five. Substrate dependent differences were also apparent from the elastic recoveries of granulates containing a binder. Generally, there was little difference between the binders with respect to the elastic recovery observed. Dicalcium phosphate granulates equilibrated at 22.5% RH generally showed a small increase in strain recovery which appeared to be independent of the binder used. This probably reflected the lower elastic modulus of the binders compared with dicalcium phosphate resulting in an increased elastic strain for the

binder-substrate matrix. The influence of plasticizer on the extent of strain recovery was not consistent for any of the polymeric binders used, but suggested a small increase in axial recovery, consistent with a plasticizer mediated decrease in binder modulus. Dicalcium phosphate granulates formed with unplasticized binders and equilibrated at the higher relative humidity also showed an increase in elastic recovery. This may be interpreted in terms of a moisture mediated decrease in the elastic moduli of the binders. Granulates containing plasticized binders at the higher humidity exhibited a slight decrease in elastic recovery reflecting the enhanced ability to dissipate elastic strain by stress-relaxation.

In contrast with the behaviour of dicalcium phosphate, binder incorporation decreased the elastic recovery of paracetamol. PVP and HPMC facilitated a greater decrease in elastic recovery than Starch 1500 or sucrose. The presence of the binder either dissipated elastic strain by stress-relaxation during compression or reduced elastic strain by preferential deformation of the more plastic binder. The presence of increasing levels of plasticizer in the polymeric binders produced small and inconsistent changes in the elastic recovery. Increased binder plasticity in granules equilibrated at the higher relative humidity showed some tendency to increase elastic recovery.

Incorporation of a plasticizer in a polymeric binder produces two contrasting actions with respect to the elasticity of a tablet. On the one hand, plasticization enhances the ability to dissipate elastic strain by stress-relaxation. On the other hand, however, the reduced binder modulus may result in a softer binder-substrate matrix which exhibits greater elastic strain under compression. The relatively small influence of binder plasticity on elastic strain recovery indicated that the predominant factor remained the elastic deformation of the base substrate.

Compression at a lower strain rate of 100mm min^{-1} had no significant influence on the elastic recovery of dicalcium phosphate or paracetamol granulated in the absence of a binder. In general a decrease in elastic strain recovery was observed for both dicalcium phosphate and paracetamol granulates containing a binder. Incorporation of a plasticizer in the polymeric binders facilitated a reduction in

elastic recovery after compression at the lower loading rate compared with the higher loading rate. There was no consistent trend noted with increasing levels of plasticizer. At slower loading rates, greater time is available for non-recoverable deformation of the plastic components of a binder-substrate matrix. The magnitude of elastic strain at slower compaction rates may be diminished either by preferential deformation of the plastic components and/or dissipation of elastic strain by concurrent stress-relaxation. A limiting elastic strain value, determined by the modulus of the binder-substrate matrix compressed to zero porosity might be expected, however.

The literature contains little information on the influence of compaction rate on elastic strain in tablets. Celik (1984) observed that the elastic strain recovery of some direct compression bases decreased with increased holding time at constant stress. Similar behaviour was observed for ibuprofen (Marshall et al., 1986). In both cases, the duration of holding was of the order of seconds and thus considerably longer than the maximum compression time of even the slowest tablet presses.

6.5 Plasto-Elasticity Indices

A considerable amount of data has been amassed in the literature which suggests that the physical properties of a tablet are dependent on the relative proportion of bonding plastic deformation (occurring during compression) and debonding elastic deformation (occurring during decompression). A number of methods, reviewed in section 1.2.7 have been proposed to quantify the bonding and debonding contributions. The Elastic Recovery Index (Celik, 1984) or plasto-elasticity ratio (Malamataris et al., 1984) have been useful developments in this area. The two approaches which are essentially identical, express the relative debonding and bonding contributions as the ratio of elastic strain recovery during decompression to strain movements occurring during a holding period at constant stress. The fundamental correctness of the approach may be questioned however. Strain in a compact held at constant stress is a creep phenomenon and may result from retarded elastic deformation in addition to plastic flow. Some workers have used the erroneous description "stress-relaxation" implying that the deformation was purely plastic rather than

viscoelastic. Strain recovery determined at some time after ejection from the die would also contain some element of retarded elasticity in addition to the ideally instantaneous response. The latter problem is largely avoided by determining elastic recovery within the die as in section 6.4

In the present work, a modified approach was adopted to assess the balance of bonding and debonding deformation in the absence of retarded elasticity. A new plasto-elasticity ratio ER/SR was defined where ER was the axial elastic strain recovery defined previously (equation 6.2) and SR was the stress-relaxation defined thus:

$$SR = [(P_{MAX} - P_{100}) / P_{MAX}] \times 100\% \quad (6.3)$$

where P_{MAX} was the maximum upper punch pressure and P_{100} was the residual upper punch pressure after 100 seconds holding time at constant strain.

Values for SR and ER were determined in separate experiments and have been reported previously in sections 6.3.3 and 6.4. In the calculation of ER/SR it was implicit that the same compression strain rate was used in the determination of both components. Table 6.19 shows the calculated plasto-elasticity ratios for paracetamol and dicalcium phosphate respectively.

Examination of the ratios revealed a number of features. The ratio was observed to be much smaller for dicalcium phosphate than for paracetamol and this was due to the smaller elastic strain recovery. Incorporation of a binder resulted in a reduction in the ratio. This was primarily due to the increased plasticity of the granulation rather than a decrease in elastic strain. Increasing the plasticity of the polymeric binders by the incorporation of a plasticizer, or equilibration at the higher humidity, further reduced the plasto-elasticity ratios. This was also due mainly to increased granular plasticity rather than decreased elastic strain. In some cases increased binder plasticity actually resulted in an increased elastic strain recovery as shown in Table 6.18. This could result from the increased densification during compression and/or the reduction in elastic modulus for plasticized binders compared with unplasticized binders.

Table 6.19 Plasto-Elasticity Ratios (ER/SR) for Paracetamol and Dicalcium Phosphate Granulates

	Dicalcium phosphate			Paracetamol			
	22.5% RH	59.5% RH		22.5% RH	59.5% RH		
Loading rate mm min ⁻¹	1000	100	1000	1000	100	1000	
Binder	Plasticizer						
	Level %						
Water	0.29	1.50	0.30	1.43	24.40	1.48	
Sucrose	0.28	1.66	0.28	0.97	6.34	0.72	
PVP	0	0.30	1.09	0.24	0.52	3.04	0.46
+ PEG 200	5	0.28	0.82	0.17	0.45	2.00	0.41
+ PEG 200	10	0.23	0.62	0.16	0.42	1.25	0.42
+ PEG 200	15	0.23	0.44	0.12	0.37	0.75	0.35
HPMC	0	0.26	1.09	0.23	0.50	2.70	0.46
+ PEG 200	10	0.26	0.86	0.19	0.40	1.64	0.33
+ PEG 200	20	0.25	0.63	0.18	0.27	0.65	0.27
+ PEG 200	30	0.20	0.54	0.13	0.21	0.40	0.26
Starch 1500	0	0.27	0.70	0.24	1.47	3.81	0.49
+ Glycerol	10	0.30	0.54	0.17	0.63	2.67	0.48
+ Glycerol	20	0.22	0.58	0.17	0.45	1.47	0.42
+ Glycerol	30	0.20	0.45	0.14	0.35	0.98	0.35

For granules compressed at the slower strain rate of 100mm min⁻¹ the magnitude of plasto-elasticity indices changed significantly although the trend in relation to the binder plasticity remained constant. This was due to the marked influence of strain rate on the magnitude of plastic deformation as determined by stress-relaxation. Elastic strain, being (ideally) independent of time was relatively unaffected by strain rate.

6.6 Conclusions

It was possible to evaluate the densification of paracetamol and dicalcium phosphate granulates using Heckel plots as the data exhibited linearity at pressures above 150MPa when plotted in this manner. Deviations from linearity were found at lower pressures, as is commonly the case, and these represented granular rearrangement and low pressure failure of the granules. The linear portion of the Heckel plot was considered to represent bulk plastic deformation of the granular mass, fracture of the primary substrate material and any elastic strain occurring during compression.

Dicalcium phosphate was more resistant to consolidation than was paracetamol because of its higher mean yield pressure. The form of the Heckel plots for both substrates was independent of the duration of compression and there was no increase in compact density during a 10 second holding period at maximum upper punch stress. The absence of time-dependence with respect to consolidation indicated that fragmentation was the primary mode of deformation for both substrates. After the incorporation of a binder, granules exhibited greater resistance to consolidation at low pressures. This was due to binder mediated granule strength. Both paracetamol and dicalcium phosphate, massed in the absence of a binder, yielded weak granules which readily failed under low pressure. At higher pressures the presence of a binder facilitated easier consolidation. This was substantiated by a reduction in the mean yield pressure. The relative ease of consolidation of the granulates was dependent on the type of binder used.

Increasing the plasticity of the polymeric binders, either by increased moisture sorption or by the inclusion of a plasticizer, resulted in increased consolidation. This was a generalised phenomenon which was independent of binder type or the substrate material. The increased consolidation resulted both from increased densification at low pressures (corresponding to the curved portion of the Heckel plot) and a decrease in the mean yield pressure (corresponding to an increased slope in the linear part of the Heckel plot). With highly plasticized binders, a paradoxical increase in mean yield pressure was observed. This was attributed to the extent

of densification occurring at lower pressures. This behaviour can be interpreted in terms of the influence of plasticization on the mechanical properties of the polymeric binder as follows. Plasticization reduces the strength of a polymeric binder resulting in a weaker granule which fails more readily at low pressures. Concurrently, plasticization decreases the apparent viscosity of plastic flow for the polymeric binder, facilitating easier deformation under compression and increasing the plastic strain per unit time.

A significant effect of binder-mediated plasticity was the induction of time-dependent consolidation behaviour characterised by increased densification at a slower loading rate, and increased densification under constant compressive stress. This phenomenon was absent for the substrate materials granulated in the absence of any binder. The extent of time-dependency was quantified for a number of granulates using a loading rate sensitivity (LRS) parameter based on mean yield pressures determined at two different rates of compression. This parameter was small, i.e. $LRS < 1$ for the substrate materials granulated in the absence of a binder. But LRS was increased by the incorporation of a binder. Increased moisture sorption or the incorporation of a suitable plasticizer markedly increased LRS for binder massed-granulates.

Stress-relaxation studies, conducted using constant strain conditions, indicated that granulates of paracetamol and dicalcium phosphate granulates exhibited a finite degree of plasticity, even in the absence of binder. These results contrasted with results obtained from Heckel plots performed at two different loading rates. Similarities in the Heckel constants at the two loading rates indicated that the densification of both substrates was independent of time. Similar stress-relaxation results were observed by Cutt (1983) for glass ballotini beads. Static fatigue failure was proposed as a possible mechanism for stress-relaxation of brittle-elastic materials and may explain the behaviour observed here. A further possibility was that, at the strain rates used for the stress-relaxation studies, application of stress was too rapid for rearrangement consolidation to be completed resulting in a dynamic resistance to consolidation. The observed stress-relaxation might then result from further particulate rearrangement, promoting closer packing during the holding period at

constant strain. On the basis of these results it was concluded that stress-relaxation techniques were generally more sensitive for the detection of plastic deformation in tableting models.

Granulation of the substrates with a binding agent increased the plasticity of the matrix resulting both in increased rate and extent of stress-relaxation. Sucrose, a brittle crystalline material, induced less stress-relaxation than the polymeric binders. The stress-relaxation of both paracetamol and dicalcium phosphate granulates was dependent on the plasticity of the incorporated binder and consequently was increased by increased moisture content and by incorporation of increased concentrations of a suitable plasticizer.

The effect of compact density on subsequent stress-relaxation was demonstrated by the reduced relaxation of compacts compressed to a peak upper punch pressure of 250MPa compared with compacts compressed to 150MPa. Studies on pressure-volume relationships for the compacts indicated that compaction over the range 0 to 350MPa compression pressures resulted in greater densification and consequently a reduced porosity to accommodate further plastic flow. This was in agreement with results obtained for powdered polymeric binders and glass ballotini granulates (Cutt, 1983). Stress-relaxation, being a time-dependent phenomenon, was found to be highly sensitive to the compression strain rate. This was true for the substrates granulated in the absence of a binder as well as those containing a binding agent. At the lower strain rate (100mm min^{-1}) the time required to achieve the holding strain was much greater than at the higher strain rate (1000mm min^{-1}). Plastic flow producing densification of the compact and coincident stress-relaxation, occurred to a greater extent at the slower strain rate. This resulted in greater compact density and reduced porosity to accommodate further plastic deformation.

The elastic strain recovery of the compressed granulates on decompression was observed to be determined primarily by the nature of the substrate material. Dicalcium phosphate granulates exhibited much lower elastic strain recovery than the corresponding paracetamol granulates. The magnitude of elastic recovery of paracetamol is well documented and has been implicated in the severe capping tendency of this material. The incorporation of a binder was associated with a

reduction in the elastic strain of paracetamol granulates but resulted in no significant effect on dicalcium phosphate granulates. Increased binder plasticity, due either to increased moisture sorption or plasticizer incorporation, did not result in a general reduction in elastic strain recovery. In many cases, the presence of a more plastic binder actually increased the measured elastic recovery. This was possibly due to the decrease in elastic modulus observed when polymers are plasticized. These results were particularly interesting since the ability of plastic binders to reduced capping tendency has frequently been attributed to a reduction in the elastic strain recovery of the compressed material. Compressing the granules at a lower strain rate of 100mm min^{-1} rather than 1000mm min^{-1} did, however, result in a reduction in the observed elastic strain recovery. The reduction was small and no consistent trend with respect to plasticizer content was identified.

In contrast to the measurement of elastic strain alone, the calculation of a plasto-elasticity index (ER/SR) revealed a number of consistent trends. Paracetamol granulates exhibited higher values for ER/SR than dicalcium phosphate granules due to the greater degree of elastic strain. Considering the tableting characteristics observed in the previous chapter, it was evident that high values for the index correlated with high friability and capping tendency. Increase in moisture sorption or the incorporation of a plasticizer in the polymeric binders resulted in a decrease in ER/SR. This correlates directly with the enhanced tablettability reported in Chapter five.

CHAPTER SEVEN

GENERAL CONCLUSIONS AND SUGGESTIONS FOR FURTHER WORK

CHAPTER SEVEN

GENERAL CONCLUSIONS AND SUGGESTIONS FOR FURTHER WORK

In the work described, it has been shown that the physico-mechanical properties of some commonly used polymeric tablet binders can be modified by plasticization. The deformation of granulates prepared by wet-massed granulation and the properties of the resultant compressed tablets is determined by fundamental material properties of the binder.

In Chapter two, it was shown that the thermodynamics of polymer solutions could be applied to problems of polymer-plasticizer compatibility and plasticizer selection. Two criteria for thermodynamic compatibility between a polymer and potential plasticizer were evaluated; these were solubility parameters and Flory-Huggins interaction parameters. Using these data, it was predicted that PVP would exhibit ideal compatibility with a number of glycols or PEGs used as potential plasticizers. In contrast, the data indicated the potential for phase separation between HPMC and glycols or PEGs. The compatibility predictions were found to be in good agreement with visual/tactile compatibility determinations in aqueous-cast polymer films. Nevertheless, limitations to the thermodynamic approach to polymer-plasticizer compatibility were observed.

PEG 200 was identified as the optimum plasticizer (from those screened) for the polymers PVP and HPMC. In the former case, the selection was based on ideal polymer-plasticizer miscibility. In the latter case, the selection was based on a lower tendency to phase-separation with PEG 200 compared with glycols or other PEGs.

Using the solubility spectrum of Burrell, it was possible to determine solubility parameter values for HPMC and PVP, but not for Starch 1500. The crystallinity of Starch 1500 results in very poor solubility characteristics, even in strongly hydrogen-bonding solvents. As a consequence, this polymer exhibits very limited compatibility with potential plasticizers.

The lattice model for polymer dissolution, proposed independently by Flory and Huggins, defines the conditions for phase equilibrium and phase separation for binary mixtures of a polymer and solvent or plasticizer. The asymmetry of the theoretical polymer-solvent phase equilibrium diagram indicates that non-solvents for a polymer may, however, dissolve in the polymer to some degree. This offers a mechanism by which non-solvent molecules may plasticize a polymer in spite of limited interaction and thermodynamic incompatibility.

An assumption implicit in both solubility parameter approach and the Flory-Huggins model of polymer solutions is that the heat of mixing is positive. This suggests that the direct measurement of heat of mixing, for example by microcalorimetry, may be useful in the evaluation of polymer-plasticizer interactions and in identifying potential plasticizers.

Tensile testing and creep rheology were used to characterise the physico-mechanical properties of binder films and, to quantify the effect of potential plasticizers on the films. Since the polymeric binders used in this work are hydrophilic, the influence of moisture sorption on physico-mechanical properties was investigated.

It was shown that the unmodified polymers differed significantly in their characteristic stress-strain relations. Thus, PVP was classified as a hard, brittle material; HPMC was classified as a hard, tough material and Starch 1500 as a soft weak material. An increase in the moisture content of the polymers, or the inclusion of sufficiently compatible plasticizers resulted in changes in mechanical properties which were consistent with a plasticizer activity. It was possible to explain the observed phenomena by reference to the thermodynamic factors controlling polymer-plasticizer compatibility and, to the gel theory of plasticization. The relative plasticizing efficiency of different molecules could not be explained in terms of the relative hydrogen-bonding potential between the polymer and plasticizer.

The ability of glycerol and, to a lesser extent, propylene glycol to plasticize Starch 1500 was unexpected considering the crystalline nature of starches and their consequent poor compatibility with

potential plasticizers. Glycerol-plasticized and unplasticized Starch 1500 films are qualitatively identical in terms of their X-ray diffraction patterns. This indicates that plasticizer activity must reside in the amorphous content of Starch 1500. The inclusion of PEG 200 in Starch 1500 films results in an antiplasticization effect. This provides further support to the concept that compatibility is prerequisite for efficient plasticization.

Plasticization of the binder films results in changes in the shape of the tensile stress-strain curves, indicative of changes in the viscoelastic characteristics. Tensile tests performed at single strain rate yield little fundamental information about time-dependent deformation. Consequently, creep rheological methods, were employed to discriminate and quantify viscoelastic properties.

In this work, an ICI microindenter was modified to enable computer logging of indentation depth versus time data for plasticized and unplasticized films of PVP, HPMC and Starch 1500. Programs were written to perform discrete and continuous spectral analysis of creep-compliance data. The resultant speed of analysis and the elimination of laborious (and potentially inaccurate) graphical methods greatly enhances the potential of this technique.

Results presented in Chapter four show that hydrophilic polymeric binders can display a spectrum of mechanical properties, depending on the presence of sorbed moisture and/or plasticizer. The measured creep-compliance of both unplasticized and plasticized binders conformed to a linear viscoelastic model. Hence, it was possible to use discrete mechanical analysis to resolve and quantify the elastic, retarded elastic and plastic components of deformation.

It was possible to determine creep curves for PVP, HPMC and Starch 1500 films dried over phosphorous pentoxide, so minimizing the influence of sorbed moisture. Dry, unplasticized binders exhibit high shear moduli and severely limited potential for time-dependent deformation. Although PVP and HPMC exhibit some retarded elastic strain, the rapid attainment of an equilibrium compliance confirms the absence of ductile flow. Starch 1500, in contrast, exhibits limited but finite plastic flow. These observations suggest that, unless the

stress required to initiate brittle failure is exceeded, the majority of binder strain occurring during the process of tablet compression will be elastic. The practical observation that overdried granulates often fail to tablet satisfactorily may reflect the predominant elasticity of dry polymeric binders.

Binders containing a significant proportion of sorbed moisture or a plasticizer (PEG 200 in the case of PVP and HPMC and glycerol in the case of Starch 1500) exhibit reduced shear moduli and decreased (Newtonian) viscosity. Consequently, the application of stress produces greater elastic strain but this is associated with increased plastic strain per unit time. The reduction in the apparent viscosity provides direct quantification polymer plasticization.

By the use of discrete mechanical analysis, it has been shown that binder plasticization increases the magnitude and complexity of retarded elastic strain. In the context of tableting, retarded elastic strain phenomena are implicated in strain-induced ageing defects in coated tablets or the appearance of capping on storage. Hiestand et al. (1987) suggested that the elastic energy dissipated in post-compression strain recovery of tablets may be utilised in further plastic deformation. Thus, plasticizer-induced retarded elasticity in tablet binders may make a contribution to the strength of tablets, in addition to that due to plastic flow during the compression event.

The use of continuous spectral analysis enabled creep-compliance data to be treated in a more fundamental manner. At low levels of plasticizer inclusion, continuous spectra were qualitatively similar in terms of peak position, although peak height was increased. This suggests that, at the molecular level, processes contributing to retardation are similar in nature. Shifts in the position of peaks in the retardation spectrum, associated with higher levels of plasticizer inclusion, indicate fundamental changes in the molecular process contributing to retardation.

Some caution is necessary in attempting to apply the results of studies on cast binder films to the real tableting situation. The duration of the creep test is many orders of magnitude longer than the duration of a typical compression cycle. The use of dynamic

rheological techniques may enable the evaluation of viscoelastic properties of polymers (and the influence of plasticization) over a time-scale similar to that of the tablet compression cycle.

The relationship between the viscoelasticity of polymers and their thermal properties, discussed in Chapter four, suggests that investigation of thermo-mechanical properties of binders at elevated temperature may be of value. Temperature rises during the compression process are well documented (see, for example Itiola and Pilpel, 1986) and may modify binder properties at the moment of compression.

An important consequence of plasticization, demonstrated by creep rheological studies on cast binder films, is the induction of time-dependency in the deformation characteristics. Consolidation studies at different loading rates and stress relaxation studies have confirmed that the time-dependent binder deformation is reflected in the compression properties of a granulate. Time-dependent deformation is not always been perceived as advantageous in tableting, however, since it confers compressing rate dependency. Nevertheless, work presented here has demonstrated that the induction of plasticity into materials which are inherently brittle or elastic can be desirable, and may be essential, for satisfactory tableting.

The results of tableting studies, presented in Chapter five, demonstrate that the mechanical properties of compressed tablets are determined both by the nature of the substrate and by the mechanical properties of the binder. Increasing binder plasticity eliminates the capping tendency of paracetamol and can result in tablets of greater tensile strength. However, an optimum level of binder plasticity exists, above which, the tensile strength of the tablets is reduced. A consistent reduction in tablet strength with increased binder plasticity was observed for dicalcium phosphate. It is deduced from these observations that, in the absence of debonding elastic strain recovery, binder strength contributes directly to tablet strength. In the breakage of a tablet, failure may occur at the binder-substrate interface or within the binder film. Studies to differentiate adhesive and cohesive failure may contribute to a better understanding of the role of binders in determining tablet strength.

The reduction in tablet friability, induced by binder plasticization, occurred irrespective of the substrate material or the effect on tablet strength. No correlation was found between the friability of tablets and the work required to cause diametral breakage. However, the data suggests resistance to impact attrition is determined by the strength and/or the rigidity or stiffness of tablets. Binder plasticization appears to induce a transition, from brittle elasticity, to more rubbery elasticity in compressed tablets. This correlates with plasticizer-induced conversion of polymeric binders from brittle glasses to ductile plastics of low modulus.

Ideally a ductile control substrate should have been included in this work. In fact, some studies were carried out using a microcrystalline cellulose (Avicel PH101, FMC Corp.) since this satisfied the selection criteria of ductile deformation and low aqueous solubility. Initial granulation studies indicated, however, that the deformation mode of microcrystalline cellulose was influenced significantly by the granulating fluid. Thus, although the unmassed substrate could be classified as ductile, after wet-massed granulation (in the absence of a binder) the resulting granules were highly elastic and did not form tablets. This behaviour has been confirmed by other workers (Staniforth et al., 1988). Other materials which exhibit ductile deformation, such as sodium chloride, were considered to be too water-soluble for use in the present work. Lead shot, however, might prove to be a suitable control for future studies.

Results presented in Chapter six demonstrate that the consolidation and plasticity of granulates is related directly to the plasticity of the binder. This behaviour has been interpreted in terms of the mechanical and rheological properties of the corresponding free binder film. The incorporation of a plasticizer or the sorption of moisture results in a decrease in the tensile strength of hydrophilic polymeric binders as observed in Chapter three. This results in greater granular consolidation at low compaction pressures, as a result of granule weakening. At higher compaction pressures, the plasticized binder facilitates easier deformation of granules into remaining voids. The binder itself can deform plastically to relieve stress at points of contact with the granule substrate or the compression tooling. This is analogous to the extrusion of binder into small voids.

Stress-relaxation provides a direct measurement of the plastic deformation of a compressed granulate. Data presented in this work shows that stress-relaxation of a granulate depends not only on the fundamental material properties but also on the compression history. Consequently, the determination of stress-relaxation without consideration of the deformation during the loading phase of compression, may give a misleading view of the deformation characteristics of the material. The inability of stress-relaxation to quantify plastic flow during the finite period of loading to maximum stress is a major limitation of the technique. The determination of maximum stress generated, by the compression of granulates to a constant strain, might characterise plastic deformation during the initial phase of compression.

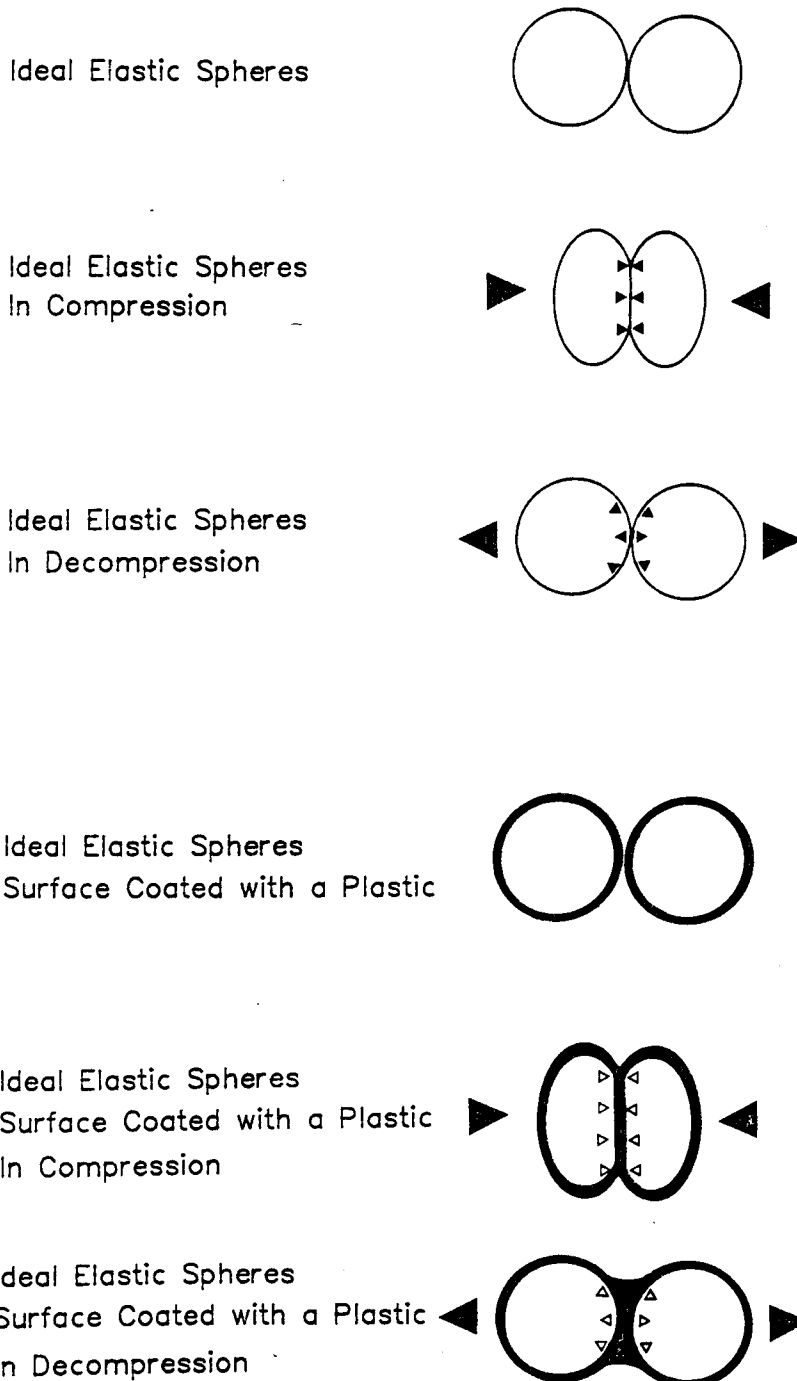
The increase in rate and extent of stress-relaxation, which occurs with increasing binder plasticity, correlates with the decrease in the viscosity of the corresponding free binder film. The relationship between binder plasticity and granule deformation appears to be a mechanical phenomenon which is independent of binder type or substrate material.

It was shown that a plasto-elasticity index (ER/SR) can be used to characterise the relative bonding and debonding deformations occurring during the compression and decompression of a tablet. Comparison of ER/SR indices with the tablet properties reported in Chapter five shows that high values correlate with high friability and capping tendency. Conversely, low values for ER/SR correlate with good tablettability. Plasticization of the polymeric tablet binders results in a decrease in the index, favouring the persistence of bonding. ER/SR does not provide a universal index of tablettability, however, since the magnitude of the index is greatly influenced by the experimental conditions under which stress-relaxation and, to a lesser extent, strain recovery are measured. Thus, when comparing different materials in this manner it is essential that identical test conditions are used.

The ability of plasticized binders to eliminate the capping tendency of paracetamol is not associated with significant reduction of elastic strain recovery. The reduction in binder elastic modulus resulting

from plasticization may, in fact, predispose the compressed granulate to greater elastic strain. It is deduced from these observations that plastic binders facilitate elastic strain recovery without catastrophic debonding. This can occur if the binder is sufficiently plastic to "give", i.e. translate elastic strain recovery into further plastic or viscoelastic deformation, hence maintaining or generating true area of contact. This concept is represented in Fig. 7.1.

Figure 7.1 Model Behaviour of Plastic Binders in Compression



The model represented by Fig. 7.1 considers the compression-decompression response of two pairs of brittle-elastic spheres, one pair being coated with a plastic polymer. For the uncoated spheres, the bonding area generated during compression is destroyed on decompression as the spheres regain their original conformation. This is analogous to the processes of capping or lamination. In contrast, although the polymer coated spheres regain their original configuration, deformation of the polymer coating maintains bonding area and prevents separation. In this case, the force required to cause separation after decompression (analogous to the tensile strength of a tablet) depends on adhesion between sphere and polymer or cohesion within the polymer film, whichever is the weakest. A critical degree of binder ductility will be required to prevent separation by brittle failure (of the binder film) on decompression. Binder plasticization beyond this limit reduces the strength of the binder film and, consequently, the strength of the interparticulate bond. The resistance of tablets to impact attrition is dependent on their ability to withstand impact shock without breakage. It has been shown that this is a function of tablet strength and stiffness. This can be modelled in terms of the strength and elastic modulus of the polymer coating the spheres in Fig. 7.1. Thus, although binder plasticization may reduce tablet strength it also confers rubbery-type impact resistance due to the reduced elastic modulus of the binder film.

Thus, the model proposed in Fig. 7.1 satisfactorily accounts for

- the ability of plasticized binders to eliminate capping and existence of an optimum degree of binder plasticity
- the decrease in tablet strength which occurs with binder plasticization
- the increased resistance to impact attrition (reduced friability) induced by binder plasticization

Data presented in this thesis indicates that, while water does not conform to traditional definitions of a plasticizer, it induces plasticity in some hydrophilic binders. Compression effects which have been attributed to the presence of moisture in a granulate, particularly the moisture sensitive compression characteristic of some granulates, probably result from binder plasticization. It is clear,

therefore, that water must be regarded as a plasticizer in this circumstance. Accordingly, binder plasticity should be considered as a factor when establishing moisture specifications for granulates.

REFERENCES

REFERENCES

- Abdul-Razzak, M.H., (1980)
M.Phil., (CNAAC), Leicester Polytechnic
- Abdul-Razzak, M.H., (1983)
Ph.D., (CNAAC), Leicester Polytechnic
- Ahmed, M. and Pilpel, N., (1967)
Manuf. Chem. & Aerosol News, 38, 37-38
- Alderborn, G. and Nystrom, C. (1984)
Acta Pharm. Suecica, 21, 1-8
- Alfrey, T, Jr., (1948)
"Mechanical Behaviour of High Polymers", Interscience Publishers,
NY
- Alfrey, T. and Gurnee, E.E., (1956)
"Rheology, Theory and Applications", Academic Press N.Y.
- Allen, D.J., Demarco, J.D. and Kwan, K.C., (1972)
J. Pharm. Sci., 61, 106-109
- Anagnostopoulos, C.E., Coran, A.Y. and Gamrath, H.R., (1965)
Modern Plastics, 43, 141-147, 187
- Armstrong, A.N. and Haines-Nutt, R.F., (1972)
J. Pharm. Pharmacol., 22, Suppl., 85
- Armstrong, A.N. and Haines-Nutt, R.F., (1974)
Powder Technol., 9, 287
- Armstrong, A.N. and Moreton, F.S.S., (1977)
J. Powder. Bulk Solids Technol., 1, 32-35
- Armstrong, A.N., Abourida, N.M.A.H. and Gough, A.M., (October, 1982)
Pharm. Tech., 66-72
- Armstrong, A.N., Abourida, N.M.A.H. and Gough, A.M., (1983)
J. Pharm. Pharmacol., 35, 320-321
- Armstrong, A.N. and Palfrey, L.P., (1987)
J. Pharm. Pharmacol., 39, 497-501
- Armstrong, A.N., (1989)
Int. J. Pharm., 49, 1-13
- Armstrong, A.N., (1990)
Pharm. Tech. Int., 2, 19-27
- ASTM D 683 - 80
- ASTM D 882 - 80a
- ASTM D 2383 - 69 (Reapproved 1976)
- ASTM D 3291 - 74 (Reapproved 1980)

- Aulton, M.E., Travers, D.N. and White, P.J.P., (1973)
 J. Pharm. Pharmacol., 25, Suppl., 79-86P
- Aulton, M.E., Tebby, H.G. and White P.J.P., (1974)
 J. Pharm. Pharmac., 26, Suppl., 59P
- Aulton, M.E. and Tebby, H.G., (1976)
 J. Pharm. Pharmacol., 28, Suppl., 66P
- Aulton, M.E. and Tebby, H.G., (1976)
 J. Pharm. Pharmacol., 28, Suppl., 66P
- Aulton, M.E., (1977)
 Mfr. Chem. & Aerosol News, 48, 23-36
- Aulton, M.E., Abdul-Razzak, M.H. and Hogan, J.E., (1980)
 Proceeding of the 2nd International Pharmaceutical Technology
 Conference, Paris
- Aulton, M.E., Abdul-Razzak, M.H. and Hogan, J.E., (1981)
 Drug Dev. Ind. Pharm., 7, 649
- Aulton, M.E. and Banks, M., (1981)
 Int. J Pharm. Tech. and Prod. Manf., 2, 24-29
- Aulton, M.E., (1982)
 Int. J Pharm. Tech. and Prod. Manf., 3, 9-16
- Eal'shin, M.Y., (1938)
 Vest. Metalloprom., 18, 124
- Bangudu, A.B. and Pilpel, N., 1985
 J. Pharm. Pharmacol., 37, 289-293
- Banker, G.S., (1966)
 J. Pharm. Sci., 55, 81-89
- Barlow, C.G., (1968)
 Chem. Engr. Lond., 46, CE196-CE200
- Barry, B.W., (1974)
 in "Advances in Pharmaceutical Sciences", Vol.4, Academic Press,
 London
- Barry, B.W. and Meyer, M.C., (1978)
 Int. J. Pharm., 2, 1-25
- Barton, A.F.N., (1982)
 J. Adhesion, 14, 33-62
- Beverley, P., (March, 1984)
 Acorn User, 115-120,
- Blecher, L., Lorenz, D.H., Lowd, H.L., Wood, A.S. and Wyman, D.P.,
 (1983), in "Handbook of Water Soluble Gums and Resins", Ed.,
 Davidson, R.L., McGraw Hill Book Co., NY

- Bohn, L., (1975)
in "CRC Polymer Handbook", Eds., Brandrup, J. and Immergut, E.H.,
Wiley Interscience Publishers
- Boyer, R.F., (1951)
through Nielson, L.E., (1977)
"Polymer Rheology", Marcel Dekker, NY
- Boyer, R.F. and Spencer, R.S., (1947)
J. Polymer Sci., 2, 157
- Bristow, G.M. and Watson, W.F., (1958 a.)
Trans. Faraday Soc., 54, 1567-1573
- Bristow, G.M. and Watson, W.F., (1958 b.)
Trans. Faraday Soc., 54, 1731-1741,
- Bristow, G.M. and Watson, W.F., (1958 c.)
Trans. Faraday Soc., 54, 1742-1747,
- Britten, J.R. and Pilpel, N., (1978)
J. Pharm. Pharmacol. 30, 673
- Buhler, V and Klodwig, U., (1984)
Acta Pharm. Technol., 30, 317-324
- Burrell, H., (1975)
"CRC Polymer Handbook", Eds., Brandrup, J. and Immergut, E.H.,
Wiley Interscience Publishers
- Burrell, H., Ed., (1983)
"CRC Handbook of Solubility and Other Cohesion Parameters", Wiley
Interscience Publishers
- Callahan, J.C., Cleary, G.W., Elefant, M., Kaplan, G., Kensler, T. and
Nash, R.A., (1982), Drug. Dev. Indust. Pharm., 8, 355-369
- Capes, C.E. and Dankwerts, P.V., (1965)
Trans. Inst. Chem. Engrs., 43, T116-T124
- Carr, R.L., (1965)
Chem. Eng., 72, (1) 169, (2) 69
- Carless, J.E. and Leigh, S., (1974)
J. Pharm. Pharmacol., 26, 289
- Carswell, T.S. and Nason, H.K., (1944)
Mod. Plast., 29, 121-126
- Casahoursat, L., Lemagnen, G., Larrouture, D., (1988)
Drug Dev. Indust. Pharm., 14, 2179-2199
- Castello, R.A. and Goyan, J.E., (1964)
J. Pharm. Sci. 53, 777

- Celik, M. and Travers, D.N., (1984)
 Proceeding of the 4th Pharmaceutical Technology Conference,
 Edinburgh
- Celik, M., (1984)
 Ph.D., (CNA), Leicester Polytechnic
- Celik, M. and Marshall, K., (1989)
 Drug Dev. Indust. Pharm., 15, 759-800
- Chalmers, A.A. and Elworthy, P.H., (1976)
 J. Pharm. Pharmac. 28, 239
- Chowan, Z.T. and Chow, Y.P. 1980
 Int. J. Pharm., 5, 139
- Chowan, Z.T. and Chow, Y.P., (1981a)
 Int. J. Pharm. Tech. & Prod. Mfr., 2, 29
- Chowan, Z.T. and Chow, Y.P., (1981b)
 J. Pharm. Sci., 70, 1134
- Church, M. and Kennerley, J. (1984)
 Proceeding of the 4th Pharmaceutical Technology Conference,
 Edinburgh
- Cole, E.T., Rees, J.E. and Hersey, J.A., (1975)
 Pharm. Acta Helv., 50, 28
- Cook, G.D. and Summers M.P., (1986)
 J. Pharm. Pharmacol., 38 suppl., 76P
- Cooper, A.R. and Eaton, L.E., (1962)
 J. Am. Ceram. Soc., 45, 97
- Cowie, J.M.G., (1965)
 Biopolymers, 3, 69-76
- Cutt, T., (1983)
 M.Sc., University of Manchester
- Danielson, W.G., Morehead, W.T. and Rippie, E.G., (1983)
 J. Pharm. Sci., 72, 342-345
- Danjo, K., Ertell, C., and Carstensen, J.T., (1989)
 Drug Dev. Indust. Pharm., 15, 1-10
- David, S.T. and Augstburger, L.L., (1977)
 J. Pharm Sci., 66, 155
- Davidson, R.L., (1983)
 "Handbook of Water Soluble Gums and Resins", McGraw Hill Book
 Co., NY
- Davis, S.S., (1974)
 Pharm. Acta. Helv., 49, 161

- de Blaey, C.J. and Polderman, J. (1970)
Pharm. Weekbl., 105, 241
- de Blaey, C.J. and Polderman, J. (1971a)
Pharm. Weekbl., 106, 57
- de Blaey, C.J., van Oudtshoorn, M.C.B. and Polderman, J. (1971b)
Pharm. Weekbl., 106, 589
- de Blaey, C.J., de Rijk, W. and Polderman, J. (1971c)
Pharm. Ind., 33, 897
- de Blaey, C.J., Weekers-Andersen, A.B. and Polderman, J. (1971d)
Pharm. Weekbl., 106, 893
- de Blaey, C.J., (1972)
Pharm. Weekbl., 107, 233
- Delporte, J.P., (1980)
Proceeding of the 2nd International Pharmaceutical Technology
Conference, Paris
- Dittgen, M., (1984)
Proceeding of the 4th Pharmaceutical Technology Conference,
Edinburgh,
- Doelker, E. and Shotton, E., (1977)
J. Pharm. Pharmacol., 29, 193
- Doelker, E., Gurny, R. and Mordier, D., (1980)
Acta Pharm. Technol., 26, 155
- Doelker, E., (1989)
Boll. Chim. Farm., 127, 37-49
- Doolittle, A.K., (1947)
J. Polymer Sci., 2, 121
- Doolittle, A.K., (1954)
"The Technology of Solvents and Plasticizers", Chapman & Hall,
London
- Doty, P.M. and Zable, H.S., (1946)
J. Polymer Sci., 1, 90-101
- Duchene, D., Puisieux, F., Veillard, M. and Bentejac, R., (1982)
Int. J. Pharm. Tech. & Prod. Mfr., 3, 100-107
- Eith, L., Stepta, R.F.T., Tomka, I., and Wittwer F., (1986)
Drug Dev. Indust. Pharm., 12, 2113-2126
- Ejiofor, O., Esezobo, S and Pilpel, N.,, 1986
J. Pharm. Pharmacol., 38, 1-7
- Entwistle, C.A. and Rowe, R.C, (1979)
J. Pharm. Pharmacol., 31, 269-272

- Esezobo, S and Pilpel, N., (1977a)
J. Pharm. Pharmacol., 29, 75
- Esezobo, S and Pilpel, N., (1977b)
J. Pharm. Sci., 66, 852
- Esezobo, S and Ambujam, V., (1982)
J. Pharm. Pharmacol., 34, 761
- Esezobo, S and Pilpel, N., (1986)
J. Pharm. Pharmacol., 38, 409-413
- Fassihi, A.R. and Parker, M.S., (1986)
Int. J. Pharm., 31, 271-273
- Fell, J.T. and Newton, J.M., (1971)
J. Pharm. Sci., 60, 1866
- Ferry, J.D., (1961)
"The Viscoelastic Properties of Polymers", Wiley Interscience
Publishers, NY
- Flory, P.J. (1942)
J. Chem. Phys., 10, 51
- Flory, P.J., (1953)
"The Principles of Polymer Chemistry", Cornell University Press,
NY
- Forrest, S.M., (1987)
Final Year Project B.Sc. (Pharm), (CNA), Leicester Polytechnic
- Fugiwara, H., Toda, J. and Kato, M., (1966)
Chem. Pharm. Bull., 14, 601
- Ganderton, D and Hunter, B.M., (1971)
J. Pharm. Pharmacol., 23, Suppl., 15
- Gee, G., (1943)
Trans. Inst. Rubber Ind., 18, 266,
- Gee, G., (1947)
Q. Rev. Chem. Soc., 1, 265-298,
- Griffith, A.A., (1920)
Philos. Trans. R. Soc., London, Ser. A, 221, 163
- Hansen, C.M. (1967a)
J. Paint Technol., 39, 104-117
- Hansen, C.M. (1967b)
J. Paint Technol., 39, 505-511
- Hansen, C.M. and Skaarup, K., (1967)
J. Paint Technol., 39, 511-515

- Hardman, J.S. and Lilley, S.A. (1973)
Proc. R. Soc., London, A333, 183
- Hawes, M.R., (1978)
"The Effect of Some Commonly Used Excipients on the Physical Properties of Film Formers Used in the Aqueous Coating of Pharmaceutical Tablets", R.P. Scherer Award
- Healey, J.N.C., Humphrey-Jones, J.F. and Walters, V., (1972)
J. Pharm. Pharmacol. 24, Suppl., 121P
- Healey, J.N.C., Humphrey-Jones, J.F. and Walters, V., (1973)
J. Pharm. Pharmacol. 25, Suppl., 110P
- Healey, J.N.C., Rubinstein, M.H. and Walters, V., (1974)
J. Pharm. Pharmacol., 26, Suppl., 41P-46P
- Healey, J.N.C., (1976)
Ph.D. (CNA), Liverpool Polytechnic
- Heckel, R.W., (1961a)
Trans. Met. Soc. AIME, 221, 671
- Heckel, R.W., (1961b)
Trans. Met. Soc. AIME. 221, 1001
- Hersey, J.A. and Rees, J.E., (1970)
Proceedings of the 2nd Particle Size Analysis Conf., Society for Analytical Chemistry, Bradford
- Hersey, J.A. and Rees, J.E., (1971)
Nature Physical Science, 230, 96
- Hersey, J.A., Cole, E.T. and Rees, J.E. (1973)
Proceedings of the 1st International Conference on the Compaction and Consolidation of Particulate Matter, London
- Hiestand E.N., Wells, J.E., Peot, C.B. and Ochs, J.F., (1977)
J. Pharm. Sci., 66, 510-519
- Hiestand, E.N and Smith, D.P., (1984)
Powder Technol., 38, 145-159
- Hiestand, E.N., (1985)
J. Pharm. Sci., 74, 768-770
- Hiestand, E.N and Smith, D.P., (1987)
Acta Pharm. Suecica, 24, 47-48
- Hiestand, E.N, Wald, R.J. and Smith, D.P., (1987)
J. Pharm. Sci., 76, S267
- Hildebrand, J.H. and Scott, R.L., (1950)
"The Solubility of Non-electrolytes", 3rd Ed., Reinhold, NY

- Ho, T. and Hersey, J.A., (1980)
J. Pharm. Pharmacol., 32, 160
- Holm, P., Jungensen, O., Schaefer, T. and Kristensen, H.G., (1983)
Pharm. Ind., 45, 806-811
- Holm, P., Jungensen, O., Schaefer, T. and Kristensen, H.G., (1984)
Pharm. Ind., 46, 97-101
- Hoy, K.L., (1970)
J. Paint Technol., 42, 76,
- Huckle, P.D., (1985)
Ph.D., London University
- Huggins, M.L., (1942a)
J. Phys. Chem., 46, 151
- Huggins, M.L., (1942b)
Ann. N. Y. Acad. Sci., 43, 1
- Huggins, M.L., (1942c)
J. Am. Chem. Soc., 64, 1712
- Huggins, M.L., (1947)
J. Chem. Phys., 44, 9-15
- Humbert-Droz, P., Doelker, E., Gurny, R. and Mordier, D., (1983)
Int. J. Pharm. Tech. & Prod. Mfr., 4, 29-35
- Hunter, B.M., Fisher, D.G., Pratt, R.M., and Rowe, R.C., (1976)
J. Pharm. Pharmacol. 28, Suppl., 65P
- Hunter, B.M. and Ganderton, D., (1973)
J. Pharm. Pharmacol. 25, Suppl., 71P
- Itiola, O.A. and Pilpel, N., (1986)
Int. J. Pharmaceutics., 31, 99-105
- Iyengar, Y and Erickson, D.E., (1967)
J. Appl. Polymer Sci., 11, 2311-2324
- Jackson, I.M., Ridgway, F. and Rubenstein, M.H., (1982)
J. Pharm. Pharmacol., 34 Suppl. 48P
- Jaegerskou, A., Holm. P., Schaefer, T and Kristensen, H.G., (1984)
Pharm. Ind., 46, 310-314
- Jaiyeoba, K.T. and Spring, M.S., (1979)
J. Pharm. Pharmacol., 31, 197
- Jarosz, P.J. and Parrott, E.L., (1982)
J. Pharm. Sci., 71, 607
- Jones, H, (1947)
"Plasticizers, Fillers, Catalysts and Accelerators", Plastics
Inst., Monograph 11

- Kanig, J.L. and Goodman, H., (1962)
J. Pharm. Sci., 51, 77-83
- Kapur, P.C. and Fuerstenau, D.W., (1964)
Trans. Am. Inst. Min. Metall. Petrol Engrs., 229, 346-355
- Kawakimi, M., Egashira, M. and Kagawa, S. (1976)
Bull. Chem. Soc. Jpn., 49, 3449-3453
- Kent, D.J., and Rowe, R.C., (1978)
J. Pharm. Pharmac., 30, 808-810
- Khan, K.A. and Musikabhumma, P., (1981)
J. Pharm. Pharmac., 33, 627
- Kristensen, H.G., and Scheafer, T. (1987)
Drug Dev. Indust. Pharm., 13, 803-872
- Krycer, I., Pope, D.G. and Hersey J.A., (1982a)
Int. J. Pharm., 12, 113-134
- Krycer, I., Pope, D.G. and Hersey J.A., (1982b)
J. Pharm. Pharmacol., 34, 802-804
- Krycer, I., Pope, D.G. and Hersey J.A., (1982c)
Powder Technol., 33, 101-111
- Krycer, I., Pope, D.G. and Hersey, J.A., (1983)
Powder Technol., 34, 39-51
- Kuhn, W., (1947)
Helv. Chim. Acta, 30, 487-493
- Kurup, T.R R. and Pilpel, N., (1977)
Powder Technol., 16, 179
- Kurup, T.R R. and Pilpel, N., (1978)
Powder Technol., 19, 147
- Lee, E.H. and Radok, J.R.M., (1960)
J. Appl. Mech., 27, 438-444
- Lehrman, G.P. and Skauen, D.M., (1958)
Drug Stand., 26, 170-175
- Leibch, W., (1943)
Kolloid-Z, 99, 107
- Leigh, S., Carless, J.E. and Burt, B.W., (1977)
J. Pharm. Sci., 56, 888
- Lever, A.E. and Rhys, J.A. (1968)
"The Properties and Testing of Plastics Materials", 3rd Ed.,
Temple Press Books, UK
- Lindberg, N.O., (1984)
Drug Dev. Indust. Pharm., 10, 45-56

- Lockett, F.J., (1972)
 "Nonlinear Viscoelastic Solids", Academic Press, London
- Long, W.M., (1960)
 Powder Metall, 6, 73
- Luenberger, H., Bier, H. and Sucker, H.B., (1979)
 Pharm. Tech. Int., July, 35-42
- Luenberger, H., (1982)
 Pharm. Acta Helv., 57, 77-82
- Majeed, S., (1984)
 M.Phil. (CNA), Leicester Polytechnic
- Malamataris, S. and Pilpel, N., (1983)
 J. Pharm. Pharmacol., 35, 1-6
- Malamataris, S., Baie, S.B. and Pilpel, N., (1984)
 J. Pharm. Pharmacol., 36, 616-617
- Manfred, G. and Obrist, J. (1927)
 Kolloid-Z 41, 348
- Mann, S., (1984)
 M.Sc. University of Bath
- Mark, H.F., (1965)
 J. Polymer Sci., Part C, 1, 1-33
- Marshall, P.V., York, P. and Richardson, R.. (1986)
 J. Pharm. Pharmacol., 38 suppl., 47P
- Marshall, K., (1989)
 Drug Dev. Indust. Pharm., 15, 2153-2176
- Martin, A., Camarata, A. and Swarbrick, J., (1983)
 "Physical Pharmacy", 3rd Ed., Lea & Febiger, Philadelphia. US
- Masilungan, F.C. and Lordi, N.G., (1984)
 Int. J. Pharm., 20, 295-305
- Mendes, R.W., (1968)
 Drug Cosmet. Ind., 103, 46-48 & 176-179
- Merck Index, (1983)
 10th Edn., Merck & Co., Inc., Rahway, USA
- Mochun, W. (1984)
 Final Year Project B.Sc. (Pharm), (CNA), Leicester Polytechnic
- Monk, C.J.H. and Wright, (1965)
 J. Oil Col. Chem. Assoc., 48, 520-528
- Morris, R.J.L., (1970)
 J. Oil Col. Chem. Assoc., 53, 761-773

- Morris, R.J.L., (1973)
J. Oil Col. Chem. Assoc., 56, 555-565
- Morton, F.S.S., (1977)
Ph.D., UWIST
- Munden, B.J., DeKay, H.G. and Banker, G.S., (1964)
J. Pharm. Sci., 53, 395-401
- Muti, H. and Othman, S. (1989)
Drug Dev. Indust. Pharm., 15, 2017-2035
- Nelson, E., Arndt, J.R. and Busse, L.W., (1957)
J. Am. Pharm. Assoc., Sci. Edn., 46, 257-262
- Newitt, D.M. and Conway-Jones, J.M., (1958)
Trans. Inst. Chem. Engrs., 36, 422
- Newton, J.M. and Fell, J.T., (1970)
J. Pharm. Sci., 59, 688-691
- Nielsen, L.E., (1977)
"Polymer Rheology", Marcel Dekker, NY
- Norwick, A.S and Berry, B.S., (1972)
"Anelastic Relaxation in Crystalline Solids", Academic Press, NY
- Nutter-Smith, A., (1949)
Pharm. J., 163, 194-195, 227-228 & 477-478
- Nyquist, H., (1983)
Int. J. Pharm. Tech. & Prod. Mfr., 4, 47-48
- Obiorah, B.A. and Shotton, E., (1976)
J. Pharm. Pharmacol., 28, 629
- Okhamafe, A.O. and York, P., (1983)
J. Pharm. Pharmacol., 35, 409-415
- Okhamafe, A.O. and York, P., (1984a)
Proceedings of the 4th Pharmaceutical Technology Conference,
Edinburgh
- Okhamafe, A.O. and York, P., (1984b)
Int. J. Pharm., 22, 273-281
- Okhamafe, A.O. and York, P., (1985)
Drug Dev. Ind. Pharm., 11, 131-146
- Okhamafe, A.O. and York, P., (1988)
J. Pharm. Sci., 77, 438-443
- Oksanen, C.A. and Zografis, G., (1990)
Pharm. Res., 7, 654-657
- Ononokopono, O.E. and Spring, M.S., (1988a)
J. Pharm. Pharmacol., 40, 126-128

- Oñonokopono, O.E. and Spring, M.S., (1988b)
J. Pharm. Pharmacol., 40, 313-319
- Osewa, S.Y. and Nasipuri, R.N., (1983)
Drug dev. Indust. Pharm., 9, 197
- Otozai, K. and Toyama, I. (1976)
Z. Anal. Chem., 281, 131-133
- Paronen, P., (1986)
Drug, Dev. Indust. Pharm., 12, 1903
- Patel, C.I. and Staniforth, J.N., (1987)
Powder Technol., 53
- Pilpel, N., (July, 1969)
Chem. Process Eng., 67-72
- Porter, S.C. and Ridgeway, K., (1977)
J. Pharm. Pharmacol., 29 suppl., 42P
- Porter, S.C., (1980)
Pharm. Tech., 4, 67-75
- Radebaugh, G.W., Murtha, J.L., Julian, T.N. and Bondi, J.N., (1988)
Int. J. Pharm., 45, 39-46
- Radebaugh, G.W., Babu, S.R. and Bondi, J.N., (1989)
Int. J. Pharm., 57, 95-105
- Ragnarsson and Sjorgren, J., (1982)
Int. J. Pharm., 12, 163-171
- Ragnarsson and Sjorgren, J., (1985)
J. Pharm. Pharmacol., 37, 145-150
- Reading, S, (1983)
Ph.D., University of Manchester
- Reading, S.J. and Spring, M.S., (1983)
J. Pharm. Pharmacol., 35, Suppl., 2P
- Reading, S.J. and Spring, M.S., (1984a)
J. Pharm. Pharmacol., 36, 421-426
- Reading, S.J. and Spring, M.S., (1984b)
Proceedings of the 4th Pharmaceutical Technology Conference,
Edinburgh
- Record, P.C., (1980)
Int. J Pharm. Tech. & Prod. Manf., 1, 32-39
- Rees, J.E. and Shotton, E., (1970)
J. Pharm. Pharmacol., 22, Suppl., 175
- Rees J.E., Rue, P.J. and Richardson, S.C., (1977)
J. Pharm. Pharmac., 29,
- Rees, J.E. and Rue, P.J., (1978a)
J. Pharm. Pharmacol., 30, 601

- Rees, J.E. and Rue, P.J., (1978b)
Drug Dev. and Ind. Pharm., 4, 131
- Rees, J.E., (1980)
"Postgraduate School on the Theory and Practice of Solid Dosage
Forms and Manufacture", London
- Rippie, E.G. and Danielson, D.W., (1981)
J. Pharm. Sci., 70, 476-482
- Ritala, M., Holm, P., Schaefer, T. and Kristensen, (1986)
Drug Dev. Indust. Pharm., 12, 1685
- Ritchie, P.D., (1972)
"Plasticizers, Stabilisers and Fillers". Iliffe Books Ltd.,
London
- Ritter, A and Sucker, H.B., (March, 1980)
Pharm. Tech. 56-65 & 128
- Roberts, R.J. and Rowe, R.C., (1985)
J. Pharm. Pharmac., 37, 377-384
- Roberts, R.J. and Rowe, R.C., (1986a)
J. Pharm. Pharmac., 38, 526-528
- Roberts, R.J. and Rowe, R.C., (1986b)
J. Pharm. Pharmac., 38, 567-571
- Robinson, D.H., (1989)
Drug Dev. Indust. Pharm., 15, 259
- Rogerson, A., Travers, D.N, and Jones, T.M., (1976)
J. Pharm. Pharmac., 28, Suppl., 67P
- Rowe, R.C., (1976a)
J. Pharm. Pharmac., 28, 310-311
- Rowe, R.C., (1976b)
Pharm. Acta Helv., 51, 330-334
- Rowe, R.C., (1982)
Int. J. Pharm. Tech. and Prod. Mfr., 3, 3-8
- Rowe, R.C., (1983)
Int. J. Pharm., 14, 355-359
- Rowe, R.C., Sakellariou, P. and White, E.F.T., (1986)
Int. J. Pharm., 31, 175-177
- Rubenstein, M.H. and Healey, J.N.C., (1973)
J. Pharm. Pharmac., 25, Suppl., 168P
- Rudin, A. and Wagner, R.A., (1975)
J. Appl. Polym. Sci., 19, 3361-3367

- Rue, P.J. and Rees, J.E., (1978)
J. Pharm. Pharmac., 30, 642
- Rue, P.J., (1980)
Proceedings of the Symposium on Tablet Technology, Stockholm
- Rue, P.J., Seager, H., Ryder, J. and Burt, I., (1980)
Int. J. Pharm. Tech. & Prod. Mfr., 1, 2-6
- Rumpf, H., (1958)
Chem. Ing. Tech., 30, 144-158 & 329-336
- Rumpf, H., (1962)
in "Agglomeration", Ed. W.A. Knepper, Interscience Publishers
Inc., NY
- Sakellariou, P., Rowe, R.C. and White, E.F.T, (1985)
Int. J. Pharm., 27, 267-277
- Sakellariou, P., Rowe, R.C. and White, E.F.T, (1986)
Int. J. Pharm., 34, 93-103
- Schwarzl, F. and Staverman, A.J. (1952)
Physica, 18, 791-798
- Seager, H., (1977)
Manuf. Chem. & Aerosol News, 48, 25
- Shaxby, J.H., and Evans, J.C., (1923)
Trans. Faraday Soc., 19, 60
- Schilderout, S.A., (1984)
J. Pharm. Pharmacol., 36, 502-505
- Shlanta, S. and Milosovich, G. (1964)
J. Pharm. Sci. 53, 562-564
- Shotton, E. and Edwards, N.J., (1974)
J. Pharm. Pharmacol., 26, Suppl., 107P
- Shotton, E. and Obiorah, B.A. (1975)
J. Pharm Sci., 64, 1213
- Shultz, A.R., and Flory, P.J., (1952)
J. Am. Chem. Soc., 74, 7624
- Skultety, P.F., and Sims, S., (1987)
Drug Dev. Indust. Phar., 13, 2209-2219
- Small, P.A., (1953)
J. Appl. Chem., 3, 71-80
- Spring, M.S. and Femi-Oyewo, M.N., (1982)
Int. J. Pharm. Tech. & Prod. Mfr., 3, 73-75
- Staniforth, J.N., Baichwal, A.R. and Hart., J.P., (1987)
Int. J. Pharmaceutics, 40, 267-269

- Stanley-Wood, N.G. and Shubair, M.S., (1979)
J. Pharm. Pharmacol., 31, 429
- Stanley-Wood, N.G. and Shubair, M.S., (1979)
Powder Technol., 25, 57
- Strickland, W.A., Busse, L.W. and Higuchi, T., (1956)
J. Am. Pharm. Assoc. Sci. Ed., 45, 482
- Summers, M., Enever, R.P. and Carless, J.E., (1976)
J. Pharm. Pharmacol., 28, 89
- Vemba, T., Gillard, J. and Roland, M. (1980)
Pharm. Acta Helv. 55, 65-71
- Tan, Y.Y. and Challa, G., (1976)
Polymer, 17, 739-740
- Tobolsky, A.V., (1971)
in "Polymer Science and Materials", Eds., Tobolsky, A.V. and
Mark, H.F., Wiley Interscience, NY
- Train, D., (1956)
J. Pharm. Pharmacol., 8, 745
- Train, D., (1957)
Trans. Instn. Chem. Engrs., 35, 258
- Travers, D.N., Celik, M and Buttery, T.C., (1983)
Drug Dev. and Indust. Pharm., 9, 139-157
- Van Krevelen, D.W. and Hoftyzer, P.J., (1976)
"Properties of Polymers: Their Estimation and Correlation with
Chemical Structure", 2nd Ed., Elsevier, Amsterdam
- Vaughan, C.D., (1985)
J. Soc. Cosmet. Chem., 36, 319-333
- Walker, E.E. (1923)
Trans. Faraday Soc., 19, 73, 83, 614
- Warburton, B. and Barry, B.W., (1967)
J. Pharm. Pharmacol., 20, 255-268
- Wells, J.I. and Walker, C.V., (1983)
Int. J. Pharm., 15, 97-111
- Wells, J.I. and Khan, K.A., (1982)
European Patent Application No. 0 070 127 A2
- Wells, J.I., Bhatt, D.A. and Khan, K.A., (1982)
J. Pharm. Pharmacol., 34, Suppl., 46P
- White, P.J.P. and Aulton, M.E. (1980)
J. Phys. E: Scientific Instruments, 13, 380-381

- Willis, C.K., Banker, G.S. and DeKay, H.G., (1965)
J. Pharm. Sci., 54, 366-372
- Wollish, E.G. and Mlodozieniec, A.R., (June, 1982)
Pharm. Tech.. 49-64
- Wurstlin, F., (1943)
Kunststoff Tech., 11, 269
- York, P. and Pilpel, N. (1973)
J. Pharm. Pharmacol., 25, Suppl. 1P
- York, P. and Baily, E.D., (1977)
J. Pharm. Pharmacol., 29, 70-74
- Zatz, J.L., Weiner, N.D., Gibaldi, M. (1968)
J. Pharm. Sci., 57, 1440-1443